UNIVERSITÀ DI PARMA

UNIVERSITA' DEGLI STUDI DI PARMA

DOTTORATO DI RICERCA IN
"*Biologia Evoluzionistica ed Ecologia*"
CICLO XXXV

Camera trapping and occupancy analyses to study tropical and temperate mammals from local to global scale

Coordinatore:
Chiar.mo Prof. Pierluigi Viaroli

Tutore:
Chiar.mo Prof. Francesco Rovero

Dottoranda: Ilaria Greco

Anni Accademici 2019/2020 – 2021/2022

Doctoral degree in

Evolutionary Biology and Ecology

Curriculum in Ethology and Ecology

IN CO-TUTELA CON:

UNIVERSITA' DEGLI STUDI DI FIRENZE

Il dottorato in Biologia Evoluzionistica ed Ecologia – XXXV ciclo è in convenzione tra le Università di Ferrara, Firenze e Parma (sede amministrativa)

Camera trapping and occupancy analyses to study tropical and temperate mammals from local to global scale

Ph.D. Thesis

Ilaria Greco

To my younger self.

To my parents.

To You.

"[…] Many have called Chernobyl the most costly environmental catastrophe in history. Sadly, this isn't true.
Something else has been unfolding, everywhere, across the globe, barely noticeable from day to day for much of the last century. This too is happening as the result of bad planning and human error. Not one hapless accident, but a damaging lack of care and understanding that affects everything we do.
It didn't begin with a single explosion.
It started silently, before anyone realized it, as a result of causes that are multifarious global and complex. Its fallout cannot be detected by a single instrument. It has taken hundreds of studies across the world to confirm that is even happening. Its effects will be far more profound that the contamination of soils and waterways in a few unfortunate countries – it could ultimately lead to the destabilization and collapse of everything we rely upon.
This is the true tragedy of our time: the spiraling decline of our planet's *biodiversity*. […]"

David Attenborough

"It is not enough to understand the natural world;
the point is to defend and preserve it"

Edward Abbey

Acknowledgements

I am very grateful to my supervisor, Prof. Francesco Rovero, for his guidance and assistance, particularly because he gave me the opportunity to work on this project and challenge myself to accomplish it. Thank you, Francesco, for everything you taught me and for all the possibilities and experiences you offered me during this PhD.

Deep gratitude is also extended to Prof. Lydia Beaudrot who hosted me in her team at Rice University and gave me significant ecological insights along my journey into macroecology, and to Dr. Simone Tenan and Prof. Chris Sutherland who provided invaluable contributions to the broader-scale community analyses. A special thank you also to Prof. Giacomo Santini, for his presence and support during these years. Thanks to Frank and Francis who took care of our server as best as possible, and to my friends and colleagues of the Ecology and Biodiversity Conservation Lab – Marina Bambi and Marco Salvatori – for the moments shared together.

Thanks to the staff of Foreste Casentinesi National Park, Reparto Carabinieri of Biodiversity of Pratovecchio and Reparto Carabinieri Forestali for their logistic support with our long-term camera-trapping project in the park. Thanks also to Martina Miscioscia and Matilde Marconi for their precious help during the data collection.

No words of gratitude are enough for the daily-based essential support of my fiancé Alberto, my mum Antonella, my dad Andrea, and my whole family. Thank you, I owe you everything.

Summary

The contemporary biodiversity crisis caused by anthropogenic disturbances calls for urgent actions to reduce the pervasive loss or decline of species that are jeopardizing the functioning of the ecosystems. Halting species decline is only achievable by understanding the causes of biodiversity changes, the responses of species to disturbances, and consequently by promoting conservation actions that can mitigate impacts. In this context, reliable population and community assessments based on sound data and robust analytical frameworks can help to guide conservation strategies. Particularly, information for monitoring changes should come from data collected systematically with tools that can detect also cryptic and rare species and acquire data on the whole community, and from analytical frameworks that can account for imperfect detection. Camera traps as a detection tool, and occupancy models as an analytical framework perfectly suit these requirements. This thesis uses tools to address various aspects of anthropogenic impact on wild mammals, by assessing the potential vulnerability of populations and communities in temperate and tropical protected areas, at both local and global scale, and with a focus on tropical forests. I targeted mammals both for the key ecological roles they play and because camera traps are particularly suitable to target this taxon. In particular, Chapters 1 - 3 focus on single populations of overlooked and elusive mammal species at a local scale (in Tanzania and Mongolia), while Chapters 4 - 5 focus on mammalian communities at a larger scale (across protected areas in Italy and in the tropics).

In Chapter 1, I analysed data from a systematic camera trapping protocol deployed in a remote reserve in Tanzania to determine the species checklist and assess vulnerability of most threatened species. Among these, the African golden cat

(*Caracal aurata*) was detected for the first time in this country, confirming a range expansion for this species and the establishment of the easternmost African population. Results from the occupancy analyses of this species indicated marked vulnerability to human encroachment in the reserve, as I estimated greater occurrence in areas of primary, closed-canopy and dense forest in the interior of the Nature Reserve and away from settlements. In Chapter 2, I used bycatch data from a systematic camera trapping project in the Mongolian steppe that primarily targeted the snow leopard (*Panthera uncia*) to study the habitat selection preferences of the neglected Pallas's cat and its relationship with livestock presence. I estimated that the preferred habitat of the Pallas's cat (*Otocolobus manul*) in the study region coincided with areas encroached by livestock, with diel activity segregation that limits direct encounters. Its dependence on areas that are used for grazing may eventually threaten the cat with habitat degradation, prey depletion, predation by dogs, and poisoning from pest control, ultimately undermining the long-term viability of the population. In Chapter 3, I used density data from acoustic distance sampling with camera trapping data to carry out the first comprehensive assessment and spatially-explicit density estimation of the endemic Sanje mangabey (*Cercocebus sanjei*), across its entire distribution range in Tanzania. I found that the higher density found in the forest of lower protection compared to previous studies instil optimism for the conservation of the species, although occupancy analysis highlighted the vulnerability of this primate to human disturbance.

In Chapter 4, we investigated the spatial and temporal patterns of mammalian communities in relation to human frequentation in four protected areas in central and northern Italy, monitored with a standardized camera trapping protocol. By using a Bayesian multi-area occupancy model for communities that also accounts for the time interval of the detection events (i.e., diurnal, crepuscular and nocturnal events), we found that wildlife consistently increased their nocturnal activity at locations with higher rates of human passage, therefore diminishing the chances to encounter humans. We also found differences in behavioural responses according to species' body size and trophic guild: larger species and omnivores tended to avoid

humans in space as well as in time, while larger species also became more diurnal further away from urban areas. Human presence may indeed promote risk perception and the creation of a landscape of fear that can result in cascading effects on the whole community. However, the adoption of a primarily nocturnal activity can act as coping mechanism to allow coexistence between humans and wildlife. Finally, in Chapter 5, I investigated pan-tropical patterns of changes in mammal communities in relation to proximity to settlements, increasing human density, habitat loss and forest fragmentation in the broader landscape surrounding protected forests. Although protected areas represent indeed a critical tool for conservation, evidence warns that human impacts around reserve threatened biodiversity within. By using camera trapping data systematically collected in 37 tropical forests, I simultaneously estimated patterns of community richness and occupancy by accounting for imperfect detection. I found that the escalating human densities around reserves impact richness within, while occupancy was not affected. Moreover, the extent of forest cover in the landscape is associated with higher richness and occupancy within reserves, with occupancy increasing with less fragmentation. These results suggest an extinction filtering of sensitive species, and a potential increase in abundance of adaptative species. While the anthropogenic impact on the landscape highly affects wildlife within reserves, I found that the viability of mammals depends on environmental changes happening beyond protected areas' boundaries.

Overall, the results of this thesis demonstrated how the use of systematic camera trapping data coupled with robust analytical framework that accounts for imperfect detection can represent a valid tool for population and community assessments in view of promoting wildlife conservation and mitigation strategies. Hence, mammal assessments are fundamental in view of the new challenge to doble the protected area estate within the upcoming years to ensure that current and future reserves can sustain viable wildlife populations.

Sommario

L’attuale crisi della biodiversità, causata da disturbi antropogenici, richiede azioni urgenti per ridurre l’estensiva perdita di specie che sta portando a una grave alterazione dell'abbondanza e della distribuzione della fauna selvatica e che sta mettendo a repentaglio il funzionamento complessivo dell'ecosistema. Arrestare il declino delle specie selvatiche è possibile solo comprendendo le cause che determinano i cambiamenti della biodiversità, le risposte della fauna selvatica ai disturbi e, di conseguenza, promuovendo azioni di conservazione che possano mitigare gli impatti. In questo contesto, valutazioni affidabili di popolazioni e di comunità basate su dati solidi e quadri analitici robusti possono contribuire a guidare le strategie di conservazione. In particolare, informazioni utili per monitorare potenziali cambiamenti nella biodiversità dovrebbero provenire da dati raccolti sistematicamente con strumenti in grado sia di rilevare le specie criptiche che di acquisire dati sull'intera comunità, e da framework analitici che possono tenere conto del rilevamento imperfetto. Quindi, l’uso di fototrappole come strumento di monitoraggio e di modelli di occupancy per l’analisi dei dati si adattano bene a questi requisiti. Questa tesi affronta vari aspetti dell'impatto antropogenico sulle specie selvatiche per valutare la potenziale vulnerabilità di popolazioni e comunità di mammiferi in relazione al disturbo, in aree protette temperate e tropicali, dalla scala locale a quella globale, con particolare attenzione alle foreste tropicali. I Capitoli 1 - 3 si concentrano su singole popolazioni a scale locale di mammiferi poco studiati, mentre i capitoli 4 - 5 si concentrano sulle comunità di mammiferi su scala più ampia. Ho usato i mammiferi come oggetto di studio sia per i ruoli ecologici chiave che svolgono sia perché le fototrappole sono strumenti particolarmente adatti allo studio di questo taxon. Pertanto, ho utilizzato dati sistematici e standardizzati ottenuti da fototrappole e abbinati al framework di

occupancy che tiene conto del rilevamento imperfetto.

Nel capitolo 1, ho utilizzato il fototrappolaggio come strumento efficace per valutare la presenza di specie rare in una remota riserva in Tanzania. Utilizzando un protocollo sistematico, è stato rilevato per la prima volta in questo paese il gatto dorato africano, confermando un'espansione dell'areale di distribuzione di questa specie e l'insediamento della popolazione africana più orientale. I risultati delle analisi di occupancy hanno suggerito la sua vulnerabilità allo sfruttamento nella riserva da parte dell'uomo, poiché ho stimato una maggiore probabilità di presenza nelle aree di foresta primaria, dense e fitte situate all'interno della Riserva Naturale. Nel capitolo 2, ho utilizzato dati secondari derivanti da un progetto di fototrappolaggio sistematico nella steppa mongola per studiare le preferenze di selezione di habitat del poco studiato gatto di Pallas e il suo rapporto con la presenza del bestiame. Ho stimato che l'habitat preferito del gatto di Pallas all'interno della regione di studio coincide con aree fortemente usate dal bestiame, mentre la segregazione dell'attività temporale limita gli incontri diretti tra gatto e bestiame. La dipendenza del felino dalle aree utilizzate per il pascolo può alla fine minacciare il gatto a causa del degrado dell'habitat, della predazione da parte dei cani da pastore, dall'avvelenamento e progressivo esaurimento delle prede, minando infine la vitalità a lungo termine della popolazione. Nel capitolo 3, ho utilizzato dati di densità ottenuti usando campionamento acustico associato alla tecnica del distance sampling con dati di fototrappolaggio per effettuare la prima stima di densità spazialmente-esplicita e la prima valutazione completa della popolazione di Sanje mangabey in tutto il suo areale di distribuzione in Tanzania. Dato il precedente disturbo, la più alta densità stimata nella foresta con minore protezione rispetto agli studi precedenti infonde ottimismo per lo stato di conservazione di questa specie endemica, sebbene l'analisi della probabilità di presenza abbia comunque evidenziato una potenziale vulnerabilità di questo primate al disturbo antropico.

Nel Capitolo 4, abbiamo indagato pattern spaziali e temporali di comunità di mammiferi in relazione alla presenza umana in quattro aree protette dell'Italia centro-settentrionale, campionate con un protocollo standardizzato di

fototrappolaggio. Utilizzando un modello Bayesiano multi-area di occupancy per comunità, che tiene conto anche dell'intervallo temporale degli eventi di rilevamento (i.e., eventi giornalieri, crepuscolari, notturni), abbiamo scoperto che la fauna selvatica ha costantemente aumentato l'attività notturna in luoghi con tassi più elevati di passaggio umano, diminuendo quindi le possibilità di incontro con l'essere umano. Abbiamo anche trovato differenze nelle risposte comportamentali in base alla dimensione corporea delle specie e alla loro gilda trofica: le specie più grandi e le specie con una dieta onnivora tendevano a evitare gli esseri umani nello spazio così come nel tempo, mentre le specie con massa corporea maggiore diventavano anche più diurne con una distanza maggiore dalle aree urbane. La presenza umana può infatti promuovere la percezione del rischio e la creazione di un paesaggio di paura che può provocare effetti a cascata sull'intera comunità. Tuttavia, l'adozione di un'attività prevalentemente notturna può rappresentare un meccanismo di adattamento che consente la convivenza tra uomo e fauna selvatica. Infine, nel capitolo 5, ho analizzato variazioni di ricchezza e probabilità di presenza a scala pantropicale delle comunità di mammiferi in relazione alla vicinanza dagli insediamenti, all'aumento della densità umana, alla perdita di habitat e alla frammentazione delle foreste nel più ampio paesaggio che circonda le aree protette. Infatti, sebbene le aree protette rappresentino uno strumento fondamentale per la conservazione, studi recenti avvertono che gli impatti umani attorno alle riserve minacciano la biodiversità al loro interno. Utilizzando dati da fototrappolaggio raccolti sistematicamente in 37 foreste tropicali, ho stimato contemporaneamente ricchezza e probabilità di presenza delle comunità, tenendo conto del rilevamento imperfetto. Ho scoperto che l'aumento della densità umana attorno alle riserve ha un impatto sulla ricchezza al loro interno, mentre non ho trovato effetti sull'occupancy. Inoltre, l'estensione della copertura forestale nel paesaggio è associata a una maggiore ricchezza e probabilità di presenza all'interno delle riserve, con un'occupancy che aumenta con una minore frammentazione. Questi risultati suggeriscono un filtro di estinzione delle specie sensibili e un aumento dell'abbondanza di quelle maggiormente adattabili e generaliste. Mentre l'impatto

antropogenico sul paesaggio impatta fortemente la fauna selvatica all'interno delle riserve, ho scoperto che la vitalità dei mammiferi dipende dai cambiamenti ambientali che avvengono al di fuori delle aree protette.

Nel complesso, i risultati di questa tesi dimostrano come l'uso di dati sistematici derivanti da fototrappolaggio, insieme all'uso di un framework analitico robusto che tenga conto del rilevamento imperfetto, possa rappresentare uno strumento valido per valutare lo status di popolazioni e di comunità per promuovere strategie di conservazione e di mitigazione delle minacce. Tali valutazioni sono fondamentali per la nuova sfida di raddoppiare l'estensione delle aree protetta entro i prossimi anni così da garantire la sopravvivenza della fauna selvatica.

List of Tables

Table 1.1 Model ranking for occupancy (ψ) and detection probability (p) of the African golden cat *Caracal aurata* detected by camera trapping in Minziro Nature Forest Reserve, Tanzania.....18

Table 1.2 Parameter estimates from the averaging of the two best supported models testing the effect of covariates on detection probability (p) and occupancy (ψ) of the African golden cat in Minziro Nature Forest Reserve.....18

Table 2.1 Number of independent events per day and naïve occupancy of domestic species (i.e., livestock, dogs, and humans) and Pallas's cat, and the number of sites where the cat was detected. Data were collected using cameras in the 4 study areas in western Mongolia, 2015–2019.....31

Table 2.2 Parameter estimates from model-averaging of the best-supported models for the occupancy (ψ) and detection (p) probability of livestock in western Mongolia, 2015–2019. For the assessment across the 4 study areas, we considered all livestock, humans, and dogs as a single category, while for the focal area assessment, we considered small- and large-sized livestock separately.....32

Table 2.3 Summary of the single-species single-season occupancy models of the Pallas's cat (*Otocolobus manul*) across the four study areas and for the focal area (i.e., Khork Serkh Strictly Protected Area), in western Mongolia. Ranking was carried out using the Akaike Information Criterion (AIC), with models having Δ AIC < 2.00 considered equally best-supported (bold). Only the ten top models and the null models are shown.....33

Table 2.4 Parameter estimates from the averaging of the best-supported models for both across the four study areas and focal area assessment of the Pallas's cat (*Otocolobus manul*) for the occupancy (ψ) and detection (p) probability in western Mongolia.....35

Table 3.1 Results of the occupancy models for the Sanje mangabey (*Cercocebus sanjei*) in two forests, Mwanihana and Uzungwa Scarp Nature Reserve in Tanzania,

detected by camera-traps in 2017. Model ranking is based on the Akaike Information Criterion (AIC), with models having ΔAIC < 2.00 considered best-supported (bold). Table also display the R-squared of each model. Table displays the top five model and the null model……52

Table 3.2 Parameter estimates from the averaging of the best-supported models of Sanje mangabey (*Cercocebus sanjei*). Table displays occupancy (ψ) and detection (p) probability estimates across the two study areas (Mwanihana forest and Uzungwa Scarp Nature Reserve) in Tanzania……52

Table 3.3 Estimated group density, number of groups, population size and individual density of the Sanje mangabey (*Cercocebus sanjei*) in Mwanihana forest (MW) and Uzungwa Scarp Nature Reserve (USNR), Tanzania……54

List of Figures

Fig. 1.1 Minziro Nature Forest Reserve, Tanzania, with camera trap sites and records of the African golden cat Caracal aurata……14

Fig. 1.2 African golden cat *Caracal aurata* photo-trapped in Minziro Nature Forest Reserve, Tanzania. The survey revealed golden/brown-reddish (a, c) and dark/light grey (b, d) morphotypes……16

Fig. 1.3 Estimated occupancy (SE in dotted lines) of the African golden cat in Minziro Nature Forest Reserve in relation to distance from the closest forest edge……17

Fig. 2.1 Map of western Mongolia with the four study areas: Siilkhem B National Park (sampled in 2015), Tavan Bogd National Park (2017), Khork Serkh Strictly Protected Area (2018), and Sutai Massif (2019). Pallas's cat distribution range is from the IUCN Red List website (Ross et al., 2020)……25

Fig. 2.2 Estimated occupancy probability (ψ) of the Pallas's cat in western Mongolia (spring 2015 – 2019) in relation to: A) the study areas, B) the three main habitat types, and C) the occupancy of domestic animals (SE in grey). Values are in probability scale and derived from the averaging of the best-supported models……34

Fig. 2.3 Occupancy probability distribution of the Pallas's cat (A) in Khork Serkh Strictly Protected Area (2018), western Mongolia. Circles indicate occupancy probability, with larger ones representing higher values. Occupancy was modelled as a function of: B) the occupancy of small-sized domestic animals (i.e., sheep and goats), C) habitat type, D) slope, and E) relative abundance of prey species……34

Fig. 2.4 Temporal overlap in activity between the Pallas's cat and livestock in western Mongolia (2015 – 2019). The figure displays the diel activity pattern of the felid (A) at sites where livestock was detected (111 sites, 63 cat's detections) and (B) at sites where livestock was not detected (105 sites, 44 cat's detections). Both Pallas's cat activity curves were plotted against the diel activity pattern of livestock across the whole area, to point out the felid's variation in activity pattern. The coefficient (Δ) assessed the degree of overlap between the diel activity curves of the two taxa (1 = complete overlap, 0 = no overlap)……36

Figure 3.1 Map of the study area in Tanzania (central panel and inset), with the two forest blocks (Mwanihana forest and Uzungwa Scarp Nature Reserve) where the Sanje mangabey (*Cercocebus sanjei*) occurs (left and right panels). In these two forests, black and white dots represent camera-trap locations (white are those where mangabeys were detected), whereas crosses represent the listening posts where acoustic surveys were made (yellow are those where mangabeys were detected)....46

Fig 3.2 Bivariate predictions of estimated occupancy probability with SE from the averaging of the predictions of the three best-supported models for the Sanje mangabey (*Cercocebus sanjei*) in relation to: a) elevation, b) forest type, and c) distance to the closest forest border. Additionally, d) shows the boxplot for site-specific occupancy values divided by forest.....51

Fig 3.3 Relationship between occupancy and acoustic density estimates derived in Mwanihana (left, N = 13 listening posts) and Uzungwa Scarp forests (right, N = 9), Tanzania, where the Sanje mangabey (*Cercocebus sanjei*) was studied. The graph represents the result of a Generalized Linear Models with Gamma distribution and log-link function. Shaded area represents SE.....53

Fig 3.4 Maps of the predicted group density of the Sanje mangabey (*Cercocebus sanjei*) in Mwanihana forest (left) and Uzungwa Scarp forest (right), Tanzania.....54

Fig 4.1 Map of the four study areas in northern and central Italy monitored with systematic camera trapping in 2020: 1) Parco Naturale Adamello Brenta, 2) Parco Naturale Paneveggio Pale di San Martino, 3) Parco Naturale Regionale delle Alpi Apuane, 4) Parco Naturale Nazionale delle Foreste Casentinesi. Protected areas are shown in green, while sampling sites are indicated by blue dots.....66

Fig 4.2 Relative abundance Index of humans (vehicles included), domestic animals and wild mammals, ordered from the most to the least detected for each area. Species identity is indicated by its silhouette and scientific name. Data derive from systematic camera trapping in four protected areas of central and northern Italy during 2020: 1) Parco Naturale Adamello Brenta, 2) Parco Naturale Paneveggio Pale di San Martino, 3) Parco Naturale Regionale delle Alpi Apuane, 4) Parco Nazionale delle Foreste Casentinesi.....73

Fig 4.3 Effects of the rate of human passage, distance from towns, elevation, and terrain slope on the number of events of wild mammals estimated with a multi-region community model. Caterpillar plots depict beta coefficients of diurnal (red),

crepuscular (orange) and nocturnal (blue) events in relation to human passage, distance from closest town, elevation, and terrain slope. Points represent the median of the full posterior distribution, and error bars represent the 90% BCI. Data derive from systematic camera trapping in four protected areas of central and northern Italy during 2020……74

Fig 4.4 Effects of the rate of human passage on the number of events at meta-community (central panel) and species level (outer panels). Stacked bar plots show the predicted number of average diurnal (red), crepuscular (orange) and nocturnal (blue) events of each species for different rates of human passage (human RAI). The species are indicated by their silhouettes and are ordered according to body mass from top left to bottom right as follows: *Ursus arctos, Cervus elaphus, Sus scrofa, Dama dama, Ovis musimon, Rupicapra rupicapra, Canis lupus, Capreolus capreolus, Meles meles, Hystrix cristata, Felis silvestris, Vulpes vulpes, Procyon lotor* (allochthonous species), *Lepus europaeus, Oryctolagus cuniculus, Martes spp., Mustela putorius, Sciurus vulgaris*. Data derive from systematic camera trapping in four protected areas of central and northern Italy during 2020, modeled through a multi-region community model……75

Fig 4.5 Post-hoc analysis of the coefficient estimates of the three time period: diurnal events (red), crepuscular events (orange) and nocturnal events (blue). From top left: regression of the coefficient estimates for the effect of human passage (Panel A) and distance from the closest town (Panel B) in relation to the body mass of mammals (logarithmic), boxplot of coefficient estimates according of human passage (Panel C) and distance from the closest town (Panel D) in relation to the trophic guild. The dotted horizontal line represents a coefficient equal to zero. Data derive from systematic camera trapping in four protected areas of central and northern Italy during 2020, modeled through a multi-region community model……78

Fig 5.1 Map of the 37 tropical forests in the *TherioTrop* database. Inset maps represent two protected areas embedded in contrasting landscapes: intact one with low human density (left) and anthropogenic one with high human density (right). Green areas in insert maps represent PA boundaries. The bottom chart shows estimated species richness (black dots) and the observed number of detected species with camera-traps (blue triangles) in each forest, which are ordered by increasing human density. See Suppl. Table E.2 for the list of site codes……90

Fig 5.2 Hypothesized processes for the influence of forest cover and human density in the landscape on species richness and community occupancy (H1 and H4) and for

the influence of forest configuration in the landscape (i.e., fragmentation and connectivity of remnant forest patches) and proximity to settlements on community occupancy (H2 and H3). Landscape is defined as the area extending 50 km from protected areas borders (DeFries et al 2005)……91

Fig 5.3 Results of predictors of estimated mammalian species richness from the multi-region, multi-species occupancy model applied to the 37 study areas across the tropics. a, standardized beta coefficients for the effects of predictors, with human density and forest cover measured on a buffer extending 50 km around the sampled area. Points indicate median of the full posterior distribution. Solid blue lines represent significant effect with 90% Bayesian Credible Interval (BCI) that do not overlap 0 (dashed vertical line). Closed grey points represent 50% BCI that do not include 0, while open grey points indicate that 50% BCI overlaps 0. b, bivariate plots of predicted species richness in relation to increasing human density, and c, increasing forest area availability (bottom). Grey shaded areas indicate 90% BCI…92

Fig 5.4 Results of predictors of estimated community occupancy probability (ψ) from the multi-region, multi-species occupancy model applied to the 37 study areas across the tropics. a, standardized coefficients for the effects of predictors, with human density, the forest patch size and forest cover measured on a buffer extending 50 km around the sampled area. Points indicate median of the full posterior distribution. Solid blue lines represent significant effect with 90% Bayesian Credible Interval (BCI) that do not overlap 0 (dashed vertical line). Closed grey points represent 50% BCI that do not include 0, while open grey points indicate that 50% BCI overlaps 0. b, bivariate plots of the predicted community occupancy probability in relation to increasing forest patch size, and c, increasing forest cover. Grey shaded areas indicate 90% BCI……93

Contents

Acknowledgements.....i

Summary.....ii

Sommario.....v

List of Tables.....viii

List of Figures.....x

General Introduction.....1

Aim and scope.....6

PART I: Assessing mammal populations at local scale

Chapter 1 The African golden cat *Caracal aurata* in Tanzania: first record and vulnerability assessment.....11

Abstract.....12

1.1 Introduction.....13

1.2 Methods.....14

1.3 Results.....15

1.4 Discussion.....17

1.5 Acknowledgements.....20

Chapter 2 Spatio-temporal occurrence of a neglected small cat in the Mongolian Altai and its sensitivity to livestock husbandry.....21

Abstract.....22

2.1 Introduction.....23

2.2 Methods.....24

2.2.1 Study area.....24

2.2.2 Motion-Sensitive Cameras.....26

2.2.3 Covariates.....27

2.2.4 Occupancy Modeling.....28

2.2.5 Analysis of Diel Activity Pattern.....29

2.3 Results.....30

2.4 Discussion.....36

2.5 Management Implications.....40

2.6 Acknowledgements.....40

Chapter 3 Calibrating occupancy to density estimations to assess abundance and vulnerability of a threatened primate in Tanzania.....41

Abstract……42
3.1 Introduction……43
3.2 Methods……45
3.2.1 Study area……45
3.2.2 Data collection: acoustic and camera-trapping surveys……46
3.2.3 Data collection: covariates……47
3.2.4 Data analyses……48
3.2.4.1 Group density estimates……48
3.2.4.2 Occupancy modeling……48
3.2.4.3 Density to occupancy calibration……50
2.3 Results……50
3.4 Discussion……55
3.5 Acknowledgements……58

PART II: Studying mammal communities at larger scale

Chapter 4 Consistent spatio-temporal responses of mammalian communities to human frequentation across Italian protected areas……60
Abstract……61
4.1 Introduction……62
4.2 Methods……65
4.2.1 Study area……65
4.2.2 Data collection……67
4.2.3 Covariates……68
3.2.4 Analyses……69
4.3 Results……72
4.4 Discussion……79
4.5 Acknowledgements……84

Chapter 5 Widespread anthropogenic extinction filtering of tropical forest mammals even within protected areas……85
Abstract……86
5.1 Introduction……87
5.2 Results……91
5.3 Discussion……94
5.4 Methods……97
5.4.1 Study areas, camera trapping and *Theriotrop* dataset……97
5.4.2 Covariates……98
5.4.3 Model formulation……99
5.5 Acknowledgements……101

General Conclusions……103

Appendix A. The African golden cat *Caracal aurata* in Tanzania: first record and vulnerability assessment……109

Appendix B. Spatio-temporal occurrence of a neglected small cat in the Mongolian Altai and its sensitivity to livestock husbandry……111

Appendix C. Calibrating occupancy to density estimations to assess abundance and vulnerability of a threatened primate in Tanzania……114

Appendix D. Consistent spatio-temporal responses of mammalian communities to human frequentation across Italian protected areas……117

D.1 JAGS code……117

Appendix E. Widespread anthropogenic extinction filtering of tropical forest mammals even within protected areas……133

E.1 Complete list of co-authors and *Theriotrop* owners……133

E.2 Covariates description and extraction……133

E.3 Nimble code and model specification……135

Bibliography……151

PDFs published articles……181

General Introduction

Biosphere integrity, i.e., biodiversity and its inherent components of taxonomic, functional and genetic diversity, is one of the nine planetary boundaries sustaining human life on Earth (Steffen et al. 2015). However, a critical decline of specie is currently taking place, such that rates of species loss are comparable with those of previous Mass Extinctions (Barnosky et al 2011; Ceballos et al 2015). The current defaunation is a critical phenomenon in the proposed Anthropocene epoch (Steffen et al. 2011, Dirzo et al. 2014; Andermann et al. 2020), and the root cause is the escalating increase of the human population (McKinney 2001), the consequent demand for greater conversion of natural environments into arable lands and infrastructures (Haddad et al 2015), and the complex web of human activities (McKinney 2001). The Millennium Ecosystem Assessment (2005) estimated that the environmental changes in the last 50 years caused by human activities have been quicker and more severe compared to any other time in human history such that the risk of abrupt and irreversible ecosystem-level changes is rising. Nowadays, 80% of the terrestrial biosphere has suffered alterations (Ellis et al. 2021) and it is estimated that only 10% of the Earth's surface will remain unaltered by 2050 (WWF 2018). While the detrimental effect caused by anthropogenic activities is pervasive across the globe, tropical forests are one of the most affected biomes, and where therefore extinction risk is the greatest (Pimm et al. 2014).

Hitherto, more than 900 species across multiple taxa have disappeared globally since 1500 (IUCN 2022), and 20% of all vertebrates are at risk of extinction in the wild (Hoffmann et al. 2010). Mammals are among the most affected orders (Chapin et al. 2000, Ceballos et al. 2015), with a quarter of the species that are threatened with extinction, half are declining - including least-concern ones, and

many species are suffering drastic range shrinkage (Gilbert et al. 2008, Ceballos et al 2017, WWF 2020, Pacifici et al. 2020a). Moreover, mammals' decline in richness and abundance has deep detrimental effects on ecosystem functioning and human well-being (Diaz et al. 2006; Cardinale et al. 2012). This is due to the critical ecological roles that mammals perform, such as landscape engineering, pest control, seed dispersal and regulation of trophic dynamics (Lacher et al. 2019).

Despite these alarming patterns, the overall biodiversity decline would have been significantly worse without conservation actions (Hoffmann et al. 2010), whereby the establishment of protected areas (PAs) is the most critical strategy to stall species' decline. Today, many mammal species persist solely within protected areas especially across the tropics (Pacifici et al. 2020b), and the need to preserve natural habitats is more urgent than ever. However, despite a number of global conservation projects such as the "half-earth" (Wilson 2013) and the "30 by 30" (Dinesteirn et al. 2019), today only 15% of the total land's surface is protected, which falls short even for the Aichi Target previously set. Furthermore, while wildlife conservation relies heavily on PAs, conserved areas are not consistently chosen to maximize conservation needs, given that they partially consist of marginal lands of low priority for human use (Joppa and Pfaff 2009). Additionally, species loss may extend also within well-protected PAs due to human influence around and within the protected borders (Laurence et al. 2012).

With most of the 2020 Aichi goals missed or only partially achieved, the post-2020 Global Biodiversity Framework of the UN Convention on Biological Diversity aims to protect 30% of land by 2030 (Kunming-Montreal Global Biodiversity Framework 2022) calls for urgent action to significantly halt species loss. A critical step towards achieving this goal is the scientific monitoring of mammals, both at the species and community level, to understand their responses to human disturbance and habitat degradation and eventually promote targeted conservation actions. However, reliable population and community assessments are only possible by using robust data, which in turn will set the ground for appropriate short-term conservation actions and future strategies. Hence, the requirement of consistent

methodologies for biological monitoring applicable at a broad spatial and temporal scale has brought the spotlight on remote monitoring techniques.

In this context, with countless independent projects running at a global scale and given the potential for methodological standardization, the use of camera traps (CTs) has become a keystone of wildlife monitoring (O'Brien et al. 2010, Ahumada et al. 2013). Camera traps are a non-invasive, automatically triggered survey tool for capturing wild animals on photos or films with minimum human interference and disturbance to wildlife (Rovero et al. 2010). The major strength of modern camera devices is their ability to remain active in the field over long periods, continuously detecting whatever passes in front of their lens. Furthermore, the production of objective records is an additional highlight compared to other survey techniques. Camera traps are cost- and effort-efficient; their autonomy and automatism readily allow for the accumulation of data, making them suitable for intensive and prolonged surveys across large and remote areas (Wearn and Glover-Kapfer 2017). They are an appropriate tool to study mammals and allow to obtain robust data also on rare and elusive species, otherwise difficult to detect (Linkie et al. 2013, Brassine and Parker 2015). Their use has exponentially increased in the last decades and successfully contributed to a range of ecological, behavioural and conservation studies (Rovero et al. 2013, Rovero and Kays 2021), including population assessments and study of community structure (Wearn and Glover-Kapfer 2017).

Together with effective detection tools, robust sampling designs are also equally important, since the location of the camera stations, their number, spacing and duration of the survey are all aspects that affect the process under investigation, as well as the strength of the statistical inference (Burton et al. 2015). Hence, a systematic design following a regular grid, with a camera deployed within each cell and collecting detections at multiple sites for multiple consecutive days, will allow the gaining of sound data for the whole mammal community. Furthermore, the spatial and temporal replicates of the survey will make it possible to estimate a multitude of state variables, whose results would be more precise than the ones obtained with a

random design since the variance in detections across sites would be lower (Burton et al. 2015). Additionally, compared to opportunistic design, results can be inferred over the entire study area. At the same time, a standardised protocol will allow data comparisons across multiple areas, setting the ground for planetary-scale monitoring networks and consistent macroecological studies (e.g., Beaudrot et al. 2016; Rovero et al. 2020). A practical application of such effort is the TEAM Network project (Tropical Ecology and Monitoring) which systematically collect camera trapping data of medium-to-large wild mammals across 16 areas in tropical forests (Rovero and Ahumada 2017).

In parallel, robust analytical frameworks contribute to gaining reliable information on the status of species and communities, with species distribution models that have been used to guide conservation practices (Guisan and Zimmermann 2000). However, many of them do not account for imperfect detection (Kery 2002, Kery and Schmidt 2008), namely the probability that a species is recorded when present (MacKenzie et al. 2002), leading to the inaccurate classification of occupied locations as empty. Hence, failing to consider imperfect detection may lead to severe misinterpretation of data (Pfaller et al. 2013; Guillera-Arroita et al. 2014), ultimately generating biased outcomes that can jeopardize the process of conservation decision-making. Alternatively, occupancy models can accommodate the observational process, correcting for variations in detection probability (p). Occupancy (ψ, probability of site-use) can be considered as a proxy of abundance and distribution, and a cost-efficient alternative metric for wildlife monitoring, given it works with detection/non-detection data and does not require the individual-level identification of animals (MacKenzie et al. 2002). For all these reasons and for its flexibility in accommodating variables of interest, the occupancy framework has gained great popularity in ecology. Therefore, the blend of remote, non-invasive, broad-spectrum biodiversity monitoring techniques, as camera trapping, with statistical models assessing species presence and distribution that account for imperfect detection, as occupancy, has become a compelling tool to predict mammals' response in relation to environmental and anthropogenic

variables.

Such combination of detection technology and analytical tool allowed the development of inferential studies on animal ecology, at both population and community level, which contributes to providing critical information on species distribution and responses to threats for conservation purposes. This is indeed the niche in which my thesis has developed.

Aim and Scope

All chapters of my thesis address various forms of anthropogenic impact on wildlife to assess the potential vulnerability of mammal populations and communities in protected areas across different biomes and spatial scales, with a specific focus on tropical forests. For my thesis, I focused on mammals not only for their wide taxonomic diversity and the broad range of ecological niches they exploit but also for the important ecological roles they perform and their great sensitivity to human-induced environmental changes (Ceballos and Ehrlich 2002, Magioli et al. 2021). For these reasons, mammals can act as ecosystem indicators of what is allegedly happening to the rest of the biota.

On this ground, the overall aim of my thesis is to understand how the human presence, together with its local and broader impact on the landscape, affects the spatial distribution of wild mammals. The unifying thread that underlines this overarching goal is the use of systematic and standardised camera trapping as the detection method, occupancy models as the framework of analyses, and occupancy probability (ψ) as the main state variable.

It is well acknowledged that understanding species' presence and distribution, as well as their responses to a set of biotic and abiotic stressors, is critical knowledge for wildlife conservation (Kéry et al. 2013). However, data paucity hampers the ability to access reliable information on population status, preventing to set adequate management strategies and conservation goals. This applies particularly to rare species, which are generally characterised by a relatively low density and narrow distribution and face the highest extinction risk (Loiseau et al. 2020). In this context, the first three chapters (part I) investigate specific populations of single target

species that are elusive and rare, that live in remote areas and that are typically difficult to be detected in the wild. These cryptic species are of conservation concerns, overlooked, with limited quantitate knowledge and frequently suffering data sparsity. Hence, populations could allegedly face decline due to anthropogenic influence without adequate knowledge to manage for threat reduction.

Thus, in Chapter 1, I underpinned the effectiveness of camera trapping as a conservation tool and its efficacy in detecting the presence of rare species in an area of unique biodiversity and conservation value. Hence, a well-designed systematic protocol allowed to detect the first population of African golden cat (*Caracal aurata*) in Tanzania (Rovero et al. 2019), the least-known and truly forest-dependent felid in Africa (Bahaa-El-Din et al., 2015a). By using presence/absence data and occupancy analyses, the main objective was to assess the population status of this species and its potential vulnerability to human encroachment in the Nature Reserve.

In Chapter 2, I used bycatch data from systematic and standardised camera trapping projects across western Mongolia to study the neglected Pallas's cat (*Otocolobus manul*). Small cats are indeed understudied, with minimum funding for conservation and suffer from poor quantitative knowledge (Brodie 2009). The aim was to use occupancy probability of the Pallas's cat to understand its habitat selection preferences and relationship with livestock husbandry. In fact, although Mongolia has a very low human density, the presence of livestock is ubiquitous also within strictly protected areas, with over 2 million head of livestock roaming in the steppe (World Bank 2018, National Statistics Office of Mongolia 2020). Here, I aimed at estimating if the presence of herds (particularly sheep and goats) triggers spatial segregation of the cat preventing the use of suitable habitats or if temporal shifts in activity patterns could promote coexistence.

In Chapter 3, I developed an innovative framework for density estimation, by coupling detection/non-detection data from camera trapping and density data from acoustic survey. Thus, I carried out the first comprehensive and quantitative population assessment of the IUCN-endangered Sanje mangabey (*Cercocebus sanjei*), an elusive primate endemic to only two disjoint forest blocks in the Udzungwa

Mountains of Tanzania (Ehardt et al. 2005; Rovero et al. 2006; McCabe et al. 2019). Main goals were to assess habitat preferences, potential vulnerability to human presence and forest exploitation, and in particular to estimate spatially-explicit group density and population size across the entire distribution range.

Furthermore, in the face of the current biodiversity loss and species decline, standardised wildlife monitoring and robust data are critical for conservation concerns to understand larger- and global-scale spatial patterns of the vulnerability of mammal communities. Besides local population assessments, the study of threats to the entire mammalian assemblage bears important ecosystem-level implications due to the ecological roles that mammals perform (Lacher et al. 2019). In this perspective, camera trapping is an efficient technology with the potential to create a large-scale monitoring network (Steenweg et al. 2017), while the conceptual clarity and flexibility of Bayesian analyses allow to fit also complex hierarchical models (Gelman and Hill 2006), like the multi-species multi-region occupancy ones. In this context, the last two chapters of my thesis (part II) focus on the study of mammal communities at a larger scale and on how various facets of communities' ecology respond to anthropogenic disturbance. The study of community ecology becomes important to understand patterns of changes beyond single-species dynamics. Research at the community level, possibly at a larger spatial scale, can indeed inform on possible common threats and comparable adaptative mechanisms to disturbance providing a broader overview of the anthropogenic impact on mammals.

In Chapter 4, by creating a network of protected areas in the Italian Alps and Apennines systematically monitored with camera traps, we developed a new framework to estimate in one single hierarchical model the spatial and temporal influence of human presence on mammal communities across four parks. The main objective was to understand if human frequentation and proximity to cities were affecting the spatial distribution of the whole mammal group (Suraci et al. 2019) or if the human influence in the reserves was triggering any coping mechanisms by shifting the mammals' temporal behaviour (Gaynor et al. 2018).

In Chapter 5, I investigated global patterns of mammal defaunation, by

assessing variations in species richness and community occupancy to anthropogenic impact across pan-tropical forests. To this purpose, I established *Theriotrop*, a new compilation of standardised camera trapping data collected systematically across three continents. I used a Bayesian multi-species multi-region model that considers imperfect detection to estimate the two metrics simultaneously in relation to forest cover, habitat configuration, human density, and proximity to settlements. The aim was to assess how mammal species richness and community occupancy within protected areas may vary in relation to anthropogenic pressures and environmental changes in the broader landscape surrounding the study forests.

Finally, I present the general conclusions of my thesis, highlighting the major contributions of the different topics to the current knowledge (Chapters 1 - 5) and the potential practical applications of my project. Additional material for every chapter is available in the appendices, while I also provide the PDFs of the published manuscripts at the back of the dissertation, with manuscript reported in Chapter 4 and Chapter 5 that are in preparation and nearing submission, respectively, at the time of writing.

PART I

Assessing mammals' populations at the local scale

Chapter 1

The African golden cat *Caracal aurata* in Tanzania: first record and vulnerability assessment

Greco, I. & Rovero, F.

Oryx – The International Journal of Conservation

55(2), 212-215

DOI: doi.org/10.1017/S003060532000040X

Abstract

We report on the first population found in Tanzania of the Vulnerable African golden cat *Caracal aurata*, extending its documented range c. 200 km to the south and south-east. This is one of the least-known and truly forest-dependent felines in Africa, ranging across the Guinea–Congolian forest block. We recorded the new population in Minziro Nature Forest Reserve, north-west Tanzania, during a 3-month survey in 2018. We deployed 70 camera traps on a regular grid and obtained 33 detection events of the golden cat at 26% of sites, with a minimum of 10 individuals across 257 km^2. We estimated occupancy and detection probability and modelled these in relation to the distance of sampling sites to the forest edge, which coincides with both the Reserve boundary and proximity to human settlements surrounding the Reserve. Mean estimated occupancy was 0.41 ± 0.12 SE (average detectability = 0.13 ± 0.05 SE), with occupancy increasing significantly with distance from the forest edge. Detectability did not vary significantly with distance from the forest edge, but increased for camera models that had a faster trigger time. Our findings add to the scant data available for this species. It appears threatened by human activity, which we recorded both outside and within the Reserve, and the presence of the species indicates Minziro Forest is an important site for its conservation.

Keywords: African golden cat, camera trapping, *Caracal aurata*, edge effect, Minziro, occupancy modelling, Tanzania

1.1 INTRODUCTION

The African golden cat *Caracal aurata* is an elusive, medium-sized felid categorized as Vulnerable on the IUCN Red List, regarded as the least-known wildcat in Africa and one of the least-studied felines (Bahaa-El-Din et al. 2015b). As the only truly forest-dwelling feline in Africa, it is threatened by deforestation, habitat destruction and snaring (Bahaa-El-Din et al. 2016). Although the population is believed to be decreasing (Bahaa-El-Din et al. 2015a), robust knowledge of the species is scant. The species occurs in West and Central Africa, with an easternmost population recently confirmed in Kenya from a roadkill in the Aberdare Mountains (Hatfield et al. 2019). Western Tanzania has been regarded as potentially suitable for the species (Butynski et al. 2012), but no records have previously been reported. Here, we present the first record and results of habitat association modelling for a population of golden cat found in Tanzania in the course of a biodiversity survey in Minziro Nature Forest Reserve. We used a camera-trap survey, and occupancy analysis, to determine the distribution of the golden cat and its association with habitat edges and human disturbance.

1.2 METHODS

Camera trapping was conducted in Minziro Nature Forest Reserve, north-west Tanzania, during 3 October – 28 December 2018. Established in 2016 and formerly a reserve with lower protection status, it comprises 257 km^2 of flat, moist forest at a mean altitude of 1,150 m (Rovero et al. 2019). The northern boundary is the country border, merging with the Sango Bay Forest Reserve in Uganda. All other boundaries border human-modified habitat with settlements, plantations and patches of drier woodland and grassland (Fig. 1.1), with Kagera river and seasonal flooding to the east, and a paved road and several villages to the west. The Reserve is the

easternmost extension in Tanzania of the Congo–Guinea forest, with fauna typical of West and Central Africa. The Reserve is heavily disturbed, with illegal logging,

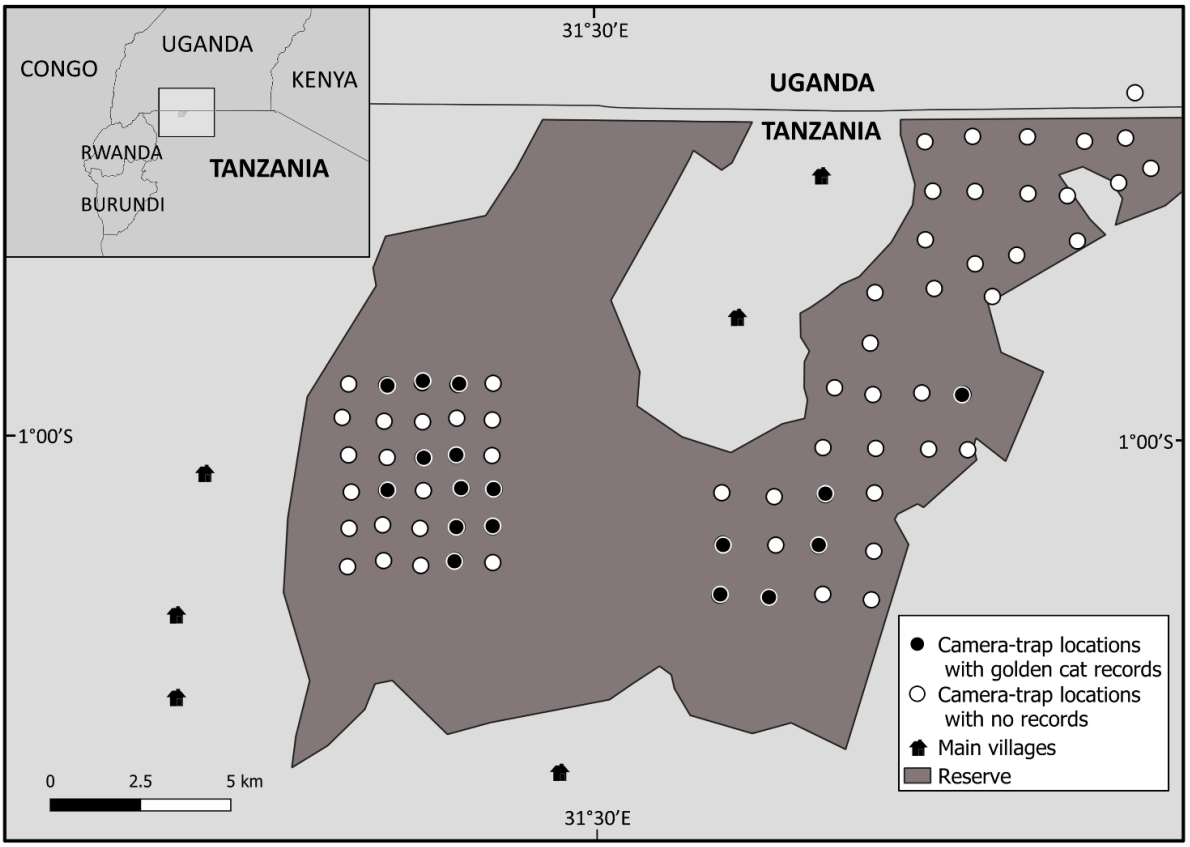

burning, livestock grazing and fishing occurring in the area (Rovero et al. 2019). We found evidence of bushmeat hunting: we encountered hunters with dogs on one occasion and found a number of snares, presumably set for ungulates but potentially a threat to the golden cat and other species.

Fig. 1.1 Minziro Nature Forest Reserve, Tanzania, with camera trap sites and records of the African golden cat *Caracal aurata*.

We surveyed 70 sites across the Reserve using a regular grid of 1–2 km^2 cell size, firstly surveying 40 camera sites and then 30 (Fig. 1.1), for a minimum of 30 days (mean 32 days) each. We used Browning (Morgan, USA), Cuddleback (Green Bay, USA) and UOVision (Shenzhen, China) cameras, with infrared flash and motion-activated sensor, 0.15 seconds trigger speed for Browning, and 1–2 seconds Cuddleback and UOVision, attached to trees at c. 50 cm from the ground, facing a

presumed animal trail and without baits.

The survey yielded 2,219 camera days from 68 camera traps (two were stolen). We annotated images using *Wild.ID* and ran analyses using *R 3.6* (R Core Team 2019). We calculated the detection of the golden cat events per day and used them to derive a relative abundance index. We plotted the species' daily activity pattern using hourly events. We then used single-season occupancy modelling (MacKenzie et al. 2002) to estimate golden cat occupancy (ψ) and detection probability (p) and their association with presumed covariates. We arranged golden cat detections/non-detections into a site-by-sampling occasion matrix; we chose 5 days as the resolution of the occasions as with poorly detected species this provides better estimation of detectability, and hence occupancy (Rovero & Spitale 2016). We built parsimonious models using the distance from each site to the closest Reserve border (i.e., forest edge) as a covariate. We derived these distances using QGIS (QGis Development Team 2019) and a 1:100,000 scale map. Based on our survey of human disturbance, we considered greater distance to the border as a proxy for increasing habitat quality and decreasing human disturbance. We assumed that both ψ and p increase with distance to border. For detection probability we also considered that camera trap model could potentially influence detection. Using *unmarked* (Fiske et al. 2019), we built all model combinations and ranked them according to the Akaike Information Criterion (AIC). We considered statistically supported models with ΔAIC < 2.00 and used *AICcmodavg* (Mazerolle 2019) to average parameter estimates.

1.3 RESULTS

After discarding 3,297 blank and set-up images, camera trapping yielded 4,244 photographs of 23 species of medium to large wild mammals (Suppl. Table A.1), including 169 images of golden cats. These corresponded to 33 independent detection events of the species within 24-hour intervals at 17 sites (naïve occupancy = 0.26; Fig. 1.1). Based on individual pelage marks, we identified a minimum of 10

individuals. Pelage colouration varied from dark brown to sandy and golden (Fig. 1.2). Animals were mainly active at night, with activity peaking at 19.00, 22.00 and 3.00, but with detections in daylight (Suppl. Fig. A.1).

Fig. 1.2 African golden cat *Caracal aurata* photo-trapped in Minziro Nature Forest Reserve, Tanzania. The survey revealed golden/brown-reddish (a, c) and dark/light grey (b, d) morphotypes.

Based on occupancy model ranking (Table 1.1), we averaged the two most supported models, and the resultant mean estimated occupancy was 0.41 ± SE 0.12. Occupancy increased significantly with distance to the Reserve border (1.30 ± SE 0.54; Table 1.2, Fig. 1.3). Average detection probability was 0.13 ± SE 0.05 and did not vary significantly with distance to the Reserve border but did vary with camera model, with Browning cameras having significantly higher values (Suppl. Table 2).

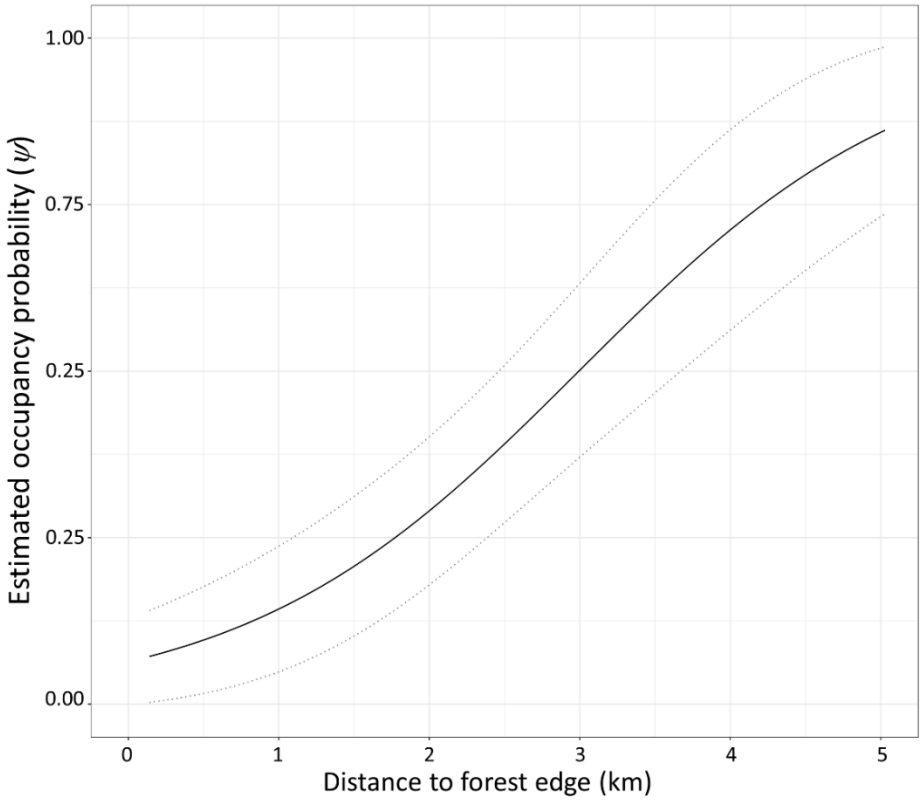

Fig. 1.3 Estimated occupancy (SE in dotted lines) of the African golden cat in Minziro Nature Forest Reserve in relation to distance from the closest forest edge.

1.4 DISCUSSION

Our findings suggest that habitat intactness and human disturbance affect golden cat occurrence, with increased occupancy with increasing distance from the Reserve border and human settlements. This matches the feline's known sensitivity to anthropogenic disturbance and its vulnerability in human-disturbed areas (Martinez Marti 2011; Bahaa-El-Din et al. 2016).

Table 1.1 Model ranking for occupancy (ψ) and detection probability (p) of the African golden cat *Caracal aurata* detected by camera trapping in Minziro Nature Forest Reserve, Tanzania.

Models	No. param	AIC[1]	Δ AIC	AIC weight	Cum. weight	R^2
p (Camera Model) ψ (Distance from closest edge)	5	198.88	0.00	0.59	0.59	0.27
p (Camera Model + Distance from closest edge) ψ (Distance from closest edge)	6	200.50	1.62	0.26	0.85	0.27
p (.) ψ (Distance from closest edge)	3	203.44	4.56	0.06	0.91	0.16
p (Distance from closest edge) ψ (Distance from closest edge)	4	204.18	5.31	0.04	0.95	0.18
p (Camera Model) ψ (.)	4	204.83	5.95	0.03	0.98	0.17
p (Camera Model + Distance from closest edge) ψ (.)	5	205.68	6.80	0.02	1.00	0.18
p (.) ψ (.)	2	212.82	13.95	<0.01	1.00	0.00
p (Distance from closest edge) ψ (.)	3	213.16	14.28	<0.01	1.00	0.03

[1]Models were ranked according to the Akaike Information Criterion (AIC), with ΔAIC < 2 considered supported.

Table 1.2 Parameter estimates from the averaging of the two best supported models testing the effect of covariates on detection probability (p) and occupancy (ψ) of the African golden cat in Minziro Nature Forest Reserve.

Model	Estimate	SE	Z	P (>|z|)
ψ Distance from closest edge	1.30	0.54	2.38	0.02
p Camera Model—Browning	1.51	0.64	2.36	0.02
p Camera Model—UOVision	–0.57	1.23	–0.47	0.64
p Distance from closest edge	–0.18	0.30	0.61	0.54

We documented a high incidence of human activities around and within the Reserve, potentially explaining the species' relatively higher occurrence in areas with dense, closed-canopy, continuous forests. A similar pattern has also been reported in Uganda (Mugerwa et al. 2012). Detection probability was greater with faster cameras, highlighting the importance of standardizing camera models in wildlife surveys: the best performing devices increase the probability of detecting elusive species. Although not exclusively nocturnal, the golden cat activity pattern showed peaks at night, mirroring the cathemeral behaviour reported by Bahaa-El-Din et al. (2015a), with peaks in activity that may overlap with periods of low human presence and higher prey activity. The minimum number of 10 individual cats detected gives a naïve density of 4 per 100 km^2, suggesting that this population may not be as abundant as in other areas. Densities of 16 individuals per 100 km^2 have been reported in pristine habitats in Gabon, and densities similar to our estimates have been reported in highly disturbed and hunted areas (Bahaa-El-Din et al. 2016). It is possible that the presence of seasonally flooded forest and swamps, mainly on the eastern side of Minziro Nature Forest Reserve, make this habitat type suboptimal for the golden cat.

This is the first record of the little-known golden cat in Tanzania, c. 200 km east-south-east from the closest known populations in Uganda and Rwanda, potentially confirming anecdotal reports of the species in the contiguous Sango Bay Forest in Uganda in the mid-1990s (T. Davenport, pers. comm. 2019). Pelage pattern suggests the population in Tanzania may be the subspecies *Caracal aurata aurata*, with spots only on the belly and limbs (Bahaa-El-Din et al. 2015a). Given its isolation and the heavily modified habitat, we assume this population is genetically isolated, and thus Minziro Nature Forest Reserve may be an important site for the species' conservation. We also recorded the tree pangolin *Phataginus tricuspis* and giant pangolin *Smutsia gigantea*, both Endangered, and the first record in Tanzania of the fire-footed rope squirrel *Funisciurus pyrropus*. Considering the human encroachment, we detected, and ineffective law enforcement, these findings indicate the need for appropriate protection of this forest.

1.5 ACKNOWLEDGMENTS

We thank the Tanzania Commission for Science and Technology (COSTECH) and Tanzania Forest Service (TFS) for providing permission and assistance to conduct this study. We thank the reserve Conservator, Mr. Bernard Mwigulu, for critical support, along with officers Hassan Omary, Twaha Mponzi, and Alfred Mlenge. Thank to Michele Menegon for lending the Browning camera traps, and to Steven Shinyambala, Ruben Mwakisoma and Mr. Bayona for invaluable field assistance, and all other local assistants.

Chapter 2

Spatio-temporal occurrence and sensitivity to livestock husbandry of Pallas's cat in the Mongolian Altai

Greco, I., Oberosler, V., Monti, I. E., Augugliaro, C., Barashkova, A. & Rovero, F.

Journal of Wildlife Management

86:e22150

DOI: doi.org/10.1002/jwmg.22150

Abstract

Biased research and conservation efforts result in some faunal groups (e.g., small felids) being understudied, and hence these groups are often declining without adequate knowledge to manage for threat reduction. The Pallas's cat (*Otocolobus manul*) occurs across central and western Asia with declining populations and the largest population is likely in Mongolia. A potential threat to this felid is livestock encroachment across its range, including within protected areas, yet we lack a clear understanding of the impact of livestock husbandry on this cat. We used motion-sensitive camera data from 216 sites in 4 study areas in western Mongolia to study the occurrence probability of Pallas's cat in relation to habitat characteristics and occurrence of livestock and conducted a local assessment within a strictly protected area where we obtained the highest number of detections. We estimated a relatively low occupancy (0.33 ± 0.10), which is associated with sites with natural vegetation, steeper slopes, and greater prey abundance. Occupancy also increased with increasing livestock occurrence, particularly large herds of sheep and goats. Such co-occurrence was partially adjusted by diel activity segregation, presumably to limit direct encounters. Our results suggest that the preferred habitat by Pallas's cat in the study region coincides with areas encroached by livestock. The Pallas's cat's habitat is specialized and its dependence on areas that are increasingly used for grazing may eventually threaten the cat with habitat degradation, prey depletion, predation by dogs, and poisoning from pest control. Relevant conservation actions should regulate livestock encroachment within protected areas and improve grazing regimes. The Pallas's cat is an indicator species of mountainous and steppe ecosystems in central Asia; hence, further research towards the preservation of its populations would also benefit other key species across its range.

Keywords: livestock husbandry, occupancy modelling, *Otocolobus manul*, Pallas's cat, regional assessment, small cat conservation, strictly protected area.

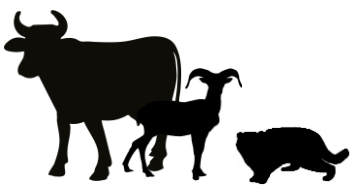

2.1 INTRODUCTION

Wildlife conservation has gained additional public attention because of the current extinction crisis (Pimm et al. 1995, Zhou et al. 2016). Research and conservation efforts are biased, with some faunal groups that are understudied and receive limited conservation funding (Lawler et al. 2006, Brodie 2009). Among mammals, the Felidae family is one of the most threatened taxa (Cardillo et al. 2004, Lamberski 2015), yet the majority of research and conservation effort has targeted the 7 species of large cats, while the 33 species of small cats have been largely overlooked (Brodie 2009). Less than 1% of conservation funding to all wild cats was devoted to small cats (Brodie 2009). Increased knowledge on the occurrence and vulnerability to changes of small cats is desirable. The use of motion-sensitive camera data from studies primarily focused on larger species or on the pool of medium to large mammals (Lama et al. 2019, Li et al. 2020, Greco and Rovero 2021) has potential to provide some of the missing data on small felids. We used data from a study on snow leopard (*Panthera uncia*) in western Mongolia to determine the spatio-temporal patterns of occurrence of the Pallas's cat (*Otocolobus manul*) and its sensitivity to environmental and anthropogenic factors, with a focus on the effects of grazing livestock.

The Pallas's cat, or manul, is a rare small felid with a vast but highly fragmented distribution in the steppes and mountainous areas of central and western Asia. Its dependence on cavities for shelter, vulnerability to aerial and terrestrial predators, and high dietary specialization underline its natural low density and patchy distribution (Ross et al. 2019*b*), making the species highly vulnerable (Purvis et al. 2000, Ross et al. 2019*b*). Although it was recently downlisted to least concern status by the International Union for Conservation of Nature (Moqanaki and Ross 2020), the species is declining (Chimed et al 2021), with many populations that are small and isolated (Ross et al. 2020). While Mongolia is the stronghold of its distribution (Ross et al. 2020), only few inferential studies on their home range, spatial distribution, and density are available (Ross et al. 2019*b*, Anile et al. 2021, Chimed et al. 2021, Greenspan and Giordano 2021). Various factors threaten the

Pallas's cat in Mongolia, including historical direct persecution for fur and medical uses (Barashkova and Smelansky 2011, Ross et al. 2020). Nonetheless, the greatest impact is thought to be caused by livestock overstocking, which causes habitat degradation due to heavy grazing (Ross et al. 2019*b*), an increase in predation by dogs (Farhadinia et al. 2016), and prey depletion due to eradication campaigns to reduce rodents (Delibes-Mateos et al. 2011, Ross et al. 2020). The number of domestic animals has exponentially increased in Mongolia in the last 20 years due to the worldwide demand for cashmere wool (National Statistical Office of Mongolia 2018). Livestock husbandry occurs throughout the country (Barashkova et al. 2007, Damdinsuren et al. 2008), and is permitted with few limitations even within protected areas according to the Mongolian Law on special protected areas (1994), with the exception of strictly protected areas (SPA). Despite the evidence that overstocking affects the Pallas's cat, quantitative knowledge on how livestock directly or indirectly affect Pallas's cat occurrence and activity pattern is scant.

We examined 4 areas across western Mongolia with different management regimes to estimate Pallas's cat occupancy (MacKenzie et al. 2002) in relation to habitat features, prey availability, and livestock grazing, and to investigate its diel activity pattern in relation to that of livestock. We hypothesized that the cat's occupancy increases at sites that are steeper, have natural vegetation cover, and higher prey availability (Ross et al. 2012); the cat's occupancy decreases at sites with higher livestock presence, or its diel activity pattern minimizes the overlap with that of domestic animals (Sévêque et al. 2020); and large herds of goats and sheep have a greater effect on cat occupancy than the small herds of free-ranging, large-sized livestock (Augugliaro et al. 2020).

2.2 METHODS

2.2.1 Study area

The Mongolian Altai Mountains extend from the northwestern part of Mongolia to the south, stretching over 900 km, and ranging 500–4,500 m above sea level. The area is

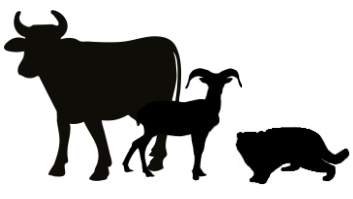

characterized by a semi-arid and cold continental climate, with long cold winters reaching temperature of −25° C in January and short summers with little precipitation averaging 45 mm in July and 20° C. The landscape is characterized by rocky, steep, and dry mountains, with high plateaus dominated by dry steppe vegetation, and valley bottoms covered by coniferous trees and sparse shrubs.

We conducted the study in 4 areas within the Altai Mountains range of Mongolia in 2015–2019 (Fig. 2.1). The Siilkhem National Park, Part B (Siilkhem B; 49°49'N, 89°44'E; 1,400 km^2) and the Tavan Bogd National Park (Tavan Bogd; 48°3'N, 88°37'E; 6,362 km^2) are located at the northwestern corner of the country, bordering Russia and China. Tavan Bogd is the largest protected area in Mongolia, with the highest elevation in the country (4,374 m) at Khuiten Uul Mountain. To the south, approximately 45 km from the Chinese border, lies the Khork Serkh (47°93'N, 90°99'E; 659 km^2), which is an SPA established in 1977, located between Bayan Olgii and Hovd provinces. The fourth area, Sutai massif (46°37'N, 93°35'E; 850 km^2), is an inland, remote and isolated area that had no legal protection when surveyed, but it was granted Nature Reserve status in 2020. All 4 study areas fell within the range of potentially suitable habitat for the Pallas's cat (Barashkova et al. 2019, Ross et al. 2020, Greenspan and Giordano 2021; Fig. 1).

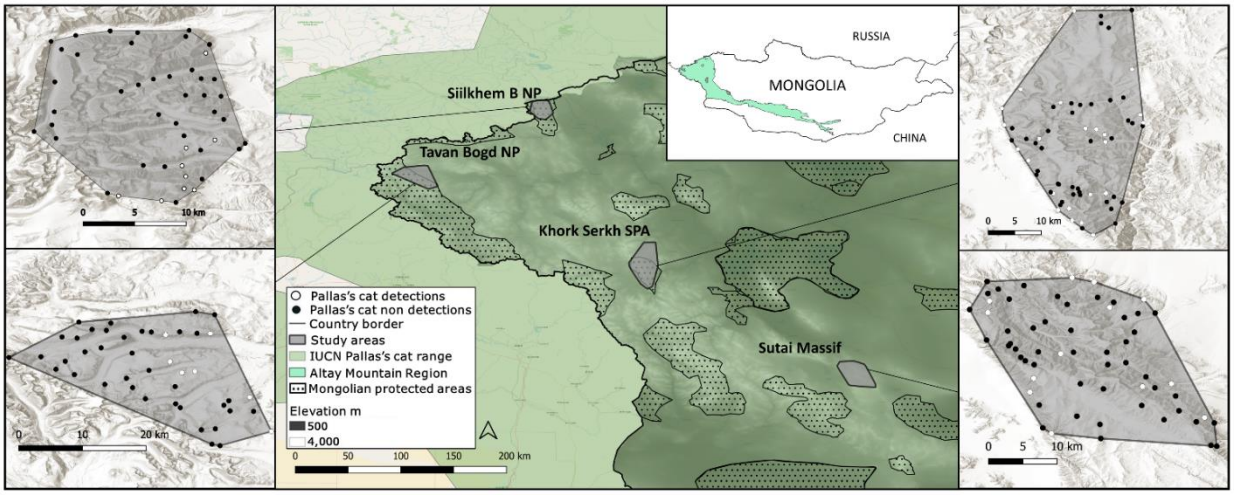

Fig. 2.1 Map of western Mongolia with the four study areas: Siilkhem B National Park (sampled in 2015), Tavan Bogd National Park (2017), Khork Serkh Strictly Protected Area (2018), and Sutai Massif (2019). Pallas's cat distribution range is from the IUCN Red List website (Ross et al., 2020).

Beside the Pallas's cat, the community of medium to large mammalian species in western Mongolia includes a variety of large and meso-carnivores including snow leopards, wolves (*Canis lupus*), wolverines (*Gulo gulo*), foxes (*Vulpes vulpes*), lynxes (*Lynx lynx*), bears (*Ursus arctos*), and mustelids. Siberian ibexes (*Capra sibirica*), argali (*Ovis ammon*), and marmots (*Marmota marmota*) are the main wild herbivores. In the study area, human density is 1.5 person/km^2, with approximately 30% of the population being pastoral nomads or semi-nomads (Dagvadorj et al. 2009, World Bank 2018). Pastoralism is the primary form of livelihood in the country, with herder families moving seasonally to different grazing areas. In the province of Bayan Olgii alone, where the first 3 study areas are located, 2.2 million head of livestock were reported in 2018, 1.9 million of which were sheep and goats (National Statistics Office of Mongolia 2020). Except for the SPAs, traditional livestock husbandry is permitted in national parks only within limited use zones. Herd size can exceed 1,000 animals (Augugliaro et al. 2020), with large livestock (e.g., cows, yaks, horses) that are usually free ranging in small clusters, while goats and sheep form large herds and are generally guarded by herders with dogs during the day and moved into corrals at night.

2.2.2 Motion-Sensitive Cameras

For every study area, we collected motion-sensitive camera data in spring (Mar – Jun) from 2015 to 2019, sampling one study area per year with the exception of 2016 (Suppl. Table B1, available in Supporting Information). We sampled 48–63 sites per study area (Suppl Table B.1) with a criterion of ≥ 1.5 km between adjacent cameras. The regular design was constrained by topography and snow cover, and hence accessibility (Fig. 2.1). Sampled sites covered 500–1,100 km^2 per study area at an elevation from 1,900 m to 3,500 m (Suppl. Table B.1). We placed motion-sensitive cameras on narrow valleys and ridges to maximize the chances to detect passing wildlife. Albeit aimed at primarily detecting snow leopards, such design and site selection proved efficient at detecting livestock and other wild mammals, (Rovero et al. 2020) including the Pallas's cat. Pallas's cat and snow leopard occur at similar altitudinal ranges in the Altai Mountains (Snow Leopard Network 2014, Moqanaki et

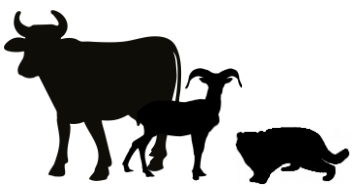

al. 2019), and display a comparable marking behavior (Allen et al. 2016). Such behavioral similarity, similar habitat preferences, and the relative homogeneity of the landscape, potentially allows the 2 species to use the same marking spots (Li et al. 2013). This further supports the effectiveness of site selection at detecting the Pallas's cat. We used heat-in-motion triggered cameras of different brands, and considered Reconyx (Holmen, WI, USA) as fast-triggered and other brands (Cuddeback, Green Bay, WI, USA; Browning, Birmingham, AL, USA; and UoVision, Shenzhen, China) as slow-triggered. We set cameras to work in continuous mode for 45–90 days (Suppl. Table B1), with no delay between photographs; we used alkaline batteries, which outperform other types at cold temperatures. We placed motion-sensitive cameras on rock piles at approximately 50 cm from the ground. Upon retrieving cameras, we annotated images using the open-source software Wild.ID (Fegraus and MacCarthy 2016). For our research, no animals were handled and permission to conduct the study was granted by the Ministry of Environment and Tourism of Mongolia (Protocol number 10/1674).

2.2.3 Covariates

We used 8 environmental and anthropogenic covariates potentially associated to Pallas's cat occupancy (ψ) and detection probability (p). We selected covariates from a broader set of candidate variables (Suppl. Table B.2, available in Supporting Information) to avoid collinearity, based on Pearson's correlation coefficient (r = 0.5 as threshold). Hence, we used the motion-sensitive camera trigger speed (fast and slow) and sampling effort (camera days) as potentially affecting detectability. We derived the relative abundance index (RAI) of the pooled domestic species (i.e., livestock), with a 15-minute interval and normalized by the sampling effort, as an indicator of the intensity of livestock passage. We used site slope, site aspect, study area, and land cover (bare ground, managed ground, natural vegetation) as predictors of occupancy, as well as the occurrence probability of livestock modeled across sampling sites. We preferred this metric over the RAI of livestock as a predictor of Pallas's cat occupancy because we assumed it more accurately measured the diffused presence of livestock across the landscape given it accounts for imperfect detection

(MacKenzie et al. 2002, MacKenzie and Royle 2005).

We conducted a second analysis using only data from Khork Serkh SPA, where we obtained the highest number of detections of both Pallas's cat and livestock, which enabled us to conduct more detailed analysis of the target species. In addition, for Khork Serkh SPA we distinguished small-sized and large-sized livestock and modeled their occupancy separately to determine the relative impact on Pallas's cat given their different herding and rearing management regimes (Augugliaro et al. 2020). The use of a greater number of motion-sensitive cameras in this area relative to other areas allowed us to also record small-sized species. Therefore, we recorded detections of voles (*Alticola* spp.) and pikas (*Ochotona* spp.) as preferred Pallas's cat prey (Ross et al. 2010*b*), and used independent photographs to compute their RAI, which we then used as a covariate of Pallas's cat occupancy.

To estimate livestock occupancy, we merged the number of domestic animals and human detections into a single category (i.e., livestock) and 2 categories (i.e., small and large livestock) for all study areas and the area sampled in 2018, respectively, and used single-season occupancy models. We modeled occupancy in relation to distance to the herders' tents or houses (i.e., ger) and elevation; we also fitted the distance to herders' houses to detectability, on the assumption that livestock herds would be more compact and hence more easily detected where closer to houses. Based on Akaike's Information Criterion (AIC) and model-averaging procedures described below, we derived occupancy estimates at motion-sensitive camera sites and used them as a covariate of Pallas's cat occupancy models. We extracted all environmental variables using the geo-processing tools available in Quantum GIS (QGIS Development Team 2019), with the land cover extracted using the GLC2000 dataset (European Commission 2003) and altitudes extracted using a 30-m digital elevation model (Jarvis et al. 2008).

2.2.4. Occupancy Modeling

We used single-season occupancy models (MacKenzie et al. 2002) to study the spatial patterns of the Pallas's cat in relation to covariates. Occupancy (ψ) is defined as the proportion of sites a species is expected to occur while accounting for imperfect

detection, expressed in probability scale. Given the limitations of estimating true occupancy from point detectors within a continuous habitat, we interpreted occupancy as the proportion of area occupied (Neilson et al. 2018). For the multiple-area analysis, we summarized detection and non-detection data in a 2-dimensional array $Y_{i,j}$ of 216 sites × 131 sampling occasions, using a resolution of 1 day. Its elements $y_{i,j}$, denoted if the cat was detected (y = 1) or undetected (y = 0) at site i during sampling occasion j. We used NA to denote that a site was not sampled during a specific occasion. We ran models using the package unmarked (Fiske and Chandler 2011) in the R environment (R Core Team 2019). We standardized continuous covariates to have mean of zero and unit variance, built models with various combinations of covariates, and included the null model (i.e., no covariates). We ranked models according to the principle of parsimony, using the AIC and considered as equally best-supported those with ΔAIC < 2 (Burnham and Anderson 2002). In the case of multiple best models, we used a model-averaging method through the package AICmodavg (Mazerolle 2019) to estimate the relative importance of the parameters and predicted occupancy and detection probabilities from the averaged models. We used the same procedure for the analysis on Khork Serkh SPA data but without using study area, and including the RAI of prey, and the occupancy of both large- and small-sized livestock as covariates. For this study area we also mapped the occupancy values estimated at the scale of motion-sensitive camera sites and derived from the averaged models.

2.2.5. Analysis of Diel Activity Pattern

To investigate activity patterns of livestock and Pallas's cat, we used a kernel density estimation function implemented in the R package overlap (Meredith and Ridout 2014), which allowed us to compute activity distribution curves for the 2 groups and carry out a pairwise comparison. Hence, we considered all the domestic species as a single category (i.e., livestock) and used the time converted in radians of each independent event (>30 min) of cats and livestock to create temporal density curves (Zimmermann et al. 2016). Specifically, to determine whether the cat shifted diel activity depending on the intensity of site use by livestock, we built 2 density curves

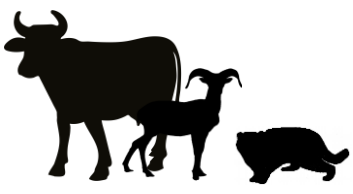

for the Pallas's cat: 1 for its detections at sites where livestock were also detected (i.e., RAI of livestock > 0) and 1 for detections at sites where livestock were not detected (RAI = 0). This resulted in 111 sites with and 105 sites without livestock occurrences, corresponding to 63 and 44 detections of Pallas's cat in the 2 subsets, respectively. Thus, to simultaneously compare Pallas's cat and livestock activities and test if the cat's diel activity shifts across the 2 scenarios, we plotted each of the cat's density curves with the one of livestock activity across the whole area. We then tested for significant differences between the 2 pairs of curves with a Wald test (Zimmermann et al. 2016). By using the R package activity (Rowcliffe et al. 2014), we computed overlap coefficient (Δ) between the 2 sets of curves, and specifically used Δ_4 for the scenario with livestock and Δ_1 for the one without livestock, in relation to the number of cat's detections (Meredith and Ridout 2014). We then computed 1,000 bootstraps iterations on the overlap values to estimate 95% confidence intervals (Ridout and Linkie 2009). The coefficient assesses the degree of overlap from 1 (complete overlap) to 0 (no overlap). Finally, we used the Welch 2-sample *t*-test to assess if the 2 generated distributions of Δ values were significantly different.

2.3 RESULTS

We obtained 1,298 images of Pallas's cats, corresponding to 107 detection events at 52 sites of the 216 sampled, between 2,223 m and 3,300 m in elevation, through 13,890 camera days across all study areas, with an average of 62 camera days per sampling unit (Tables 2.1, Suppl. Table B.1).

Table 2.1 Number of independent events per day and naïve occupancy of domestic species (i.e., livestock, dogs, and humans) and Pallas's cat, and the number of sites where the cat was detected. Data were collected using cameras in the 4 study areas in western Mongolia, 2015–2019.

Study area	Protection level	Livestock		Pallas's cat		
		Events	Naïve ψ	Events	Naïve ψ	Number of successful sites
Siilkhem B	National Park	316	0.44	11	0.19	9
Tavan Bogd	National Park	138	0.29	10	0.16	7
Khork Serkh	Strictly protected	538	0.60	62	0.37	23
Sutai Massif	Unprotected	244	0.62	24	0.21	13

We detected 7 domestic species (Suppl. Table B.3, available in Appendix B.) at 111 sites, with an overall mean estimated occurrence probability of 0.51 (Siilkhem B ψ = 0.55, Tavan Bogd ψ = 0.41, Khork Serkh SPA ψ = 0.57, Sutai Massif ψ = 0.52). The highest numbers of raw detections (538) and occupancy (0.57) of livestock were recorded at Khork Serkh SPA. Livestock occupancy (as a whole category and considering small- and large-sized livestock separately) increased at lower elevations and in proximity to the herders' camps across the 4 study areas and in the focal area (Table 2.2; Suppl. Table B.4, available in Supporting Information).

For both the overall and the focal area assessment, multiple Pallas's cat occupancy models were best-supported (Table 2.3). Pallas's cat average estimated occupancy was 0.33 ± 0.10 (SE) and was lower in Tavan Bogd compared to other study areas (Fig. 2.2A). Estimated detection probability was low (p = 0.02 ± 0.003) and increased where cameras had faster (p = 0.03 ± 0.003) than slower trigger speeds (p = 0.01 ± 0.004).

Occupancy was higher in areas with sparse and natural vegetation (ψ = 0.73 ± 0.11) than with bare and managed ground (Table 2.4; Fig. 2.2B) and it increased significantly with livestock occupancy (Table 2.4; Fig. 2.2C). In Khork Serkh, the occurrence probability of the Pallas's cat increased significantly with increasing

occupancy of sheep and goats (β = 1.25 ± 0.47, P < 0.01; Fig. 2.3; Table 2.4) and the occupancy of large livestock was not retained in the best models, showing a positive but non-significant effect. Similar to the model for all areas, the cat's occupancy increased in habitat with natural vegetation (ψ = 0.70 ± 0.12, P = 0.01). Moreover, occupancy tended to increase with increasing steepness of the terrain (β = 0.79 ± 0.42, P = 0.05), and higher relative abundance of rodents (β = 0.67 ± 0.41, P = 0.09; Table 2.4; Fig. 2.3).

Table 2.2 Parameter estimates from model-averaging of the best-supported models for the occupancy (ψ) and detection (p) probability of livestock in western Mongolia, 2015–2019. For the assessment across the 4 study areas, we considered all livestock, humans, and dogs as a single category, while for the focal area assessment, we considered small- and large-sized livestock separately.

Parameter	**Estimates**	**SE**	***Z***	***P***
Four areas, western Mongolia – livestock				
ψ Distance to closest ger	−1.11	0.50	2.21	0.03
ψ Elevation	−0.38	0.31	1.23	0.21
p Distance to closest ger	−0.62	0.18	3.41	<0.01
Focal area, Khork Serkh – small-sized livestock				
ψ Distance to closest ger	−1.92	0.64	−2.99	<0.01
ψ Elevation	−0.84	0.35	−2.36	0.02
p Distance to closest ger	−0.63	0.24	−2.66	<0.01
Focal area, Khork Serkh – large-sized livestock				
ψ Distance to closest ger	−0.57	0.49	1.16	0.25
ψ Elevation	−0.38	0.31	1.25	0.22
p Distance to closest ger	−0.45	0.23	1.96	0.04

Table 2.3 Summary of the single-species single-season occupancy models of the Pallas's cat (*Otocolobus manul*) across the four study areas and for the focal area (i.e., Khork Serkh Strictly Protected Area), in western Mongolia. Ranking was carried out using the Akaike Information Criterion (AIC), with models having Δ AIC < 2.00 considered equally best-supported (bold). Only the ten top models and the null models are shown.

Models	nPars	AIC	Δ AIC	AICwt
Across the four areas - western Mongolia				
***p* (Trigger speed) ~ *ψ* (Habitat cover + Area)**	**8**	**1145.84**	**0.00**	**5.9E-01**
***p* (Trigger speed) ~ *ψ* (Occupancy domestics + Habitat cover)**	**6**	**1147.33**	**1.50**	**2.8E-01**
p (Trigger speed) ~ *ψ* (Habitat cover)	5	1149.45	3.61	9.8E-02
p (Trigger speed) ~ *ψ* (Aspect + Area + Habitat cover)	9	1159.93	6.09	2.8E-02
p (Trigger speed) ~ *ψ* (Aspect + Habitat cover)	8	1167.31	21.48	1.3E-05
p (Trigger speed) ~ *ψ* (Aspect + Area + Habitat cover)	11	1167.83	21.99	9.9E-06
p (Trigger speed) ~ *ψ* (Slope + Area)	7	1170.19	24.36	3.1E-06
p (Trigger speed) ~ *ψ* (Slope + Habitat cover)	6	1170.27	24.43	2.9E-06
p (Trigger speed) ~ *ψ* (Aspect + Occupancy domestics + Slope + Habitat cover)	10	1171.01	25.17	2.0E-06
p (Trigger speed) ~ *ψ* (Slope + Occupancy domestics + Area)	8	1171.54	25.70	1.6E-06
p (1) ~ *ψ* (1)	2	1180.76	34.63	9.0E-09
Focal area - Khork Serkh Strictly Protected Area				
***p* (Trigger speed + RAI domestics) ~ *ψ* (Occupancy small livestock + RAI prey + Slope + Habitat cover)**	**9**	**581.12**	**0.00**	**4.3E-01**
***p* (Trigger speed + RAI domestics) ~ *ψ* (Occupancy small livestock + Slope + Habitat cover)**	**8**	**582.74**	**1.62**	**1.9E-01**
p (Trigger speed + RAI domestics) ~ *ψ* (Slope * Occupancy small livestock + Habitat cover)	9	583.98	2.86	1.0E-01
p (Trigger speed + RAI domestics) ~ *ψ* (Occupancy small livestock + Habitat cover)	7	584.70	3.58	7.2E-02
p (Trigger speed + RAI domestics) ~ *ψ* (Occupancy large livestock + Habitat cover + Slope)	8	586.05	4.93	3.7E-02
p (Trigger speed + RAI domestics) ~ *ψ* (Occupancy small livestock + Slope)	6	586.20	5.08	3.4E-02
p (Trigger speed + RAI domestics) ~ *ψ* (Slope * Occupancy small livestock)	7	586.97	5.85	2.3E-02
p (Trigger speed + RAI domestics) ~ *ψ* (Occupancy small livestock + RAI prey + Slope)	7	587.05	5.93	2.2E-02
p (Trigger speed + RAI domestics) ~ *ψ* (Occupancy large livestock + Habitat)	7	588.60	7.48	1.0E-02
p (Trigger speed + RAI domestics) ~ *ψ* (RAI prey + Habitat cover + Slope)	8	588.68	7.56	9.9E-03
p (1) ~ *ψ* (1)	2	647.60	66.48	1.6E-15

ψ = occupancy probability; p = detection probability

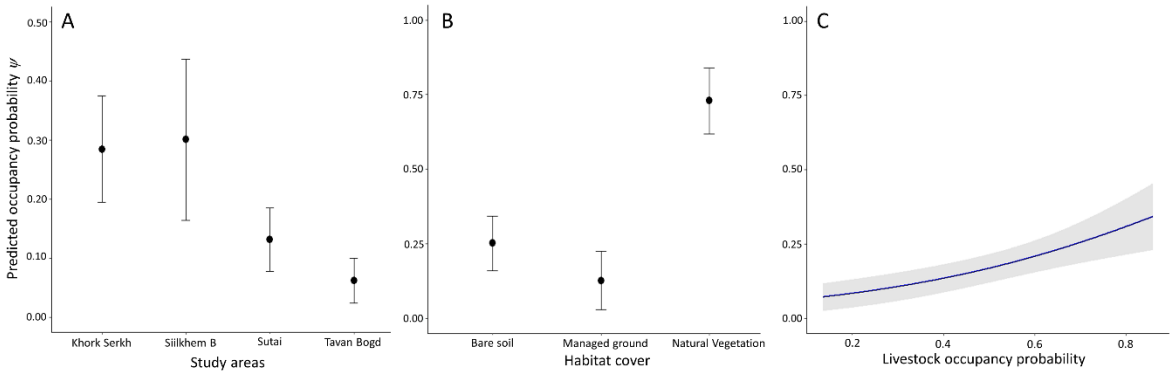

Fig. 2.2 Estimated occupancy probability (ψ) of the Pallas's cat in western Mongolia (spring 2015 – 2019) in relation to: A) the study areas, B) the three main habitat types, and C) the occupancy of domestic animals (SE in grey). Values are in probability scale and derived from the averaging of the best-supported models.

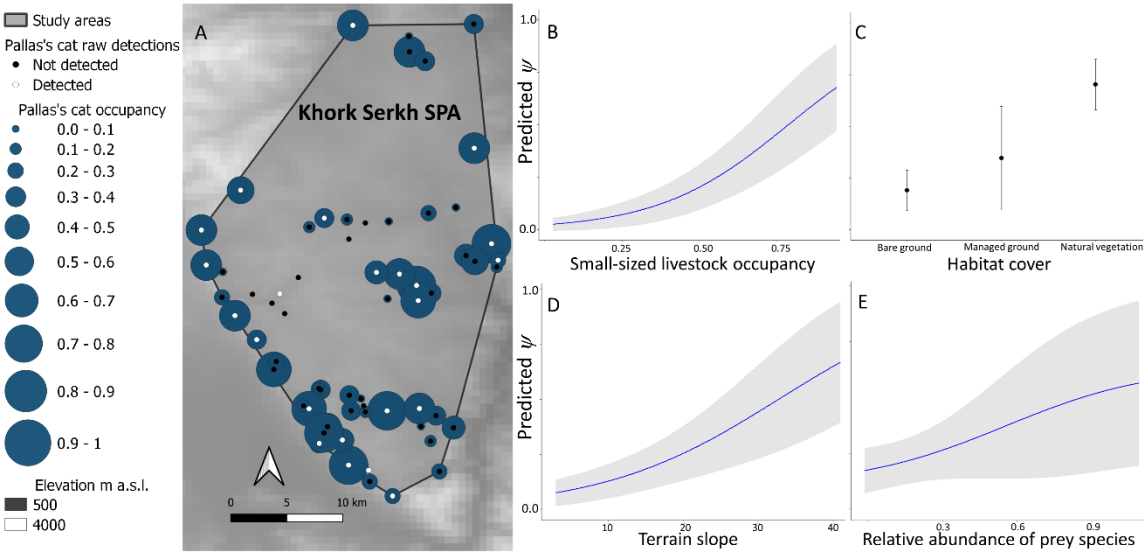

Fig. 2.3 Occupancy probability distribution of the Pallas's cat (A) in Khork Serkh Strictly Protected Area (2018), western Mongolia. Circles indicate occupancy probability, with larger ones representing higher values. Occupancy was modelled as a function of: B) the occupancy of small-sized domestic animals (i.e., sheep and goats), C) habitat type, D) slope, and E) relative abundance of prey species.

Table 2.4 Parameter estimates from the averaging of the best-supported models for both across the four study areas and focal area assessment of the Pallas's cat (*Otocolobus manul*) for the occupancy (ψ) and detection (p) probability in western Mongolia.

Parameter	Estimates	SE	Z	P(>|z|)
Across the four areas - western Mongolia				
ψ Habitat cover – Natural vegetation	2.11	0.49	4.30	< 0.001
ψ Habitat cover – Managed ground	-0.88	0.83	1.06	0.29
ψ Occupancy of domestic animals	0.44	0.22	1.96	0.04
ψ Area – Tavan Bogd NP	-1.78	0.68	2.63	< 0.01
ψ Area – Siilkhem B NP	0.07	0.72	0.11	0.92
ψ Area – Sutai Massif	-0.96	0.55	1.75	0.08
p Trigger speed – slow	-0.77	0.36	2.17	0.03
Focal area - Khork Serkh Strictly Protected Area				
ψ Abundance of small-sized livestock	1.25	0.47	2.62	< 0.01
ψ Habitat cover – Natural vegetation	2.52	1.00	2.52	0.01
ψ Habitat cover – Managed ground	1.42	1.41	1.01	0.31
ψ Slope	0.79	0.42	1.88	0.05
ψ Relative abundance of prey species	0.67	0.41	1.66	0.09
p Trigger speed – slow	-1.68	0.57	2.96	< 0.01
p RAI domestics	-0.15	0.13	1.14	0.26

Overall, Pallas's cat displayed a cathemeral behavior with multiple peaks of activity through the 24 hours (Fig. 2.4), with detections during 1400–1700 that were less frequent. Across the 4 areas, the overlap between Pallas's cat and livestock curves was lower at sites where livestock was also detected (Δ = 0.28, 95% CI = 0.25–0.31) than at sites where livestock was not detected (Δ = 0.45, 95% CI = 0.41–0.49; Fig. 2.4). The difference in activity pattern was significant in the former case (W = 20.44, P < 0.001) and non-significant in the latter (W = 2.26, P = 0. 13). The t-test for differences in activity overlaps between the 2 scenarios had a significant outcome (P < 0.001).

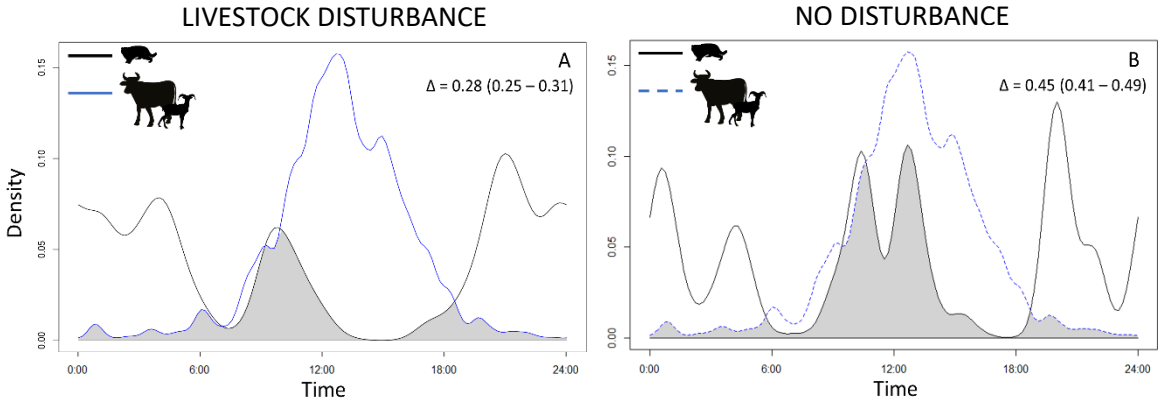

Fig. 2.4 Temporal overlap in activity between the Pallas's cat and livestock in western Mongolia (2015 – 2019). The figure displays the diel activity pattern of the felid (A) at sites where livestock was detected (111 sites, 63 cat's detections) and (B) at sites where livestock was not detected (105 sites, 44 cat's detections). Both Pallas's cat activity curves were plotted against the diel activity pattern of livestock across the whole area, to point out the felid's variation in activity pattern. The coefficient (Δ) assessed the degree of overlap between the diel activity curves of the two taxa (1 = complete overlap, 0 = no overlap).

2.4 DISCUSSION

Motion-sensitive camera detections of Pallas's cat from snow leopard surveys in the Mongolian Altai Mountains enabled us to evaluate the spatio-temporal patterns and responses of this little-known felid to a suite of covariates, with a particular focus on the sensitivity to grazing livestock. Previous information on Pallas's cat occupancy was limited to local ecological knowledge (Chimed et al. 2021). We are aware of the limitations of our sampling that primarily targeted the snow leopard (Rovero et al. 2020), and we acknowledge that occupancy may simply reflect the proportion of area used by the Pallas's cat (Efford and Dawson 2012, Neilson et al. 2018). Yet, being a metric that accounts for imperfect detection, its usefulness to assess habitat associations has been revealed by many studies (Niedballa et al. 2015, Gompper et al. 2016, Moll et al. 2016, Greco et al. 2021).

Moreover, our inference is related to the gradient of protected areas encroached by livestock (2 national parks, 1 SPA, 1 area that was not protected at the

time of sampling), and not to the wider steppe ecosystem in western Mongolia. The moderate occupancy and very low detectability we estimated are broadly consistent with the presumed low density of this species (Ross et al. 2012, Anile et al. 2021), while the proportion of sites used on sites sampled is comparable with that of Chimed et al. (2021). The significantly lower occupancy in Tavan Bogd may indicate that this area is suboptimal for this felid, likely because it is generally higher in elevation and has more extensive glacial and snow cover relative to the other areas (Ganyushkin et al. 2018). The Pallas's cat appears to prefer areas that are steep, with natural vegetation and higher occurrence of prey, matching the high habitat and dietary specialization known for this species (Ross et al. 2019*a*, Chimed et al. 2021, Greenspan and Giordano 2021). The importance of areas with vegetation emerged clearly from both analyses (i.e., the entire region and the focal area of Khork Serkh SPA), while a weak preference for steep areas only emerged from the focal area. For this area we could also consider prey availability in the model, and this variable too resulted to be weakly associated to Pallas's cat's occupancy. The weak association may have been affected by natural fluctuations in the abundance of prey (Andreassen et al. 2021, Otgonbayar and Buyandelger 2021) or our placement of motion-sensitive cameras to target snow leopard may have biased low the detection of small animals. Similarly to the effect of land cover, the positive association with the occupancy of livestock was revealed in both assessments, and it was relatively more attributable to small-sized livestock in the focal area. Pallas's cat was significantly more detectable in all study areas when using fast-trigger motion-sensitive cameras, as reported for other elusive felids and small mammals (Wellington et al. 2014, Greco and Rovero 2021).

The positive association of the Pallas's cat with vegetated and prey-rich habitat where also grazing livestock occur is partially in contrast to our hypothesis. Such spatial association may be due to the higher abundance of prey species near camps due to fertilization promoting vegetation growth (Bulow-olsen 1980, Ross 2009) or areas with natural vegetation that are associated with a greater presence of pikas and other small rodents (Ross 2009). The presence of livestock could also

trigger a form of mesopredator release, with herding dogs and livestock that might disperse larger carnivores (Ross 2009, Anile et al. 2021). The convergence in habitat preferences between domestic species and Pallas's cat suggests that the preferred habitat by the cat in the study region coincides with areas encroached by livestock. The spatial association is especially pronounced with sheep and goats that are managed as massive herds and represent the majority of livestock, being therefore of potential greater impact on the vegetated areas (Augugliaro et al. 2020). Thus, the Pallas's cat is able to populate the preferred habitat despite its use by livestock; however, in line with our hypothesis, a coping mechanism is the shift in the diel activity pattern of the felid at grazing sites in the direction of minimizing temporal activity overlap with livestock, which are usually corralled at night in the study region, particularly for small-sized livestock (Augugliaro et al. 2020). In view of these results, we suggest that the convergence between Pallas's cat preferred habitat and grazing areas of livestock may represent a serious, impending threat to the felid, as suggested by its shift in diel activity pattern to limit direct encounters. Temporal niche partitioning in response to anthropogenic disturbance is known from a range of other study systems where wild species co-occur with humans and livestock, with animals minimizing risk by shifting the temporal, rather than the spatial niche (Poudel et al. 2015, Oberosler et al. 2017, Gaynor et al. 2018).

When considering that livestock numbers have markedly increased across Mongolia over the last decades (Berger et al. 2013, Pfeiffer et al. 2018), and that we also recorded diffused livestock presence into protected areas (this study, Augugliaro et al. 2020, Rovero et al. 2020), our findings are of conservation concern for a number of reasons. First, the Pallas's cat is specialized in its habitat choice, and only uses a small fraction of area available within the steppe ecosystem (10 – 30%; Ross et al. 2019*a*); it is dependent on areas that are protected but also increasingly used for grazing, which may eventually threaten the cat from habitat degradation affecting the abundance of small rodents, hence progressively reducing prey availability (Cao et al. 2016, Schieltz and Rubenstein 2016). Second, the proximity of preferred areas to herders' houses and camps implies higher chances of Pallas's cat predation by dogs,

considered one of the most important causes of human-related deaths of these cats (Ross 2009; Barashkova 2012, 2017), and poisoning, directly as a predator control method or as consequence of poisoning of Pallas's cat's primary prey for pest or disease control (Tseveenmyadag and Nyambayar 2002). This latter threat is particularly critical for Mongolia (Winters 2006). The detrimental effects of such practices and overharvesting are also currently threatening marmot (*Marmota* spp.) species (Zahler et al. 2004, Clayton 2016), on whose cavities Pallas's cats are dependent on for denning and resting sites (Ross et al. 2010*a*). These concerns are augmented when considering that hunting of Pallas's cats is still permitted in Mongolia (Murdoch et al. 2007, Barclay et al. 2019) where Pallas's cats were traded until recently on local markets (Wingard et al. 2018), poaching of this species within protected areas has been documented as frequently occurring (Murdoch et al. 2007), and Pallas's cats are occasionally shot when mistaken for marmots (Ross et al. 2019*b*). Field observations from our sampling reported Pallas's cat skins found in several nomads' tents across 3 out of 4 areas (F. Rovero, University of Florence, and C. Augugliaro, University of Lausanne, personal observation).

Habitat degradation resulting from livestock grazing has detrimental effects on large mammals (Ripple et al. 2014, 2015; Soofi et al. 2018), while a general trend of total abundance declining with grazing is also documented for small mammals (Schieltz and Rubenstein 2016). But studies on the specific effects on small carnivores are few and with contrasting outcomes (Blaum 2007*a*, 2007*b*, 2009; Bösing et al. 2014; Williams et al. 2018). For example, a study in South Africa reported that stocking rate of livestock was inversely related to local abundance of small- and medium-sized predators, including felids (Blaum et al. 2009). While our data on the Pallas's cat do not provide for inference on population trends, the consistency in the results across study areas with different protection regimes and between the regional and the focal area indicates that the causalities we suggest explaining the spatio-temporal responses of Pallas's cat to livestock are founded.

2.5 MANAGEMENT IMPLICATIONS

We suggest that the most relevant conservation actions for Pallas's cat should include regulations of livestock encroachment within protected areas by improving enforcement efficacy. Additionally, in consideration of the cat's association with natural vegetation and prey abundance, we suggest improving protection for this habitat and to ban the eradication campaigns of rodents through poisoning. We further believe that a review of its legal status in Mongolia based on updated and quantitative evidence should be carried out. Because our knowledge of Pallas's cat ecology, behavior, distribution, and population status is scarce, further research on their populations is required for the conservation of the species and to benefit other key species across its range.

2.6 ACKNOWLEDGMENTS

We are grateful to the J. K. Sheppard, and 2 anonymous reviewers for valuable comments to an earlier version of the manuscript. We thank the Ministry of Environment and Tourism of Mongolia for providing the research permit, the Altai Mountain Protected Area Authority, and C. Janchvlamdan for the technical support and help with logistics. Fototrappolaggio, UNIL, Altai Institute for Research and Conservation, and Snow Leopard Conservancy provided a share of the motion-sensitive cameras. We are thankful to all participants in the expeditions, particularly M. Krofel, C. Groff, R. Havmøller, R. Rizzoli, B. Rosembaum, D. Ciaramella, F. Zimmermann, P. Christe, and P. Zorer for the valuable contribution to the fieldwork. We also thank students for classifying camera images. The study was funded by Panthera (Sabin Snow Leopard Grants to FR); MUSE - Museo delle Scienze, Italy; Green Initiative; Natural History Museum of Denmark; University of Lausanne; Irbis Mongolia; Altai Institute for Research and Conservation; Parco Natura Viva, Italy; and Herbette Foundation, Switzerland. VO was supported by the Gino Zobele Fund.

Chapter 3

Calibrating occupancy to density estimations to assess abundance and vulnerability of a threatened primate in Tanzania

Greco, I., Paddock, C. L., McCabe, G. M., Barelli, C. Shinyambala, S., Mtui, A. S. & Rovero, F.

Ecosphere

14(3), e4427

DOI: doi.org/10.1002/ecs2.4427

Abstract

The current decline of mammals worldwide makes quantitative population assessments crucial, especially for range-restricted and threatened species. However, robust abundance estimations are challenging for elusive or otherwise difficult to detect species. Alternative metrics requiring only presence/absence data, i.e. occupancy, are possible but calibration with independent density estimates should be foreseen, although rarely performed. Here, we calibrated density estimates from acoustic surveys to occupancy estimates from camera-trapping detections to derive the abundance of the IUCN-Endangered Sanje mangabey (*Cercocebus sanjei*) across its entire range in the Udzungwa Mountains of Tanzania. We found marked occupancy-density relationships for the two forest blocks where this primate occurs and used them to derive spatially-explicit density estimates. Occupancy increased in montane forest zones at mid-elevation but decreased slightly with proximity to forest borders. We predicted an average density (±SE) of 0.26 ± 0.05 groups/km2 in the national park and 0.24 ± 0.06 in the nature reserve. Accordingly, and given the much larger area of the reserve, the average predicted individual abundance was 1,555 ± 325 and 2,471 ± 571 in the national park and nature reserve, respectively. We found higher density and abundance in the nature reserve compared to previous studies. Given the past disturbance and poorer protection in the nature reserve relative to the national park, our results instil optimism for the status of the species, although occupancy analysis highlighted the potential vulnerability of this primate to human disturbance. Our approach appears valuable for spatially-explicit density estimations of elusive species, and provides robust assessments of vulnerability and identification of priority areas for conservation of threatened populations.

Keywords: acoustic distance sampling, camera-trapping, *Cercocebus sanjei*, density estimation, endangered species, occupancy, Udzungwa Mountain National Park.

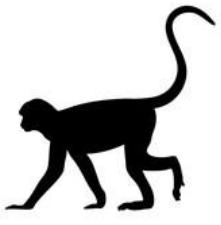

3.1 INTRODUCTION

In the Anthropocene, wildlife species are experiencing an unprecedented decline, with 26% of mammals currently threatened with extinction (IUCN 2022). While the highest concentration of threatened and range restricted species are found in tropical forests, these represent one of the most affected biomes, with habitat loss and harvesting that disproportionally impact mammals (Schipper et al. 2008, Roberts et al. 2021). Non-human primates are among the most threatened order of mammals, with ~65% of the 504 existing species being threatened with extinction and ~75% of the populations facing decline (Estrada et al. 2017; Fernández et al. 2022). By functioning as seed dispersers, these species serve a critical ecological role in forest regeneration, affecting plant species diversity and demography (e.g., Holbrook and Loiselle 2009; Lambert 2010; Andersen et al. 2018). For these reasons, non-human primates are considered excellent ecological indicators and are highly sensitive to anthropogenic disturbance (Marsh 2003; Rodrìguez-Luna et al. 2013). Therefore, research and conservation efforts focused on primates may have the added benefits of preserving important ecological functions as well as other species (Gippoliti and Sousa 2004; Martins and Valladres-Padua 2005; Lambert 2010). However, the quantitative knowledge on abundance, conservation status and vulnerability of threatened primates needed to promote sound conservation remains limited (Estrada et al. 2017), and rarely does this cover the entire range of species (e.g., Davenport et al. 2022).

A key limiting issue of such assessments is the pervasive difficulty of estimating population abundance and its spatial variation, especially for rare and elusive free-ranging animals. Hence, accounting for imperfect detection is important especially for species that are difficult to detect, and methods that include it are highly recommended (e.g., Spehar et al. 2015; Cavada et al. 2019). In place of direct counts of individuals or groups, a practical approach is the use of detection/non-detection data (Joseph et al. 2006; Kühl et al. 2008). The latter are suitable for estimating occupancy, which is broadly considered a surrogate for abundance, and can be

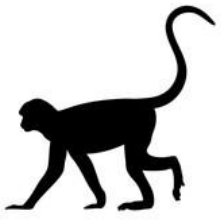

modelled with spatial covariates to assess species response to drivers of change (MacKenzie et al. 2002; 2006; Kéry and Royle 2016; Linden et al. 2017). However, the assumption of a positive relationship between the two metrics is often untested, and ideally requires the calibration of occupancy with independently derived density estimates (Linden et al. 2017).

Here, we present the results of an approach that calibrates occupancy from camera trapping detections to density from acoustic surveys to estimate population abundance and spatial variation of an endangered primate in relation to both environmental and anthropogenic factors. We selected the Sanje mangabey (*Cercocebus sanjei*, Mittermeier et al. 2006) for this study, an IUCN-Endangered, predominantly ground-dwelling, and frugivorous primate first described in 1979 and occurring only in two separated forests in the Udzungwa Mountains of south-central Tanzania (Ehardt et al. 2005; Rovero et al. 2006; McCabe et al. 2019). The area is of outstanding importance for biodiversity conservation (Burgess et al. 2007; Rovero et al. 2014b) and a high priority area for primate conservation in Tanzania (Davenport et al. 2013).

Despite several ecological studies, robust knowledge on population abundance and habitat association remains preliminary, with studies rarely targeting the whole species range with consistent methodology. Earlier estimations of population abundance were based on crude extrapolations of home-range data from a few groups (e.g., Ehardt et al. 2001; 2005; Rovero et al. 2009). More recently, Paddock et al. (2020) used acoustic detections to estimate density using a distance sampling approach, hence taking into account imperfect detection. This method enabled group detection using the distinctive mangabey whoop-gobble long-call which is given by males in each group in the mornings, allowing for remote sensing without the need for visual observations of this elusive species. However, effort was limited to a single survey across a spatially- and numerically-limited set of listening posts, and the analysis did not consider spatial covariates. Similarly, habitat associations have been studied with camera-traps but only for parts of the species range (Rovero et al. 2014a; Martin et al. 2015; Oberosler et al. 2020a) and considered

only a few environmental and anthropogenic variables. Studies showed that camera-traps are very efficient at detecting this ground-dwelling species (Hegerl et al. 2017; Martin et al. 2016; Oberosler et al. 2020a) which is instead very rarely sighted by human observations (Rovero et al. 2012; Barelli et al. 2013).

Here, we aimed to provide more accurate quantification of abundance and density of this elusive and iconic species by integrating camera-trapping and acoustic data to overcome previous limitations, particularly the difficulties associated with collecting systematic and spatially comprehensive density data from acoustic detections. Thus, we used camera-trap data collected consistently in both forests, and hence across most of the species' range, to calibrate spatially-explicit occupancy estimates to density from acoustic surveys, and used the regression to derive density estimates across the species' range. Moreover, by integrating visual counts of group size, we also predicted individual densities and total population abundance. Lastly, we also aimed to determine spatial patterns of occurrence in relation to both habitat and potential anthropogenic disturbance to better assess habitat associations and vulnerability of this endangered and iconic primate.

3.2 METHODS

3.2.1 Study area

The Udzungwa Mountains in south-central Tanzania (7°40'– 8°40'S and 35°10'–36°50', Fig 3.1) represent the largest block within the Eastern Arc Mountains and the richest in biodiversity (Rovero et al. 2014b). Part of the area is protected as Udzungwa Mountain National Park (1,990 km2), established in 1992, whereas the remaining part is preserved either as Nature Reserve or Forest Reserve (Rovero et al. 2009). The two forests where the Sanje mangabeys occur are Mwanihana (MW, 167 km2) within the Udzungwa Mountain National Park, and Uzungwa Scarp (USNR, 372 km2) which is a nature reserve, approx. 150 km to the south-west (Fig 3.1). These areas are both east-facing escarpment slopes ranging in elevation between 290 and 2100 m a.s.l., with a gradient of vegetation cover from lowland deciduous to montane

evergreen and upper montane bamboo forests. Lowland zones in both areas are dominated by regenerating and secondary forest due to past logging and degradation, whereas the higher elevations are mainly characterized by undisturbed, closed canopy forest. The two forests share similar ecological characteristics (Suppl. Table C.1), but different management regimes: MW has effective law enforcement being in a well-protected national park, while USNR is less efficiently protected (Rovero et al. 2012), and more degraded (Rovero et al. 2014b; Oberosler et al. 2020a). In fact, the nature reserve is a forest island surrounded by small villages and suffers from logging, habitat destruction and illegal hunting, whereas MW has minor anthropogenic disturbance from the villages located east of the park boundary.

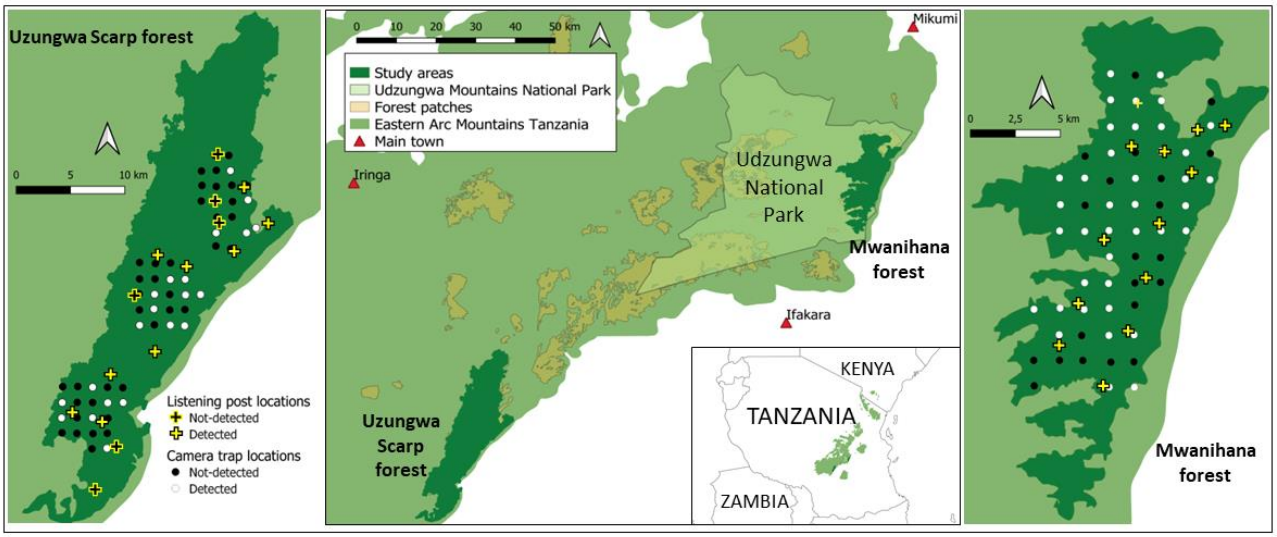

Figure 3.1 Map of the study area in Tanzania (central panel and inset), with the two forest blocks (Mwanihana forest and Uzungwa Scarp Nature Reserve) where the Sanje mangabey (*Cercocebus sanjei*) occurs (left and right panels). In these two forests, black and white dots represent camera-trap locations (white are those where mangabeys were detected), whereas crosses represent the listening posts where acoustic surveys were made (yellow are those where mangabeys were detected).

3.2.2 Data collection: acoustic and camera-trapping surveys

Acoustic detection data were collected by Paddock et al. (2020) during the dry season (June – November 2017), at 28 survey locations (MW: N = 13; USNR: N = 15; Fig 3.1).

The listening posts were located randomly inside cells of a systematic grid, with a minimum distance between locations of 2 km (Fig 3.1), which is in line with the known home-range size of the target species (Ehardt et al. 2005). The distance to each mangabey vocalization heard was estimated by three independent observers and the distance and direction mapped to estimate the position of the group. Estimates included in the analyses were truncated at 1km as it was unlikely calls were accurately detectable over this distance. Data collection was carried out in the morning, between 07:00 and 09:00, when the Sanje mangabey is known to call at the highest frequencies (Ehardt et al. 2005), and every survey was conducted once (further details in Paddock et al. 2020).

Camera-trapping surveys were conducted in both forests in the same period as the acoustic survey (i.e., July – November 2017). Data in MW were collected through the Tropical Ecology Assessment Monitoring (TEAM) Network project (Rovero and Ahumada, 2017), that follows a standardized and systematic protocol for monitoring medium-to-large terrestrial mammals, and the same protocol was extended in USNR. Thus, for each forest, we placed three consecutive arrays of 20 camera-traps (Reconyx HC500, Reconyx Inc., Holmen, WI, USA), for a total of 60 camera stations per forest (Fig 3.1). Cameras were located based on a systematic grid of 2 km2 cell size and deployed in the field for a minimum of 30 consecutive days. Inside each cell, camera traps were placed on the closest wildlife trail to the centroid of the cell, and attached to trees at approximately 50 cm from to the ground, facing the presumed trail at approximately 2 – 3 m distance. Total sampling effort yielded 1,839 camera days for MW, and 1,792 for USNR (Suppl. Table C.1) from 117 camera-trap sites overall, as three were damaged, with a mean effort per camera of 31 days for both study areas.

3.2.3 Data collection: covariates

We derived six covariates that could affect the species spatial distribution both in terms of density and occupancy and used them as proxies of environmental and anthropogenic factors. Thus, we considered: i) habitat cover, extracted from the GLC2000 dataset (European Commission 2004) and based on FAO habitat

classification (i.e., broadleaf evergreen forest and deciduous forest), ii) elevation, extracted from a 90 m DEM raster, iii) ground slope, iv) distance from the camera location to the closest river, v) distance to the closest forest border, and vi) study area (i.e., the two forests with contrasting management regimens). Values were extracted using the built-in tools in the open-source software QGIS (QGIS Development Team 2019). Based on the Pearson's correlation coefficient (threshold = 0.5), these variables were not collinear.

3.2.4 Data analyses

3.2.4.1 Group density estimates

We re-analysed data from Paddock et al. (2020) with the aim of building density estimation models with account of anthropogenic and environmental covariates. We used the package "Distance" (Miller et al. 2019) in R (R Core Team 2019) to model the probability of detection and estimate Sanje mangabey groups' density from distance data. We built and compared several model combinations using different detection functions and covariates, to find the best-fitting detection function. The best model was selected using Akaike's information criteria (AIC) where the best model was considered at ΔAIC = 0. We did not use adjustment terms as covariates were involved (Miller et al. 2019). Given the limited sample size (N = 28 listening posts), we only used elevation, ground slope, and distance to the closest reserve border as density covariates (see next section on assumptions of covariate relationship with density and occupancy). We averaged covariate value across a 1 km buffer around each listening post since Sanje mangabeys are generally heard within such area. Group densities were calculated for each study forest and then extrapolated considering the total available forest area (MW = 150.59 km2 and USNR = 314.48 km2: Marshall et al., 2010).

3.2.4.2 Occupancy modelling

Sanje mangabey occupancy (ψ) accounting for imperfect detection (p) was estimated using single-species single-season occupancy modelling (MacKenzie et al. 2002). Occupancy is the proportion of sites where the target species is expected to occur when the likelihood to record it is smaller than 1, namely when the non-detection of

the species does not imply its absence from the site (MacKenzie et al. 2002). We built a single model for both forests. The input data consisted of a matrix of sampled sites i by the sampling occasions j, filled with species detections (1) and non-detections (0). This consisted in a matrix of 117 sites and 137 sampling occasions. We scored as NA a site that was not sampled during a specific occasion. We first built a null model with constant detection and occupancy, and then selected the best-supported model for the detection probability by fitting distance to the closest forest border and habitat type. In fact, previous studies assessed that the former could influence the detection probability of a range of species in either direction (Rovero et al 2014a; Greco & Rovero 2021), likely triggering increasing shyness or boldness. Moreover, detectability could also be affected by the density of forest floor vegetation in different habitat types, leading to changes in the efficiency of camera at detecting animals (Greco et al. 2021). We did not use camera trap effort as potential covariate for the detection probability because our effort was homogeneous across cameras. We then used the best-supported detection model (Suppl. Table C.2) to model occupancy. Occupancy probability was modelled as a function of i) habitat type, ii) elevation, iii) ground slope, iv) distance to the closest reserve border, and v) distance to the closest river. We expected occupancy to increase away from the forests' borders, where anthropogenic disturbance may be higher, and that would increase in association with an optimal environment for the Sanje mangabeys, such as closer to watercourses, in association to broadleaves evergreen forests, and at mid-elevation. We also expected averaged site-specific occupancy to be higher in the national park compared to the nature reserve (Oberosler et al 2020a; Paddock et al 2020). Finally, we ranked all the occupancy models with different combinations of variables against the null model. Models were run using the package "unmarked" (Fiske and Chandler 2011) in R. Model selection and ranking was based on the AIC score, with $\Delta AIC < 2$ representing best-supported models. If multiple models resulted top-ranked, we followed Dormann et al. (2008)'s procedure to averaging predictions: we computed predictions on link-scale for each best supported model, back-transformed them to response scale, and averaged predictions. Using the best models, we predicted

occupancy across the forest areas by using a grid of 100 x 100 m pixels populated with site covariate values (Rovero and Spitale 2016). This was done by using the 'predict' function and plotted the result on a map using the 'levelplot' function in the R package 'lattice' (Sarkar et al., 2021).

3.2.4.3 Density to occupancy calibration

Given that listening post locations might not perfectly overlap with just one pixel of predicted occupancy, we averaged predicted occupancy values from the nine pixels centred on each listening post. We then regressed density values from survey sites on these predicted occupancy values to determine the relationships. We used Generalised Linear Models with a gamma distribution and log-link function for each population within the two forests to test the relationship between the two metrics, with occupancy values as the independent variable and density values as the dependent variable (N = 13 sites for MW and N = 9 sites for USNR). Contrary to MW, USNR had sites with no acoustic records, and we assumed that these reflected non-detections rather than absence. Hence, we did not include them in the analyses. We chose a gamma distribution as the data are continuous and positive (Bolker 2014) and because we hypothesized that the relationship might not be linear. This is because as occupancy increases along the 0 – 1 gradient density may increase at a higher rate given it is not bounded. Based on the calibration results, we derived density (± SE) estimates from the occupancy values at the 100 x 100 m resolution, using the function "predict" in the package "stats" (Chambers and Hastie 1992). We averaged density values to predict group density in each forest and multiplied them by the forest area to predict group abundance. Lastly, we derived individual density and abundance by using an average count of 39.2 individuals per group in MW (N = 5) and 31.7 in USNR (N = 3; Paddock et al. 2020).

3.3 RESULTS

Three occupancy models were best-supported (Table 3.1), resulting in an average (±

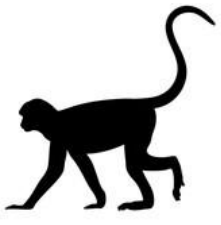

SE) site-specific estimated occupancy probability (ψ) of 0.64 ± 0.10 and 0.48 ± 0.09 in MW and USNR, respectively (Fig 3.2), with lower occupancy in USNR than MW (Welch two sample t-test: t = 3.57; df = 110.32; p-value < 0.001). In addition, occupancy decreased with elevation (ψ = -1.36 ± 0.41; p < 0.01), it was higher in broadleaf evergreen forest (ψ = 2.38 ± 0.71; p < 0.01) and increased with distance to protected area border (ψ = 0.58 ± 0.31; p = 0.06; Fig 3.2; Table 3.2). Conversely, the detection probability (p) decreased away from the border (p = -0.24 ± 0.09; p < 0.01; Table 3.2). Spatially-explicit occupancy maps are shown in Suppl. Figure C.1.

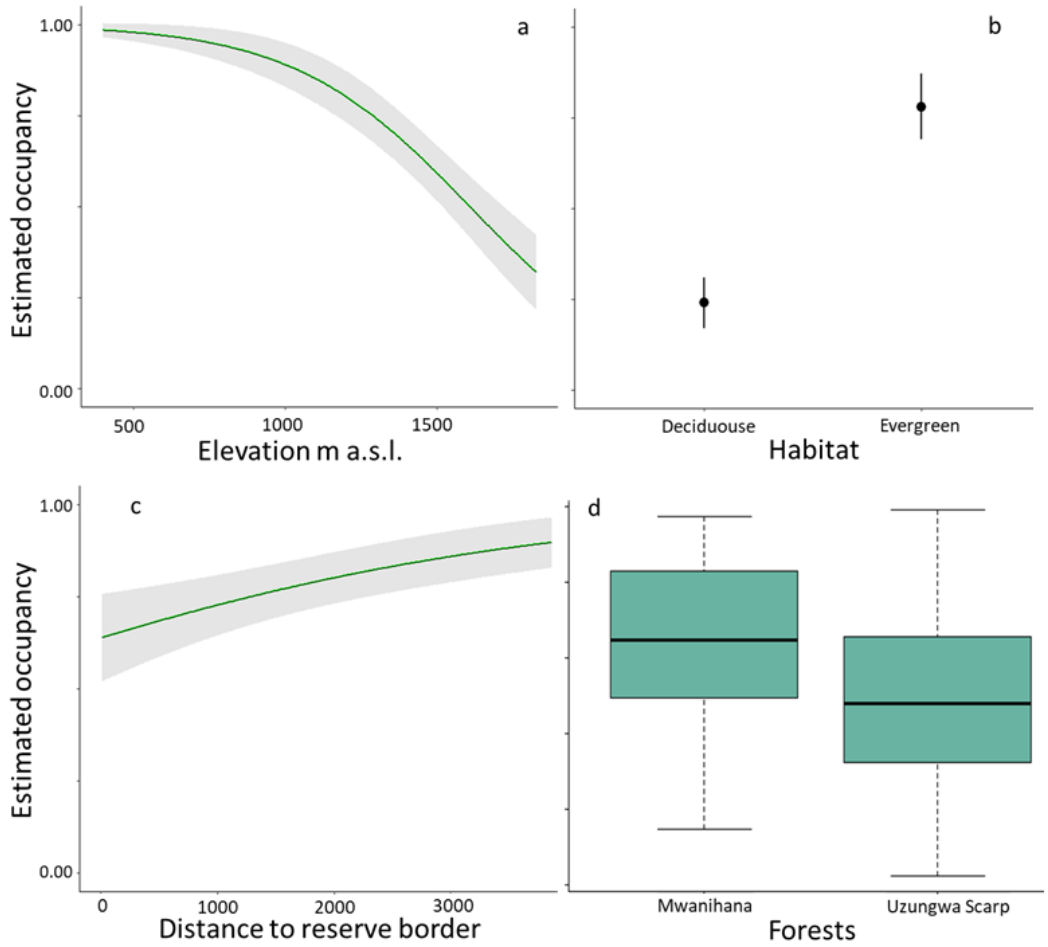

Fig 3.2 Bivariate predictions of estimated occupancy probability with SE from the averaging of the predictions of the three best-supported models for the Sanje mangabey (*Cercocebus sanjei*) in relation to: a) elevation, b) forest type, and c) distance to the closest forest border. Additionally, d) shows the boxplot for site-specific occupancy values divided by forest.

Table 3.1 Results of the occupancy models for the Sanje mangabey (*Cercocebus sanjei*) in two forests, Mwanihana and Uzungwa Scarp Nature Reserve in Tanzania, detected by camera-traps in 2017. Model ranking is based on the Akaike Information Criterion (AIC), with models having ΔAIC < 2.00 considered best-supported (bold). Table also display the R-squared of each model. Table displays the top five model and the null model.

Occupancy models	n. param.	AIC	ΔAIC	Rsq
p (Distance to closest reserve border) ~ ψ (Distance to closest reserve border + Habitat + Elevation)	**6**	**1228.26**	**0.00**	**0.57**
p (Distance to closest reserve border) ~ ψ (Distance to closest reserve border + Habitat + Elevation + Distance to closest river + Slope)	**8**	**1229.92**	**1.66**	**0.58**
p (Distance to closest reserve border) ~ ψ (Distance to closest reserve border + Habitat + Elevation + Slope)	**7**	**1230.09**	**1.84**	**0.57**
p (Distance to closest reserve border) ~ ψ (Distance to closest reserve border + Elevation)	5	1241.59	13.33	0.51
p (Distance to closest reserve border) ~ ψ (Distance to closest reserve border + Habitat + Distance to closest river)	4	1241.73	13.47	0.51
p (1) ~ ψ (1)	2	1320.06	91.81	0.00

Table 3.2 Parameter estimates from the averaging of the best-supported models of Sanje mangabey (*Cercocebus sanjei*). Table displays occupancy (ψ) and detection (p) probability estimates across the two study areas (Mwanihana forest and Uzungwa Scarp Nature Reserve) in Tanzania.

Parameters	Estimate	SE	z-value	p-value
ψ Distance to closest edge	0.58	0.32	1.85	0.06
ψ Habitat - Evergreen	2.38	0.70	3.38	< 0.01
ψ Elevation	-1.36	0.41	3.29	< 0.01
ψ Slope	0.12	0.26	0.47	0.64
ψ Distance to closest river	0.36	0.25	1.44	0.15
p Distance to closest edge	-0.24	0.09	2.71	< 0.01

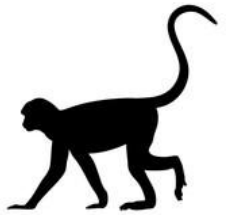

Acoustic density estimations were best-fitted by a half-normal detection function and with the distance to the closest reserve border as the variable retained (goodness of fit = 0.69; Table S2). Occupancy values at the listening posts successfully predicted density estimates from acoustic surveys for both MW (ψ = 1.90 ± 0.92 SE; p = 0.03; R2 = 0.32) and USNR (ψ = 2.49 ± 0.93 SE; p = 0.03; R2 = 0.36; Fig 3.3).

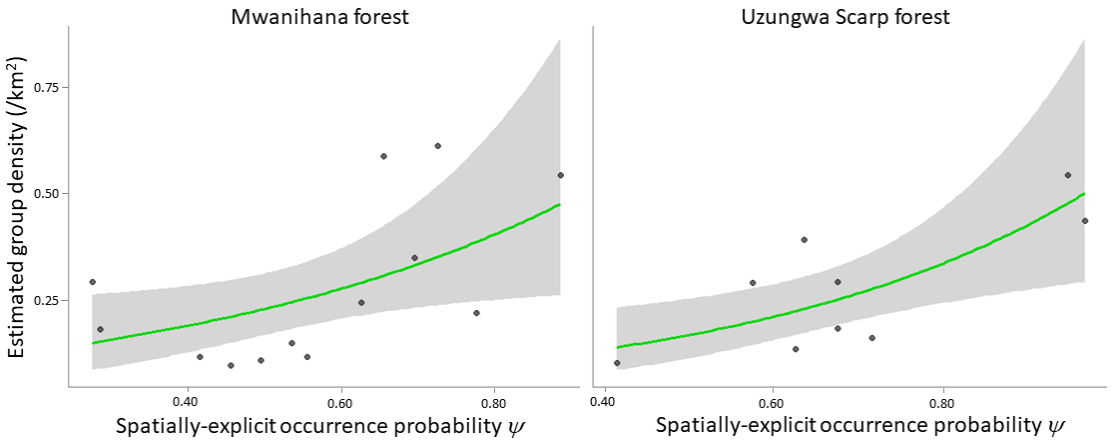

Fig 3.3 Relationship between occupancy and acoustic density estimates derived in Mwanihana (left, N = 13 listening posts) and Uzungwa Scarp forests (right, N = 9), Tanzania, where the Sanje mangabey (*Cercocebus sanjei*) was studied. The graph represents the result of a Generalized Linear Models with Gamma distribution and log-link function. Shaded area represents SE.

The spatially-explicit densities derived from such relationships (Fig 3.4) were significantly higher in MW than in USNR (Welch two Sample t-test: t = 16.65; df = 51988; p-value < 0.001), and resulted in an estimated mean ± SE density of 0.26 ± 0.05 groups/km^2 and 0.24 ± 0.06, respectively. These estimates translated into 39.66 ± 8.28 mangabey groups across MW and 77.94 ± 18.01 across USNR. Predicted population size using available mean group counts resulted of 1,555 ± 324.58 and 2,471 ± 570.88 individual monkeys in MW and USNR, respectively, corresponding to an estimated individual density of 10.32 ± 2.16 ind./km^2 in MW and 7.86 ± 1.82 in USNR (Table 3.3).

Table 3.3 Estimated group density, number of groups, population size and individual density of the Sanje mangabey (*Cercocebus sanjei*) in Mwanihana forest (MW) and Uzungwa Scarp Nature Reserve (USNR), Tanzania.

Metric	Forest	Parameter estimate	± SE	Range
Group density/km^2	MW	0.26	0.05	0.12 - 0.47
	USNR	0.24	0.06	0.05 - 0.56
Number of groups	MW	39.66	8.28	19.22 - 70.93
	USNR	77.94	18.01	16.24 - 177.18
Population size	MW	1,554.63	324.58	753.48 - 2,780.34
	USNR	2,470.63	570.88	514.86 - 5,616.59
Individual density/km^2	MW	10.32	2.16	5.00 - 18.46
	USNR	7.86	1.82	1.64 - 17.86

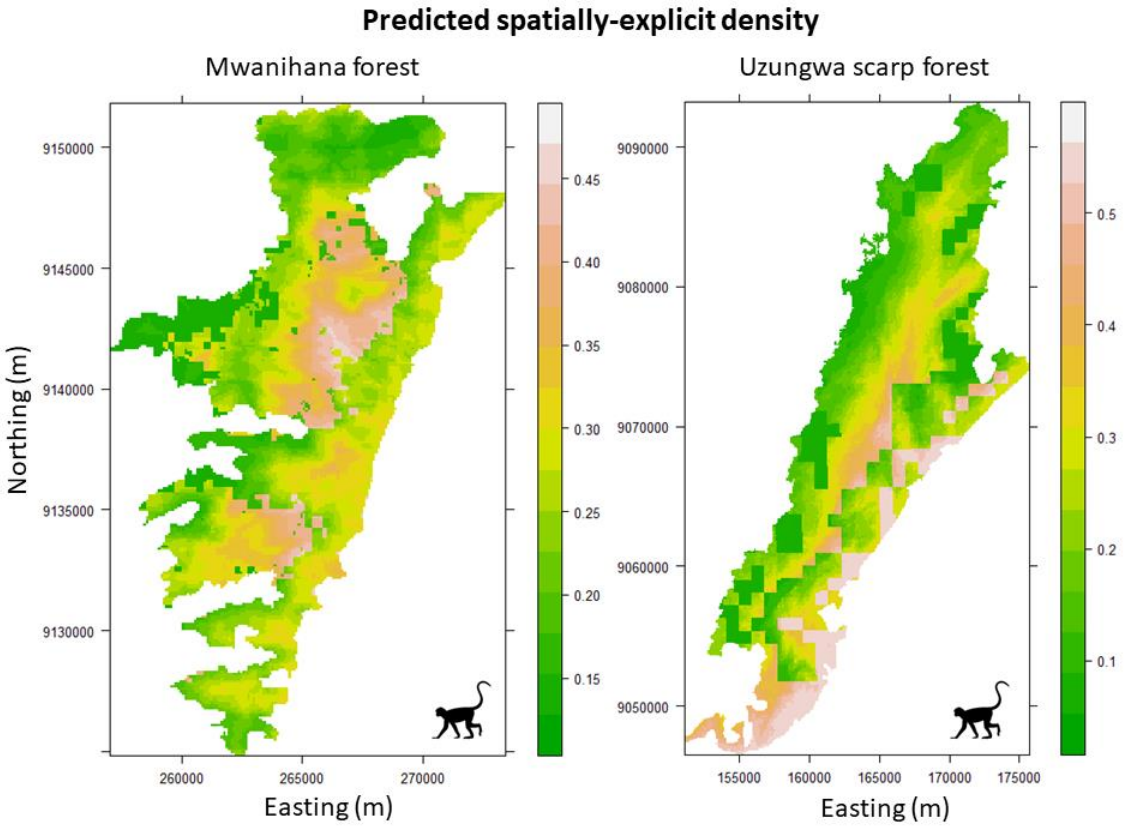

Fig 3.4 Maps of the predicted group density of the Sanje mangabey (*Cercocebus sanjei*) in Mwanihana forest (left) and Uzungwa Scarp forest (right), Tanzania.

3.4 DISCUSSION

By integrating density estimation from acoustic surveys with spatially-explicit occupancy predictions, we derived density with account for spatial heterogeneity across the entire range of the endangered Sanje mangabey, hence refining the population estimates by Paddock et al. (2020), which were based on acoustic surveys at a limited sample of sites. Occupancy modelling also allowed us to determine habitat associations across the species' range and assess potential vulnerability of this non-human primate species to anthropogenic disturbance.

The use of occupancy as a cost-effective population assessment tool when abundance estimation is complex has long been recognized (e.g., MacKenzie et al. 2005; Noon et al. 2012; Wilson and Schmidt 2015), and rests on an assumed positive relationship between occupancy and density (MacKenzie and Nichols 2004). Such relationship is inherently complex because occupancy asymptotes at 1. In our study, the design of 2 km^2 grid cell size used for camera-trapping broadly matched the documented home-range of Sanje mangabey (Ehardt et al. 2005; Mwamende 2009). Hence, given that the grid cell size was close to the target species' home range, occupancy and abundance should broadly correspond (Linden et al., 2017), which likely underlines the occupancy-density relationship we found. Indeed, several studies highlighted how the spacing of detectors in relation to the home-range and movement pattern of the target species influenced the relationship (Tempel and Gutiérrez 2013; Rogan et al. 2019), with appropriate designs being those where such spacing matches the target species' home-range size, so to assume independence of detections (Tempel and Gutiérrez 2013; Clare et al. 2015; Wilson and Schmidt 2015). In addition, the use of camera-trapping to estimate occupancy in continuous habitats is problematic due to the inherent violation of the closure assumption, given that camera-traps are point detectors and animals regularly move in and out of sampled "sites" (Neilson et al. 2018). However, this issue makes estimated occupancy from camera detections a biased approximation of true occupancy especially when low-density species move fast across large areas, hence saturating occupancy when density may be low (Lewis

et al. 2015; Parsons et al. 2017; Neilson et al. 2018).

Findings from studies that investigated both forests found that the northern forest appears well protected compared to the southern one (Oberosler et al. 2020b), with the population in the nature reserve forest that has suffered decades of poor protection and, as a result, it is highly threatened and with lower density (Paddock et al. 2020). Our predictions of average group density per forest are broadly in line with those presented by Paddock et al. (2020) in that density was significantly higher in MW than in USNR; however, we estimated relatively higher density in USNR than from the acoustic distance sampling data alone (i.e., 0.22 vs 0.15 groups/km^2, and 69.6 vs 45.9 groups for ours and the earlier study, respectively). This divergence may be caused by the spatially limited sample of listening posts used by Paddock et al. (2020) in comparison to the diffuse grid of camera-traps we deployed, as well as the single acoustic survey event conducted for that study that may have caused a lower overall detection of the target species. The higher group density we estimated in USNR compared to previous studies translated into a higher overall abundance of approximately 4.026 ± 875.61 individuals in both forests (versus 3,167 ± 436.62 estimated by Paddock et al., 2020), 61% of which are estimated to occur in USNR given its much larger area than MW. We caution that the conversion from groups to individuals' abundance may be biased by the relatively small sample of group counts available (N = 8; Paddock et al. 2020) and needs therefore to be considered with this limitation in mind for future improvements. However, population estimates with methods that account for imperfect detection (Paddock et al. 2020) and with data from across the species' range (this study) were lacking (see review in Paddock et al. 2020); hence, our study provides for an important and comprehensive contribution to refine the species' conservation status and as a baseline for future studies.

The lower group density in USNR compared to MW mirrors results from earlier occupancy analyses from camera-trapping data (Hegerl et al. 2017; Oberosler et al. 2020a, Oberosler et al. 2020b) and is likely explained by the elevated anthropogenic encroachment that has affected USNR for decades, mainly in form of illegal hunting, tree cutting and charcoal making (Rovero et al. 2012, Oberosler et al. 2020a). Such

disturbance is seemingly more impactful on the strictly arboreal and folivorous colobine monkeys that underwent severe declines in USNR, being the target of selective hunting techniques (Rovero et al. 2012; 2015), while the predominantly ground-dwelling and frugivorous mangabeys appear not to be specifically targeted by hunters and better adapted to exploit more heterogeneous and lightly disturbed habitats (Ehardt et al. 2005; Rovero et al. 2014a; Lloyd 2017). Yet, their lower density in USNR than MW (with a seemingly lower group size in the former forest; Paddock. et al., 2020) and the results of occupancy analyses suggest that the mangabey is vulnerable to human disturbance. In fact, the decreasing occupancy in proximity to protected area borders coincides in the insulated USNR with proximity to densely human populated areas, that surround the entire forest block. Indeed, the grid of camera-traps distributed across most of the species' range allowed us to study spatial variation in occurrence, and hence abundance. Elevation and gross habitat type emerged as important predictors consistently for both populations. Sanje mangabeys displayed a general preference for sub-montane forest at mid-elevation, with higher density occurring roughly between 500 and 1,000 m asl. These areas of presumed optimal habitat for the species generally consist of evergreen forest with greater mean basal area than elsewhere (Cavada et al. 2016), indicating predominance of closed-canopy and old-growth forest. Nonetheless, our results indicated that deciduous forest zones were also used, likely reflecting the great niche flexibility of the Sanje mangabey, which is known to exploit mosaic forests thanks to its diet predominantly based on seeds and invertebrates (Ehardt et al., 2005; Rovero et al. 2012; Lloyd 2017; McCabe et al. 2013).

In conclusion, the approach we tested, based on calibrating occupancy to independent density estimations, appears valuable for spatially-explicit density estimations of poorly detected species such as the Sanje mangabey, provided that the sampling design is appropriate to relate the two inherently different metrics. Our analysis provided for the first comprehensive assessments of the abundance and vulnerability of this primate, identifying priority areas for conservation, especially the forest areas at lower elevation and close to human settlements. While the

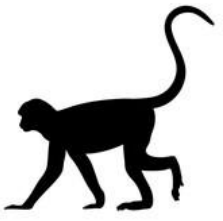

relatively higher abundance of Sanje mangabeys in the less protected USNR than earlier reported gives cause for optimism, this forest continues to suffer from illegal human encroachment, calling for the need of increased protection and mitigation of anthropogenic threats.

3.5 ACKNOWLEDGMENTS

We thank the Subject-matter Editor and two reviewers for their insightful comments and suggestions that helped us improve the original manuscript. We are grateful to the Tanzania Wildlife Research Institute, Tanzania Commission for Science and Technology, Tanzania National Parks, Tanzania Forest Service Agency, and Tanzania Commission for Science and Technology for research permissions. Wardens and staff of TANAPA's Udzungwa Mountains National Park and TFS's Uzungwa Scarp Nature Reserve are particularly thanked for the invaluable assistance and support given. For camera trapping, we thank Ruben Mwakisoma, Emilian Omari, Aggrey Uisso and several other field assistants. For the Sanje Mangabey Project, we thank all field assistants for their critical help, particularly Yahaya Sama, Bakari Ponda, Loy Loishoki and Saidi Malendula. We also thank Dr. Andrew Bowkett for participating in the baseline camera-trapping survey in Uzungwa Scarp, and Dr. David Fernandez as co-director of the Sanje Mangabey Project. Funding and equipment for camera-trapping was provided by Fondazione Foresta Futura (Italy), Wild Planet Trust (UK), MUSE – Museo delle Scienze and the Tropical Ecology Assessment and Monitoring (TEAM) network. Funding for the acoustic surveys was provided by a UK Natural Environment Research Council (NERC; CASE Studentship NE/N007980/1), Bristol Zoological Society as the NERC CASE industry partner, and Primate Conservation Inc. (#1443).

PART II

Studying mammals' communities at regional and global scale

Chapter 4

Consistent spatio-temporal responses of mammalian communities to human frequentation across Italian protected areas

Salvatori, M.*, Greco, I.*, Cappai, N., Dorigatti, E., Massolo, A., Miscioscia, M., Natucci, L., Oberosler, V., Partel, P., Pedrini, P., Petroni, L., Volcan, G., & Rovero, F.

In preparation

*Equal contribution

Abstract

Protected areas (PAs) networks are a pivotal tool to conserve nature under the current biodiversity crisis, yet they often need to balance their primary mission of nature conservation with the social and economic need of giving opportunity for outdoor recreation. Recreation in natural areas is important for human health in an increasingly urbanised society and fosters public support for nature protection. However, it remains an overlooked factor that can trigger disturbance of wild animals and prompt behavioural modifications or space use shifts. These responses have the potential to affect population dynamics and modify important ecological processes like trophic cascades and nutrient cycling. Rarely, however, have these responses being studied across multiple PAs and using standardized, field detection methods. We deployed a systematic camera trapping protocol at over 200 sites along trails and forestry roads to sample the community of medium and large mammals in four PAs within the European Natura 2000 network and neighbouring zones to address spatio-temporal responses of wild mammals to human frequentation, proximity to settlements and topographical variables. We detected a total of 18 mammalian species and a widespread presence of humans, engaged in recreational activities, in the range of one to two orders of magnitude higher than wild mammals. By applying multi-area and multi-species models on the number of diurnal, crepuscular and nocturnal detections and on occurrence probability we estimated both species-specific and meta-community level effects, finding that increased nocturnality and lower site use appear the main strategies that mammals consistently use to cope with human disturbance, thereby diminishing the probability to encounter humans. We also found differences in behavioural responses according to species' body size: larger species more markedly decreased diurnality at sites with intense human passage and increased it further away from urban areas. Our results show the effectiveness of standardized field sampling and provide relevant insights for planning the expansion of PAs as foreseen by the Kunming-Montreal Global biodiversity framework.

4.1 INTRODUCTION

The progressive artificialization of the planet is eroding and modifying natural habitats through structural alterations of the environment such as deforestation, wetland reclamation, and urbanization, ultimately resulting in wildlife population declines (Elhacham et al. 2020, Living Planet Report 2022). At the same time humans can influence animal physiological and cognitive processes also through mortality risk perception, noise emission, artificial light, and chemical pollution (non-structural alterations). These anthropogenic impacts often co-occur and interact, merging into a complex and multimodal sensory pollution (Halfwerk et al. 2015), impacting wild animals' perception and leading to human-induced behavioural changes, with potentially noxious consequences on foraging and reproductive efficacy, and therefore survival (Wilson et al. 2020, Challéat et al. 2021). Among the top-down effects of humans on animal behaviour, the spatial and temporal modification of perceived risk caused by human presence in the environment can provoke fear responses that often surpass those caused by natural predators both in magnitude and extent (Ciuti et al. 2012). As perceived super-predators, humans shape a landscape of fear that affects not only herbivore or meso-carnivore behaviour and movement, but also that of apex predators, de facto limiting their ecosystem role as top consumers and disrupting trophic cascades (Wilmers et al. 2021, Wooster et al. 2022, Londber-Holm et al. 2019). Where humans do not exert a direct mortality effect on prey through hunting or poaching, prey species can instead take advantage of the presence of people as shield against predators, altering predator-prey dynamics (Berger 2007, Muhly et al. 2011). Behavioural modifications elicited by fear of humans include increased vigilance and elusiveness (Jayakodi et al. 2008, McBlain et al. 2020), home range contraction (Plante et al. 2018), spatial shifts towards less accessible areas (Richard et al. 2016) and increased nocturnality (Diao et al. 2021). Some life traits seem to correlate with the sensitivity of mammals to human disturbance and landscape anthropization, particularly large body size, slow maturation, and wide home ranges, due to high

energetic and spatial requirements of larger species and a demographic recruitment too slow to counterbalance anthropogenic mortality (Suraci et al. 2021).

The landscape of human fear is not restricted to densely settled areas, but penetrates also into natural and protected areas (PAs), for example when humans visit them for outdoor recreation and nature tourism. PAs are one of the most important instruments in the conservation biology toolbox and are considered pivotal for the long term conservation of ecosystems under the current biodiversity crisis (Hoffman et al. 2018). Despite evidence shows that biological communities are faring better within PAs compared to unprotected landscapes (Geldmann et al. 2013, Gray et al. 2016), many PAs suffer from insufficient funding for implementing effective management and enforce protection, and are subject to urban and infrastructure development (Coad et al. 2019). One of the most overlooked threats that PAs are currently facing is represented by human disturbance linked to outdoor recreational activities. This pressure is among the most widespread within PAs globally, and is the most frequently reported threat in high-income countries (Schulze et al. 2018). Even if the emphasis on nature protection has progressively shifted towards a multi-functional role of PAs that includes social, recreational, and economic contributions to local human communities (Schmitz et al. 2012, Gavin et al. 2015), the sustainability of recreational and economic activities should be robustly measured to assure their harmonisation with biodiversity conservation (Eagles et al. 2002). Unfortunately, quantitative assessments of the effects of human disturbance on biological communities are often lacking, hindering the implementation of science-based management strategies to mitigate potential impacts (Marion et al. 2020).

In Europe, the Natura 2000 network is the backbone of the EU's Biodiversity Strategy for 2030 (European Commission 2021), but efficient monitoring and research projects across network sites are generally hampered by a lack of consistency in data collection methods, spatial scales and analytical approaches (McKenna et al. 2014). Yet, drawing generalized conclusions about the effectiveness of the Natura 2000 network and the threats insisting on PAs clearly requires

standardized and systematic approaches, whereby the same methodology is applied at the same spatial scale to multiple sites of the ecological network (Lindenmayer et al. 2013).

In this study we aimed to contribute to fill this gap and sampled mammalian communities within and around four PAs in northern and central Italy through systematic camera trapping carried out during 2020 on a total of 204 sites. We took advantage of the ability of camera traps to detect both wild mammals and human outdoor activities simultaneously, and aimed to evaluate wildlife responses to human presence. Specifically, we addressed the following research questions: 1) Do recreational activities and the proximity to human settlements decrease the probability of site use of mammals? 2) Do mammals adjust their diurnality (proportion of diurnal activity) in relation to human activities and the proximity to settlements? 3) If spatio-temporal avoidance of anthropogenic disturbance occurs, does it depend on species' characteristics such as body size and trophic guild? 4) Do prey species avoid humans or exploit them as shield against predators? We predicted that increasing rates of human outdoor activities would decrease mammal site use (prediction P1A) and force mammals towards more crepuscular and nocturnal activity (prediction P1B). We also predicted that mammals' use of sites would increase at increasing distance from human settlements (prediction P2A) as would their tendency to diurnality (prediction P2B). Furthermore, we predict that species with larger body size would display a more evident spatio-temporal displacement by humans (prediction P3A) and avoidance of human settlements (P3B), whereas carnivores would be more elusive to the human presence especially during diurnal hours (P3C) and omnivores would potentially be more attracted by settlements, especially during nocturnal hours, for the additional trophic resources (P3D). We also predicted that predator spatio-temporal avoidance of humans would be higher than that of prey, under the human shield hypothesis (P4). By rolling out a first network of PAs that implement standardized mammal assessment, we also aimed to evaluate the potential of our protocol and approach to scale-up at national and European level.

4.2 METHODS

4.2.1 Study area

In 2020 we surveyed one national park and three regional protected areas in northern and central Italy. The study areas (Fig. 4.1) include: (1) Parco Naturale Adamello Brenta (Area 1; 46° 6' N, 10° 56' E), a regional protected area in the central Italian Alps, with highest elevation of 3558 m a. s. l., was surveyed between the first day of June and the last of August. One third of Area 1 is covered by forest, dominated by broadleaved species at lower elevation, which are gradually replaced by conifers from 1000 to 2000 m a.s.l. Above the tree line the landscape is characterized by extensive grasslands and pastures, which precede steep slopes and cliffs of dolomite rocks. (2) Parco Naturale Paneveggio Pale di San Martino (Area 2; 46° 12' N, 11° 48' E), a regional protected area in the eastern Italian Alps, with the highest peak at 3192 m a.s.l, was surveyed between early September and late November. This area is characterized by a vast coniferous forest, bordering a high and rocky dolomitic massif. (3) Parco Regionale Naturale delle Alpi Apuane (Area 3; 44° 4' N, 10° 15' E), located in the northern part of Apennini mountain range, central Italy, with the highest elevation of 1946 m a.s.l., and surveyed from June to November. This mountainous area is detached from the main Apennines ridge and neighbours the Ligurian Sea coast. Area 3 has a typical alpine-like environment, with widespread cliffs and peaks composed of limestone and white marble rocks, whose extraction involves many quarries intercluded and around the protected area. Vegetation is mainly represented by broadleaved woods followed by grasslands above the tree line. (4) Parco Nazionale Foreste Casentinesi (Area 4; 44° 4' N, 10° 15' E), a National Park of 368 km^2 located in the centre-northern Apennines and gazetted in 1993, with the highest peak reaching 1658 m a.s.l. The park was surveyed between early September and late November. The area is characterized by dense forests, in particular ancient fir forests, beech woods, and mixed forests, as well as a sub-montane vegetation area dominated by oak forests and chestnut groves, and pastures

at higher elevations.

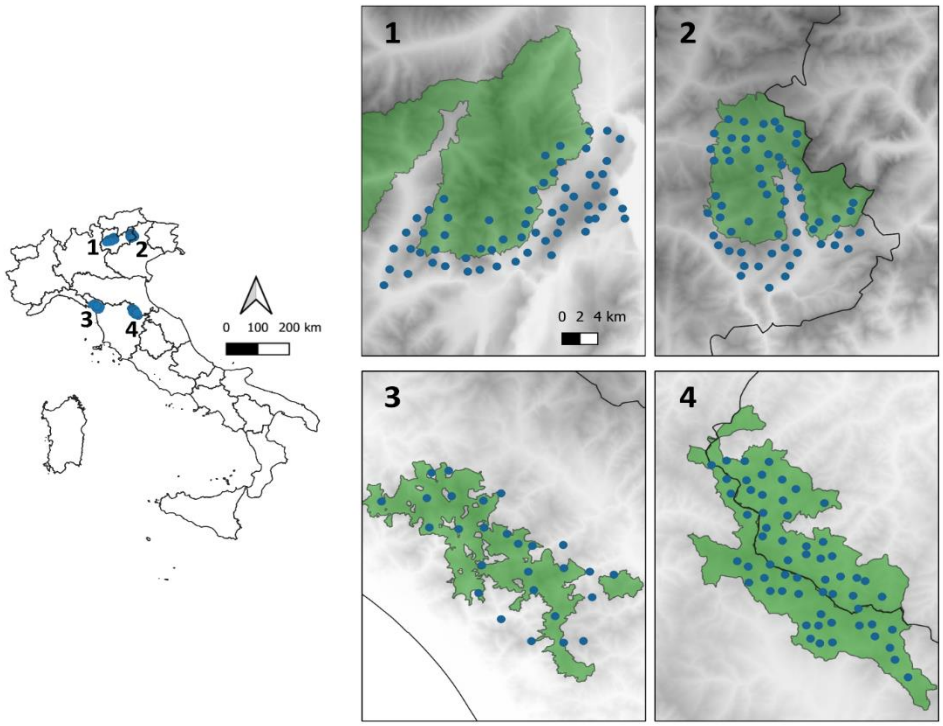

Fig. 4.1 Map of the four study areas in northern and central Italy monitored with systematic camera trapping in 2020: 1 - Parco Naturale Adamello Brenta, 2 – Parco Naturale Paneveggio Pale di San Martino, 3 – Parco Naturale Regionale delle Alpi Apuane, 4 – Parco Naturale Nazionale delle Foreste Casentinesi. Protected areas are shown in green, while sampling sites are indicated by blue dots.

All four areas are popular tourist destinations for outdoor recreation and have an extensive network of forestry roads, hiking and biking trails, and numerous touristic facilities. In areas 1 and 2 forestry roads are accessible by car only for residents, hunters and forestry personnel, while in area 4 their use by vehicles is restricted to forestry personnel and, upon authorization, to researchers for scientific purposes. In areas 1, 2 and 4 mushroom collection is strictly regulated, while in areas 1 and 2 visitors are not allowed to leave the trails within the core areas of the park. The core of Area 4 is included within the Integral Nature Reserve “Sasso Fratino”, which is a strictly protected biogenetic area and part of the UNESCO World Heritage, where human access is limited to research and scientific activities only.

In Area 3 and 4 hunting is not permitted within the parks’ boundaries, although this

activity is carried out in adjacent areas, with wild boar (*Sus scrofa*) and red deer (*Cervus elaphus*) that are among the most targeted species. Instead, except for state-own lands, hunting is practiced in Area 1 and 2 also within the parks' territories, and hunting season is mainly between October – November. Here, red deer, roe deer (*Capreolus capreolus*), mouflon (*Ovis orientalis*), and wild boar are the targeted species. Hence, giving that 2 out of 4 areas are not affected by any form of hunting activities, and that in Area 1 hunting season does not overlap with the sampling season, we decided to not consider such activity in the analyses and to focus on the effect on human frequentation within the parks.

4.2.2 Data collection

The sampling design applied in the four areas has been used in Area 1 since 2015 (Oberosler et al. 2017, Salvatori et al. 2023) and is adapted from the Tropical Ecology Assessment and Monitoring Network (TEAM Network 2011, Jansen et al. 2014), a pan-tropical biodiversity monitoring program (Rovero and Ahumada 2017). Differences with the TEAM Network protocol include a larger spacing between camera locations to maximize the overall area monitored and to account for the larger home range size of the mammals of temperate forests compared to species in tropical rainforests. We designed a regular grid with side of cells of 2/3 km and placed one camera-trap site per cell, evenly spaced and positioned to cover the whole altitudinal gradient (Fig. 4.1). In areas 1, 2, and 4 the number of sampling sites was 60, and 45 in Area 3, due to the smaller spatial extent of this study area. Within each cell, we randomly selected one trail or forestry road and positioned a random point on it, that was then located in the field based on accessibility. Cameras were installed on trees at about 60 cm above the ground and at a distance of 3-5 meters from the target trail or road. For all areas, baits were not used, and cameras stayed active in the field for a minimum of 30 consecutive days. For this study, we used heat-in-motion triggered cameras of different brands: Reconyx (Holmen, WI, USA), Browning (Birmingham, AL, USA), UWAY Outdoor Products (Norcross, GA, USA), Bushnell Outdoor Products (Overland Park, KA, USA), Boly Inc. (Santa Clara, CA, USA) and Apemans (Shenzhen, China). The pictures collected were classified at the species level by the authors

through the software Wild.ID (Rovero and Zimmermann 2016). The only exception refers to the sympatric species *Martes foina* and *Martes martes*, which were classified at the genus level only, due to the impossibility to distinguish them with certainty from camera trap detections. Since the sampling sites were positioned on trails and roads, our inference is generally related to wild mammals' and humans' use of these features only, and not of the whole study area (see Discussion). For the present study, trail-based sampling was necessary to monitor both wildlife and human site use, and thus to evaluate the potential consequences of human passage on wild mammals.

4.2.3 Covariates

To model large-scale effects of human frequentation on the spatial distribution and temporal behavior of the mammalian communities in the four study areas, we extracted a set of four anthropogenic and environmental variables: i) the Relative Abundance Index (RAI) of humans at camera level (RAIHUMAN), ii) the distance from the camera to the closest settlement (SETTL), iii) elevation (ELEV), and iv) slope (SLOPE). These variables were minimally or not collinear based on the Pearson correlation coefficient (threshold = 0.5). The RAI of humans (vehicles included) represented a proxy of the diffuse presence of people in the reserves as well as a measure of the direct human passage at the camera stations. Site-level RAIs were calculated by extracting the number of independent events and dividing it by the number of sampling days and multiplying by 100. We defined events as photographic sequences separated by at least 15 minutes (Rovero and Zimmermann 2016). RAIs thus summarized the site-specific average number of independent events every 100 days of sampling. The distances from each camera station to the closest settlement were computed as the Euclidean distance and represented proximity to town centers (excluding isolated houses). Site elevation and site slope were used to correct for possible environmental influences while investigating focal anthropogenic effects on mammals, and were extracted from Digital Elevation Models (DEMs) by using the built-in tools for geospatial analyses in QGis (QGis 2020). Since we used a mix of camera trap brands, we categorized the photographic devices based on their trigger speed (CAM_TYPE), with "fast" = 1 for cameras with trigger speed <0.2s, and

"moderate" = 2 for the others.

4.2.4 Analyses

The composition of the mammalian communities in the four study areas was initially explored by calculating the RAI of wild mammals following the same procedure described above for the RAI of humans. Thus, for each study area, by ordering the species according to their RAI value, we could descriptively appraise the composition in terms of the number of photographic events of the mammalian species in each community (Fig. 4.2). Additionally, to explore the overall activity patterns of wildlife (all species considered together) and humans for each study area, we visually reported the pairwise overlap between the activity distribution curve of wildlife and humans, estimating and then overlapping the Kernel density curves of the two categories through the package overlap (Meredith and Ridout 2014).

To model global spatio-temporal variations of mammal communities across the four study areas we adapted the multi-region occupancy model developed by Sutherland et al. (2016) to accommodate not only presence/absence data for estimating detection and occupancy probability, but also independent events in three different time slots (day, crepuscular hours, and night) to model potential variations in mammal site use intensity in relation to time of day and anthropogenic covariates. This model extends the community occupancy model of Dorazio and Royle (2005) by linking data collected at multiple spatially independent regions, thus information is connected across sites and species, but also across different study areas (R = 4), while also accounting for different faunal species compositions. In this way, the coefficients of regressions are not only linked across species *i* of the same community through a random effect with a common mean, but also across regions R through a global random effect with a common mean for different study areas. This allowed us to assess the effect of covariates of interest as global effects on multiple independent communities as well as to assess covariate effects on each species in each region.

The number of diurnal, crepuscular and nocturnal photographic events were modelled through a sub-model with Poisson distribution, area-specific intercepts, and species- and area-specific slopes drawn from a normal distribution. Response

data were organized as independent tridimensional arrays, populated by the number of diurnal, crepuscular and nocturnal photographic events for each species *i*, at each site *j*, and in each area *r*. These data were expressed as discrete counts, and a single value was assigned for each species at each site in each area. We defined diurnal events those obtained between one hour after astronomical sunrise and one hour before sunset; crepuscular events those obtained within one hour before and after sunrise or sunset; and nocturnal events those obtained between one hour after sunset and one hour before sunrise. Sunrise and sunset times were extracted through the R package 'suncalc' (Thieurmel 2022). For each species *i* in region *r*, the events in the three time intervals were modelled using a Poisson distribution with the following structure:

$$day_{ijr} \sim Poisson(\lambda day_{ijr})$$
$$crep_{ijr} \sim Poisson(\lambda crep_{ijr})$$
$$night_{ijr} \sim Poisson(\lambda night_{ijr})$$

where day_{ijr}, $crep_{ijr}$, and $night_{ijr}$ represent the species-, site- and region-specific number of events for each time interval. Species-specific and global variations of the number of events in each temporal interval were then modelled as functions of covariates, such that:

$$\log(\lambda day_{ijr}) = \mu\lambda day_{r} + \beta 1 day_{ir} * RAIHUMAN_{jr} + \beta 2 day_{ir} * SETTL_{jr} + \beta 3 day_{ir} * ELEV_{jr} + \beta 4 day_{ir} * SLOPE_{jr}$$
$$\log(\lambda crep_{ijr}) = \mu\lambda crep_{r} + \beta 1 crep_{ir} * RAIHUMAN_{jr} + \beta 2 crep_{ir} * SETTL_{jr} + \beta 3 crepi_{r} * ELEV_{jr} + \beta 4 crep_{ir} * SLOPE_{jr}$$
$$\log(\lambda night_{ijr}) = \mu\lambda night_{r} + \beta 1 night_{ir} * RAIHUMAN_{jr} + \beta 2 night_{ir} * SETTL_{jr} + \beta 3 night_{ir} * ELEV_{jr} + \beta 4 night_{ir} * SLOPE_{jr}$$

For the occupancy sub-model, data were again organized as tridimensional array of species by sites by area (*I*J*R*). Detection/non-detection data (*Y*) corresponded to the imperfect observation of the true occupancy state (*Z*). This latter was modelled as a

Bernoulli random variable such that $z_{jir} \sim$ Bernoulli(ψ_{jir}), with $z_{jir} = 1$ if site *j* was occupied by species *i* in region *r*, and $z_{jir} = 0$ if unoccupied. Here, ψ_{jir} is the species-specific occupancy probability of species i at site j in region r. The true occupancy states Z were then related to the observed data (*Y*) with the observational sub-model through a Binomial random variable $y_{jir} \sim$ Binomial(K_{ir}, p_{jir}, z_{jir}), where Kir represent the number of sampling occasions, thus the number of days each camera was active in every forest, and p_{jir} is the detection probability of species i at site j of region r. Region-specific detection and occupancy probability were modelled as a function of covariates through a logistic link, such that:

$$\text{logit}(p_{jir}) = \alpha 0_r + \alpha 1_{ir} * \text{SETTL}_{jr} + \alpha 2_{ir} * \text{equals}\ (\text{CAM\_TYPE}_{jr}, 2)$$

$$\text{logit}(\psi_{jir}) = \beta 0_r + \beta 1_{ir} * \text{RAIHUMAN}_{jr} + \beta 2_{ir} * \text{SETTL}_{jr} + \beta 3_{ir} * \text{ELEV}_{jr} + \beta 4_{ir} * \text{SLOPE}_{jr}$$

Region-specific variations in both detection and occupancy probability were accounted for by the intercepts ($\alpha 0_r$, $\beta 0_r$), modelled as random effects drawn from normally distributed hyperparameters of common mean and variance.

The overall model was executed in JAGS (Plummer 2003) in the Bayesian framework through the package jagsUI (Kellner and Meredith 2021), in R (R Core TEAM 2022). Posterior distributions of the parameters were estimated by using 3 Markov Chain Monte Carlo of 750,000 iterations (500,000 burn-in and 250,000 post-burn in, and thinning = 10). We visually assessed model performances by inspecting the convergence of the chains for every parameter of interest, by using the R-hat diagnostic with R-hat < 1.1 indicating good convergence, and by checking the number of samplings from the posterior distribution. For further details on priors and the model formulation we provide the JAGS code in the supplementary material.

Furthermore, we tested whether the diurnal, crepuscular and nocturnal responses to human passage and proximity to urban areas changed according to body size or trophic guild. For the first case, we regressed coefficient estimates of the three event types and two anthropogenic covariates against the log of each species body mass with post-hoc linear regressions (Salvatori et al. 2022). For the second case, we

performed a post-hoc analyses of variance by testing the coefficient estimates of the three event types and two anthropogenic covariates against the three trophic guilds (i.e., carnivore, herbivore, and omnivore).

We discuss all our numerical results considering strength of evidence as a gradient rather than excluding parameters strictly relying on p-values and confidence intervals as in traditional significance testing (see Muffs et al. 2021).

4.3 RESULTS

We collected 359,400 pictures through 8,619 camera days, from 204 sites sampled across the four areas (Suppl. Table D.1). Pictures of humans or vehicles corresponded to 73.5% of total pictures collected in Area 1, 58.8% in Area 2, 31.0% in Area 3, and 51.8% in Area 4.

In all four areas the number of photographic events of humans was far greater than that of any other species, with higher values in the Alpine areas (RAI_{human} in Area 1 = 194.6; RAI_{human} in Area 2 = 250.0) compared to the Apennine ones (RAI_{human} in Area 3 = 150.9; RAI_{human} in Area 4 = 152.8; Fig. 4.2). These latter two areas showed a higher number of wild mammalian species (12 in Area 3 and 15 in Area 4) compared to the first two (10 in Area 1 and 9 in Area 2). In Area 3 and 4 the second and third most detected species were red fox (Area 3: 43.65; Area 4: RAI = 57.43) and wild boar (Area 3: RAI = 41.27; Area 4: RAI = 32.92), before domestic animals, at the fourth place (Area 3: RAI = 29.47; Area 4: RAI = 30.99). Domestic animals were instead the second most detected species after humans in the two Alpine areas (Area 1: RAI = 30.63; Area 2: RAI = 47.85). Red fox was the most detected wild species in all areas except Area 2, where red deer ranked first (RAI = 37.03).

According to the Kernel density curves, in all four areas wild mammals showed reduced diurnal activity, with most of the independent photographic events that were concentrated at night and twilight hours (Suppl. Fig. D.1). Conversely, humans were active in the parks from 6 am to 6 pm with peaks in activity during midday. These trends were particularly pronounced in areas 1, 2 and 4 in which the overall

diurnal activity for all wild species dropped consistently highlighting a reduced temporal overlap with the human presence in the park. Instead, in Area 3, the wildlife temporal activity was more evenly spread across the day, although a reduction of activity during diurnal hours was still present (Suppl. Fig. D.1).

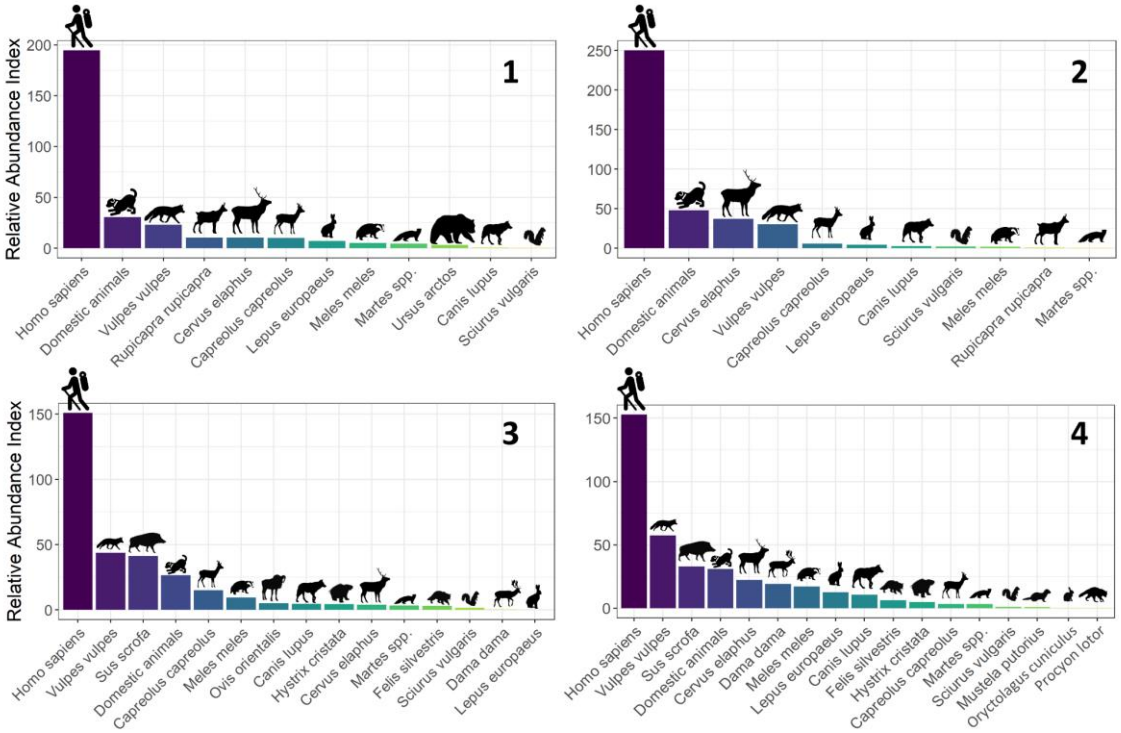

Fig. 4.2 Relative abundance Index of humans (vehicles included), domestic animals and wild mammals, ordered from the most to the least detected for each area. Species identity is indicated by its silhouette and scientific name. Data derive from systematic camera trapping in four protected areas of central and northern Italy during 2020: 1 - Parco Naturale Adamello Brenta, 2 – Parco Naturale Paneveggio Pale di San Martino, 3 – Parco Naturale Regionale delle Alpi Apuane, 4 – Parco Nazionale delle Foreste Casentinesi.

Across the four areas, we found a global consistent spatio-temporal response of mammals to human frequentation (Fig. 4.3, Suppl. Table D.2). In particular, the number of diurnal events decreased with increasing rates of human passage ($\beta 1_{day}$ = -0.48; 90% Bayesian Credible Interval, BCI: -0.67, -0.29; Fig. 4.3 and Fig. 4.4). Crepuscular events followed the same pattern, even though with a weaker effect size ($\beta 1_{crep}$ = -0.16; BCI: -0.31, -0.02), while the number of nocturnal events did not vary with human passage ($\beta 1_{night}$ = 0.01; BCI: -0.11, 0.13). Overall then, the number of

total events decreased and became mostly nocturnal at increasing rates of human passage. We found a lack of effect of distance from the closest town on diurnal events ($\beta 2_{day}$ = -0.09; BCI: -0.34, 0.18; Fig. 4.3), and a negative effect on crepuscular ($\beta 2_{crep}$ = -0.22; BCI: -0.43, -0.02) and nocturnal ($\beta 2_{night}$ = -0.26; BCI: -0.49, -0.03) ones, suggesting a tendency for a general decrease of nocturnality at increasing distance from urbanized areas (Fig. 4.3). All event types (diurnal, crepuscular and nocturnal) increased at higher elevation ($\beta 3_{day}$ = 0.51; $\beta 3_{crep}$ = 0.38; $\beta 3_{night}$ = 0.58) and steeper slopes ($\beta 4_{day}$ = 0.14; $\beta 4_{crep}$ = 0.15; $\beta 4_{night}$ = 0.29), and all their 90% credible intervals did not overlap 0, except for the effect of terrain slope on diurnal events (BCI: -0.04, 0.34, Fig. 4.3).

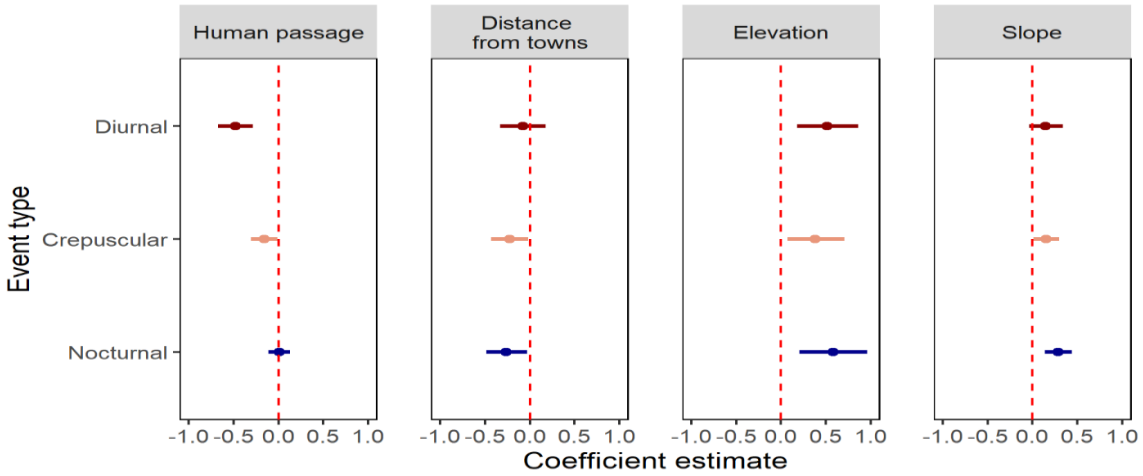

Fig. 4.3 Effects of the rate of human passage, distance from towns, elevation, and terrain slope on the number of events of wild mammals estimated with a multi-region community model. Caterpillar plots depict beta coefficients of diurnal (red), crepuscular (orange) and nocturnal (blue) events in relation to human passage, distance from closest town, elevation, and terrain slope. Points represent the median of the full posterior distribution, and error bars represent the 90% BCI. Data derive from systematic camera trapping in four protected areas of central and northern Italy during 2020.

The relationship between the rate of human passage and the number of events was lower for diurnal than nocturnal ones in all species with the only exception of the red fox, meaning that at increasing human frequentation of sites mammalian behaviour became more nocturnal and that this pattern was consistent across species (Fig. 4.4, Suppl. Fig. D.2, Suppl. Fig. D.6 and Suppl. Fig. D.10). Most species

showed a marked decrease in diurnal events leading to a strong disproportion towards nocturnal behaviour (e.g., Wild boar: $\beta 1_{day}$ = -1.70; BCI: -3.50, 0.22; Red deer: $\beta 1_{day}$ = -0.78; BCI: -1.67, -0.10; Roe deer: $\beta 1_{day}$ = -0.74; BCI: -1.46, -0.14; Fig. 4.4). Many species also showed a general tendency to decrease their total number of events in response to human frequentation, namely the coefficient was negative for diurnal, crepuscular and nocturnal events alike (e.g., Brown bear: $\beta 1_{day}$ = -0.59; $\beta 1_{crep}$ = -0.54; $\beta 1_{night}$ = -0.29; Mouflon: $\beta 1_{day}$ = -0.88; $\beta 1_{crep}$ = -0.20; $\beta 1_{night}$ =-0.19). The red fox showed a similar tendency to decrease its average number of events at increasing human disturbance, but its activity was concentrated during night-time even at low disturbance rates (Red fox: $\beta 1_{day}$ = -0.21; $\beta 1_{crep}$ = 0.28; $\beta 1_{night}$ = -0.41).

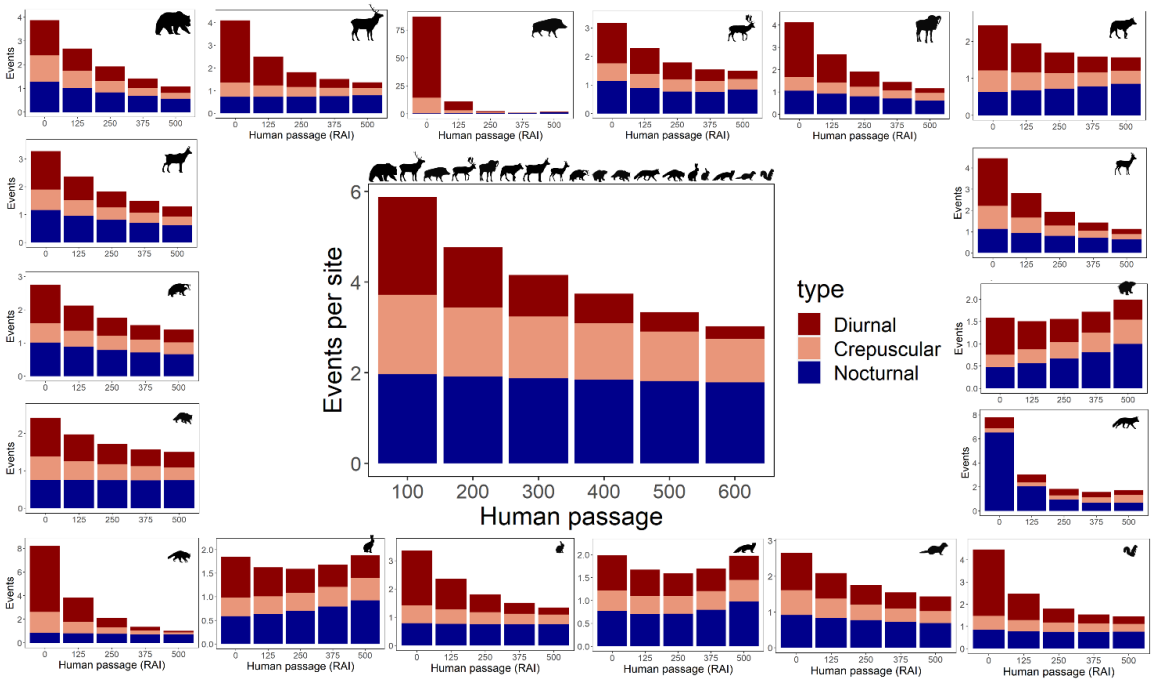

Fig. 4.4 Effects of the rate of human passage on the number of events at meta-community (central panel) and species level (outer panels). Stacked bar plots show the predicted number of average diurnal (red), crepuscular (orange) and nocturnal (blue) events of each species for different rates of human passage (human RAI). The species are indicated by their silhouettes and are ordered according to body mass from top left to bottom right as follows: *Ursus arctos, Cervus elaphus, Sus scrofa, Dama dama, Ovis musimon, Rupicapra rupicapra, Canis lupus, Capreolus capreolus, Meles meles, Hystrix cristata, Felis silvestris, Vulpes vulpes, Procyon lotor* (allochthonous species), *Lepus europaeus, Oryctolagus cuniculus, Martes spp., Mustela putorius, Sciurus vulgaris*. Data derive from systematic camera trapping in four protected areas of central and northern Italy during 2020, modeled through a multi-region community model.

Crested porcupine, hare and *Martes spp.* did not show pronounced variations in their number of events at growing rates of human frequentation, with the decrease in diurnal events compensated by an increase in nocturnal ones. Red squirrel, though being the smallest species, displayed a pattern similar to the largest ones, with a general decrease in all event types, especially diurnal ones (Red squirrel: $\beta 1_{day}$ = -0.55; $\beta 1_{crep}$ = -0.17; $\beta 1_{night}$ = -0.02).

The effect of distance from the closest settlement was less consistent across species, with some species, especially larger ones, exhibiting an increase in the number of diurnal events further away from towns (e.g., Brown bear: $\beta 2_{day}$ = 0.96; BCI: 0.40, 1.57; Mouflon: $\beta 2_{day}$ = 0.71; BCI: 0.53, 0.88; Suppl. Fig. D.3, Suppl. Fig. D.7 and Suppl. Fig. D.11), whereas other species, especially the small and medium sized ones, showed a general decrease in the total number of events at greater distances from towns (e.g., Wild cat: $\beta 2_{day}$ = -1.07, $\beta 2_{crep}$ = -0.69, $\beta 2_{night}$ = -0.63; crested porcupine: $\beta 2_{day}$ = -1.02, $\beta 2_{crep}$ = -0.81, $\beta 2_{night}$ = -0.60).

Most species level effects of elevation were positive or close to zero (Suppl. Fig. D.4, Suppl. Fig. D.8 and Suppl. Fig. D.12), and the stronger relations, especially on the diurnal and crepuscular component, were shown by polecat ($\beta 3_{day}$ = 2.13; BCI: 1.03, 3.34), wildcat ($\beta 3_{day}$ = 2.12; BCI: 1.02, 3.33), crested porcupine ($\beta 3_{day}$ = 2.38; BCI: 1.20, 3.70), chamois ($\beta 3_{day}$ = 0.59; BCI: 0.05, 0.93), mouflon ($\beta 3_{crep}$ = 1.13; BCI: 0.72, 1.56) and bear ($\beta 3_{day}$ = 0.41; BCI: -0.03, 0.84). Terrain slope did not have marked effects at species level (Suppl. Fig. D.5, Suppl. Fig. D.9 and Suppl. Fig. D.13), with the exception of the positive response of nocturnal events of brown bear ($\beta 4_{night}$ = 0.92; BCI: 0.55, 1.29), wild boar ($\beta 4_{night}$ = 0.61; BCI: -0.02, 1.69), mouflon ($\beta 4_{night}$ = 0.21; BCI: 0.02, 0.40), chamois ($\beta 4_{night}$ = 0.64; BCI: 0.21, 1.01), crested porcupine ($\beta 4_{night}$ = 0.62; BCI: -0.02, 1.51) and rabbit ($\beta 4_{night}$ = 0.26; BCI: 0.03, 0.48). Roe deer showed a decrease of diurnal events at increasing steepness ($\beta 4_{night}$ = -0.56; BCI: -1.20, 0.01).

Additionally, we also estimated area and species-specific effects on occupancy. Coefficient estimates at area level were centered around zero (Suppl. Fig. D.14), as expected when species within a community present contrasting effect that cancel

each other out in the common mean. Only the hare occupancy increased at increasing rates of human passage in Area 1, whereas we estimated no significant variations for any other species in the other areas (Suppl. Fig. D.15). Furthermore, roe deer, western polecat, crested porcupine, badger and brown bear all decreased their occupancy at increasing distance from towns, while the opposite pattern was estimated for the wolf and wild boar, which consistently increased their occupancy further away from settlements (Suppl. Fig. D.16). Conversely, red squirrel and red fox had contrasting coefficients in the four areas or did not present any significant trend. Occupancy was also negatively correlated with terrain elevation for red squirrel, Martes spp., badger, wild boar, and wild cat, while there was a positive association for rabbit, hare, raccoon, roe deer and fallow deer. All the other species had either inconsistent coefficients in the four areas, indicating local responses to topography and habitat characteristics specific to each area, or did not present strong associations for any area (Suppl. Fig. D.17). Finally, we found no marked trend between the species-specific occupancy probability and terrain slope, except for fallow deer in Area 4 (Suppl. Fig. D.18).

The post-hoc linear regressions indicated that the coefficient estimate for number of events in relation to human passage was inversely proportional to the log of body mass for diurnal (β = -0.21 ± 0.12 SE; Fig. 4.6A) and crepuscular events (β = -0.14 ± 0.10 SE), but not for nocturnal ones (β = 0.00 ± 0.07 SE). The log of body mass was positively related to the coefficients of distance from towns on number of events, more strongly for diurnal events (β = 0.46 ± 0.16 SE; Fig. 4.6B), and less pronouncedly for crepuscular (β = 0.38 ± 0.15 SE), and for nocturnal ones (β = 0.36 ± 0.19 SE). Furthermore, in relation to human passage, all three guilds presented a higher mean coefficient estimate for nocturnal events compared to the diurnal and crepuscular ones (Fig. 4.6C), with herbivores in particular having significant differences among the temporal activity in the three time intervals ($F_{(2,69)}$=13.41, $p<0.001$), and the most significant difference between diurnal and nocturnal events ($p<0.001$). Additionally, omnivores had a significantly different diurnal behavior compared to the other guilts ($F_{(2,135)}$=3.53, p=0.03), with significantly lower diurnal

coefficient estimates (p=0.04, Fig. 4.6C). Conversely, we did not find significant trends among guilds and temporal activity in the three time interval in relation to the proximity to the closest town (Fig. 4.6D).

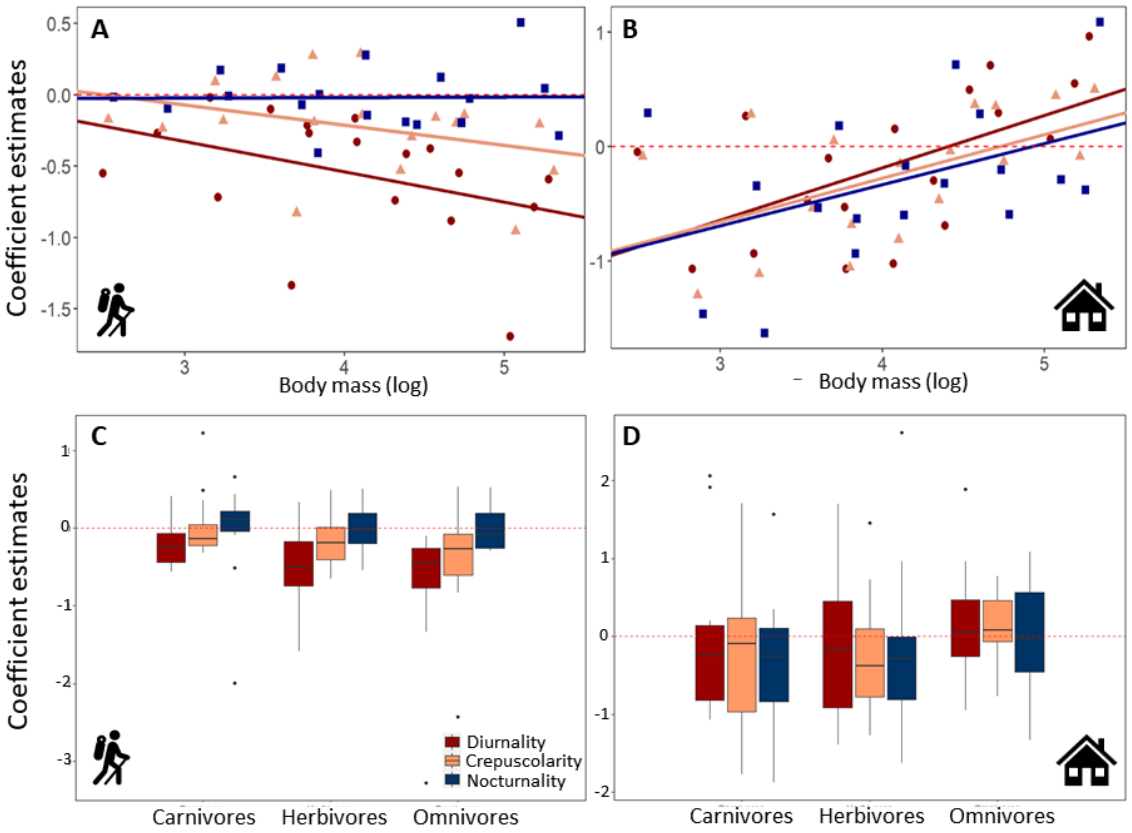

Fig. 4.5 Post-hoc analysis of the coefficient estimates of the three time period: diurnal events (red), crepuscular events (orange) and nocturnal events (blue). From top left: regression of the coefficient estimates for the effect of human passage (Panel A) and distance from the closest town (Panel B) in relation to the body mass of mammals (logarithmic), boxplot of coefficient estimates according of human passage (Panel C) and distance from the closest town (Panel D) in relation to the trophic guild. The dotted horizontal line represents a coefficient equal to zero. Data derive from systematic camera trapping in four protected areas of central and northern Italy during 2020, modeled through a multi-region community model.

4.4 DISCUSSION

By systematically monitoring the community of medium and large-sized mammals in four PAs of the European Natura 2000 network and neighboring areas, we found that wildlife consistently tended to decrease site use and increase nocturnality at higher rates of human passage. Indeed, we first reported that across the four areas, wildlife had a predominant crepuscular and nocturnal behavior and little overlap with the temporal activity of humans in the parks, which were exclusively diurnal. Despite this, we also found that this trend became more evident at sites with more intense human activity since the number of diurnal events decreased sharply, and crepuscular events mildly in response to increased human frequentation. Instead, nocturnal events remained essentially unvaried, thus becoming the relative majority. This effect was consistent across species, since all had a response to human passage that was more negative for diurnal than for nocturnal events, except for the red fox. However, this pattern was stronger for species with larger body mass, for which the decrease in diurnal events led to a dramatic drop in the general use of sites with high human frequentation. Crested porcupine, hare and martens did not show an overall decrease in site use with growing human passage, but rather a shift towards nocturnal activity. Therefore, the mammalian species we studied did not differ in the tendency to increase nocturnal behavior at higher human frequentation but more in the strategy adopted to avoid disturbance: large-bodied species and omnivores, together with badger, wildcat and squirrel avoided humans both in space and time by diminishing the passage at more disturbed sites and concentrating it during the night, whereas other medium-sized species avoided humans only temporally, since their total events either remained constant or even increased at more disturbed sites, but anyway focalized at night-time. Thus, our prediction P1A (lower site-use in response to human outdoor activities) was generally confirmed, even if most of the reduction was in diurnal and crepuscular events, supporting our prediction P1B (increased nocturnality in response to human outdoor activities). The spatio-temporal avoidance of human

passage was generally stronger for species with larger body mass, confirming prediction P3A. Instead, contrary to our prediction P3C, we found that omnivores rather than carnivores displayed a more marked human avoidance, which is reflected in a reduction of their diurnal activity and a limitation in the use of sites more frequently visited by trekkers. This trend was recently found also for omnivorous species in south-east Asia, where the human presence caused a shift in their temporal and foraging activities from diurnal to nocturnal hours (Osugi et al. 2022). Conversely, our prediction P4 (prey use humans as shield against predators) was not confirmed, since ungulates and even small prey such as squirrels and rabbits showed marked spatio-temporal avoidance of humans.

At sites further away from towns, crepuscular and nocturnal events decreased at community level, while diurnal events did not change. Therefore, our prediction P2B (increased diurnality further from towns) was confirmed since diurnal events became the relative majority. However, our prediction P2A (increased use of site further from towns) was not confirmed at community level, since the decline of crepuscular and nocturnal site use further from towns resulted in an overall reduction of site use. Opposite to the trophic guilds for which we did not find any relevant trend (prediction P3D not met), larger species seemed to avoid towns more markedly than smaller ones, confirming prediction P3B (spatio-temporal avoidance of towns by larger species) displaying an increase in the number of events at greater distances from human settlements, especially for diurnal events. On the contrary several small and medium mammals showed even a decrease in total number of events at more remote sampling sites. This pattern could be due to higher spatial requirements of bigger species, needing less fragmented and modified habitats, but possibly also to parallel habitat preferences if suitable environments for small sized species are more common close to towns. Hares and rabbits, for example, are known to favor more heterogeneous landscapes with presence of grasslands and agricultural fields (Naldi et al. 2020), that in our study areas are located around human settlements, and that give way to dense continuous forests further away from settlements, at PAs cores. In turn, lower density of small prey at greater distances

from urban areas might explain the higher site use in proximity to settlements in the case of polecat and wild cat. Yet we detected a higher variability between areas in the spatio-temporal effect of the distance from human settlements than that of human outdoor activities, suggesting that the local configuration of the coupled human-modified and natural systems likely plays a role. Ultimately, these results also indicate that human active disturbance can be a stronger driver of mammalian behavioral change than structural landscape modifications, as already found by previous research (Corradini et al. 2021, Nickel et al. 2020).

Overall, our target communities heightened their site use at higher elevation and steeper slopes. Though this might partially reflect ecological preferences by some species, like chamois and mouflon, it may also derive from a further strategy to avoid human activities, generally concentrated at low elevations and along valley bottoms. This is especially relevant for those species like brown bear or wildcat, that do not possess specific adaptations for the mountainous environment or rugged terrain, and that regularly utilize lowlands in pristine areas with low human presence (Tammeleht et al. 2020, Ferretti et al. 2022). Interestingly, the topographical variables did not relate with site use differentially during diurnal, crepuscular and nocturnal hours, in contrast to the anthropogenic variables that induced behavioral responses with an inherent temporal component.

The sampling design chosen targeted trails and unpaved roads, hence the inferences we obtained must be interpreted in light of such non-random placement of detectors and cannot be extended to the whole extent of the studied areas. Spatio-temporal responses of mammals to human passage and to proximity to towns might be different in locations outside of the trail and road networks, for example with a lower tendency to nocturnality in dense forest stands where humans cannot access (Tanwar et al. 2021). Indeed further research is needed to understand the spatial extent of the impact provoked by recreational activities outside the network of trails. However, our camera-trap placement was functional to the aim of simultaneously detecting the whole pool of medium and large wild mammals and humans, and previous research suggests that this sampling design is more cost-effective, more

efficient at detecting rare species and species such as large carnivores that mainly travel along well-established paths and can give similar community metrics compared to random designs (Tanwar et al. 2021, Cusak et al. 2015). Interestingly moreover, the patterns we observed using photographic events as dependent variable were not evident with occupancy modelling. This is not surprising and matches previous research highlighting that since occupancy quickly asymptotes to 1 it cannot measure a gradient of site use intensity once 100% occurrence probability has been reached, due to the binary nature of presence/absence data (Suraci et al. 2019, Salvatori et al. 2023). For these reasons occupancy might not be the ideal variable to represent gradients of animal space use in continuous habitats (Efford and Dawson 2012, Parsons et al. 2017).

Our results suggest that human outdoor recreation and the proximity to urban areas might affect the behavior and movement patterns of larger mammals more than that of smaller species, since the increase in nocturnality with more intense human frequentation was proportional to species body mass, as was the case for the increase in diurnality moving away from urban areas. Suraci et al. (2021) found that body mass and spatial requirements were among the best predictors of the degree with which mammals used areas with high human footprint (i.e., intense structural modifications) at a continental scale, with smaller species exhibiting tolerance towards landscape modification and larger ones displaying spatial avoidance. Yet, they did not find a similar pattern regarding the intensity of human frequentation, most probably because the avoidance of human presence, largely diurnal, has a preeminent temporal component, as shown by our results. This general activity shift towards nocturnality may imply that terrestrial mammals not only have less room to roam (Tucker et al. 2018, Wilcove et al. 2008), but also less time to be active. By avoiding diurnal humans and seeking refuge during night-time, animals might experience greater pressure from ecological competitors and predators, all forced to exploit darkness hours (Gaynor et al. 2018, Bonnot et al. 2020). However, spatial avoidance of trails intensely used by human recreationists and a temporal shift towards nocturnal hour, though potentially implying

physiological costs for wildlife (Larson et al. 2016), might not directly affect survival and reproduction. Indeed, long-term results from one of our target areas show that wild mammals display stable and increasing trends even under intense human visitation of their habitat (Salvatori et al. 2023). Nonetheless, this plastic behavioral responses to human presence can potentially modify inter-specific dynamics and ecological processes (Reed et al. 2008). High human risk perception in natural areas, by concentrating wild mammals within more densely covered forests, that provide more efficient shields to human disturbance, has been suggested to even modify the nitrogen biogeochemical cycle, with the potential for soil eutrophication (Segar et al. 2022). Similarly, the avoidance of humans and their infrastructures can intensify forest browsing by ungulates in the less disturbed and more secluded areas, with potential negative impacts on forest dynamics (Mathisen et al. 2018). Both scenarios are in line with our findings that ungulates consistently avoided areas with high rates of human frequentation, possibly resulting in aggregation of herbivores in less disturbed and accessible areas. That brown bear and wolf tended to avoid humans and towns in space and time, especially during daylight, is encouraging for the large carnivore-human coexistence, thanks to a low encounter probability, but is concerning for the weakened ecological role that large carnivores can assume under an intense landscape of human fear (Ordiz et al. 2013). With these concerns in mind, avoidance behaviors by wildlife such as those detected in the present study give ground for optimism towards the harmonization of wildlife protection and touristic access in natural and protected areas. Nonetheless, other faunal taxonomic groups such as reptiles, amphibians and ground dwelling birds may suffer disturbance from outdoor recreation more compared to mammals, and in extreme cases experience severe population declines (e.g., Garber et al. 1995).

As world governments pledge to protect 30% of lands and seas through the Kunming-Montreal Global biodiversity framework, protected areas will cover a pivotal role in the global challenge to halt the biodiversity crisis (CBD 2022). Since protected area management is fundamental to reach desired conservation outcomes (Wauchope et al. 2022), knowledge on human frequentation and wildlife responses

along trails and roads is functional to managing human-wildlife coexistence ee.g., through spatial and temporal zoning of access (Reed et al. 2008, Whittington et al. 2019). Many protected areas however currently lack adequate funding or personnel to enforce existing regulations and to manage mass tourism, whose magnitude within PAs is increasing worldwide, and is projected to grow further in the future (Balmford et al. 2015, National Park Service 2023, Smith et al. 2019). Furthermore, our results call for caution when planning new roads or trails within natural and protected areas, as this may translate into further behavioral impact on wildlife. Finally, our study underscores the need for harmonizing wildlife monitoring techniques and protocols across the sites of an ecological network in order to collect comparable results and gain insight on general ecological phenomena while also accounting for local specificities.

4.5 ACKNOWLEDGMENTS

We are very grateful to the managers and other personnel of the following institutions involved in the project for facilitating data collection: Parco Naturale Adamello-Brenta, Parco Naturale Paneveggio-Pale di San Martino, Parco Nazionale delle Foreste Casentinesi, Parco Regionale delle Alpi Apuane, Servizio Faunistico of the Provincia Autonoma di Trento, Reparto Carabinieri Forestali and Reparto Carabinieri Biodiversità of Pratovecchio. We also thank all the people that assisted us invaluably during fieldwork or sampling design, especially Claudio Groff, Michele Zeni, Marzia Pin, Yuri Valler, Renato Rizzoli, Paolo Pedrini, Giulia Bombieri, Luca Roner, Mirta Checcacci, Lorenzo Petralia, Giulia Bianchi, and Alberto Masoni. F.R. and I.G. also thank Marco Zaccaroni for assistance with material and Stefano Anile for help with the identification of wild cat images from area 4.

Chapter 5

Widespread anthropogenic extinction filtering of tropical forest mammals even within protected areas

Greco, I., Beaudrot, L., Sutherland, C., Tenan, S., Gorczynski, D., Hsieh, C., *Theriotrop owners** & Rovero, F.

In preparation

* Complete list of co-authors provided in Appendix E.1.

Abstract

The severity and drivers of the 'Anthropocene defaunation' remain debated. Humans are particularly destructive for tropical forests, where many threatened mammals only survive within protected areas. While protected areas are the primary strategy for conserving wildlife, their effectiveness has been questioned, because human pressure in surrounding landscapes may threaten biodiversity within. However, empirical evidence from global-scale, in situ data on wildlife is lacking. Here, by leveraging an unprecedented dataset from >2000 camera-traps we show how the richness and occupancy of mammal communities from 37 tropical forests respond to landscape-scale deforestation, fragmentation, human density, and infrastructure development. We found that fragmentation was negatively associated with occupancy and forest loss was negatively associated with species richness and occupancy, while human density was only negatively associated with species richness. Such decoupling suggests that high human density has contributed to local extinctions that filtered out the most sensitive species, while occurrence rates of persisting taxa remained relatively unchanged. Our results demonstrate that the conservation of tropical forest mammals in protected areas depend on anthropogenic pressures far beyond their borders. Therefore, the Kunming-Montreal target of protecting 30% of land by 2030 may not achieve desired conservation outcomes if threats surrounding protected areas are not addressed.

5.1 INTRODUCTION

An outstanding question in the current biodiversity crisis concerns the severity of the Anthropocene defaunation (Dornelas et al. 2014, Leung et al. 2020). Loss of animals – from local population declines and range contractions to species extinction (Dirzo et al. 2014) – disproportionally affects tropical forests (Schipper et al. 2008). While tropical forests represent the richest biome on earth, human population growth and associated land conversion make habitat loss, fragmentation, and unsustainable hunting major drivers of vertebrate decline (Ripple et al. 2017, Archer et al. 2020), with mammals especially impacted. This results in many tropical mammals now surviving almost exclusively in protected areas (PAs; Pacifici et al. 2020a) or in sparsely populated areas far from major urban centres (Benítez-López et al., 2017). However, the effectiveness of the existing PA network for fully protecting mammals from extinction has been questioned, not only due to their inadequate size and number, but also the lack of connectivity among them (Williams et al. 2022) and a general inability to buffer increasing human pressure, especially in the tropics (Geldmann et al. 2013). Indeed, evidence suggests that increasing anthropogenic threats outside PAs also threatens biodiversity within (DeFries et al. 2005, Laurance et al. 2012, Geldmann et al. 2019, Jones et al. 2018). However, empirical evidence from in situ data on how landscape-scale conditions impact wildlife communities within PAs is lacking. For example, DeFries et al. (2005) estimated that forest loss in the surrounding 50 km outside PAs triggers a decline in tree species richness within PAs, yet empirical evidence and assessments of the consequences of forest loss on wildlife are untested. As governments commit to increasing the global PA estate following the Kunming-Montreal Global Biodiversity Framework6 (2022), such knowledge is foundational for identifying the most effecting conditions for sustaining biodiversity within existing and future PAs (Geldmann et al. 2019).

In this study we test four non-mutually exclusive hypotheses for mechanisms linking variations in tropical mammal community richness and occupancy within PAs to landscape-scale anthropogenic processes outside PAs boundaries (i.e., habitat loss, fragmentation, increasing human density and proximity to infrastructure). We do this

using a buffer that extends 50 km around PAs (DeFries et al. 2005), by investigating anthropogenic effects on species richness and community occupancy. Species richness represents the size of the mammalian community and here we focused on its geographic (among-area) variation, while community occupancy represents the central tendency of site use probability for all species belonging to a community. Occupancy is a proxy of distribution and abundance (sensu Mackenzie and Nichols 2004) that accounts for imperfect detection and a useful metric to overcome the inherent difficulties of abundance estimation. It reflects vulnerability to local pressures that can ultimately affect variation in species richness. Hence community occupancy and species richness provide complementary information on how mammalian communities respond to anthropogenic pressures (Supp et al. 2014). To date, both data quality and scaling issues have prevented rigorous examination of how these key state variables vary at the global-scale. Indeed, large-scale assessments of mammalian species richness are typically based on range maps (e.g., Rondinini et al. 2011, Howard et al. 2020), which can overestimate species presence (Di Marco et al. 2017) and do not contain information on abundance. For mobile species, moreover, range maps confound absence with non-detection, potentially biasing the estimation of true community size (Dorazio et al. 2006). Meta-analyses drawn from the literature are prone to biases due to heterogeneity in data quality and spatio-temporal scales (Stewart 2010), which prevents addressing questions requiring standardized designs. On the contrary, when collected at large and representative scales, systematic monitoring yields in situ data that produce more robust inferences that are more appropriate for empirically testing ecological hypotheses at the global scale (Fraser et al. 2013).

Our first hypothesis is that as PAs become isolated forest islands, species-area effects alter their capacity to sustain both viable populations and the full complement of species. Hence, we predict lower mammalian richness and occupancy with decreasing forest cover at the landscape-scale (H1.P1). Second, we hypothesize that the size and shape of remnant forest patches in the landscape (i.e., habitat configuration) can affect source-sink dynamics across PAs and their surrounding landscapes (Hansen et al. 2011). Reduced patch area and increasing isolation

between them have been associated with reduced abundances for a range of taxa, including mammals (Haddad et al. 2015). Similarly, global assessments have shown reduced mammal distributions with higher fragmentation (Crooks et al. 2017). Hence, we predict reduced mammalian occupancy in PAs surrounded by more fragmented forest cover (H2.P1).

Third, we hypothesize that the presence of settlements and roads in the landscape surrounding PAs favours human permeability into forest interiors, driving the exploitation of resources and hunting (Benítez-López et al., 2017) and may force wildlife distributions towards suboptimal habitats (Scott et al. 2001). We therefore predict lower mammalian occupancy near infrastructure (H3.P1). Conversely, anthropogenic edges can promote the use of open habitats and agricultural matrices by some species for additional/complementary dietary resources or refugia (Clough et al. 2011), hence resulting in no overall variation in community occupancy as some species increase in occupancy while others may spatially avoid these places (H3.P2). Fourth, we hypothesize that increasing human population density around PAs represents both a direct stressor to wildlife and a proxy for threats that are unknown or difficult to measure, such as fear or forest resource extraction (Pacifici et al. 2020b, Gaynor et al. 2019). Human density can affect species distributions, resulting in either range expansions or contractions for species that exploit anthropogenic environments or not, respectively (Pacifici et al. 2020b, Suraci et al. 2021), and thus no net change in average community occupancy (H4.P1). Additionally, for 16 tropical forest PAs, surrounding human density was associated with lowered richness of area-demanding and habitat specialist guilds, particularly insectivores (Rovero et al. 2020). In US parks, greater human density in a 50 - 100 km buffer predicted mammal extinction inside PAs (Parks and Harcourt 2002), thus, we predict lower mammalian richness in PAs with higher surrounding human density due to the potential loss of sensitive species (H4.P2).

Camera trapping has revolutionized wildlife monitoring (Rovero and Kays 2022), and its potential for scaling-up and standardization is unmatched (Steenweg et al. 2017). Here, we establish *TherioTrop*, an original dataset of detections for 241 primarily ground-dwelling mammalian species in 37 forest areas across the tropics

collected by 2,021 camera-traps (Fig. 5.1). *TherioTrop* areas span a gradient of anthropogenic pressure and legal protection status, from nearly intact to severely fragmented, human-dominated landscapes, and from PAs to multiple-use and unmanaged forests, thus providing an unprecedented opportunity to quantify the effects of anthropogenic disturbance on tropical mammal richness and occupancy globally.

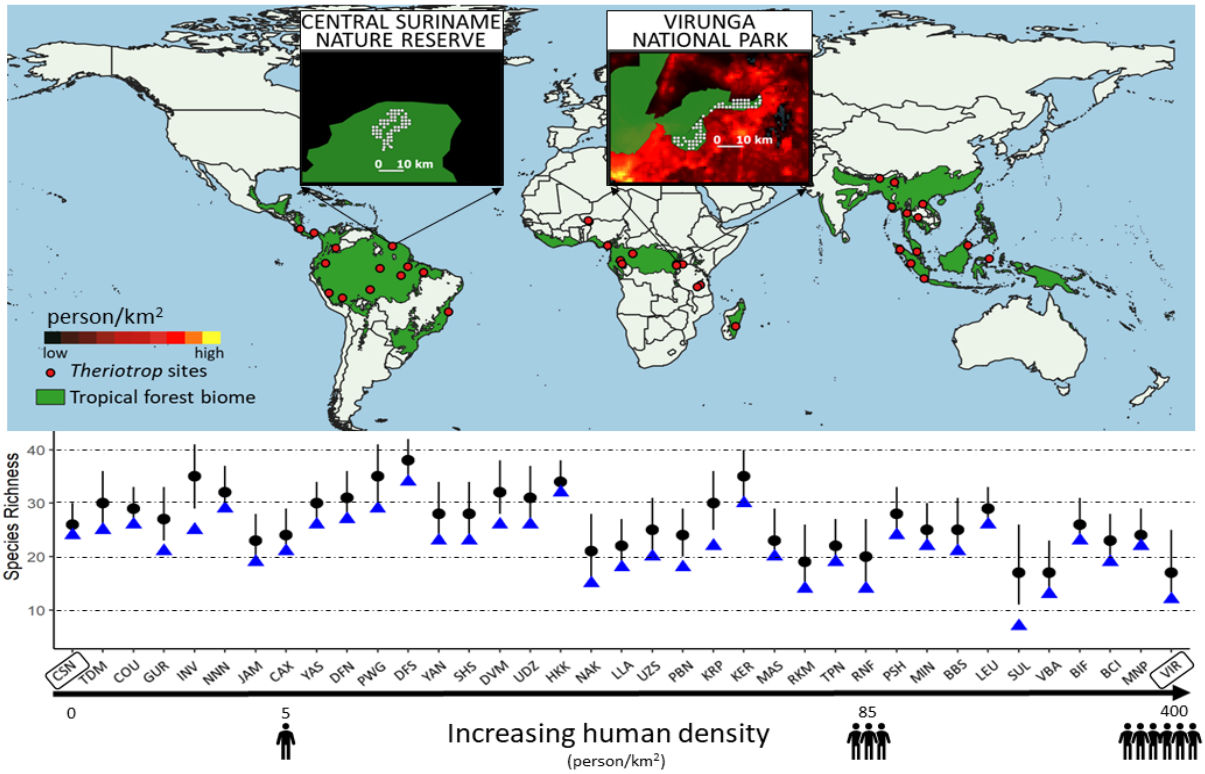

Fig. 5.1 Map of the 37 tropical forests in the TherioTrop database. Inset maps represent two protected areas embedded in contrasting landscapes: intact one with low human density (left) and anthropogenic one with high human density (right). Green areas in insert maps represent PA boundaries. The bottom chart shows estimated species richness (black dots) and the observed number of detected species with camera-traps (blue triangles) in each forest, which are ordered by increasing human density. See Suppl. Table D.2 for the list of site codes.

We apply a Bayesian multi-species multi-region occupancy model to the *TherioTrop* data to simultaneously quantify drivers of species richness and occupancy to test the four hypotheses above by relating variation in richness and occupancy to forest cover, habitat configuration, human density, and proximity to infrastructures (Fig. 5.2). We also include the size and habitat productivity of the sampled areas, as well as

continent, to account for their potential influences on species richness.

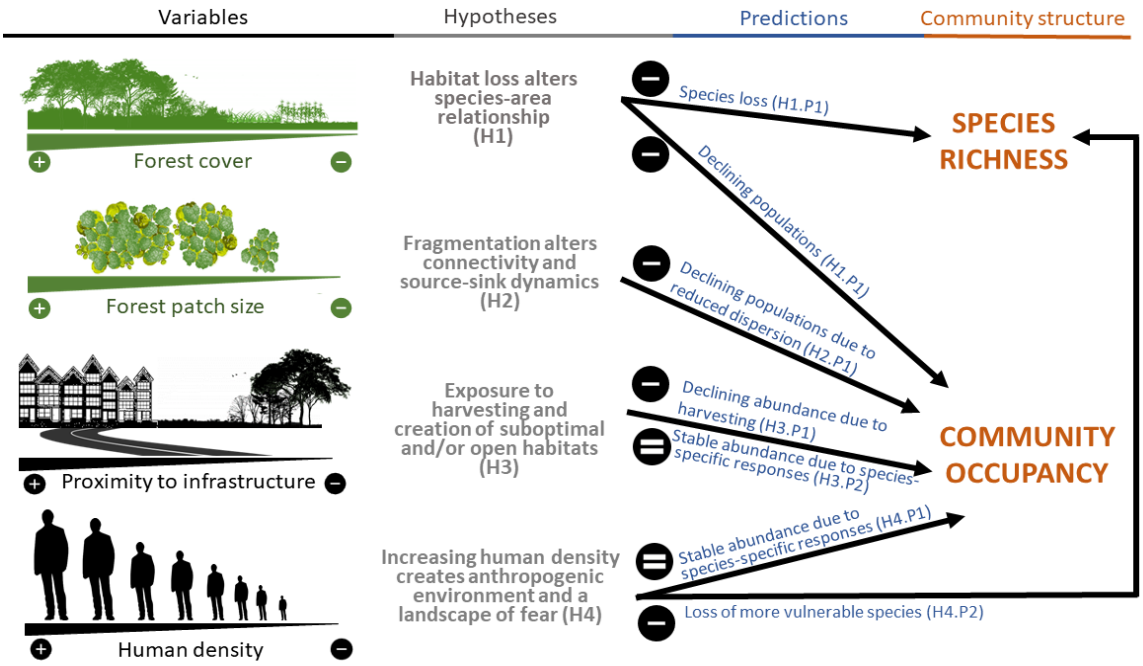

Fig. 5.2 Hypothesized processes for the influence of forest cover and human density in the landscape on species richness and community occupancy (H1 and H4) and for the influence of forest configuration in the landscape (i.e., fragmentation and connectivity of remnant forest patches) and proximity to settlements on community occupancy (H2 and H3). Landscape is defined as the area extending 50 km from protected areas borders (DeFries et al 2005).

5.2 RESULTS

Estimated richness ranged from 17 species in Virunga National Park, DRC (90% Bayesian Credible Interval, CI: 13 – 22) and Volcan Barva, Costa Rica (CI: 14 – 23), to 38 species (CI: 35 – 41) in Djoum, Cameroon (Fig. 1). Species richness was lower in the Neotropics (β = -0.31, CI: -0.62 – -0.05) than other continents (Neotropics = 25 ± 1.0 SE, Afrotropics = 29 ± 1.7 SE, Indo-Malayan tropics = 27 ± 1.7 SE species; Fig. 5.3; Suppl. Table 1). Richness was significantly and positively associated with landscape-scale forest cover (β = 0.12; CI: 0.01 – 0.24) and was significantly and negatively associated with landscape-scale human population density (β = -0.19; CI: -0.31 – -0.06; Fig. 5.3). These results support the hypotheses that higher forest cover sustains

richer communities (H1.P1) and that human pressure due to increasing population density in tropical forests negatively impacts species richness (H4.P1). In contrast, mammalian richness was not significantly associated with the size or NDVI of the sampled areas (Fig. 5.3; Suppl. Table E.1).

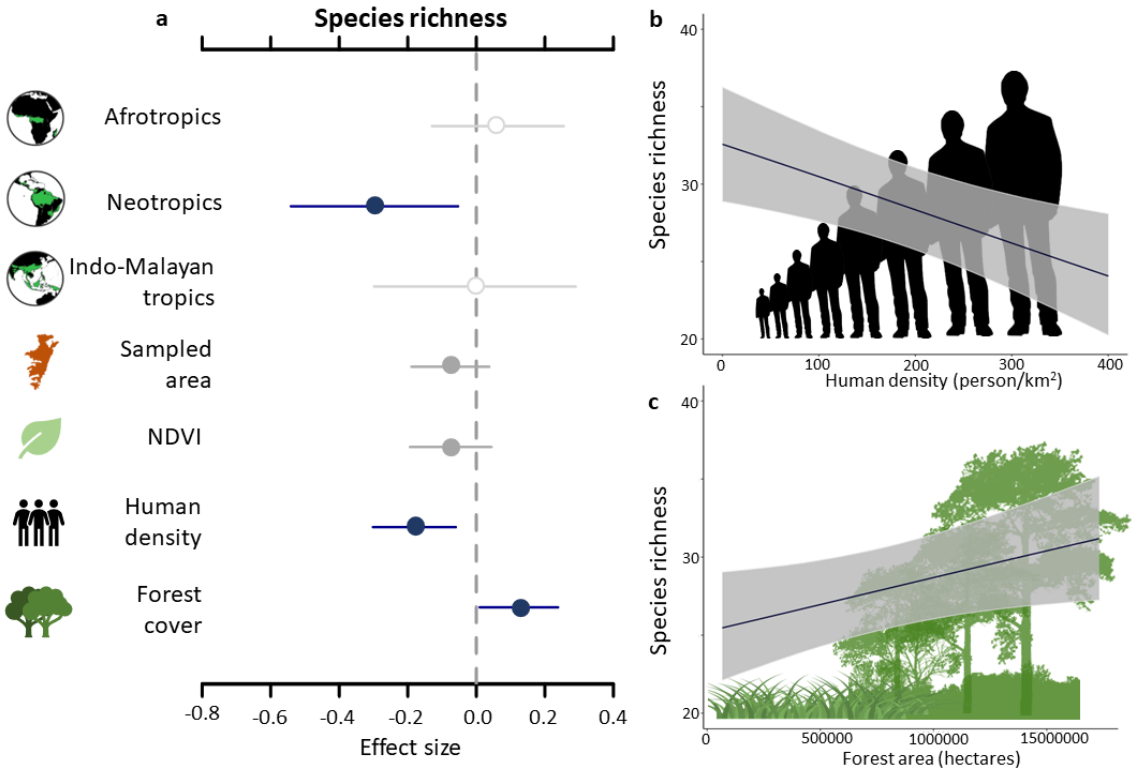

Fig. 5.3 Results of predictors of estimated mammalian species richness from the multi-region, multi-species occupancy model applied to the 37 study areas across the tropics. **a**, standardised beta coefficients for the effects of predictors, with human density and forest cover measured on a buffer extending 50 km around the sampled area. Points indicate median of the full posterior distribution. Solid blue lines represent significant effect with 90% Bayesian Credible Interval (BCI) that do not overlap 0 (dashed vertical line). Closed grey points represent 50% BCI that do not include 0, while open grey points indicate that 50% BCI overlaps 0. **b**, bivariate plots of predicted species richness in relation to increasing human density, and **c**, increasing forest area availability (bottom). Grey shaded areas indicate 90% BCI.

The relationships between average species-specific occupancy and anthropogenic conditions were broadly similar to those of richness, but with some important differences that support the value and complementarity of richness and community occupancy. Like species richness, occupancy was significantly and positively

associated with higher landscape-scale forest cover (θ = 0.16; CI: 0.01 – 0.32; Fig. 5.4), and habitat configuration (θ = 0.40; CI: 0.2 – 0.57). Hence, the species within a community occupied a greater portion of the landscape when this consisted of larger and more continuous forest patches. Consequently, as predicted, habitat loss and fragmentation were negatively associated with community occupancy (H1.P1 and H2.P1, respectively). Unlike species richness, however, community occupancy was not significantly associated with landscape-scale human density (H4.P1) or distance to infrastructure (H3.P2, Fig. 5.4).

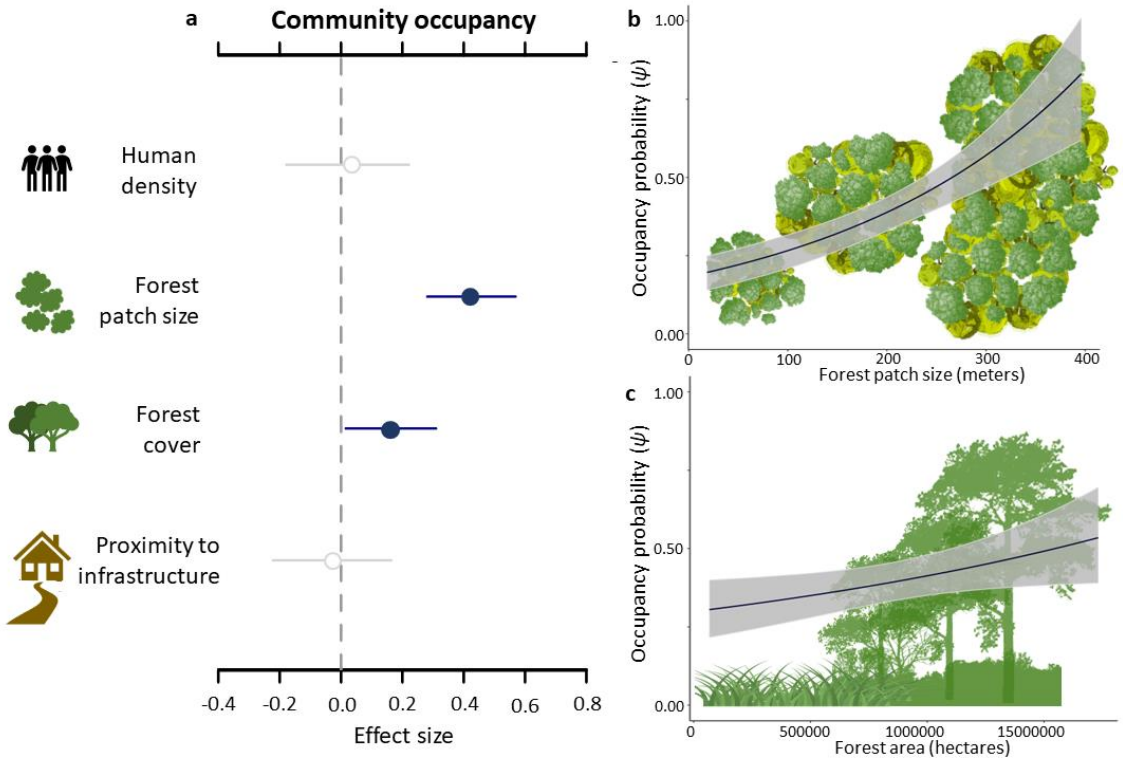

Fig. 5.4 Results of predictors of estimated community occupancy probability (ψ) from the multi-region, multi-species occupancy model applied to the 37 study areas across the tropics. **a**, standardised coefficients for the effects of predictors, with human density, the forest patch size and forest cover measured on a buffer extending 50 km around the sampled area. Points indicate median of the full posterior distribution. Solid blue lines represent significant effect with 90% Bayesian Credible Interval (BCI) that do not overlap 0 (dashed vertical line). Closed grey points represent 50% BCI that do not include 0, while open grey points indicate that 50% BCI overlaps 0. **b**, bivariate plots of the predicted community occupancy probability in relation to increasing forest patch size, and **c**, increasing forest cover. Grey shaded areas indicate 90% BCI.

5.3 DISCUSSION

Our results suggest that human density, habitat loss, and fragmentation have detrimental consequences for tropical forest wildlife in protected areas worldwide. The extent of forest cover in the landscapes surrounding PAs was critical for sustaining both the number of species and their average occupancy, with PAs surrounded by more extensive forest cover supporting more wildlife. To our knowledge, this is the first study that has tested predictors of mammal community size and occupancy throughout the tropics using standardised in situ data. By simultaneously evaluating both aspects of community structure, we were able to identify key differences in the effects of anthropogenic pressures on species richness versus occupancy. Specifically, we found that protected forests surrounded by higher human population density had significantly fewer mammal species. Moreover, average mammal occupancy was lower in PAs surrounded by smaller remnant forest patches. Combined, these findings indicate that landscape fragmentation contributes to the decline of mammal occupancy, ultimately leading to local extinctions in highly populated landscapes. Therefore, accounting for human density and anthropogenic pressures far beyond sampling locations is critical for understanding the drivers of tropical mammal community composition even within protected areas (DeFries et al. 2010).

That richness decreased with higher surrounding human population density is arguably the most robust evidence to date based on field data that documents the effects of human density on wildlife within PAs. High human density may lead to extirpation from overhunting (Benítez-López et al. 2019) and species loss from other detrimental human activities (Pacifici et al. 2020). In contrast to the effect on richness, human density did not significantly predict variation in occupancy. Therefore, in areas with high landscape-scale human density and lower richness the distribution and abundance of remaining species were primarily associated with habitat extent and configuration. Such decoupling in the responses of richness and occupancy to human density suggests that local extinction filtering (Balmford 1996) has occurred. Hence, average occupancy may be driven by ‘winners’, i.e., species that survive, or even thrive, in human-dominated landscapes, while ‘losers’ have become

locally extinct. Proximity to infrastructure did not significantly predict average community occupancy. Infrastructure may positively affect occupancy for some species and negatively affect occupancy for others, hence neutralizing each other out (Pacifici et al. 2020, Semper-Pascual et al. 2022). While successful species generally have fast life-history and opportunistic diets (Pacifi et al. 2020, Suraci et al. 2021), more work is required to identify which functional traits predict tropical mammal forest winners and losers (Devictor et al. 2008).

Landscapes with greater forest cover supported richer communities of mammals, supporting the prediction that the anthropogenic alteration of species-area processes leads to reduced local species richness (Newmark 1986). Furthermore, communities had higher occupancy when forest cover was more extensive and less fragmented. Hence, larger and better-connected forest habitat sustains populations with wider distributions (Bedoya-Durán et al. 2021). That the effect of the landscape-scale habitat configuration on community occupancy was even higher than of forest cover may be attributable to fragmentation altering source-sink population dynamics and hence the resulting reduced capacity of species to recolonize forest fragments (Saura et al. 2014).

Our results suggest that the anthropogenic alteration of the landscape challenges the capacity of PAs to buffer disturbance. For example, estimated species richness was lowest (17) in Virunga National Park, Rwanda, which is a well-protected stronghold for the mountain gorilla (*Gorilla beringei beringei*) surrounded by a highly fragmented landscape (28% of forest cover) and among the highest human population density (400 persons/km^2) in the dataset. In contrast, estimated species richness was among the highest (34) in PWG, a sustainable logging concession in Gabon surrounded by the largest estimated forest area in the landscape (92% of forest cover) and low human population (6.57 persons/km^2). While we acknowledge that local climatic or habitat characteristics may also influence species richness, this signal was also consistent among PAs within the same ecosystem that had similar environmental and historical characteristics but contrasting human pressure. For example, in the Udzungwa Mountains of Tanzania reduced richness and occupancy in the Uzungwa Scarp Nature Reserve compared to the Udzungwa Mountains National

Park are associated with decades of isolation of the former forest, with mounting anthropogenic pressures and less ground protection (Oberosler et al. 2020).

Despite the well-known relationship of large sampling areas (Newmark 1986) and more productive forests (Gebert et al. 2019) supporting more species, we found that landscape-scale anthropogenic pressures had a marked effect on species richness while sampling area and plant productivity were not significantly associated with richness. In addition to the variables we examined, variation in richness among areas has likely been influenced by other factors, particularly variation in biogeographic history, such as regional differences in historical extinctions (Stuart 2015). In particular, the significantly lower richness estimated for the Neotropics may reflect the disproportionally high Pleistocene megafauna extinctions, in which the continent lost ca 80% of large-bodied mammals, which were primarily ground-dwelling (Stuart 2015).

By focussing on mammals in tropical forests, where similar environments support communities with similar functional composition and vulnerability to anthropogenic pressures (Penone et al. 2016, Rovero et al. 2020), and by using in situ data from the largest number of sites with the widest gradient of protection to date, we have revealed that landscape-scale anthropogenic conditions are highly detrimental to wildlife within PAs. Our results demonstrate that the composition of tropical forest mammal communities is tied to anthropogenic pressures and environmental changes that stretch far beyond the immediate area where they occur (Laurance et al. 2012, Geldmann et al. 2019). Protected areas may be the last refugia to prevent extinction of many charismatic and keystone species throughout the tropics (Jones et al. 2018, Pacifici et al. 2020). Nevertheless, our study demonstrates existing challenges that need to be confronted to ensure the effectiveness of current and future PAs for maintaining biodiversity. The landscape surrounding these areas provides vital habitat for wildlife and ecosystem processes (Williams et al. 2022, Woodroffe and Ginsberg 1998, Hansen and DeFries 2007). Hence habitat and connectivity restoration, establishment of buffer zones, and sustainable land-uses throughout PA landscapes, are some much needed measures (Wells and McShane 2004), especially given the UN's Kunming-Montreal Global Biodiversity Framework

now committed to effectively protect 30% of land by 2030 (Kunming-Montreal Global biodiversity framework 2022). With half of the world population expected to reside in tropical regions by 2050 (Archer et al. 2020), the fate of tropical biodiversity depends on effective conservation more urgently than ever.

5.4 METHODS

5.4.1 Study areas, camera trapping and *Theriotrop* dataset

We collated data from camera trapping conducted in 37 areas across the tropical forest biome, from 19 countries in three continents (Fig. 5.1): Afrotropics (N = 12), Neotropics (N = 13), and Indo-Malayan tropics (N = 12). Seventeen of these areas form the TEAM Network (Rovero and Ahumada 2017), all being well-protected PAs except for Manaus (Brazil) which is managed for scientific research. The additional areas extend the gradient of protection regime, anthropogenic disturbance, and landscape configuration, as they include PAs of different status (from National Parks and Nature Reserves to Wildlife sanctuary), and areas managed as plantations or logging concessions (Suppl. Table E.2). The landscape surrounding the study forests held a wide range of human population density, from virtually unpopulated to highly populated (Fig. 5.1). We selected the additional datasets using the literature or by asking scientists, based on adherence to the TEAM protocol and to achieve a balanced number of areas across continents (Suppl. Fig. E.1). Camera trapping in TEAM areas followed a standardized protocol rolled out during one dry season (in 2014 or 2015), consisting of the systematic sampling of 60 camera trap sites evenly spaced 1 to 2 km apart. In the additional areas data were collected for a single-season during the period 2010 to 2019 with similar spacing among sites as TEAM's and a range of 32 to 68 sites sampled. Effort varied, and we selected the first 30 days of sampling when it exceeded (Suppl. Table E.3).

As a result, TherioTrop collates camera trap images from the 37 areas collected at 2,021 camera-trap sites (mean of 54.76 per area) sampled through 63,041 camera-trap days (range 1,088 - 2,280, mean 1,703). For the analyses we used 559,585 images of wild mammalian species with average body mass >100 g (Beaudrot et al.

2016) that were predominantly terrestrial, as smaller species are not well detected by camera traps and can be of difficult identification. We used IUCN taxonomy (IUCN 2022). This resulted into 241 mammal species in 47 families, 17 orders, and 144 genera (Suppl. Table E.4).

5.4.2 Covariates

For each forest, we derived the following suite of covariates and selected a subset of candidate variables for the model based on collinearity, with Pearson's = 0.5 as the threshold. Covariates related to (a) habitat features, (b) human disturbance, and (c) sampling. The former included: (1) forest cover extending 50 km from the sampled areas, as a measure of available forest habitat, with more forest habitat assumed to support higher biological diversity and richness (Watson et al. 2018, Fahrig 2013); (2) forest patch size, or forest compactness, in a buffer extending 50 km the study forest and representing the average distance one can move in a random direction within the patch, as a measure of decreasing fragmentation and hence greater connectivity (Wintle et al. 2019, Flensted et al. 2016); (3) the Normalized Difference Vegetation Index (NDVI) as an indicator of vegetation biomass and environmental productivity in the sampled area (Pettorelli et al. 2005). Human disturbance variables included: (4) distance from camera trap sites to the closest settlement, representing proximity to cities, forest accessibility to humans (Benítez-López et al., 2017) and higher vulnerability to hunting pressure (Van Kuijk et al. 2022); (5) the human population density extending 50 km around the sampled area, as a measure of human presence and its impact on the landscape (Parks and Harcourt 2002, Harcourt et al. 2001, Verter et al. 2016). Sampling variables included: (6) camera-trap trigger speed, given different camera models can perform differently in detecting species, especially elusive ones (Greco and Rovero 2021); (7) sampled area as an adjustment term for the different sampling effort across forests; (8) continents (i.e., Afrotropics, Neotropics, Indo-Malayan tropics) to account for the different locations and their evolutionary-history and phylogeny of different faunal groups (Lomolino et al. 2016). We standardized all continuous covariates to have mean zero and unit standard deviation. See Supplementary Methods for details on covariates extractions.

5.4.3 Model formulation

We modelled the effect of covariates on species richness and community occupancy on R = 37 forests (hereafter regions) across the tropics, using a multi-region community model (Sutherland et al. 2016), that uses the parameter-expanded data augmentation technique to account for unseen species (Dorazio and Royle 2005). Encounter frequencies of detected species were organized as a three-dimensional array Y, with elements y_{ijr} representing the number of days species *i* was observed at site *j* in region *r*, out of a total of K_{jr} days that the camera was operational. True occupancy states array Z contains elements z_{ijr} representing the species-by-site occupancy states during each survey, conditional on the species being a member of the community in each region (see below). Occupancy states were defined as Bernoulli random variables, with $z_{ijr} = 1$ indicating the site *j* is occupied by species *i*, and $z_{ijr} = 0$ if the site is empty: $z_{ijr} \sim \text{Bern}(\psi_{ir}\, \omega_{ir})$. Parameter ω_{ir} is a species-specific indicator variable denoting whether the species is present in a region, and ψ_{ir} is the species-specific occupancy probability in each region (assumed equal across sites), conditional on species *i* being a member of the r^{th} community. Based on data augmentation, an arbitrary number $M_r = M = 55$ (for all regions) of all-zero encounter frequencies, which can be seen as potentially unobserved species, was added to the detection array Y. The number of unobserved species in each community can therefore be estimated by evaluating which of the $M - n_r$ species (rows of the augmented dataset, where nr is the number of species detected in a region) are members of the r^{th} community (sampling zeros, $\omega_{ir} = 1$) or not (structural zeros, $\omega_{ir} = 0$). The indicator variable ω_{ir} was assumed a random Bernoulli variable with probability Ωr that species i of the augmented array is a member of the r^{th} community of size N_r (i.e., species richness). The data augmentation technique converts the problem of estimating N_r into the equivalent problem of estimating Ω_r, and species richness is derived parameter by summing up the latent indicators ω_{ir}, since the expectation of Nr is equal to Mr Ω_r. Inference at the community level was focused on modelled variation in Ω_r as a function of different covariates (see below). The observation model relates array Z to array Y, such that $y_{ijr} \sim \text{Binomial}(K_{jr}, p_{ijr}\, z_{ijr})$, with K_{jr} denoting the number of sampling occasions (i.e., camera trap days for each

site *j* in region *r*) and p_{ijr} the detection probability. Following this general model formulation, we investigated covariate effects at both community and species level.

Variations in region-specific species richness were investigated with a logit-link model that accounted for region-level variables. We assumed richness to vary in relation to human density (HDEN) and available forest cover (FOREST) in the landscape. We also added the mean NDVI and the size of area sampled by camera traps (AREA) to account for species-area relationship (MacArthur & Wilson 1967) and differences in the sampling effort, and a continent effect (CONTINENT, with Afrotropics as reference level) to account for differences in faunal groups.

$$\text{logit}(\Omega_r) = \beta0 + \beta1 * \text{NEOTROPICSr} + \beta2 * \text{INDO-MALAYAN}_r + \beta3 * \text{AREA}_r + \beta4 * \text{NDVI}_r + \beta5 * \text{HDEN}_r + \beta6 * \text{FOREST}_r$$

Global patterns of variations in occupancy probability were investigated by using species- and region-specific logit-linear model with region-level covariates (Kéry and Royle 2008). We expected occupancy of species i in region r to vary in relation to the human density in the area (HDEN), the available forest habitat (FOREST), forest patch size and compactness (P_SIZE) and the mean distance to the closest settlement:

$$\text{logit}(\psi_{ir}) = \theta0_{ir} + \theta1 * \text{HDEN}_r + \theta2 * \text{FOREST}_r + \theta3 * \text{P\_SIZE}_r + \theta4 * \text{SETTL}_r + \varepsilon_{\psi,ir}$$
$$\text{with } \varepsilon_{\psi,ir} \sim \text{Normal}(0, \sigma_{\psi,r})$$

Detection and occupancy probability were regressed using a logit-link function. We expected detection probability (p_{ijr}) of species *i* at site *j* in region *r*, to be potentially affected by the camera trigger speed (CAM_TYPE) and by the distance from each *j* to the closest settlement (SETTL):

$$\text{logit}(p_{ijr}) = \alpha0_{ir} + \alpha1 * \text{CAM\_TYPE}_{jr} + \alpha2 * \text{SETTL}_{jr} + \varepsilon_{p,ir}$$
$$\text{with } \varepsilon_{p,ir} \sim \text{Normal}(0, \sigma_{p,r})$$

Species- and region-specific variations in occupancy and detection probability were

accommodated by random effects ($\varepsilon_{\psi,ir}$ and $\varepsilon_{p,ir}$) with region-specific random standard deviation ($\sigma_{\psi,r}$ and $\sigma_{p,r}$). This structure allowed us to improve the precision and the predictive capability of the model since data-deficient species can be accounted for by using information from data-rich species (Ovaskainen and Soininen 2011, Zipkin et al. 2009).

We fitted a single model with a fixed number of covariates for which we had ecological a-priori justifications (Zipkin et al. 2009, Zipkin et al. 2010) that these variables could affect state parameters based on ecological relevance. We fitted the multi-region community model in a Bayesian framework using Markov Chain Monte Carlo, and inference was based on 400,000 post-burn-in posterior samples (3 chains, default thinning of 1, and burn-in of 100,000). We assessed model effectiveness by verify chains convergence for every parameter and by using the R-hat diagnostic, with R-hat ≈ 1.01 for successful convergence. The hierarchical model was implemented in Nimble (de Valpine et al. 2017, de Valpine et al. 2021), through R (R Core Team 2022). For details on prior specification of model parameters see Supplementary Method.

5.5 ACKNOWLEDGMENTS

We thank all protected area managers and staff, and all people involved in fieldwork. Part of the data were provided by the TEAM Network initiative, previously a collaboration between Conservation International, the Smithsonian Institution and the Wildlife Conservation Society, and we gratefully thank all TEAM funders and contributors. For Thailand data, we would like to thank Kasetsart University, Kittiwara Siripattaranukul, and the Department of National Parks, Wildlife and Plant Conservation. Fieldwork at Gurupi, Jamari and Terra do Meio was conducted as part of the Brazilian in situ monitoring program of Federal Protected Areas (Programa Monitora ICMBio). At Manas National Park we thank the Department of Forests, Government of Assam, Bodoland Territorial Council, and IUCN-KfW, Panthera and NTCA for financial support. For Myanmar's data we would like to thank all the Istituto Oikos staff for their participation in monitoring activities in the region of Rakhine and

also the Wildlife Conservation Society (WCS Myanmar) for their support and work in the region of Sagaing. Data collection in Gabon, under the research permits (AR0043/18; AE19004), was supported by a FRIA grant of the Fonds de la Recherche Scientifique (FNRS) in Belgium and the "Programme de Promotion de l'Exploitation Certifiée des Forêts" (PPECF), with technical and logistic support provided by the Sustainable Wildlife Management (SWM) Project local staff and the Precious Woods Gabon - Compagnie Equatoriale des Bois (PWG-CEB) logging company. D. Sheil was supported by The Research Council of Norway (project NFR301075). Funding for sampling in Sulawesi was provided by the Global Environmental Facility, as administered through the United Nations Development Programme's Enhancing the Protected Area System of Sulawesi project, Fondation Segré and Mandai Nature. We are grateful for the collaboration of the data collection with the Natural Resources Conservation Agency (BKSDA) North Sulawesi, the Bogani Nani Wartabone National Park, Universitas Sam Ratulangi Manado and the Wildlife Conservation Society Indonesia. Data collection in RPPN Estação Veracel and Pau Brasil National Park (PBN) was supported by Veracel Celulose S.A., and autohrized by SISBIO (#60641). Data collection for Colombia was supported by an Australian Laureate Fellowship awarded to Prof. William F. Laurance (2010), COLCIENCIAS's Postgraduate Scholarship Scheme Francisco José de Caldas, and support from National Federation of Oil Palm Growers (FEDEPALMA). Data collection in Tanzania was conducted under COSTECH and TAWIRI permission to F. Rovero, and funded by the Fondazione Foresta Futura, Wild Planet Trust, Provincia Autonoma di Trento, MUSE – Museo delle Scienze and other donors.

General Conclusions

This thesis shows how the use of standardised and systematic monitoring techniques able to collect information at both species level (including the most cryptic and elusive ones) and community level, coupled with the use of analytical framework able to correct for detection biases, can produce robust assessments on the status and vulnerability of mammal populations and communities, across different scales and geographic areas. In particular, the use of camera traps proved to be a valuable detection method to assess species presence in remote areas, accumulate data for robust statistical analyses in relatively limited time, and simultaneously detect multiple species, including humans and livestock. In our analyses, we estimated that fast-triggered camera models are most suitable for recording fast-moving and elusive species since they are associated with higher detection probabilities. However, although standardization of camera performances (i.e., similar technical characteristics) would always be preferred, we also highlighted that the occupancy analysis can account for potential variations in detection probability due to differences in camera models. Furthermore, the analytical framework of occupancy, and its ability to incorporate ecological factors and adjust for detection variations (MacKenzie et al. 2003, Royle and Kery 2007), provided new insights into species distribution (Chapters 1-3), adaptative strategies (Chapters 2 and 4) and ecological responses (Chapter 5). In addition, the use of comparable camera trapping protocols facilitated the creation of a network of areas consistently monitored (Rovero and Ahumanada 2017, Chapter 4), while the use of standardised data across multiple areas enabled to search for potential large-scale generalisable responses of mammal communities to threats (Penone et al. 2016, Rovero et al. 2020, Chapter 5), that may open the doors to shared conservation measures.

At the ecological level, my thesis shows that the human influence on the environment

has a pervasive and detrimental effect on both mammal populations (part I) and the entire community (part II). Indeed, direct anthropogenic effects such as forests exploitation, livestock husbandry, and human presence inside reserves (Chapters 1-4) cause spatial displacement and contraction of species distribution ranges, as well as changes in the temporal niche, forcing mammals to occupy the interior of the forests and to be active mainly during nocturnal hours, progressively leading to reduced space and temporal interval for surviving. Furthermore, indirect effects such as habitat loss, fragmentation, infrastructure development and the increasing human population beyond the reserves' boundaries are clearly associated with a decline in the number of species and in their abundances also within well-protected forests (Chapter 5), potentially promoting disturbance-adaptative species while causing local extinction of the most specialised ones.

In Chapter 1, I pinpointed that a systematic camera trapping design allows to monitor mammals in unexplored remote areas, detecting species of conservation concern that are elusive and rare, and otherwise difficult to find. Indeed, camera trapping is a suitable tool for comprehensive mammalian monitoring which, with an excellent cost-effectiveness ratio, allows to have a synopsis of the terrestrial wild fauna. Here, camera trapping revealed a new population of African golden cat, likely the subspecies *Caracal aurata aurata*, representing an expansion of its geographic range of ca. 200 km. However, results from occupancy analyses indicated a gradient of greater cat presence further away from the proximity to forest edge and settlements, pointing out the sensitivity of this species to human presence and encroachment, and its dependence on closed-canopy, undisturbed moist forests.

In Chapter 2, I reported how camera trap bycatch data can still bear critical information to improve the current and limited knowledge of an overlooked species, such as the Pallas's cat, while occupancy analyses revealed hidden risks that can affect the long-term viability of the population that I studied in western Mongolia. In fact, while major recognized threats come in the forms of hunting and black-market trades, the spatial association between the felid and cattle warns of the consequences derived from such coexistence, such as shepherd dogs' predation, prey depletion, secondary poisoning and environmental degradation caused by pasture. Even though

results show evidence of a shift in activity patterns between the felid and cattle, this avoidance strategy may not be enough to compensate for the longstanding indirect effects of husbandry, especially if even Strictly Protected Areas are not undisturbed but largely populated by sheep and goats. In this perspective, living in livestock grazing areas might be an ecological trap for the Pallas's cat (Schlaepfer et al. 2002, Hale and Swearer 2016), which would progressively lead to reduced fitness and survivorship in this mistakenly most-suitable habitat, progressively increasing local extinction risk (Battin 2004). Therefore, a regulation of this livelihood must be considered, both for the well-being of wild species roaming in the steppe and for the protection of the ecosystem. Such regulation may be translated into the selection of areas dedicated to wildlife conservation that would become truly restricted to livestock husbandry, together with a strict ban on poisoning practices.

In Chapter 3, I focused on an IUCN-endangered primate, the Sanje mangabey, highly endemic to two disjoint forest blocks in Tanzania, and used it as study species to test a new approach for spatially-explicit density estimation for elusive species. By calibrating camera trapping data with density data from acoustic distance sampling, I was able to estimate the group density and population size across the entire distribution range of the mangabey. Occupancy analyses allowed me to provide the first comprehensive assessment of the species estimating the habitat selection preferences and potential vulnerability to human disturbance. Concurrently, this approach allowed me to overcome key limitations of density estimation, such as the difficulties in detecting cryptic species and individually recognising unmarked animals. At the ecological level, the Sanje mangabey appears to fare moderately well also in the reserve of lower protection and with a recent history of exploitation and poaching, pointing out the ecological flexibility and adaptability of this species that was previously unknown due to data sparsity. However, the greater presence further away from the reserves' borders also suggests its vulnerability to human presence.

Chapter 4 shows the potential and the strength of a standardized camera trapping field sampling, while an innovative Bayesian multi-region occupancy model for communities estimated variations in the spatio-temporal presence of mammals. We indeed estimated how the human presence, in the form of outdoor recreation

inside protected areas, can generate a landscape of fear and cause a consistent spatio-temporal avoidance response by mammals that is reflected across species, communities, and multiple areas. In particular, we found that species increased their nocturnal activity as a strategy to avoid humans, while we also recorded a decrease in detection events at sites with greater rates of human passage. Interestingly, across all areas, the temporal and spatial shifts were more pronounced for large-bodied and for omnivorous species. Results suggest that options to regulate the human presence inside protected areas should be considered to ensure a safe environment for wild mammals and preserve ecological processes. In this perspective, portions of the parks could be restricted to human access, as in the case of Sasso Fratino integral reserve in Foreste Casentinesi National Park, or authorities should encourage visitors not to leave the main trails, as in the case of Brenta and Paneveggio Nature Parks. Additionally, there might be important seasonal variations in the spatio-temporal displacement of mammals which could be related to the different intensities of human frequentation throughout the year (Schirpke et al. 2018). Indeed, avoidance may be even greater during summertime when outdoor recreation peaks, while it may be reduced during winter, when human frequentation is localised close to infrastructure (Schirpke et al. 2018). However, we could not test these trends given that our sampling included only one season. Moreover, we acknowledge that our results are solely related to the use of trails and roads and that such a shift toward a nocturnal behaviour may lack in the innermost areas of the parks. Hence, future research could further explore these adaptative mechanisms by testing seasonal differences and differences between trails/roads and internal forest areas.

In Chapter 5, I assembled an unprecedent standardised dataset of camera trap detections across 37 pan-tropical forests, augumenting the TEAM Network data (Rovero and Ahumada 2017) in terms of number of sites and consistency across continents. The resulting dataset allowed me to analyse global-scale effects of human density, proximity to infrastructure, forest cover and configuration in the broader landscape on mammal communities within protected areas. I used an advanced Bayesian multi-region community model that simultaneously estimated species richness and community occupancy. I found that forest cover in the landscape is

positively associated with both richness and occupancy within reserves, with occupancy also increasing where habitat is less fragmentated, while human density negatively impacts richness but not occupancy. Results suggest that the viability of mammalian communities inside reserves is bound to environmental changes happening far beyond the protected area boundaries. Furthermore, the decoupling of richness and occupancy in relation to human population density in the surrounding landscape might indicate that a local extinction filtering is extirpating sensitive species while more adaptable species are potentially becoming more abundant. This outcome represents solid evidence that adds on the current knowledge which is almost exclusively based on range maps and literature reviews (e.g., Ceballos et al. 2002, McKinney et al. 2001). Thanks to these findings, it is particularly evident that the area surrounding protected forests should be managed to promote a sustainable use which, beyond biodiversity conservation, would also enhance local welfare and reduce deforestation (Campos-Silva et al. 2021). Most importantly, limiting human expansion (i.e., settlements and inhabitants) in the proximity to PAs' borders could help reduce its perceived effect within. Future research could test different extensions of forest buffers to understand how large a buffer zone should be to damp the anthropogenic disturbance coming from the landscape, hence halting species' local extinction. Such knowledge would indeed have outstanding conservation and management implications.

Overall, my thesis adopted consistent methodological approaches deployed in different contexts to gather robust data that produced solid inference on ecological patterns of both mammal species and communities. These two levels I addressed are important because i) knowledge of species' ecological requirements and their responses to disturbance are relevant to understanding the viability of populations (Chapters 1-3), and ii) changes at the population level lead to changes at the community level, with potential consequences not only in form of spatio-temporal shifts of communities (Chapter 4), but also on the richness, taxonomic and, potentially, functional composition of communities (Chapter 5). These latter changes can trigger cascading effects on the ecosystem and human well-being (Díaz et al.

2006). Indeed, the ever-increasing focus of animal ecology on the functional trait distribution of communities is becoming of progressively increasing relevance to conservation (e.g., Rovero et al. 2020; Pacifici et al. 2020b). Towards this end more work is required and, as a future avenue I believe that *Theriotrop* dataset could play a role in investigating pan-tropical variations of mammal functional traits in relation to anthropogenic impacts.

From a conservation management perspective, a core part of my thesis highlighted some of the direct and indirect impacts PAs and its wildlife face, suggesting the most favourable conditions to enhance their effectiveness and improve wildlife conservation. Particularly, I highlighted the vulnerability of tropical forest reserves subdued to an increasing anthropogenic environment, pointing out how conservation strategies that include the broader landscape should be carefully planned to minimize the effects of the anthropogenic impacts on wildlife viability. This is especially so in view of the projected increasing deforestation and habitat loss rates, and given that half of the world population is estimated to reside in tropical areas by 2050 (Archer et al. 2020).

Appendix A. The African golden cat *Caracal aurata* in Tanzania: first record and vulnerability assessment

Suppl. Table A.1. Checklist of wild mammals detected with camera trapping, with raw indices of detection: number of events per day, Relative Abundance Index (RAI – events/100 camera days), and the naïve occupancy. Bold highlights data for the African golden cat records.

Taxonomic order	Latin name	Common name	Events (1 day)	RAI	Naïve occupancy
Afrotheria	*Loxodonta africana*	African elephant	4	0.180	0.031
Carnivores	*Atilax paludinosus*	Marsh mongoose	7	0.315	0.094
	Caracal aurata	**African golden cat**	**33**	**1.487**	**0.262**
	Civettictis civetta	African civet	7	0.315	0.094
	Genetta maculata	Large-spotted genet	30	1.352	0.309
	Herpestes sanguineus	Slender mongoose	1	0.045	0.016
	Mellivora capensis	Honey badge	9	0.406	0.094
	Nandinia binotata	African palm civet	3	0.135	0.047
Laurasiatheria	*Phataginus tricuspis*	Tree pangolin	3	0.135	0.047
	Smutsia gigantea	Giant pangolin	2	0.090	0.031
Primates	*Cercopithecus ascanius*	Red-tailed monkey	2	0.090	0.031
	Cercopithecus mitis	Blue monkey	6	0.270	0.078
	Colobus angolensis	Angolan colobus	1	0.045	0.016
	Lophocebus albigena	Grey-cheeked mangabey	3	0.135	0.047
	Papio anubis	Olive baboon	32	1.442	0.297
Rodents	*Cricetomys gambianus*	Gambian pouched rat	14	0.631	0.141
	Funisciurus pyrropus	Fire-footed rope squirrel	37	1.667	0.141
Ungulates	*Kobus ellipsiprymnus*	Waterbuck	1	0.045	0.016
	Philantomba monticola	Blue duiker	191	8.607	0.594
	Potamochoerus larvatus	Bushpig	13	0.586	0.172
	Redunca redunca	Bohor reedbuck	1	0.045	0.016
	Syncerus caffer	African buffalo	1	0.045	0.016
	Tragelaphus scriptus	Hernessed bushbuck	11	0.496	0.094

Suppl. Table A.2. Predicted values of detection probability (*p*) from the average model for the effect of camera trap brand.

Model	Predicted value	SE	Lower	Upper
(p) Browning	0.23	0.05	0.14	0.35
(p) Ambush	0.06	0.04	0.02	0.18
(p) UOVision	0.04	0.04	< 0.01	0.25

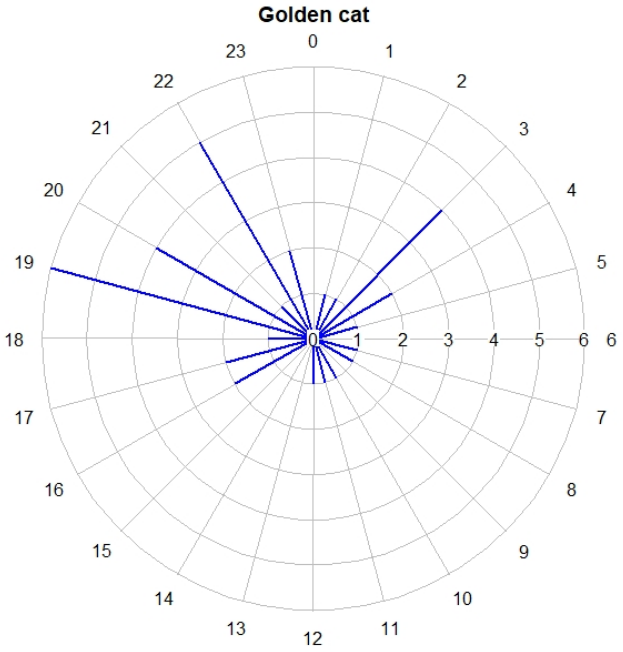

Suppl. Fig. A.1 Activity pattern of the African golden cat in the Minziro Nature Forest Reserve based on camera trapping survey, performed with the total number of captures (n = 37). Numbers in the outer part of the graphs represent hours (x-axes), whereas circular grid line (y-axes) represent the number of events in each time slot.

Appendix B. Spatio-temporal occurrence and sensitivity to livestock husbandry of Pallas's cat in the Mongolian Altai

Suppl. Table B.1 Summary of the survey information for each study area, with sampled area estimated using a Minimum Convex Polygon around the camera sites, sampling effort indicating the total number of active camera days, and sampling effort. The surveys were conducted in the Altai Mountains, western Mongolia.

Area name	Sampling period	N. cameras (working cameras)	Elevation range (m a.s.l)	Sampled area (Km^2)	Sampling effort	Mean active days per camera
Siilkhem B	17 Mar – 29 Jun 2015	49 (48)	2,231 - 3,123	513	2,186	46.5 ± 6.6
Tavan Bogd	4 Apr – 2 Jun 2017	60 (44)	2,488 - 3,072	720	2,078	48.2 ± 1.6
Khork Serkh	16 Mar – 1 Jun 2018	77 (63)	1,965 - 3,072	1,110	4,063	65.2 ± 5.8
Sutai Massif	18 Mar – 29 Jun 2019	66 (61)	2,115 - 3,527	843	5,563	92.1 ± 15.3

Suppl. Table B.2 Environmental and anthropogenic variables used to model the occupancy (ψ) and detection (p) probabilities of the Pallas's cat (*Otocolobus manul*) in western Mongolia.

Covariate	Description	Value	Type	Modelled on	Note
Camera sensitivity	Speediness and sensitivity of the camera triggers	Low - High	Categorical	p	-
Sampling effort	Number of camera days per area	14 – 100	Continuous	p	Not in the best model
RAI domestics	Relative Abundance Index of domestic species, dogs and humans	0 - 5.70	Continuous	p	Not in the best model for the landscape assessment
Terrain slope	Steepness of the terrain at sites	1.30 - 43.60	Continuous	ψ	-
Terrain roughness	Irregularity in the surface of the terrain	3 - 119	Continuous	-	Deleted due to collinearity
Aspect	Orientation of the slopes	N - S - W - E	Categorical	ψ	-
Landcover	Observed biophysical cover of the surface	Managed ground Sparse vegetation Bare soil	Categorical	ψ	-
Area	Sampled areas	Siilkhem B NP Tavan Bogd NP Khork Serkh SPA Sutai Massif	Categorical	ψ	Used only for the landscape assessment
RAI prey	Relative Abundance Index of available main wild prey in Khork Serkh	0 - 1.05	Continuous	ψ	Used only for the focal area
Occupancy of livestock	Occupancy probability of domestic species, dogs and humans modelled using the distance to the closest ger and elevation	0.04 - 0.92	Continuous	ψ	Only used for the landscape assessment
Distance to ger	Distance of the camera trap station to the closest dwelling	264 - 16,273 m	Continuous	ψ	Used to model the occupancy of livestock
Elevation m a.s.l.	Altitudinal range across the study sites	1,800 - 3,810 m a.s.l.	Continuous	ψ	Used to model the occupancy of livestock
Occupancy of small-sized livestock	Occupancy probability of sheep and goats	0.03 – 0.94	Continuous	ψ	Used only for the focal area
Occupancy of large-sized livestock	Occupancy probability of cattle	0.44 – 0.66	Continuous	ψ	Used only for the focal area

Suppl. Table B.3 List of domestic species detected through camera trapping in western Mongolia, during 2015 – 2019. The table reports the number of independent events across the four study areas.

Taxonomic order	Scientific name	Common name	N. of events
Artiodactyla	*Bos sp.*	Cow/yak	173
	Camel sp.	Camel	15
	Capra ovis	Goat	451
	Equus ferus	Horse	140
	Ovis aries	Sheep	193
Carnivorae	*Canis lupus familiaris*	Dog	140
Primates	*Homo sapiens*	Human	223

Appendix C. Calibrating occupancy to density estimations to assess abundance and vulnerability of a threatened primate in Tanzania

Suppl. Table C.1 Area and camera-trapping sampling design specifications of the two study areas in Tanzania.

Study area	Management regime	Area (Km^2)	Altitudinal range (m asl)	Mean annual rainfall (mm)	Mean annual temp. (°C)	N. cameras (working cameras)	Sampling effort
Mwanihana forest	National Park (1992)	167	300 - 2,100	1,750 - 2,000	21 - 31	60 (59)	1,839
Uzungwa Scarp forest	Nature Reserve (2016)	371	300 - 2,068	1,800 - 2,000	19 - 27	60 (58)	1,792

Suppl. Table C.2 Model selection using the Akaike Information Criterion (AIC) for the best-fitting detection model (bold).

Detection models	n. param.	AIC	ΔAIC
p (Distance to closest reserve border) ~ ψ (1)	**3**	**1249.99**	**0.00**
p (Habitat) ~ ψ (1)	3	1252.35	2.35
p (1) ~ ψ (1)	2	1320.06	70.07

Suppl. Table C.3 Model selection using the Akaike Information Criterion (AIC) for the best-fitting detection function (bold) for the estimation of the detection probability. CvM referred to Cramér-von Mises, while Pa is the average detectability with its related error.

Density models	Key function	CvM *p*	Pa	SE Pa	ΔAIC
~Distance to closest border	**Half-normal**	**0.69**	**0.31**	**0.06**	**0.00**
~1	Half-normal	0.66	0.33	0.06	0.13
~ Distance to closest border	Hazard-rate	0.92	0.52	0.06	0.34
~1	Hazard-rate	0.96	0.52	0.07	0.47
~Slope + Distance to closest border	Hazard-rate	0.97	0.50	0.06	0.73
~Elevation + Distance to closest border	Hazard-rate	0.61	0.56	0.05	0.73
~Elevation + Distance to closest border	Half-normal	0.72	0.31	0.07	0.76
~Slope + Distance to closest border	Half-normal	0.56	0.31	0.06	0.98
~Elevation	Half-normal	0.67	0.33	0.06	1.84
~Elevation + Slope	Hazard-rate	0.96	0.51	0.06	1.84
~Elevation	Hazard-rate	0.96	0.52	0.07	2.31
~Elevation + Slope + Distance to closest border	Half-normal	0.62	0.30	0.07	2.51
~Elevation + Slope	Half-normal	0.51	0.32	0.06	2.52
~Elevation + Slope + Distance to closest border	Hazard-rate	0.92	0.52	0.06	2.53

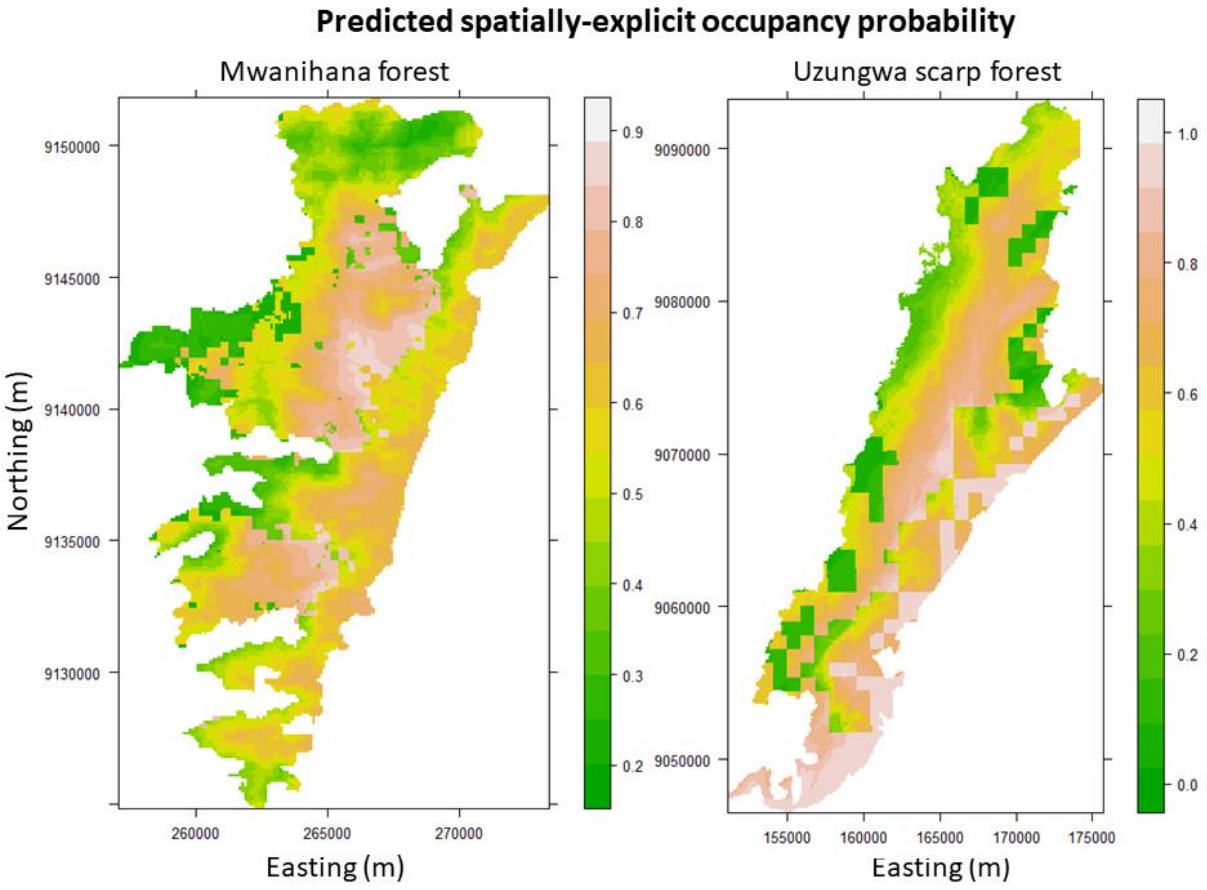

Suppl. Figure C.1 Maps of predicted occupancy probability of the Sanje mangabey (*Cercocebus sanjei*) in Mwanihana forest and Uzungwa Scarp forest, Tanzania.

Appendix D. The night as refuge from humans: responses of mammalian communities to human presence in four Italian protected areas sampled with a standardized camera trapping protocol

D.1 JAGS code

```
#########
# model formulation
cat("
model {
#Prior for covariates
mu.alpha1.global ~ dnorm(0,(1/(2.25^2)))     #slope p (continuous) = DIST SETTL
tau.alpha1.global ~ dgamma(0.1, 0.1)
mu.alpha2.global ~ dnorm(0,(1/(2.25^2)))     #slope p (continuous) = RAI.human
tau.alpha2.global ~ dgamma(0.1, 0.1)
mu.alpha3.global ~ dnorm(0,(1/(2.25^2)))     #slope p (factorial) = CAMERA
tau.alpha3.global ~ dgamma(0.1, 0.1)
mu.alpha4.global ~ dnorm(0,(1/(2.25^2)))     #slope p (factorial) = CAMERA
tau.alpha4.global ~ dgamma(0.1, 0.1)

mu.beta1.global ~ dnorm(0,(1/(2.25^2)))      #slope psi (continuous) = RAI human
tau.beta1.global ~ dgamma(0.1, 0.1)
mu.beta2.global ~ dnorm(0,(1/(2.25^2)))      #slope psi (continuous) = DIST SETTL
tau.beta2.global ~ dgamma(0.1, 0.1)
mu.beta3.global ~ dnorm(0,(1/(2.25^2)))      #slope psi (continuous) = elevation
tau.beta3.global ~ dgamma(0.1, 0.1)
mu.beta4.global ~ dnorm(0,(1/(2.25^2)))      #slope psi (continuous) = slope
tau.beta4.global ~ dgamma(0.1, 0.1)

#effetti globali tratti
mu.betaD1.global ~ dnorm(0,(1/(2.25^2)))
tau.betaD1.global ~ dgamma(0.1, 0.1)
mu.betaD2.global ~ dnorm(0,(1/(2.25^2)))
tau.betaD2.global ~ dgamma(0.1, 0.1)
mu.betaN1.global ~ dnorm(0,(1/(2.25^2)))
tau.betaN1.global ~ dgamma(0.1, 0.1)
mu.betaN2.global ~ dnorm(0,(1/(2.25^2)))
tau.betaN2.global ~ dgamma(0.1, 0.1)
mu.betaC1.global ~ dnorm(0,(1/(2.25^2)))
tau.betaC1.global ~ dgamma(0.1, 0.1)
mu.betaC2.global ~ dnorm(0,(1/(2.25^2)))
```

```
tau.betaC2.global ~ dgamma(0.1, 0.1)

 #priors for heterogenity among species
    lpsi <- log(psi.mean) - log(1-psi.mean)           #regional psi means
    psi.mean ~ dunif(0,1)
    tau.lpsi <- pow(sigma.psi,-2)
    sigma.psi ~ dunif(0,10)

     lp <- log(p.mean) - log(1-p.mean)                #region lp means
     p.mean ~ dunif(0,1)
     tau.lp <- pow(sigma.p,-2)
     sigma.p ~ dunif(0,10)

     lday <- log(day.mean) - log(1-day.mean)       #regional diurnality mean
    day.mean ~ dunif(0,1)
    tau.lday <- pow(sigma.day,-2)
    sigma.day ~ dunif(0,10)

     lnight <- log(night.mean) - log(1-night.mean)    #region nocturnality means
     night.mean ~ dunif(0,1)
     tau.lnight <- pow(sigma.night,-2)
     sigma.night ~ dunif(0,10)

     lcrep <- log(crep.mean) - log(1-crep.mean)      #region nocturnality means
     crep.mean ~ dunif(0,1)
     tau.lcrep <- pow(sigma.crep,-2)
     sigma.crep ~ dunif(0,10)

 for(r in 1:R){
        mu.alpha1[r] <- mu.alpha1.global
        tau.alpha1[r] <- tau.alpha1.global
        mu.alpha2[r] <- mu.alpha2.global
        tau.alpha2[r] <- tau.alpha2.global
        mu.alpha3[r] <- mu.alpha3.global
        tau.alpha3[r] <- tau.alpha3.global
        mu.alpha4[r] <- mu.alpha4.global
        tau.alpha4[r] <- tau.alpha4.global

        mu.beta1[r] <- mu.beta1.global
        tau.beta1[r] <- tau.beta1.global
        mu.beta2[r] <- mu.beta2.global
        tau.beta2[r] <- tau.beta2.global
        mu.beta3[r] <- mu.beta3.global
        tau.beta3[r] <- tau.beta3.global
        mu.beta4[r] <- mu.beta4.global
```

```
        tau.beta4[r] <- tau.beta4.global
         }

  for(r in 1:R){
   for(k in 1:M){
      alpha1[k,r] ~ dnorm(mu.alpha1[r],tau.alpha1[r])
      alpha2[k,r] ~ dnorm(mu.alpha2[r],tau.alpha2[r])
      alpha3[k,r] ~ dnorm(mu.alpha3[r],tau.alpha3[r])
      alpha4[k,r] ~ dnorm(mu.alpha4[r],tau.alpha4[r])

      beta1[k,r] ~ dnorm(mu.beta1[r],tau.beta1[r])
      beta2[k,r] ~ dnorm(mu.beta2[r],tau.beta2[r])
      beta3[k,r] ~ dnorm(mu.beta3[r],tau.beta3[r])
      beta4[k,r] ~ dnorm(mu.beta4[r],tau.beta4[r])
          } }

for(r in 1:R){
        mu.betaD1[r] <- mu.betaD1.global
        tau.betaD1[r] <- tau.betaD1.global
        mu.betaD2[r] <- mu.betaD2.global
        tau.betaD2[r] <- tau.betaD2.global
        mu.betaN1[r] <- mu.betaN1.global
        tau.betaN1[r] <- tau.betaN1.global
        mu.betaN2[r] <- mu.betaN2.global
        tau.betaN2[r] <- tau.betaN2.global
        mu.betaC1[r] <- mu.betaC1.global
        tau.betaC1[r] <- tau.betaC1.global
        mu.betaC2[r] <- mu.betaC2.global
        tau.betaC2[r] <- tau.betaC2.global
}

for(r in 1:R){
   mu.lambda.day[r] ~ dnorm(lday, tau.lday)            #diurnality
   mu.lambda.night[r] ~ dnorm(lnight, tau.lnight)      #nocturnality
   mu.lambda.crep[r] ~ dnorm(lcrep, tau.lcrep)         #crepuscolarity

for(k in 1:M){
# #PRIOR COV DIURNALITY
betaD1[k,r] ~ dnorm(mu.betaD1[r],tau.betaD1[r])    #SLOPE diurnality RAI.human
betaD2[k,r] ~ dnorm(mu.betaD2[r],tau.betaD2[r])   #SLOPE diurnality Dist to Settl

#  #PRIOR COV NOCTURNALITY
betaN1[k,r] ~ dnorm(mu.betaN1[r],tau.betaN1[r])   #SLOPE nocturn. RAI.human
 betaN2[k,r] ~ dnorm(mu.betaN2[r],tau.betaN2[r])    #SLOPE nocturn. Dist to Settl
```

```
# #PRIOR COV1 CREPUSCOLARITY
betaC1[k,r] ~ dnorm(mu.betaC1[r],tau.betaC1[r])      #SLOPE crepusc. RAI.human
betaC2[k,r] ~ dnorm(mu.betaC2[r],tau.betaC2[r])      #SLOPE crepusc. Dist to Settl
   } }

# #####
for (r in 1:R) {
 for (k in 1:M) {
   for(i in 1: nsite[r]) {
      day[k,i,r] ~ dpois(lambda.day[i,k,r])              # diurnality
      night[k,i,r] ~ dpois(lambda.night[i,k,r])          # nocturnality
      crep[k,i,r] ~ dpois(lambda.crep[i,k,r])            # crepuscolarity
   } } }

##MODELLING CONTINUOUS TRAIT -> DIURNALITY
 for (r in 1:R) {
 for (k in 1:M){
for (i in 1:nsite[r]) {
   log(lambda.day [i,k,r]) <-  mu.lambda.day[r] + betaD1[k,r] * RAI.human [i,r] +
betaD2[k,r] * DSet[i,r]

 ##MODELLING CONTINUOUS TRAIT -> NOCTURNALITY
   log(lambda.night [i,k,r]) <-  mu.lambda.night[r] + betaN1[k,r] * RAI.human [i,r] +
betaN2[k,r] * DSet[i,r]

## MODELLING CONTINUOUS TRAIT -> CREPUSCOLARITY
    log(lambda.crep [i,k,r]) <- mu.lambda.crep[r] + betaC1[k,r] * RAI.human[i,r] +
betaC2[k,r] * DSet[i,r]
 } } }

 # state process
 for (r in 1:R){
  #heterogenity among species
            beta0[r] ~ dnorm(lpsi, tau.lpsi)       #occupancy
            alpha0[r] ~ dnorm(lp, tau.lp)          #detection
  for (k in 1:M){
  for (i in 1:nsite[r]) {

# link
# ecological model for occupancy
 logit(psi[k,i,r]) <- beta0[r] + beta1[k,r] *  RAI.human[i,r] + beta2[k,r] * DSet[i,r] +
beta3[k,r] * Elev[i,r] + beta4[k,r] * Slope[i,r]
# observation model
 logit(p[k,i,r]) <- alpha0[r] + alpha1[k,r] * DSet[i,r] + alpha2[k,r] * RAI.human[i,r]
            + alpha3[k,r] * equals(Cam_tot[i,r],2) +
```

```
            alpha4[k,r] * equals(Cam_tot[i,r],3)

            mu.p[k,i,r] <- p[k,i,r]*z[k,i,r]
            z[k,i,r] ~ dbern(psi[k,i,r])                    #true presence/absence
            yaug[k,i,r] ~ dbin(mu.p[k,i,r], nrep[i,r])
        }     }  }
 #end model

}", fill = TRUE, file="multiR_TRATTI_MODEL.txt")

#######################################
#data
bugs.data1 <- list(M=M, R=R, nrep=K_tot_ITA, nspecies=nSpecies, nz=nz, yaug=Y_tot,
nsite=nCameras, DSet=DistS_tot3, RAI.human=RAI.H_tot2, Elev=Elev_tot2,
Slope=Slope_tot2, Cam_tot=Cam_tot, day=DAY2_tot, night=NIGHt2_tot,
crep=CREP2_tot)

##initial values
inits <- function() {list(z=zst)}

parameters <- c("psi.mean", "psi", "sigma.psi","p.mean", "sigma.p", "lpsi", "lp",
"lday", "lnight", "lcrep", "mu.beta1.global", "mu.beta2.global", "mu.beta3.global",
"mu.beta4.global", "beta0", "beta1", "beta2", "beta3", "beta4", "alpha0",
"mu.alpha1.global", "mu.alpha2.global","mu.alpha3.global", "mu.alpha4.global",
 "day.mean", "lambda.day", "mu.lambda.day", "betaD1", "betaD2",
"mu.betaD1.global", "mu.betaD2.global", "night.mean", "lambda.night",
"mu.lambda.night", "betaN1", "betaN2", "mu.betaN1.global", "mu.betaN2.global",
"crep.mean", "lambda.crep", "mu.lambda.crep", "betaC1", "betaC2",
"mu.betaC1.global", "mu.betaC2.global")

#mcmc settings
n.adapt <- 250000              #pre-burnin
n.burnin <- 500000             #burnin
n.iter <- 750000               #iterations post-burnin
n.thin <- 10
n.chains<-3

start.time = Sys.time()
Tratti_ita_OUTPUT  <- jags(data=bugs.data1,
                           parameters.to.save = parameters,
                           model="multiR_TRATTI_MODEL.txt",
                           inits = inits, n.burnin = n.burnin,
                           n.adapt = n.adapt, n.iter = n.iter,
                           n.thin = n.thin, n.chains = n.chains,
                           parallel = T, bugs.format = T)
```

Suppl. Table D.1 Summary of the number of sampling sites and effort (expressed as number of the cumulative number of days cameras were active) for each area, with the resulting number of pictures collected, in total and divided by category (humans, vehicles, domestic animals and wild mammals).

Area	1	2	3	4
Sites	58	60	27	59
Effort (camera days)	2032	2100	2519	1968
All photos	81420	86154	66852	124974
Humans	53971	45772	20106	55446
Vehicles	5901	4874	562	9252
Domestic animals	10032	9546	2569	21480
Wild mammals	12082	15129	24428	57421

Suppl. Table D.2 Global parameters from the multi-region occupancy model. α- and β-coefficients are parameters used to model detection (p) and community occupancy probabilities (ψ), β_{day}-, β_{night}- and β_{crep}-coefficients are parameters used to model diurnality, nocturnality, and crepuscolarity, respectively. Table depicts the mean of the full posterior distribution, SD, and the 5% - 95% Bayesian Credible Interval (BCI).

Sub-model	Parameter	Variable	mean	SE	5% BCI	95% BCI	R-hat	n.eff
Diurnality	μλday[1]	intercept diurnality Area 1	-0.5	0.11	-0.72	-0.28	1.00	35336
	μλday[2]	intercept diurnality Area 2	-0.34	0.08	-0.49	-0.19	1.00	75000
	μλday[3]	intercept diurnality Area 3	-1.57	0.08	-1.74	-1.41	1.00	25470
	μλday[4]	intercept diurnality Area 4	-1.81	0.11	-2.03	-1.59	1.00	75000
	μβ1day global	RAI Human	-0.48	0.13	-0.67	-0.29	1.00	38227
	μβ2day global	Dist. To Settlements	-0.08	0.14	-0.33	0.18	1.00	26775
	μβ3day global	Elevation	0.51	0.13	0.18	0.86	1.00	75000
	μβ4day global	Terrain slope	0.15	0.14	-0.04	0.34	1.00	59323
Nocturnality	μλnight[1]	intercept nocturnality Area 1	-0.22	0.09	-0.39	-0.06	1.00	75000
	μλnight[2]	intercept nocturnality Area 2	1.47	0.03	1.41	1.52	1.00	73159
	μλnight[3]	intercept nocturnality Area 3	0.99	0.02	0.94	1.04	1.00	75000
	μλnight[4]	intercept nocturnality Area 4	0.72	0.03	0.65	0.78	1.00	75000
	μβ1night global	RAI Human	0.00	0.07	-0.11	0.13	1.00	2222
	μβ2night global	Dist. To Settlements	-0.13	0.11	-0.31	0.05	1.00	75000
	μβ3night global	Elevation	-0.26	0.13	-0.49	-0.04	1.00	75000
	μβ4night global	Terrain slope	0.29	0.14	0.14	0.44	1.00	21066
Crepuscularity	μλcrep[1]	intercept crepuscularity Area 1	-0.78	0.11	-1.00	-0.57	1.00	12133
	μλcrep[2]	intercept crepuscularity Area 2	0.35	0.05	0.25	0.45	1.00	75000
	μλcrep[3]	intercept crepuscularity Area 3	-0.52	0.05	-0.62	-0.42	1.00	24661
	μλcrep[4]	intercept crepuscularity Area 4	-0.44	0.06	-0.55	-0.33	1.00	75000
	μβ1crep global	RAI Human	-0.17	0.08	-0.32	-0.02	1.00	58161
	μβ2crep global	Dist. To Settlements	-0.23	0.11	-0.42	-0.02	1.00	75000
	μβ3crep global	Elevation	0.39	0.13	0.07	0.70	1.00	75000
	μβ4crep global	Terrain slope	0.16	0.14	0.00	0.31	1.00	75000
Detection probability	α0[1]	intercept detection Area 1	-1.95	0.07	-2.07	-1.82	1.00	75000
	α0[2]	intercept detection Area 2	-1.99	0.36	-2.676	-1.48	1.00	896
	α0[3]	intercept detection Area 3	-1.81	0.05	-1.89	-1.73	1.00	12215
	α0[4]	intercept detection Area 4	-1.58	0.03	-1.63	-1.53	1.00	75000
	μα1 global	Dist. To Settlements	0.10	0.10	-0.07	0.27	1.00	33815
	μα2 global	RAI Human	-0.07	0.07	-0.19	0.04	1.00	75000
	μα3 global	Camera	-0.81	0.32	-1.33	-0.28	1.00	3028
	μα4 global	Camera	-1.28	0.64	-2.33	-0.21	1.00	3328
Occupancy probability	β0[1]	intercept occupancy Area 1	-0.41	0.21	-0.76	-0.07	1.00	30331
	β0[2]	intercept occupancy Area 2	0.7	0.28	0.26	1.06	1.00	29770
	β0[3]	intercept occupancy Area 3	0.41	0.15	0.16	0.66	1.00	75000
	β0[4]	intercept occupancy Area 4	-0.37	0.15	-0.63	-0.12	1.00	75000
	μβ1 global	RAI Human	0.10	0.09	-0.04	0.25	1.00	75000
	μβ2 global	Dist. To Settlements	-0.28	0.16	-0.55	-0.01	1.00	16834
	μβ3 global	Elevation	0	0.21	-0.34	0.33	1.00	75000
	μβ4 global	Slope	0	0.09	-0.14	0.13	1.00	75000

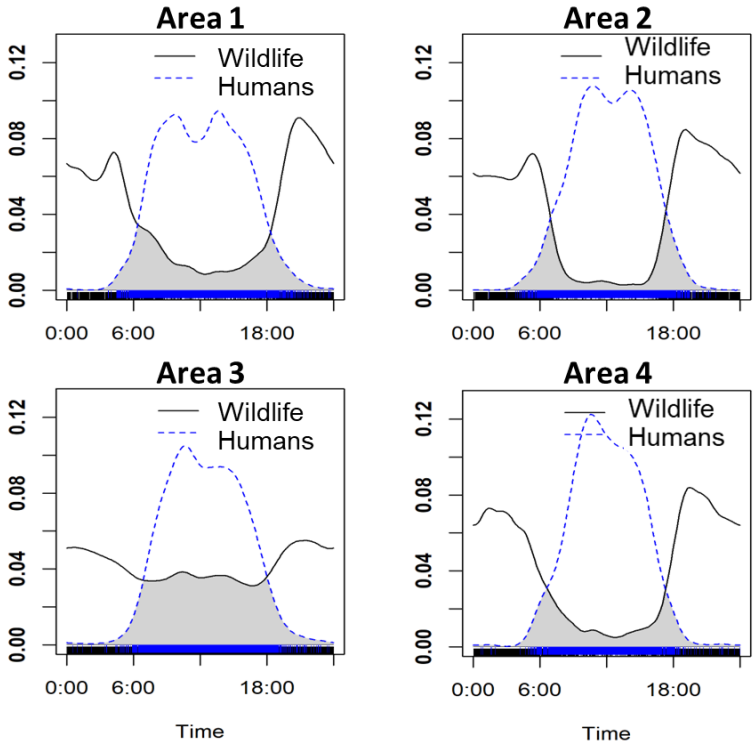

Suppl. Fig. D.1 Temporal activity overlap between wildlife (all wild mammal species considered together) and humans for each of the four study areas.

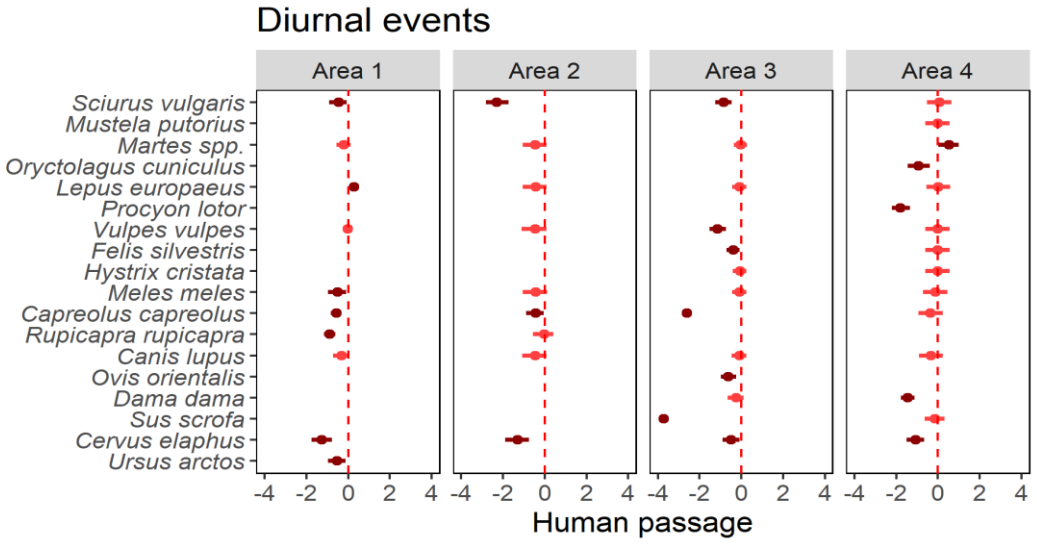

Suppl. Fig D.2 Species- and region-specific diurnal site-use probabilities in relation to human passage (RAI of humans), estimated from the multi-region regression model. Caterpillar plots depict beta coefficients with mean and 90% BCI. Darker red color indicates coefficients whose 90% BCI does not overlap 0, whereas coefficients in light red present a 90% BCI that does overlap 0.

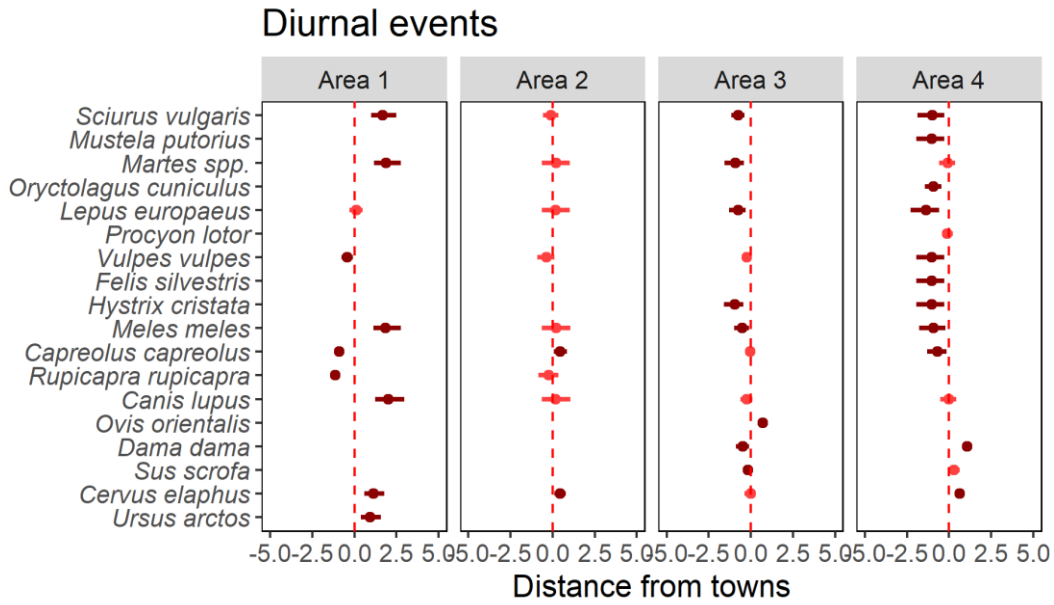

Suppl. Fig. D.3 Species- and region-specific diurnal site-use probabilities in relation to distance from closest town, estimated from the multi-region regression model. Caterpillar plots depict beta coefficients with mean and 90% BCI. Darker red color indicates coefficients whose 90% BCI does not overlap 0, whereas coefficients in light red present a 90% BCI that does overlap 0.

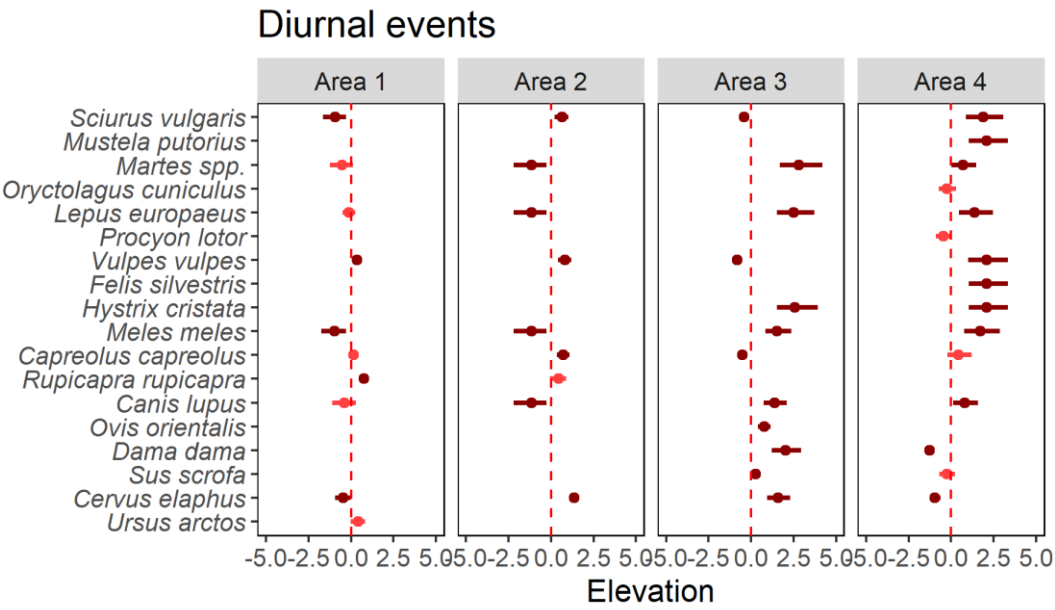

Suppl. Fig. D.4 Species- and region-specific diurnal site-use probabilities in relation to the elevation, estimated from the multi-region regression model. Caterpillar plots depict beta coefficients with mean and 90% BCI. Darker red color indicates coefficients whose 90% BCI does not overlap 0, whereas coefficients in light red present a 90% BCI that does overlap 0.

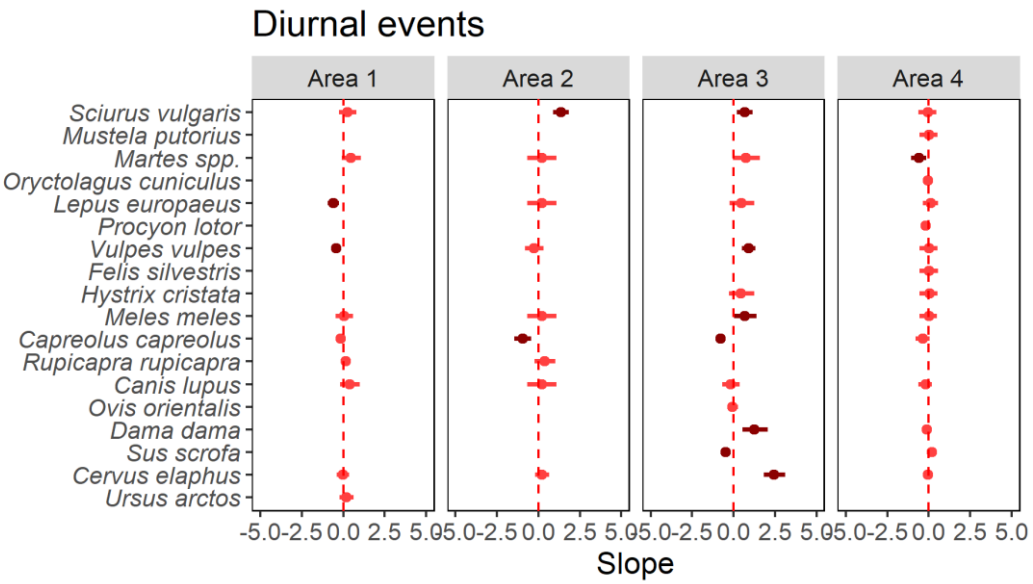

Suppl. Fig. D.5 Species- and region-specific diurnal site-use probabilities in relation to the slope of the terrain, estimated from the multi-region regression model. Caterpillar plots depict beta coefficients with mean and 90% BCI. Darker red color indicates coefficients whose 90% BCI does not overlap 0, whereas coefficients in light red present a 90% BCI that does overlap 0.

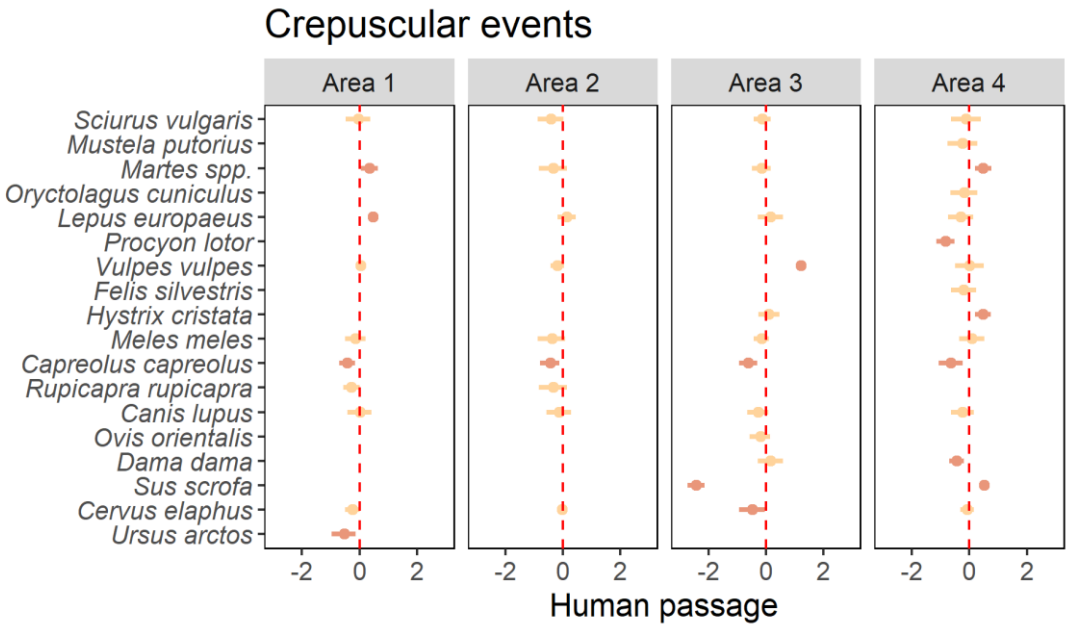

Suppl. Fig. D.6 Species- and region-specific crepuscular site-use probabilities in relation to human passage (RAI of humans), estimated from the multi-region regression model. Caterpillar plots depict beta coefficients with mean and 90% BCI. Darker orange color indicates coefficients whose 90% BCI does not overlap 0, whereas coefficients in light orange present a 90% BCI that does overlap 0.

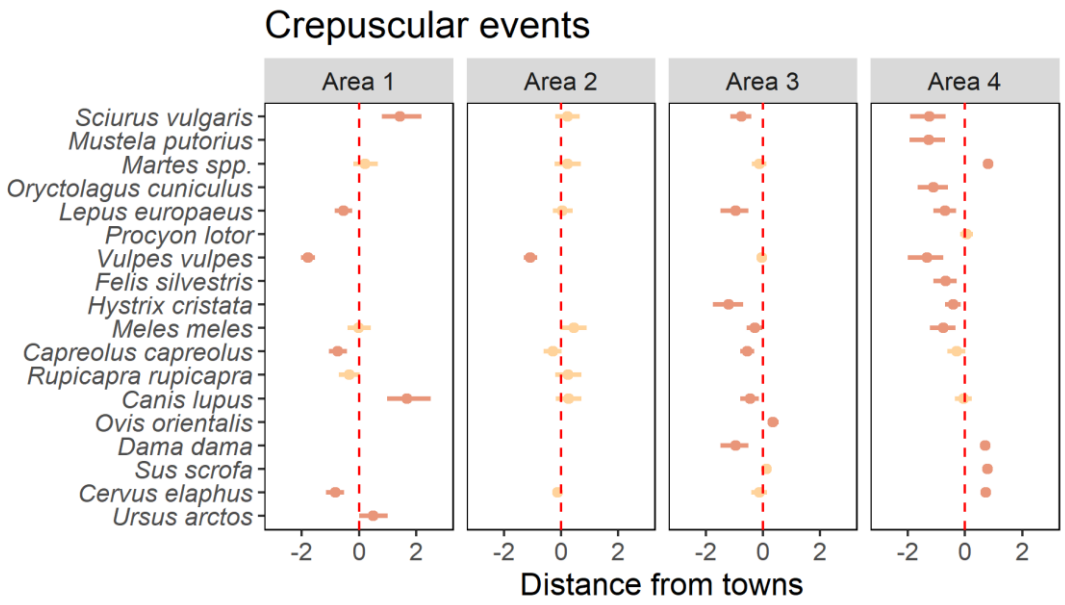

Suppl. Fig D.7 Species- and region-specific crepuscular site-use probabilities in relation to distance to the closest town, estimated from the multi-region regression model. Caterpillar plots depict beta coefficients with mean and 90% BCI. Darker orange color indicates coefficients whose 90% BCI does not overlap 0, whereas coefficients in light orange present a 90% BCI that does overlap 0.

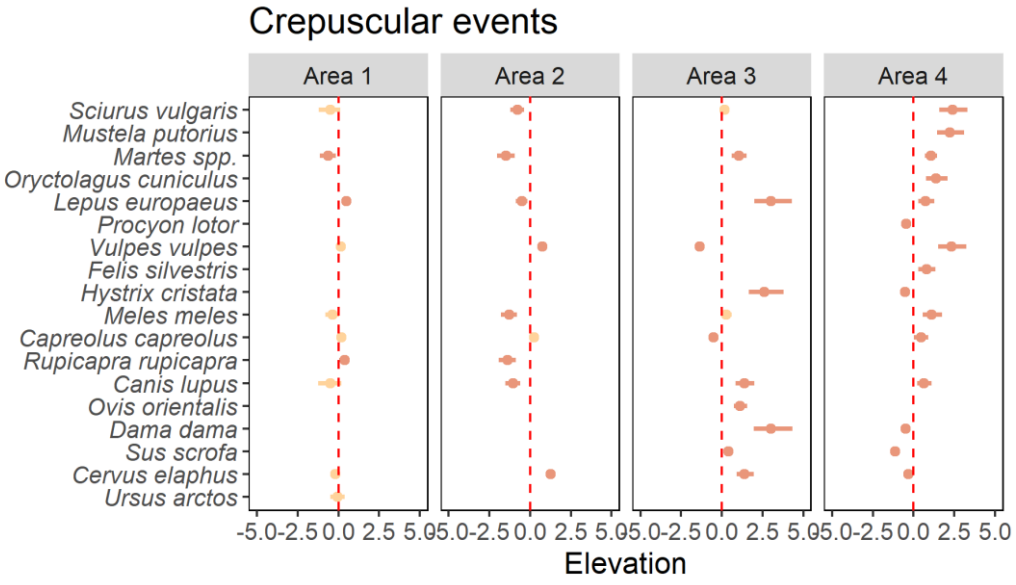

Suppl. Fig D.8 Species- and region-specific crepuscular site-use probabilities in relation to the elevation, estimated from the multi-region regression model. Caterpillar plots depict beta coefficients with mean and 90% BCI. Darker orange color indicates coefficients whose 90% BCI does not overlap 0, whereas coefficients in light orange present a 90% BCI that does overlap 0.

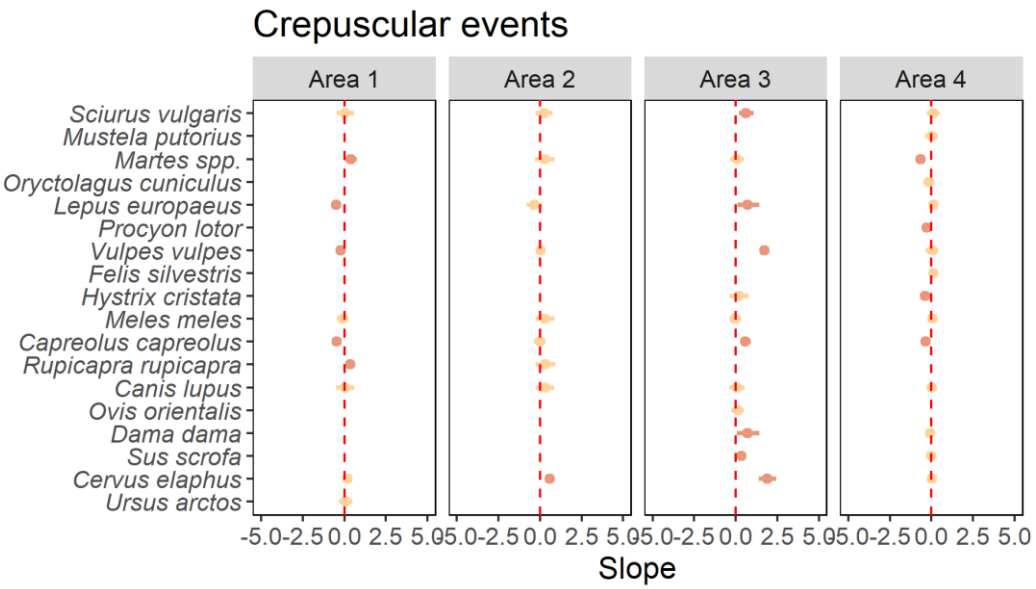

Suppl. Fig D.9 Species- and region-specific crepuscular site-use probabilities in relation to the slope of the terrain, estimated from the multi-region regression model. Caterpillar plots depict beta coefficients with mean and 90% BCI. Darker orange color indicates coefficients whose 90% BCI does not overlap 0, whereas coefficients in light orange present a 90% BCI that does overlap 0.

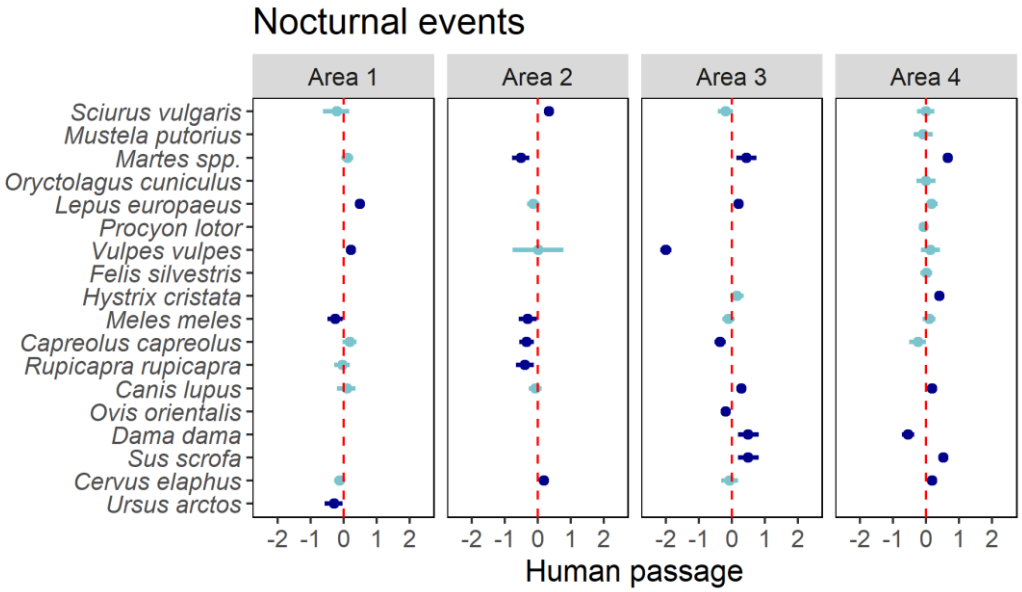

Suppl. Fig. D.10 Species- and region-specific nocturnal site-use probabilities in relation to human passage (RAI of humans), estimated from the multi-region regression model. Caterpillar plots depict beta coefficients with mean and 90% BCI. Darker blue color indicates coefficients whose 90% BCI does not overlap 0, whereas coefficients in light blue present a 90% BCI that does overlap 0.

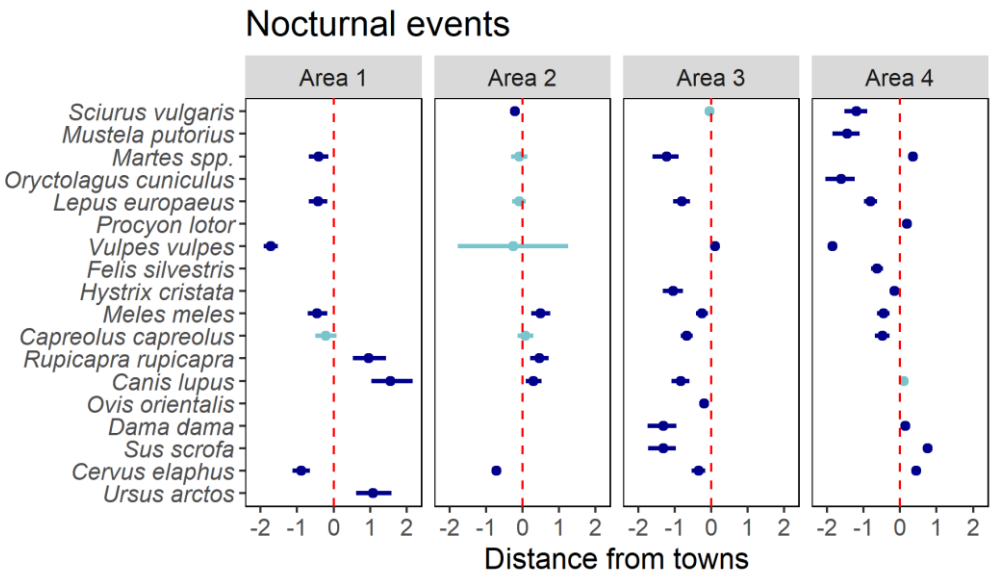

Suppl. Fig D.11 Species- and region-specific nocturnal site-use probabilities in relation to distance to the closest town, estimated from the multi-region regression model. Caterpillar plots depict beta coefficients with mean and 90% BCI. Darker blue color indicates coefficients whose 90% BCI does not overlap 0, whereas coefficients in light blue present a 90% BCI that does overlap 0.

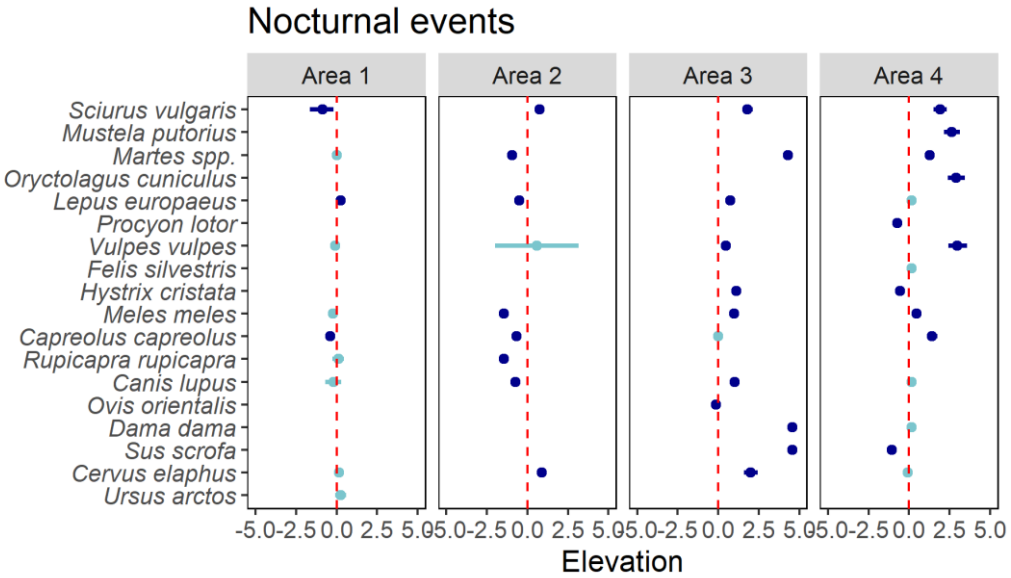

Suppl. Fig D.12 Species- and region-specific nocturnal site-use probabilities in relation to the elevation, estimated from the multi-region regression model. Caterpillar plots depict beta coefficients with mean and 90% BCI. Darker blue color indicates coefficients whose 90% BCI does not overlap 0, whereas coefficients in light blue present a 90% BCI that does overlap 0.

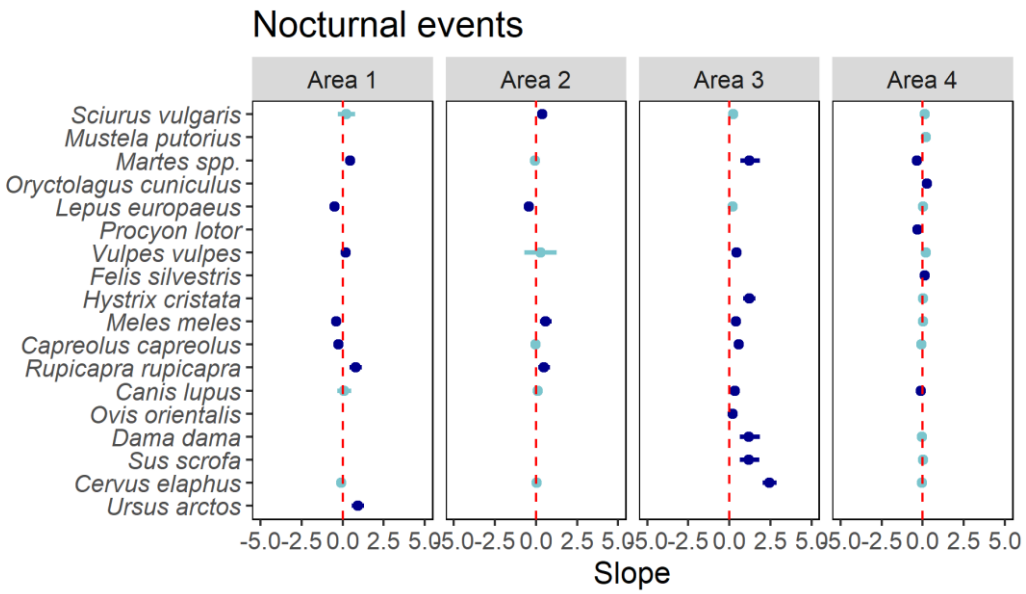

Suppl. Fig D.13 Species- and region-specific nocturnal site-use probabilities in relation to the slope of the terrain, estimated from the multi-region regression model. Caterpillar plots depict beta coefficients with mean and 90% BCI. Darker blue color indicates coefficients whose 90% BCI does not overlap 0, whereas coefficients in light blue present a 90% BCI that does overlap 0.

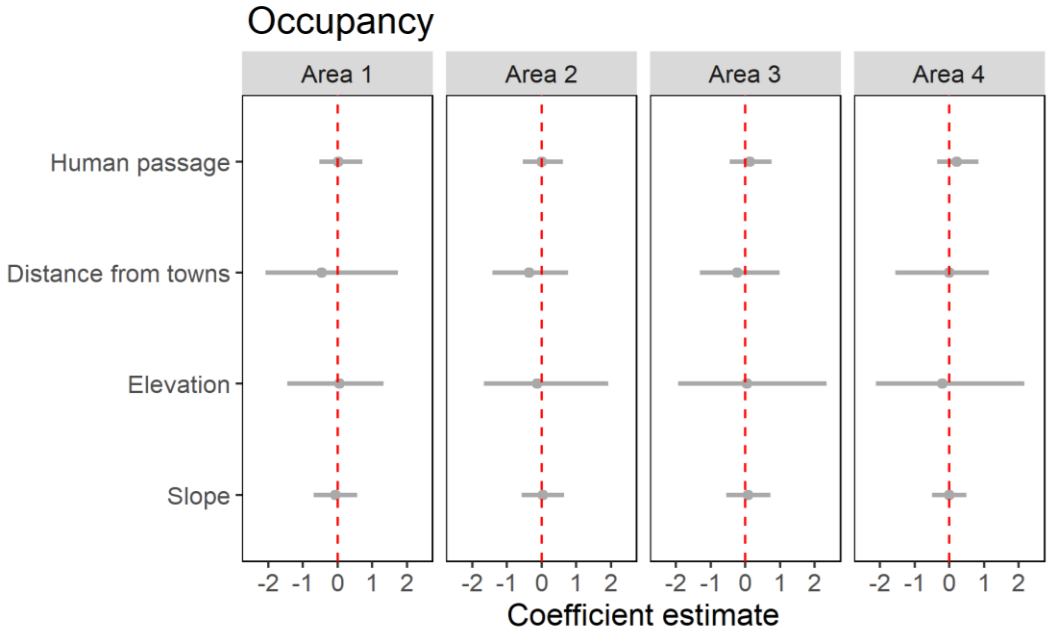

Suppl. Fig. D.14 Region- specific coefficient estimates for the effect of anthropogenic and environmental variables on community occupancy. Caterpillar plots show mean estimates and 90% BCI.

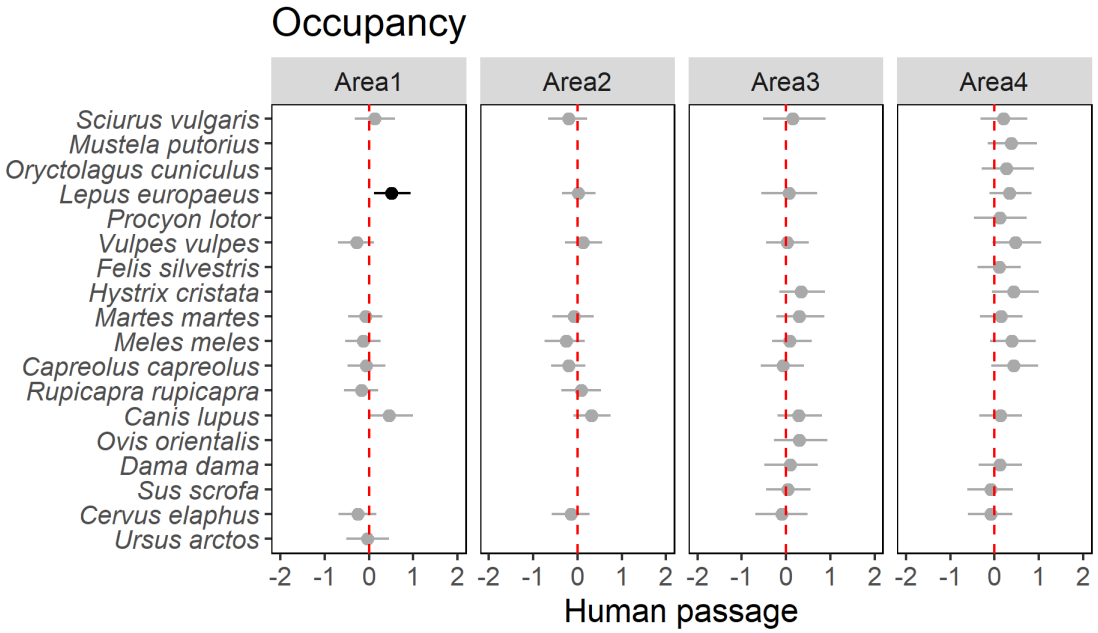

Suppl. Fig. D.15 Region- and species- specific coefficient estimates for the effect of human passage (RAI of humans) on occupancy. Caterpillar plots show mean estimates and 90% BCI. Black color indicates coefficients whose 90% BCI does not overlap 0, whereas gray color indicates coefficients whose 90% BCI does overlap 0.

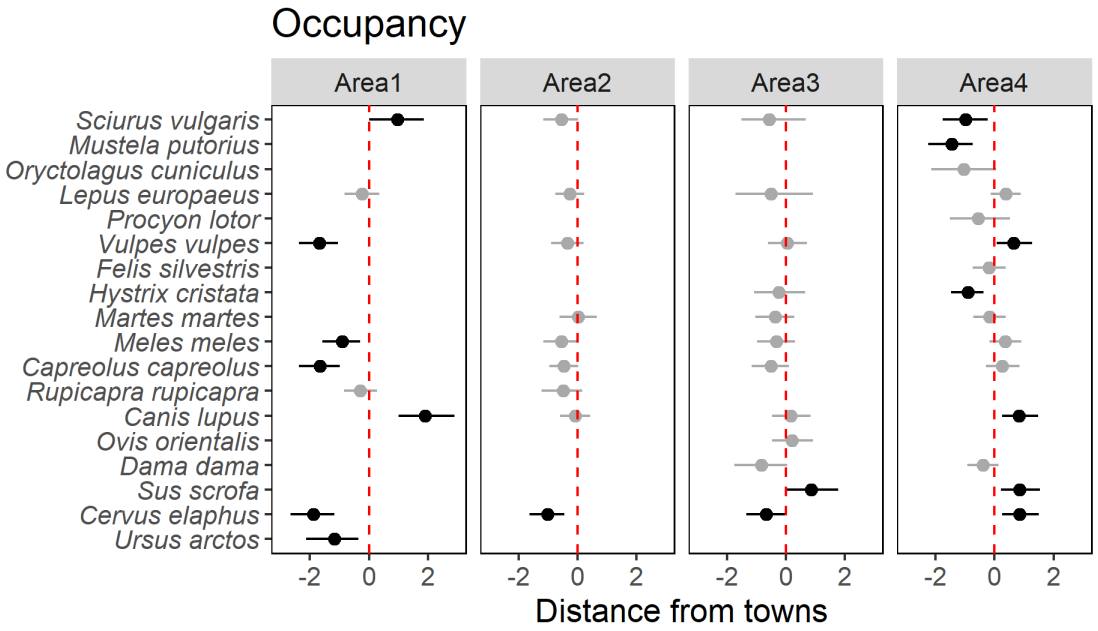

Suppl. Fig. D.16 Region- and species- specific coefficient estimates for the effect of distance from closest town on occupancy. Caterpillar plots show mean estimates and 90% BCI. Black color indicates coefficients whose 90% BCI does not overlap 0, whereas gray color indicates coefficients whose 90% BCI does overlap 0.

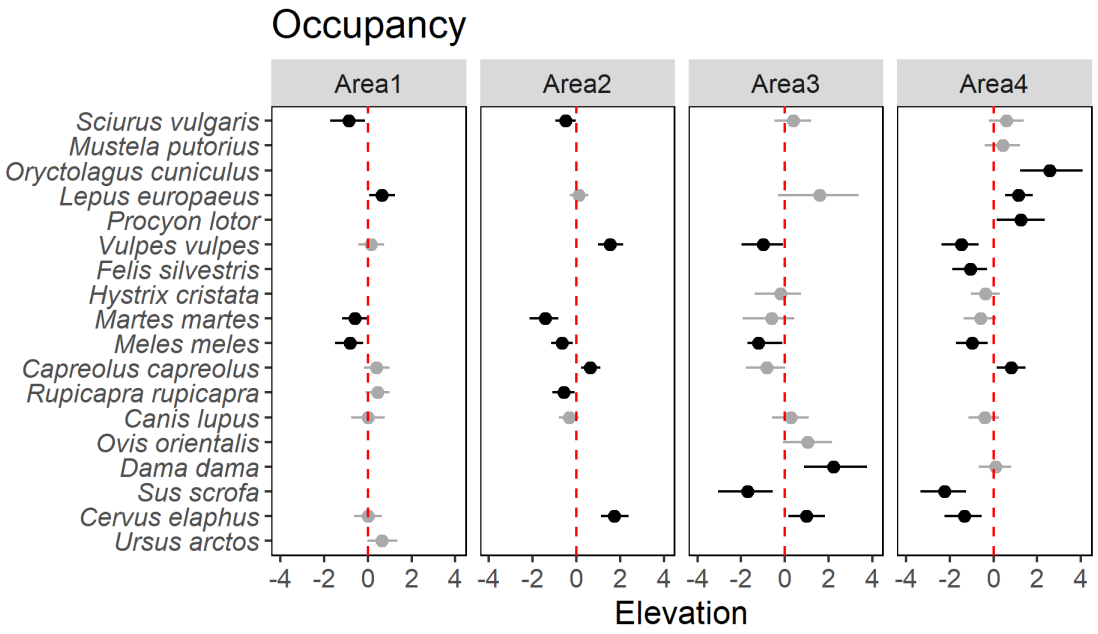

Suppl. Fig. D.17 Region- and species- specific coefficient estimates for the effect of site elevation on occupancy. Caterpillar plots show mean estimates and 90% BCI. Black color indicates coefficients whose 90% BCI does not overlap 0, whereas gray color indicates coefficients whose 90% BCI does overlap 0.

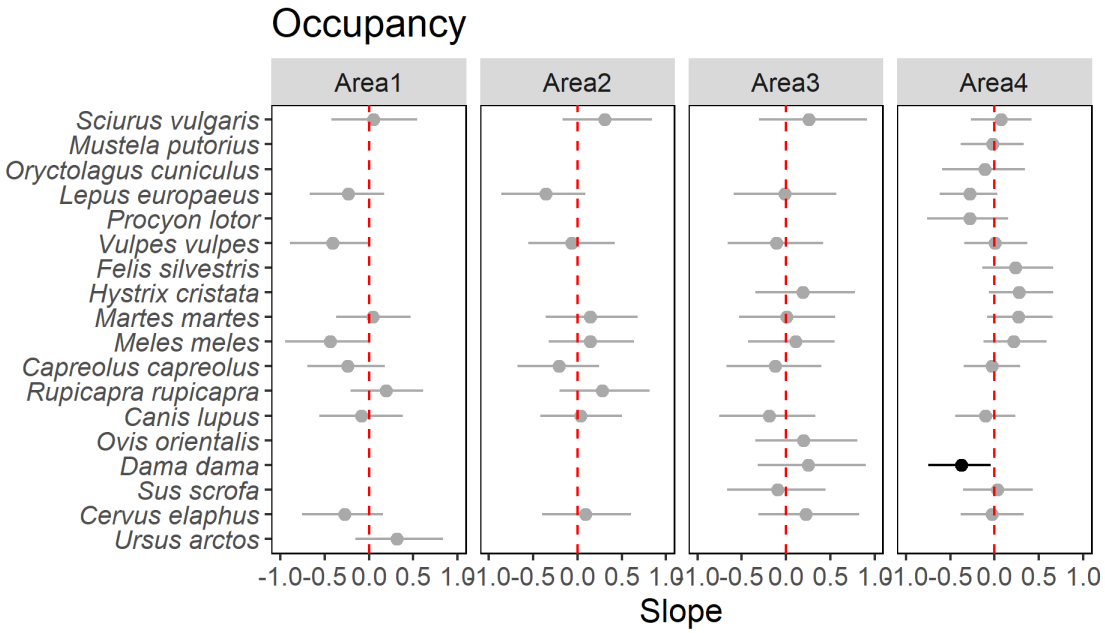

Suppl. Fig. D.18 Region- and species- specific coefficient estimates for the effect of terrain slope on occupancy. Caterpillar plots show mean estimates and 90% BCI. Black color indicates coefficients whose 90% BCI does not overlap 0, whereas gray color indicates coefficients whose 90% BCI does overlap 0.

Appendix E. The pantropical decline of mammals is associated to human density and forest fragmentation in the broader landscape

E.1 Complete of co-authors and *Theriotrop* owners

Ilaria Greco, Lydia Beaudrot, Chris Sutherland, Simone Tenan, Daniel Gorczynski, Chia Hsieh, Mohammad Firoz Ahmed, Jorge Ahumada, Rajan Amin, Mahandry Hugues Andrianarisoa, Megan Baker-Watton, Ramie Husneara Begum, Francesco Bisi, Robert Bitariho, Jedediah Brodie, Ahimsa Campos-Arceiz, Elildo A. R. Carvalho Jr., Daniel Cornélis, Giacomo Cremonesi, Virgínia Londe de Camargos, Iariaella Elimanantsoa, Santiago Espinosa, Adeline Fayolle, Davy Fonteyn, Abishek Harihar, Harry Hilser, Alys Granados, Patrick A. Jansen, Mohd-Azlan Jayasilan, Caspian Johnson, Steig Johnson, Dipankar Lahkar, Marcela Guimarães Moreira Lima, Matthew Scott Luskin, Marcelo Magioli, Emanuel H. Martin, Adriano Martinoli, Ronaldo Gonçalves Morato, Badru Mugerwa, Lain E. Pardo, Julia Salvador, Fernanda Santos, Douglas Sheil, Cédric Vermeulen, Patricia C. Wright, and Francesco Rovero

E.2 Covariates description and extraction

Covariates were first selected based on collinearity (Pearson's = 0.5 as the threshold), then on ecological relevance. The eight covariates selected for this research were extracted as follows:

1) Forest cover was estimated as the sum of forest cover patches within a buffer extending 50 km from the camera trap arrays. It was computed using the R package "landscapemetrics" (Hesselbarth et al. 2021), with forest cover dataset obtained from the Global Forest Cover available in the R package "gfcanalysis" (Cooper and Zvoleff, 2020).
2) Forest patch size and compactness was estimated as the averaged radius of gyration of all forest patches within a buffer extending 50 km from the camera trap arrays, where a greater mean radius coincides with greater patch size. The variable was extracted using the R package "landscapemetrics" (Hesselbarth et al. 2021), with forest cover dataset obtained from the Global Forest Cover available in the R package "gfcanalysis" (Cooper and Zvoleff, 2020).

3) Normalized Difference Vegetation Index (NDVI) was calculated by averaging the cell values of the 16-days MODIS NDVI images (L3 Global 250m). Data acquisition in each study forest matched the year in which wildlife was sampled.
4) Distance to the closest settlement, calculated as the Euclidean distance between each camera-trap station and the nearest settlement. Data were extracted from the Human Settlement layer at 250 m resolution from 2015 (ghsl.jrc.ec.europa.eu/ghs_bu2019.php). Such distance was collinear with the distance to the closest roads ($r = 0.71$, $P < 0.001$) hence the variable used in the analyses (i.e., proximity to infrastructure) is intended to reflect both settlements and roads. Besides the estimation at camera-level, distances within every study area were averaged to obtain an area-level value.
5) Human density was calculated by averaging the cell values of the Gridded Population of the World raster (CIESIN, 2018) within a buffer extending 50 km from the camera trap arrays. Data extraction was carried out using the R package "raster" (Hijmans et al. 2021).
6) Camera-trap trigger speed (1= fast, 2= moderate) quantified the trigger speed of camera models (i.e., the time from when the animal enters the field of view to when the camera takes a picture). Camera models were denoted as fast when the trigger speed was ca. 0.2 sec. (i.e., Reconyx and Panthera), while the other brands were denoted as moderate as trigger speed ranged from 0.25 to 1 sec..
7) Sampled area was estimated by creating and summing a buffer of 1 km around each camera-trap station.
8) Biogeographic regions (i.e., Afrotropics, Neotropics, Indo-Malayan tropics) were assigned according to the location of each study forest.

Polygons of the study forests were extracted from the World Database of Protected Area (www.protectedplanet.net), with the exception for the non-protected areas for which we created a 1 km buffer polygon around the camera traps. Such polygons and

the 50 km buffers around camera trap arrays were created with the built-in tools in QGis (QGIS Development Team, 2019).

The covariates excluded from the analyses were the following: i) size of the protected area extracted from the World Database of Protected Area, which was collinear with the distance to closest settlements (r = 0.73) and human density (r = -0.56); ii) mean forest patch area (the average patch area of all forest patches within the 50 km buffer from the camera traps), calculated with the R package "landscapemetrics" (Hesselbarth et al. 2021) with forest cover data from the R package "gfcanalysis" (Cooper and Zvoleff, 2020), which was collinear with forest patch size (r = 0.98); iii) percentage of forested landscape (the percentage of the landscape covered by forest - as opposed to non-forest - within the 50 km buffer from camera trap arrays, calculated as above, which was collinear with forest cover (r = 0.85); iv) forest patch density (number of forest patches per unit area of the landscape within the 50 km buffer from the camera trap arrays), calculated as above, which was collinear with forest cover (r = -0.57).

E.3 Nimble code and model specification

```
# r: area
#j: sampling sites (camera trap unit)
#i: species
mr_FixCovCov <- nimbleCode({
#####Data:
  # - y: observations
  # - z: known occupancy
  # - sp_in_region: known occupancies
#####Constants:
  # - n_region (scalar: number of regions)
  # - n_species (scalar: max number of species defined by our species list)
  # - n_cameras (vector: region specific number of cameras)
  # - cam_days (matrix: region x camera integer of days camera was operational)
  # - n_psi_coef (scalar: number of coefficients in the state model)
  # - psi_covs (matrix: region x covariate matrix of region-specific covariate values
for psi)
  # - psi_zeros: a vector of zeros (hyper parameter means)
```

```
 # - mv_psi: a 0 matrix with sd's on the diagonal (hyper parameter sds)
 # - n_p_coef (scalar: number of coefficients in the observation model)
 # - p_covs (matrix: region x covariate of region-specific covariate values for p)
 # - p_zeros: a vector of zeros (hyper parameter means)
 # - mv_p: a 0 matrix with sd's on the diagonal (hyper parameter sds)

 # hyperparameters
 psi_coefs[1:n_psi_coef] ~ dmnorm(mean = psi_zeros[1:n_psi_coef],
                                  prec = mv_psi[1:n_psi_coef,1:n_psi_coef])
 p_coefs[1:n_p_coef] ~ dmnorm(mean = p_zeros[1:n_p_coef],
                              prec = mv_p[1:n_p_coef,1:n_p_coef])
reg_coefs[1:n_reg_coef] ~ dmnorm(mean = reg_zeros[1:n_reg_coef],
                                 prec = mv_reg[1:n_reg_coef,1:n_reg_coef])

 for(r in 1:n_region){
  logit_psi[r] <- (psi_coefs[1:n_psi_coef] %*% psi_covs[r,1:n_psi_coef])[1,1]
  psi_sds[r] ~ dunif(min=0, max=5)
  p_sds[r] ~ dunif(min=0, max=5)
 }
 # ------------------------------------------------------------------------------------
 # Likelihood
 for(r in 1:n_region){
  #sr_prop[r] ~ dbeta(0.001,1)  #sr_prop[r] ~ dunif(0, 1)

 for(i in 1:n_species){
    sp_in_region[i,r] ~ dbern(sr_prop[r])
    psi_ranef[i,r] ~ dnorm(mean = 0, sd = psi_sds[r])
    p_ranef[i,r] ~ dnorm(mean = 0, sd = p_sds[r])
    logit(sp_in_reg_psi[i,r]) <-  logit_psi[r] + psi_ranef[i,r]

 for(j in 1:n_cameras[r]){
     logit(sp_in_reg_p[i,j,r]) <- ((p_coefs[1:n_p_coef] %*%
p_covs[j,1:n_p_coef,r])[1,1]) + p_ranef[i,r]
     z[i,j,r] ~ dbern(sp_in_reg_psi[i,r]*sp_in_region[i,r])
     y[i,j,r] ~ dbin(sp_in_reg_p[i,j,r]*z[i,j,r],cam_days[r,j])
   }}}
 # ------------------------------------------------------------------------------------
 # Derived
 for(r in 1:n_region){
```

```
   NSpp[r] <- sum(sp_in_region[1:n_species,r])
   #qui si dovrebbe aggiungere omega
   logit(sr_prop[r]) <- ((reg_coefs[1:n_reg_coef] %*% reg_covs[r,1:n_reg_coef])[1,1])
 }})
################################
# Fitting
################################
# load libraries ------------------------------------------------------
library(nimble)
library(ggplot2)
library(ggthemes)
library(see)
library(MCMCvis)
library(abind)

# load objects --------------------------------------------------------
source("./Model.R")
load("./data.RData")
# Build model ---------------------------------------------------------
wi_model <- nimbleModel(code = mr_FixCovCov,
                        constants = wi_constants,
                        data = wi_data)
# Configure MCMC ------------------------------------------------------
wi_conf <- configureMCMC(wi_model,monitors = c("NSpp",
                          "psi_sds", "p_sds", "psi_coefs", "p_coefs", "sp_in_reg_psi",
                          "sr_prop", "reg_coefs"))
# Build MCMC ----------------------------------------------------------
wi_mcmc <- buildMCMC(wi_conf, useConjugacy = FALSE)

# Compile MCMC --------------------------------------------------------
wi_compiled_model <- compileNimble(wi_model)
wi_compiled <- compileNimble(wi_mcmc, project = wi_model)
# Run MCMC ------------------------------------------------------------
wi_samples <- runMCMC(wi_compiled,
          niter = 500000,
          nburnin = 100000,
          nchains = 3
         samplesAsCodaMCMC = T,
          summary = T)
```

Suppl. Table E.1 Summary of the main parameters of interest from the multi-region occupancy model. α-coefficients represent variables used to model the detection probability (p), γ- coefficients represent parameters used to model community occupancy probability (ψ), and the β- coefficients are parameters used to model species richness. Table depicts the mean of the posterior distribution, the related SD, and the 2.5% - 97.5% Bayesian CRI. It additionally shows the potential scale reduction statistics (R-hat), with values close to 1 indicating chains' convergence, and the number of sampling (n.eff) from the posterior distribution.

Submodel	Parameter	Variable	mean	sd	2.50%	50%	97.50%	Rhat	n.eff
Detection	*α0*	Intercept	-3.97	0.10	-4.19	-3.97	-3.78	1.01	528
	α1	Camera sensitivity	-0.16	0.08	-0.31	-0.16	-0.01	1.00	2428
	α2	Distance to closest settlements	-0.05	0.09	-0.25	-0.05	0.13	1.01	359
Occupancy	*θ0*	Intercept	-0.92	0.10	-1.13	-0.92	-0.74	1.01	979
	θ1	Human density	0.03	0.12	-0.23	0.04	0.26	1.01	950
	θ2	Forest continuity	0.42	0.09	0.25	0.42	0.60	1.00	1745
	θ3	Forest availability	0.16	0.09	-0.01	0.16	0.34	1.00	1330
	θ4	Distance to closest settlements	-0.02	0.12	-0.27	-0.02	0.20	1.00	1135
Richness	*β0*	Intercept	0.06	0.12	-0.16	0.06	0.30	1.00	14584
	β1	Neotropics	-0.30	0.15	-0.59	-0.30	-0.01	1.00	18718
	β2	Indo-Malay	-0.00	0.18	-0.35	-0.00	0.35	1.00	18568
	β3	Sampled area	-0.08	0.07	-0.21	-0.08	0.06	1.00	22565
	β4	NDVI	-0.07	0.07	-0.22	-0.07	0.07	1.00	18814
	β5	Human density	-0.18	0.07	-0.33	-0.18	-0.03	1.00	12633
	β6	Forest availability	0.12	0.07	-0.01	0.12	0.26	1.00	13576

Suppl. Table E.2. List of the 37 areas included in the *TherioTrop* dataset with location, management type and environmental characteristics. Mean elevation (m.a.s.l.) of camera trap sites was sourced from the Global Biodiversity Information facility via package `rgbif` (Chamberlain et al. 2023), mean annual precipitation (mm) and mean maximum temperature (°C) were sourced from the Worldclim historical monthly weather data (Harris et al. 2014), while the dominant landcover type was sourced from the MODIS Land Cover Type Yearly L3 Global 500 m. (Friedl and Sulla-Menashe 2022).

ID	Area name	Biogeographic region	Country	Management Regime	Mean elevation	Mean annual precipitation (mm)	Mean max temperature (°C)	Dominant landcover
BBS	Bukit Barisan	Indo-Malayan	Indonesia	National Park	122.93	2969.64	29.64	Evergreen broadleaf forest
BCI	Barro Colorado	Neotropics	Panama	Nature Monument	95.95	2472.87	31.05	Evergreen broadleaf forest
BIF	Bwindi	Afrotropics	Uganda	National Park	1906.58	1396.56	22.36	Evergreen broadleaf forest
CAX	Caxiuanã	Neotropics	Brazil	National Forest	43.48	2199.68	33.44	Evergreen broadleaf forest
COU	Cocha Cashu	Neotropics	Perù	Biological Station	350.39	2627.93	32.00	Evergreen broadleaf forest
CSN	Central Suriname	Neotropics	Suriname	Nature Reserve	45.70	2146.96	33.67	Evergreen broadleaf forest
DFN	Somalomo	Afrotropics	Cameroon	Faunal Reserve	599.31	1586.50	31.51	Evergreen broadleaf forest
DFS	Djoum	Afrotropics	Cameroon	Faunal Reserve	606.35	1585.24	31.05	Evergreen broadleaf forest
DVM	Danum Valley	Indo-Malayan	Malaysia	Conservation Area	235.93	2560.83	30.45	Evergreen broadleaf forest
GUR	Gurupi	Neotropics	Brazil	Biological Reserve	143.19	1721.15	33.08	Evergreen broadleaf forest
HKK	HKK Wildlife Sanctuary	Indo-Malayan	Thailand	Wildlife Sanctuary	388.66	1425.52	35.18	Evergreen/Deciduous broadleaf forest
INV	Ivindo NP	Afrotropics	Gabon	National Park	432.39	1649.46	31.08	Evergreen broadleaf forest
JAM	Jamari	Neotropics	Brazil	National Forest	127.66	2369.55	33.47	Evergreen broadleaf forest
KER	Kerinci Seblat	Indo-Malayan	Indonesia	National Park	615.88	2645.40	29.18	Evergreen broadleaf forest
KRP	Korup	Afrotropics	Cameroon	National Park	169.93	2578.08	31.55	Evergreen broadleaf forest/Wetand
LEU	Gunung Leuser	Indo-Malayan	Indonesia	National Park	314.65	2966.20	30.57	Evergreen broadleaf forest
LLA	Llanos	Neotropics	Colombia	Oil Palm Plantation	254.21	2655.57	32.79	Evergreen broadleaf forest/Woody savanna
MAS	Manaus	Neotropics	Brazil	Area of ecological interest	106.15	2287.86	33.18	Evergreen broadleaf forest
MIN	Minziro	Afrotropics	Tanzania	Nature Reserve	1160.64	1328.08	27.13	Evergreen broadleaf forest
MNP	Manas National Park	Indo-Malayan	India	National Park	859.72	3977.81	27.21	Evergreen broadleaf forest/Woody savanna
NAK	Nam Kading	Indo-Malayan	Lao P.D.R.	Conservation Area	659.12	2711.84	31.15	Evergreen broadleaf forest
NNN	Nouabalé Ndoki	Indo-Malayan	Congo	National Park	462.87	1630.74	31.47	Evergreen broadleaf forest
PBN	Pau Brasil/Veracel	Neotropics	Brazil	National Park & private	91.90	1419.72	30.80	Evergreen broadleaf forest
PSH	Pasoh	Indo-Malayan	Malaysia	Forest Reserve	295.77	2220.00	31.39	Evergreen broadleaf forest
PWG	PWG-CEB	Afrotropics	Gabon	Logging Concession	341.61	1730.38	30.93	Evergreen broadleaf forest
RKM	Rakhine	Indo-Malayan	Myanmar	Non-Protected	138.02	4163.10	34.17	Evergreen broadleaf forest/Woody savanna
RNF	Ranomafana	Afrotropics	Madagasca	National Park	111.80	1540.84	26.11	Evergreen broadleaf forest
SHS	Sagaing Htamanthi	Indo-Malayan	Myanmar	Wildlife Sanctuary	207.24	2780.64	32.76	Evergreen broadleaf forest

SUL	Sulawesi	Indo-Malayan tropics	Indonesia	National Park & Wildlife Sanctuary & Non-Protected	645.77	2288.54	26.88	Evergreen broadleaf forest
TDM	Terra do Meio	Neotropics	Brazil	Ecological Station	175.97	1693.96	32.98	Evergreen broadleaf forest
TPN	Ta Phraya NP	Indo-Malayan	Thailand	National Park	274.75	1112.82	33.95	Evergreen broadleaf forest
UDZ	Udzungwa	Afrotropics	Tanzania	National Park	1155.10	1369.55	25.87	Evergreen broadleaf forest
UZS	Uzungwa scarp	Afrotropics	Tanzania	Nature Reserve	1345.85	1413.02	26.29	Evergreen broadleaf forest
VBA	Volcan Barva	Neotropics	Costa Rica	National Park	705.43	3525.41	30.87	Evergreen broadleaf forest
VIR	Virunga	Afrotropics	Rwanda	National Park	3010.63	1544.34	19.79	Evergreen broadleaf forest/Woody savanna
YAN	Yanachaga	Neotropics	Peru	National Park	708.63	1972.05	30.99	Evergreen broadleaf forest
YAS	Yasuni	Neotropics	Brazil	National Park	192.40	1879.26	30.25	Evergreen broadleaf forest

Suppl. Table E.3. Details on sampling effort and design for the 37 areas included in the *TherioTrop* dataset. 'Sampling effort (camera days)' is calculated as the total number of 24-h periods camera traps (CT) worked; 'Season' attributes if data collection was conducted during the dry (period of reduced precipitation) or the wet season (period when most of the yearly rain is concentrated); 'Area' is the sum of the 1-km area around each camera-trap station.

ID	Number of CT sites	Sampling effort (camera days)	Mean camera Days	Sampling year	Sampling period	Season	Average CT distance (km)	Area (km^2)
BBS	46	1058	23	2014	Apr - Jul	DRY	1.4	138
BCI	55	1760	32	2014/2015	Dec - Mar	DRY	1.4	151
BIF	59	1475	25	2014	May - Jul	DRY	1	106
CAX	58	1914	33	2014	Aug - Oct	DRY	1.4	133
COU	59	1711	29	2014	Jun - Aug	DRY	1.5	144
CSN	50	1500	30	2014	Sep - Dec	DRY	1.4	130
DFN	32	1056	32	2015	Nov-May	DRY	1.9	125
DFS	37	1080	30	2017	May-Jun	WET	1.8	121
DVM	42	1260	30	2015	Jun - Jul	DRY	1	73
GUR	57	1824	32	2016	Oct - Nov	DRY	1.4	139
HKK	65	2015	31	2010/2011	Nov - Mar	DRY	1.2	151
INV	35	1400	40	2019	May - Jun	DRY	1	55
JAM	53	1643	31	2017	Sept - Nov	DRY	1.7	134
KER	48	1344	28	2014	May - Aug	DRY	1.5	156
KRP	59	1770	30	2014	Jan - Apr	DRY	1.4	128
LEU	54	2160	40	2014	Jan - Mar	DRY	1.5	168
LLA	45	1350	30	2014/2015	Sept - Jan	DRY	2.2	167
MAS	59	1888	32	2010	Jul - Nov	DRY	1.4	142
MIN	68	2244	33	2018	Oct - Dec	DRY	1.1	130
MNP	60	1860	31	2016/2017	Dec - Jan	DRY	1.6	167
NAK	56	1848	33	2014/2015	Oct - Jan	DRY	1.4	151
NNN	53	2226	42	2014/2015	Dec - Mar	DRY	1.4	131
PBN	57	1767	31	2018	Aug - Sep	DRY	1.4	150
PSH	57	1653	29	2014	May - Jul	DRY	1.3	128
PWG	54	1512	28	2018/2019	Sep - Jan	WET	1.4	132
RKM	60	1980	33	2017/2018	Nov - Feb	DRY	1	130
RNF	59	1593	27	2013/2014	Nov - Feb	DRY	1.4	162
SHS	61	1952	32	2017/2018	Dec - Mar	DRY	1.1	134
SUL	49	1519	31	2018	Apr - Jul	DRY	5	161
TDM	58	1914	33	2016	Jun - Jul	DRY	1.3	133

TPN	62	1488	24	2010	Nov - Feb	DRY	1.5	165
UDZ	59	1829	31	2014	Jul - Nov	DRY	1.4	135
UZS	60	1860	31	2017	Jul - Nov	DRY	1.5	140
VBA	59	1770	30	2014	Jan - Apr	DRY	1.4	115
VIR	58	1914	33	2015	Jul - Oct	DRY	1.4	146
YAN	58	1624	28	2014	Jul - Sept	DRY	1.4	133
YAS	60	2280	38	2014	Feb - May	DRY	1.4	140

Suppl. Table E.4 Species list of wild mammals recorded in the 37 forests across the globe, and number of forests with at least one detection, per biogeographic region. Species are listed in alphabetic order by taxonomic order.

Wild mammals detected			Num. of forests		
Order	**Familiy**	**Species**	**Afrotropics**	**Neotropics**	**Indomalayan-tropics**
Afrosoricida	Tenrecidae	*Hemicentetes semispinosus*	1	0	0
Afrosoricida	Tenrecidae	*Tenrec ecaudatus*	1	0	0
Artiodactyla	Cervidae	*Axis porcinus*	0	0	1
Artiodactyla	Suidae	*Babyrousa celebensis*	0	0	1
Artiodactyla	Bovidae	*Bos gaurus*	0	0	3
Artiodactyla	Bovidae	*Bos javanicus*	0	1	2
Artiodactyla	Bovidae	*Bubalus arnee*	0	1	3
Artiodactyla	Bovidae	*Bubalus depressicornis*	0	0	1
Artiodactyla	Bovidae	*Capricornis milneedwardsii*	0	0	2
Artiodactyla	Bovidae	*Capricornis sumatraensis*	0	0	3
Artiodactyla	Bovidae	*Cephalophus callipygus*	5	0	0
Artiodactyla	Bovidae	*Cephalophus dorsalis*	4	0	0
Artiodactyla	Bovidae	*Cephalophus harveyi*	2	0	0
Artiodactyla	Bovidae	*Cephalophus leucogaster*	4	0	0
Artiodactyla	Bovidae	*Cephalophus nigrifrons*	5	0	0
Artiodactyla	Bovidae	*Cephalophus ogilbyi*	3	0	0
Artiodactyla	Bovidae	*Cephalophus silvicultor*	7	0	0
Artiodactyla	Bovidae	*Cephalophus weynsi*	1	0	0
Artiodactyla	Bovidae	*Cephalophus spadix*	2	0	0
Artiodactyla	Bovidae	*Kobus ellipsiprymnus*	1	0	0
Artiodactyla	Bovidae	*Neotragus batesi*	2	0	0
Artiodactyla	Bovidae	*Nesotragus moschatus*	2	0	0
Artiodactyla	Bovidae	*Philantomba monticola*	8	0	0
Artiodactyla	Bovidae	*Redunca redunca*	1	0	0
Artiodactyla	Bovidae	*Syncerus caffer*	6	0	0
Artiodactyla	Bovidae	*Tragelaphus eurycerus*	2	0	0
Artiodactyla	Bovidae	*Tragelaphus scriptus*	6	0	0
Artiodactyla	Bovidae	*Tragelaphus spekii*	3	0	0
Artiodactyla	Cervidae	*Mazama americana*	0	8	0
Artiodactyla	Cervidae	*Mazama gouazoubira*	0	2	0

Artiodactyla	Cervidae	*Mazama nemorivaga*	0	6	0
Artiodactyla	Cervidae	*Mazama temama*	0	3	0
Artiodactyla	Cervidae	*Muntiacus atherodes*	0	0	1
Artiodactyla	Cervidae	*Muntiacus montanus*	0	0	3
Artiodactyla	Cervidae	*Muntiacus muntjak*	0	0	8
Artiodactyla	Cervidae	*Muntiacus vaginalis*	0	0	2
Artiodactyla	Cervidae	*Odocoileus hemionus*	0	1	0
Artiodactyla	Cervidae	*Odocoileus virginianus*	0	2	0
Artiodactyla	Cervidae	*Rusa unicolor*	0	0	9
Artiodactyla	Suidae	*Hylochoerus meinertzhageni*	1	0	0
Artiodactyla	Suidae	*Potamochoerus larvatus*	5	0	0
Artiodactyla	Suidae	*Potamochoerus porcus*	6	0	0
Artiodactyla	Suidae	*Sus barbatus*	0	0	2
Artiodactyla	Suidae	*Sus celebensis*	0	0	1
Artiodactyla	Suidae	*Sus scrofa*	0	1	10
Artiodactyla	Tragulidae	*Hyemoschus aquaticus*	5	0	0
Artiodactyla	Tragulidae	*Tragulus javanicus*	0	0	1
Artiodactyla	Tragulidae	*Tragulus kanchil*	0	0	4
Artiodactyla	Tragulidae	*Tragulus napu*	0	0	4
Artiodactyla	Tayassuidae	*Pecari tajacu*	0	12	0
Artiodactyla	Tayassuidae	*Tayassu pecari*	0	7	0
Carnivora	Canidae	*Atelocynus microtis*	0	3	0
Carnivora	Canidae	*Canis adustus*	2	0	0
Carnivora	Canidae	*Canis aureus*	0	0	1
Carnivora	Canidae	*Canis latrans*	0	1	0
Carnivora	Canidae	*Cerdocyon thous*	0	4	0
Carnivora	Canidae	*Cuon alpinus*	0	0	6
Carnivora	Canidae	*Speothos venaticus*	0	3	0
Carnivora	Eupleridae	*Cryptoprocta ferox*	1	0	0
Carnivora	Eupleridae	*Fossa fossana*	1	0	0
Carnivora	Eupleridae	*Galidia elegans*	1	0	0
Carnivora	Eupleridae	*Galidictis fasciata*	1	0	0
Carnivora	Herpestidae	*Atilax paludinosus*	9	0	1
Carnivora	Herpestidae	*Bdeogale crassicauda*	2	0	0
Carnivora	Herpestidae	*Bdeogale nigripes*	6	0	0
Carnivora	Herpestidae	*Crossarchus obscurus*	1	0	0

Carnivora	Herpestidae	*Crossarchus platycephalus*	2	0	0
Carnivora	Felidae	*Caracal aurata*	7	0	0
Carnivora	Felidae	*Felis chaus*	0	0	1
Carnivora	Felidae	*Leopardus pardalis*	0	12	0
Carnivora	Felidae	*Leopardus tigrinus*	0	2	0
Carnivora	Felidae	*Leopardus wiedii*	0	6	0
Carnivora	Felidae	*Leptailurus serval*	2	0	0
Carnivora	Felidae	*Neofelis nebulosa*	0	0	5
Carnivora	Felidae	*Neofelis diardi*	0	0	1
Carnivora	Felidae	*Panthera onca*	0	10	0
Carnivora	Felidae	*Panthera pardus*	5	0	3
Carnivora	Felidae	*Panthera tigris*	0	0	6
Carnivora	Felidae	*Pardofelis marmorata*	0	0	5
Carnivora	Felidae	*Pardofelis temminckii*	0	0	4
Carnivora	Felidae	*Prionailurus bengalensis*	0	0	11
Carnivora	Felidae	*Puma concolor*	0	11	0
Carnivora	Felidae	*Puma yagouaroundi*	0	9	0
Carnivora	Herpestidae	*Herpestes brachyurus*	0	0	3
Carnivora	Herpestidae	*Herpestes naso*	4	0	0
Carnivora	Herpestidae	*Herpestes sanguineus*	1	0	0
Carnivora	Herpestidae	*Herpestes urva*	0	0	4
Carnivora	Herpestidae	*Herpestes javanicus*	0	0	1
Carnivora	Herpestidae	*Mungos mungo*	2	0	0
Carnivora	Mustelidae	*Arctonyx collaris*	0	0	2
Carnivora	Mustelidae	*Eira barbara*	0	12	0
Carnivora	Mustelidae	*Galictis vittata*	0	1	0
Carnivora	Mustelidae	*Martes flavigula*	0	0	6
Carnivora	Mustelidae	*Mellivora capensis*	6	0	0
Carnivora	Mustelidae	*Melogale personata*	0	0	2
Carnivora	Mustelidae	*Mustela strigidorsa*	0	0	1
Carnivora	Mephitidae	*Mydaus javanensis*	0	0	1
Carnivora	Nandiniidae	*Nandinia binotata*	10	0	0
Carnivora	Procyonidae	*Nasua narica*	0	2	0
Carnivora	Procyonidae	*Nasua nasua*	0	10	0
Carnivora	Procyonidae	*Potos flavus*	0	1	0
Carnivora	Procyonidae	*Procyon cancrivorus*	0	5	0

Carnivora	Ursidae	*Helarctos malayanus*	0	0	9
Carnivora	Ursidae	*Ursus thibetanus*	0	0	2
Carnivora	Viverridae	*Arctictis binturong*	0	0	3
Carnivora	Viverridae	*Civettictis civetta*	5	0	0
Carnivora	Viverridae	*Cynogale bennettii*	0	0	1
Carnivora	Viverridae	*Genetta genetta*	2	0	0
Carnivora	Viverridae	*Genetta maculata*	1	0	0
Carnivora	Viverridae	*Genetta servalina*	9	0	0
Carnivora	Viverridae	*Genetta tigrina*	2	0	0
Carnivora	Viverridae	*Hemigalus derbyanus*	0	0	5
Carnivora	Viverridae	*Macrogalidia musschenbroekii*	0	0	1
Carnivora	Viverridae	*Paguma larvata*	0	0	4
Carnivora	Viverridae	*Paradoxurus hermaphroditus*	0	0	10
Carnivora	Viverridae	*Viverra tangalunga*	0	0	4
Carnivora	Viverridae	*Viverricula indica*	0	0	2
Carnivora	Viverridae	*Viverra zibetha*	0	0	5
Cingulata	Chlamyphoridae	*Cabassous centralis*	0	1	0
Cingulata	Chlamyphoridae	*Cabassous tatouay*	0	1	0
Cingulata	Chlamyphoridae	*Cabassous unicinctus*	0	3	0
Cingulata	Chlamyphoridae	*Priodontes maximus*	0	7	0
Cingulata	Dasypodidae	*Dasypus kappleri*	0	5	0
Cingulata	Dasypodidae	*Dasypus novemcinctus*	0	13	0
Didelphimorphia	Didelphidae	*Didelphis aurita*	0	1	0
Didelphimorphia	Didelphidae	*Didelphis marsupialis*	0	12	0
Didelphimorphia	Didelphidae	*Metachirus nudicaudatus*	0	5	0
Didelphimorphia	Didelphidae	*Philander mondolfii*	1	0	0
Didelphimorphia	Didelphidae	*Philander opossum*	0	4	0
Eulipotyphla	Erinaceidae	*Echinosorex gymnura*	0	0	3
Hyracoidea	Procaviidae	*Dendrohyrax arboreus*	1	0	0
Hyracoidea	Procaviidae	*Dendrohyrax validus*	2	0	0
Lagomorpha	Leporidae	*Caprolagus hispidus*	0	0	1
Lagomorpha	Leporidae	*Lepus nigricollis*	0	0	1
Lagomorpha	Leporidae	*Sylvilagus brasiliensis*	0	3	0
Macroscelidae	Macroscelididae	*Petrodromus tetradactylus*	2	0	0
Macroscelidae	Macroscelididae	*Rhynchocyon cirnei*	2	0	0
Macroscelidae	Macroscelididae	*Rhynchocyon udzungwensis*	1	0	0

Perissodactyla	Rhinocerotidae	*Rhinoceros unicornis*	0	0	1
Perissodactyla	Rhinocerotidae	*Rhinosciurus laticaudatus*	0	0	1
Perissodactyla	Tapiridae	*Tapirus bairdii*	0	1	0
Perissodactyla	Tapiridae	*Tapirus indicus*	0	0	4
Perissodactyla	Tapiridae	*Tapirus terrestris*	0	10	0
Pholidota	Manidae	*Manis javanica*	0	0	6
Pholidota	Manidae	*Manis pentadactyla*	0	0	1
Pholidota	Manidae	*Phataginus tricuspis*	8	0	0
Pholidota	Manidae	*Smutsia gigantea*	6	0	0
Pilosa	Myrmecophagidae	*Myrmecophaga tridactyla*	0	10	0
Pilosa	Myrmecophagidae	*Tamandua mexicana*	0	1	0
Pilosa	Myrmecophagidae	*Tamandua tetradactyla*	0	10	0
Primates	Atelidae	*Lagothrix cana*	0	1	0
Primates	Callitrichidae	*Saguinus fuscicollis*	0	1	0
Primates	Cercopithecidae	*Cercocebus agilis*	3	0	0
Primates	Cercopithecidae	*Cercocebus sanjei*	2	0	0
Primates	Cercopithecidae	*Cercocebus torquatus*	1	0	0
Primates	Cercopithecidae	*Cercopithecus ascanius*	2	0	0
Primates	Cercopithecidae	*Cercopithecus cephus*	2	0	0
Primates	Cercopithecidae	*Cercopithecus lhoesti*	1	0	0
Primates	Cercopithecidae	*Cercopithecus mitis*	4	0	0
Primates	Cercopithecidae	*Cercopithecus nictitans*	2	0	0
Primates	Cercopithecidae	*Cercopithecus pogonias*	1	0	0
Primates	Cercopithecidae	*Lophocebus albigena*	1	0	0
Primates	Cercopithecidae	*Macaca arctoides*	0	0	3
Primates	Cercopithecidae	*Macaca fascicularis*	0	0	5
Primates	Cercopithecidae	*Macaca leonina*	0	0	5
Primates	Cercopithecidae	*Macaca mulatta*	0	0	1
Primates	Cercopithecidae	*Macaca nemestrina*	0	0	5
Primates	Cercopithecidae	*Macaca nigra*	0	0	1
Primates	Cercopithecidae	*Macaca nigrescens*	0	0	1
Primates	Cercopithecidae	*Mandrillus leucophaeus*	2	0	0
Primates	Cercopithecidae	*Papio anubis*	2	0	0
Primates	Cercopithecidae	*Papio cynocephalus*	2	0	0
Primates	Cercopithecidae	*Presbytis melalophos*	0	0	2
Primates	Cercopithecidae	*Procolobus gordonorum*	1	0	0

Primates	Cercopithecidae	*Trachypithecus obscurus*	0	0	2
Primates	Haplorhini	*Saimiri boliviensis*	0	1	0
Primates	Haplorhini	*Saimiri sciureus*	0	2	0
Primates	Hominidae	*Pan troglodytes*	6	0	0
Primates	Hominidae	*Pongo abelii*	0	0	2
Primates	Lemuridae	*Eulemur fulvus*	1	0	0
Primates	Lemuridae	*Eulemur rufifrons*	1	0	0
Primates	Hominidae	*Gorilla beringei*	2	0	0
Primates	Hominidae	*Gorilla gorilla*	4	0	0
Primates	Lemuridae	*Hapalemur aureus*	1	0	0
Primates	Lemuridae	*Hapalemur griseus*	1	0	0
Proboscidea	Elephantidae	*Elephas maximus*	0	0	7
Proboscidea	Elephantidae	*Loxodonta africana*	7	0	0
Rodentia	Caviidae	*Galea spixii*	0	1	0
Rodentia	Caviidae	*Hydrochoerus hydrochaeris*	0	1	0
Rodentia	Cricetidae	*Euryoryzomys nitidus*	0	1	0
Rodentia	Cricetidae	*Tylomys watsoni*	0	1	0
Rodentia	Cuniculidae	*Cuniculus paca*	0	13	0
Rodentia	Dasyproctidae	*Dasyprocta fuliginosa*	0	3	0
Rodentia	Dasyproctidae	*Dasyprocta leporina*	0	4	0
Rodentia	Dasyproctidae	*Dasyprocta prymnolopha*	0	1	0
Rodentia	Dasyproctidae	*Dasyprocta punctata*	0	4	0
Rodentia	Dasyproctidae	*Dasyprocta ruatanica*	0	1	0
Rodentia	Dasyproctidae	*Myoprocta acouchy*	0	2	0
Rodentia	Dasyproctidae	*Myoprocta pratti*	0	2	0
Rodentia	Echimyidae	*Dactylomys peruanus*	0	1	0
Rodentia	Echimyidae	*Proechimys brevicauda*	0	1	0
Rodentia	Echimyidae	*Proechimys semispinosus*	0	2	0
Rodentia	Erethizontidae	*Coendou prehensilis*	0	2	0
Rodentia	Hystricidae	*Atherurus africanus*	7	0	0
Rodentia	Hystricidae	*Atherurus macrourus*	0	0	5
Rodentia	Hystricidae	*Hystrix africaeaustralis*	1	0	0
Rodentia	Hystricidae	*Hystrix brachyura*	0	0	10
Rodentia	Hystricidae	*Hystrix crassispinis*	0	0	1
Rodentia	Hystricidae	*Hystrix indica*	0	0	1
Rodentia	Hystricidae	*Trichys fasciculata*	0	0	2

Rodentia	Muridae	*Leopoldamys sabanus*	0	0	1
Rodentia	Muridae	*Maxomys rajah*	0	0	1
Rodentia	Muridae	*Rattus rattus*	3	0	0
Rodentia	Muridae	*Rattus tiomanicus*	0	0	1
Rodentia	Nesomyidae	*Cricetomys emini*	7	0	0
Rodentia	Nesomyidae	*Cricetomys gambianus*	4	0	0
Rodentia	Nesomyidae	*Eliurus tanala*	1	0	0
Rodentia	Nesomyidae	*Nesomys rufus*	1	0	0
Rodentia	Sciuridae	*Callosciurus erythraeus*	0	0	1
Rodentia	Sciuridae	*Callosciurus finlaysonii*	0	0	1
Rodentia	Sciuridae	*Dremomys rufigenis*	0	0	1
Rodentia	Sciuridae	*Funisciurus anerythrus*	1	0	0
Rodentia	Sciuridae	*Funisciurus carruthersi*	1	0	0
Rodentia	Sciuridae	*Funisciurus isabella*	2	0	0
Rodentia	Sciuridae	*Funisciurus leucogenys*	1	0	0
Rodentia	Sciuridae	*Funisciurus pyrropus*	4	0	0
Rodentia	Sciuridae	*Lariscus insignis*	0	0	2
Rodentia	Sciuridae	*Menetes berdmorei*	0	0	3
Rodentia	Sciuridae	*Paraxerus vexillarius*	2	0	0
Rodentia	Sciuridae	*Protoxerus stangeri*	4	0	0
Rodentia	Sciuridae	*Rheithrosciurus macrotis*	0	0	1
Rodentia	Sciuridae	*Sciurus aestuans*	0	2	0
Rodentia	Sciuridae	*Sciurus granatensis*	0	1	0
Rodentia	Sciuridae	*Sciurus ignitus*	0	1	0
Rodentia	Sciuridae	*Sciurus igniventris*	0	1	0
Rodentia	Sciuridae	*Sciurus spadiceus*	0	1	0
Rodentia	Thryonomyidae	*Thryonomys swinderianus*	3	0	0
Scandentia	Tupaiidae	*Tupaia belangeri*	0	0	3
Scandentia	Tupaiidae	*Tupaia glis*	0	0	2
Tubulidentata	Orycteropodidae	*Orycteropus afer*	4	0	0

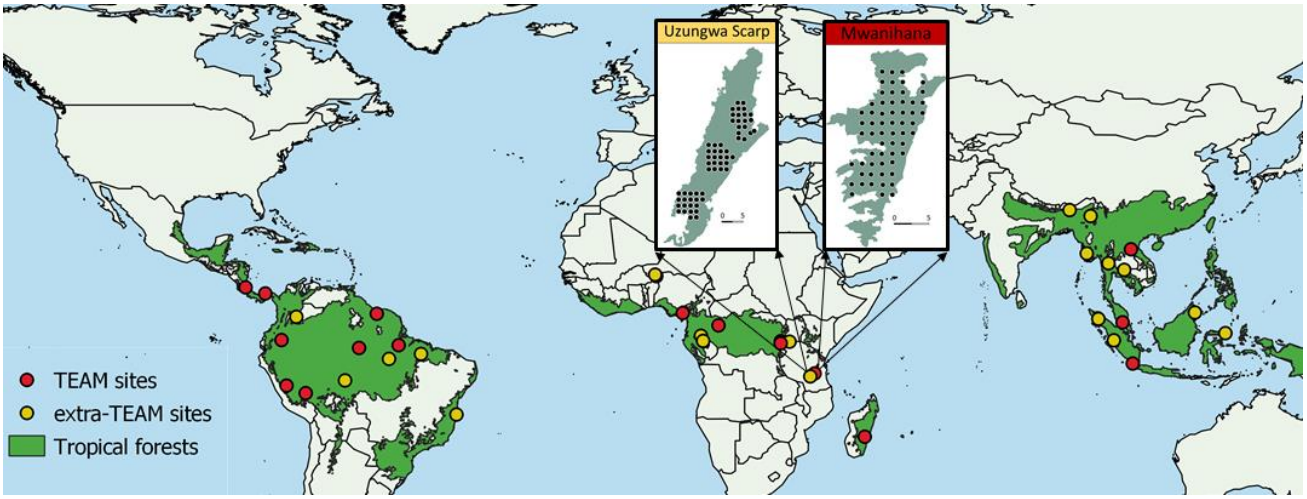

Suppl. Fig. E.1 *Theriotrop* study forests formed by the TEAM sites (red dots) and by the added sites (yellow). Insert maps display an example of the comparable sampling design between the TEAM sites (red) and the added sites (yellow).

Bibliography

Ahumada, J.A., J., Hurtado and D., Lizcano. 2013. Monitoring the status and trends of tropical forest terrestrial vertebrate communities from camera trap data: a tool for conservation. PLoS ONE 8: e73707.

Allen, M., H. Wittmer, E. Setiawan, S. Jaffe, and A. J. Marshall. 2016. Scent marking in Sunda clouded leopards (*Neofelis diardi*): novel observations close a key gap in understanding felid communication behaviours. Scientific Report 6:35433.

Andermann, T., S., Faurby, S. T., Turvey, A., Antonelli and D., Silvestro. 2020. The past and future human impact on mammalian diversity. Science Advances 6(36): eabb2313.

Andreassen, H. P., J. Sundell, F. Ecke, S. Halle, M. Haapakoski, H. Henttonen, O. Huitu, J. Jacob, K. Johnsen, E. Koskela, et al. 2021. Population cycles and outbreaks of small rodents: ten essential questions we still need to solve. Oecologia 195:601–622.

Andresen, E., V. Arroyo-Rodriguez and M. Ramos-Robles. 2018. Primate seed dispersal: old and new challenges. International Journal of Primatoly 39(3): 443 – 465.

Anile, S., C. Augugliaro, B. Munkhtsog, F. Dartora, A. Vendraminn, G. Bombieri, and C. Nielsen. 2021. Density and activity patterns of Pallas's cats *Otocolobus manul* in central Mongolia. Wildlife Research 48:264–272.

Archer, C. et al. 2020. State of the Tropics 2020 Report. Available at: https://www.jcu.edu.au/state-of-the-tropics/publications/state-of-the-tropics-2020-report

Augugliaro, C., P. Christe, C. Janchivlamdan, H. Baymanday, and F. Zimmermann. 2020. Patterns of human interaction with snow leopard and co-predators in the Mongolian western Altai: current issues and perspectives. Global Ecology and Conservation 24: e01378.

Bahaa-El-Din, L., P. Henschel, T. Butinsky, D. W. MacDonald, R. Slotow and L. Hunter. 2015a. The African golden cat *Caracal aurata*: Africa's least known feline. Mammal Review 45, 63–77.

Bahaa-El-Din, L., D. Mills, L. Hunter and P. Henschel. 2015b. *Caracal aurata.* In *The IUCN Red List of Threatened Species* 2015: e.T18306A50663128. dx.doi.org/10.2305/IUCN.UK.2015-2.RLTS.T18306A50663128.en [accessed 8 July 2020].

Bahaa-El-Din, L., R. Sollmann, L. Hunter, R. Slotow, D. W. MacDonald and P. Henschel 2016. Effects of human land-use on Africa's only forest-dependent feline: the African golden cat *Caracal aurata*. Biological Conservation 199, 1–9.

Balmford, A. 1996. Extinction filters and current resilience: the significance of past selection pressures for conservation biology. Trends in Ecology & Evolution 11: 193 – 196.

Barashkova, A., I. Smelansky, V. Kirilyuk, S. Naidenko, A. Antonevich, M. Gritsina, K. Zhumabai Uulu, M. Koshkin, N. Battogtokh, B. Otgonbayar, A. Grachev, and A. Lissovsky. 2019. Distribution and status of the manul in Central Asia and adjacent areas. Cat News Special Issue 13:14–23.

Barashkova, A. N. 2017. Manul. Pages 313–317 *in* Red Data Book of the Altai Republic. Government of Altai Republic, Gorno-Altaisk, Russia. [In Russian].

Barashkova, A. 2012. New data on Pallas's cat in Tyva. Steppe Bulletin 35:44–48. [In Russian].

Barashkova, A., and I. Smelansky. 2011. Pallas's cat in the Altai Republic, Russia. Cat News 54:4–7.

Barashkova, A., I. Smelansky, S. Goryunova, and S. Naidenko. 2007. Pallas's cat: investigation for saving (clarifying conservation status in Russia). Siberian Environmental Center, Novosibirsk, Russia.

Barclay, D., I. Smelansky, E. Nygren, and A. Antonevich. 2019. Legal status, utilisation, management and conservation of manul. Cat News Special Issue 13:37–40.

Barelli C., J. F. Gallardo Palacios and F. Rovero 2013. Variation in primate abundance along an elevational gradient in the Udzungwa Mountains of Tanzania. In:

Grow, N., S. Gursky-Doyen and A. Krzton (eds) High Altitude Primates. Developments in Primatology: Progress and Prospects. Springer, New York, NY.

Barnosky, A., N., Matzke, S., Tomiya, et al. 2011. Has the Earth's sixth mass extinction already arrived? Nature 471: 51–57.

Battin J. 2004. When good animals love bad habitats: ecological traps and the conservation of animal populations. Conservation Biology 18: 1482 – 1491.

Beaudrot, L., J. A., Ahumada, T., O'Brien, P., Alvarez-Loayza, K., Boekee, et al. 2016. Standardized Assessment of Biodiversity Trends in Tropical Forest Protected Areas: The End Is Not in Sight. PLOS Biology 14(1): e1002357.

Bedoya-Durán, M. J., O. E., Murillo-García, and L. C., Branch. 2021. Factors outside privately protected areas determine mammal assemblages in a global biodiversity hotspot in the Andes. Global Ecology and Conservation 32: e01921.

Benítez-López, A., et al. 2017. The impact of hunting on tropical mammal and bird populations. Science 356: 180 – 183.

Benítez-López, A., L., Santini, A. M., Schipper, M. Busana, and M. A. J., Huijbregts. 2019. Intact but empty forests? Patterns of hunting-induced mammal defaunation in the tropics. PLOS Biology 17: e3000247.

Berger J. 2007. Fear, human shields and the redistribution of prey and predators in protected areas. Biology Letters 3620 – 623.

Berger, J., B. Buuveibaatar, and C. Mishra. 2013. Globalization of the cashmere market and the decline of large mammals in Central Asia. Conservation Biology 27:679–689.

Blaum, N., B. Tietjen, and E. Rossmanith. 2009. Impact of livestock husbandry on small- and medium-sized carnivores in Kalahari savannah rangelands. Journal of Wildlife Management 73:60–67.

Blaum, N., E. Rossmanith, A. Popp, and F. Jeltsch. 2007*a*. Shrub encroachment affects mammalian carnivore abundance and species richness in semiarid rangelands. Acta Oecologica–International Journal of Ecology 31:86–92.

Blaum, N., E. Rossmanith, M. Schwager, and F. Jeltsch. 2007*b*. Responses of mammalian carnivores to land use in arid savanna rangelands. Basic and Applied Ecology 8:552–564.

Bolker, B. M. 2008. Probability and Stochastic Distributions for Ecological Modeling. In: Ecological Models and Data in R (pp. 103–146). Princeton University Press. https://doi.org/10.2307/j.ctvcm4g37.7

Bonnot, N. C., O., Couriot, A., Berger, F., Cagnacci, S., Ciuti, J. E., De Groeve, et al. 2020. Fear of the dark? Contrasting impacts of humans versus lynx on diel activity of roe deer across Europe. Journal of Animal Ecology, 89(1): 132 - 145.

Bösing, B. M., D. H. Haarmeyer, J. Dengler, J. U. Ganzhorn, and U. Schmiedel. 2014. Effects of livestock grazing and habitat characteristics on small mammal communities in the Knersvlakte, South Africa. Journal of Arid Environments 104:124–131.

Brassine, E. and D., Parker. 2015. Trapping Elusive Cats: Using Intensive Camera Trapping to Estimate the Density of a Rare African Felid. PLOS ONE 10(12): e0142508.

Brodie, J. F. 2009. Is research effort allocated efficiently for conservation? *Felidae* as a global case study. Biodiversity and Conservation 18:2927–2939.

Bülow-Olsen, A. 1980. Changes in the species composition in an area dominated by *Deschampsia flexuosa* (L) trin. as a result of cattle grazing. Biological Conservation 18:257–270.

Burnham, K. P., and D. R. Anderson. 2002. Model selection and multimodel inference. Springer, New York, New York, USA.

Burgess, N. D., T. M. Butynski, N. J. Cordeiro, N. H. Doggart, J. Fjeldså, K. M. Howell, F. B. Kilahama, S. P. Loader, J. C. Lovett, B. Mbilinyi, M. Menegon, D. C. Moyer, E. Nashanda, A. Perkin, F. Rovero, W. T. Stanley and S. N. Stuart. 2007. The biological importance of the Eastern Arc Mountains of Tanzania and Kenya. Biological Conservation 134: 209 – 231.

Butynsky, T. M., H. Douglas-Dufresne, and Y.A. De Jong. 2012. Identification, distribution and conservation status of the African golden cat *Caracal aurata*

in Kenya. Journal of East African Natural History 101, 3–16.

Campos-Silva, J. V., C. A. Peres, J. E. Hawes, T. Haugaasen, C. T. Freitas, R. J. Ladle and P. F. M. Lopes. 2021. Sustainable-use protected areas catalyze enhanced livelihoods in rural Amazonia. Proceedings of the National Academy of Sciences 118(40): e2105480118.

Cao, C., L. Shuai, X. Xin, Z. Liu, Y. Song, and Z. Zeng. 2016. Effects of cattle grazing on small mammal communities in the Hulunber meadow steppe. PeerJ 4:e2349.

Cardillo, M., A. Purvis, W. Sechrest, J. L. Gittleman, J. Bielby, and G. M. Mace. 2004. Human population density and extinction risk in the world's carnivores. PLoS Biology 2: e197.

Cardinale, B., J., Duffy, A., Gonzalez, et al. 2012. Biodiversity loss and its impact on humanity. Nature 486: 59–67.

Cavada, N., S. Tenan, C. Barelli and F. Rovero 2019. Effects of anthropogenic disturbance on primate density at the landscape scale. Conservation Biology 33: 873 – 882.

Cavada, N., C. Barelli, M. Ciolli and F. Rovero 2016. Primates in human-modified and fragmented landscapes: the conservation relevance of modelling habitat and disturbance factors in density estimation. PLoS ONE 11: e0148289.

Ceballos, G., and P. R., Ehrlich. 2002. Mammal Population Losses and the Extinction Crisis. Science 296: 904 – 907.

Ceballos, G., P. R., Ehrlich, A. D., Barnosky, A., García, R. M., Pringle and T. M., Palmer. 2015. Accelerated modern human–induced species losses: Entering the sixth mass extinction. Science Advances 1(5): e1400253.

Ceballos, G., P. R., Ehrlich and R., Dirzo. 2017. Biological annihilation via the ongoing sixth mass extinction signaled by vertebrate population losses and declines. Proceedings of the National Academy of Sciences 2017-07-25 114(30): E6089-E6096.

Challéat, S., K., Barré, A., Laforge, D., Lapostolle, M., Franchomme, C., Sirami, et al. 2021. Grasping darkness: the dark ecological network as a social-ecological framework to limit the impacts of light pollution on biodiversity. Ecology and

Society 26(1): 15.

Chambers, J. M. and T. J. Hastie 1992. Statistical Models in S (eds). Wadsworth and Brooks/Cole.

Chapin III, F., E., Zavaleta, V., Eviner, et al. 2000. Consequences of changing biodiversity. Nature 405: 234–242.

Chimed, O., J. S. Alexander, G. Samelius, P. Lkhagvajav, L. Davaa, N. Bayasgalan, and K. Sharma. 2021. Examining the past and current distribution of Pallas's cat in Southern Mongolia. Mammalian Biology 101:in press. doi.org/10.1007/s42991-021-00132-3.

Ciuti, S., J. M., Northrup, T. B., Muhly, S., Simi, M., Musiani, J. A., Pitt, and M. S., Boyce. 2012. Effects of humans on behaviour of wildlife exceed those of natural predators in a landscape of fear. PloS one 7(11): e50611.

Clare, J. D., E. M. Anderson and D. M. MacFarland. 2015. Predicting bobcat abundance at a landscape scale and evaluating occupancy as a density index in central Wisconsin. Journal of Wildlife Management 79(3): 469 – 480.

Clayton, E. 2016. *Marmota sibirica*. The IUCN Red List of Threatened Species 2016: e.T12832A22258643.

Clough, Y., et al. 2011. Combining high biodiversity with high yields in tropical agroforests. Proceedings of the National Academy of Sciences 108: 8311 – 8316.

Coad, L., J. E. M., Watson, J., Geldmann, N. D., Burgess, F., Leverington, M., Hockings, K., Knights, and M., Di Marco. 2019. Widespread shortfalls in protected area resourcing undermine efforts to conserve biodiversity. Frontiers in Ecology and the Environment 17(5): 259– 264.

Convention on Biological Diversity. 2021. First Draft of the Post-2020 Global Biodiversity Framework. https://www.cbd.int/meetings/WG2020-03.

Crooks, K. R., et al. 2017. Quantification of habitat fragmentation reveals extinction risk in terrestrial mammals. Proceedings of the National Academy of Sciences 114: 7635 – 7640.

Cusack J. J., A. J., Dickman, J. M. Rowcliffe, C. Carbone, D. W. Macdonald, et al. 2015.

Random versus Game Trail-Based Camera Trap Placement Strategy for Monitoring Terrestrial Mammal Communities. PLOS ONE 10(5): e0126373.

Dagvadorj, D., L. Natsagdorj, J. Dorjpurev, and B. Namkhainyam. 2009. Mongolian assessment report on Climate Change 2009. Ministry of Environment, Nature and Tourism, Ulan Bator, Mongolia.

Damdinsuren, B., J. E. Herrick, D. A. Pyke, B. T. Bestelmeyer, and K. M. Havstad. 2008. Is rangeland health relevant to Mongolia? Rangelands 30:25–29.

Davenport, T. R. B., K. Nowak and A. Perkin 2013. Priority Primate Areas in Tanzania. Oryx 48(1): 39 – 51.

Davenport, T. R. B., S. J. Machaga, N. E. Mpunga, S. P. Kimiti, W. Mwalwengele, O. Mwaipungu and P. M. Makumbule 2022. A Reassessment of the Population Size, Demography, and Status of Tanzania's Endemic Kipunji Rungwecebus kipunji 13 Years on: Demonstrating Conservation Success. International Journal of Primatology 43: 317 – 338.

de Valpine, P. et al. 2017. Programming With Models: Writing Statistical Algorithms for General Model Structures With NIMBLE. Journal of Computational and Graphical Statistics 26: 403 – 413.

de Valpine, P. et al. 2021. NIMBLE – An R package for programming with BUGS models and compiling parts of R. https://r-nimble.org/.

DeFries, R., A., Hansen, A. C., Newton, and M. C., Hansen. 2005. Increasing Isolation of Protected Areas in Tropical Forests Over the Past Twenty Years. Ecological Applications 15: 19 – 26.

Delibes-Mateos, M., T. A. Smith, C. N. Slobodchikoff, and J. E. Swenson. 2011. The paradox of keystone species persecuted as pests: a call for the conservation of abundant small mammals in their native range. Biological Conservation 144:1335–1346.

Devictor, V., R. Julliard, and F., Jiguet. 2008. Distribution of Specialist and Generalist Species along Spatial Gradients of Habitat Disturbance and Fragmentation. Oikos 117: 507 – 514.

Di Marco, M., J. E. M., Watson, H. P., Possingham, and O., Venter. 2017. Limitations and

trade-offs in the use of species distribution maps for protected area planning. Journal of Applied Ecology 54: 402 – 411.

Diao, Y., Q., Zhao, Y., Weng, et al. 2021. Temporal shifts as elusive responses to anthropogenic stressors in a mammal community. Biodiversity Conservation 30: 2529 – 2544.

Díaz, S., J., Fargione, F. S. III, Chapin and D., Tilman. 2006. Biodiversity Loss Threatens Human Well-Being. PLOS Biology 4(8): e277.

Dinerstein, E., C., Vynne, E., Sala, A. R., Joshi, S., Fernando, T. E., Lovejoy, J., Mayorga, D., Olson, G. P., Asner, J. E. M., Baillie, N. D., Burgess, K., Burkart, R. F., Noss, Y. P., Zhang, A., Baccini, T., Birch, N., Hahn, L. N., Joppa and E., Wikramanayake. 2019. A Global Deal For Nature: Guiding principles, milestones, and targets. Science Advances 5(4): eaaw2869.

Dirzo, R., H. S., Young, M., Galetti, G., Ceballos, N. J. B., Isaac and B., Collen. 2014. Defaunation in the Anthropocene. Science 345(6195): 401–406.

Dorazio, R. M., J. A., Royle, B., Söderström, and A., Glimskär. 2006. Estimating Species Richness and Accumulation by Modeling Species Occurrence and Detectability. Ecology 87: 842 – 854.

Dormann, C. F., J. M. Calabrese, G. Guillera-Arroita, E. Matechou, V. Bahn, Bartoń K, Beale CM, Ciuti S, Elith J, Gerstner K, Guela, J, Keil P, Lahoz-Monfort JJ, Pollock LJ, Reineking B, Roberts DR, Schröder B, Thuiller W, Warton DI, Wintle BA, Wood SN, Wüest RO, Hartig F (2018) Model averaging in ecology: a review of Bayesian, information-theoretic, and tactical approaches for predictive inference. Ecol Monogr, 88: 485-504.

Dornelas, M., et al. 2014. Assemblage Time Series Reveal Biodiversity Change but Not Systematic Loss. Science 344: 296 – 299.

Eagles, P. F., S. F., McCool, and C. D., Haynes. 2002. Sustainable tourism in protected areas: Guidelines for planning and management (No. 8). IUCN.

Efford, M. G., and D. K. Dawson. 2012. Occupancy in continuous habitat. Ecosphere 3(4):1–15.

Ehardt, C. L. 2001. The endemic primates of the Udzwunga Mountains, Tanzania. Afr

Primates 4: 15 – 26.

Ehardt, C. L., T. P. Jones and T. M. Butynski. 2005. Protective status, ecology and strategies for improving conservation of *Cercocebus sanjei* in the Udzungwa Mountains, Tanzania. International Journal of Primatology 263: 557 – 583.

Elhacham, E., L., Ben-Uri, J., Grozovski, et al. 2020. Global human-made mass exceeds all living biomass. Nature 588: 442 – 444.

Ellis, E. C., N., Gauthier, K. K., Goldewijk, R. B., Bird, N., Boivin, S., Díaz, D. Q., Fuller, J. L., Gill., J. O., Kaplan, N., Kingston, H., Locke, C. N. H., McMichael, D., Ranco, T. C., Rick, M. R., Shaw, L., Stephens, J. C., Svenning and J. E. M., Watson. 2021. People have shaped most of terrestrial nature for at least 12,000 years. Proceedings of the National Academy of Sciences 2021-04-27 118(17): e2023483118.

Estrada, A., P. A. Garber, A. B. Rylands, C. Roos, E. Fernandez-Duque, A. Di Fiore, K. A. I. Nekaris, V. Nijman, E. W. Heymann, J. E. Lambert, F. Rovero, C. Barelli, J. M. Setchell, T. R. Gillespie, R. A. Mittermeier, L. V. Arregoitia, M. de Guinea, S. Gouveia, R. Dobrovolski, S. Shanee, N. Shanee, S. A. Boyle, A. Fuentes, K. C. MacKinnon, K. R. Amato, A. L. S. Meyer, S. Wich, R. W. Sussman, R. L. Pan, I. Kone and B. G. Li 2017. Impending extinction crisis of the world's primates: Why primates matter. Science Advances 3: e1600946.

European Commission. 2003. Global Land Cover 2000 database. European Commission, Joint Research Center. https://forobs.jrc.ec.europa.eu/products/glc2000/glc2000.php.

European Commission. 2004. Global Land Cover for the Year 2000. In: Bartholomé E, A. Belward, R. Beuchle, H. Eva, S. Fritz, A. Hartley, P. Mayaux and H. J. Stibig (eds). Luxembourg Office for Official Publications of the European Communities catalogue number LB-55-03-099-ENC.

European Commission. 2021. Directorate-General for Environment, EU biodiversity strategy for 2030 : bringing nature back into our lives, Publications Office of the European Union, https://data.europa.eu/doi/10.2779/677548

Farhadinia, M. S., E. M. Moqanaki, and M. A. Adibi. 2016. Baseline information and status assessment of manul (Pallas's cat; *Otocolobus manul* Pallas, 1776) in

Iran. Cat News Special Issue 2016:38–42.

Fahrig, L. 2013. Rethinking patch size and isolation effects: the habitat amount hypothesis. Journal of Biogeography 40: 1649 – 1663.

Fegraus, E., and J. MacCharty. 2016. Camera trap data management and interoperability. Chapter 4 *in* F. Rovero, and F. Zimmermann, editors. Camera trapping for wildlife research. Pelagic Publishing, Exeter, United Kingdom.

Fernández, D., D. Kerhoas, A. Dempsey, J. Billany, G. McCabe and E. Argirova 2022. The Current Status of the World's Primates: Mapping Threats to Understand Priorities for Primate Conservation. International Journal of Primatology 43: 15–39.

Fiske, I., and R. Chandler. 2011. Unmarked: an R package for fitting hierarchical models of occurrence and abundance. Journal of Statistical Software 43:1– 23.

Fiske, I., R. Chandler, D. Miller, et al. 2019. unmarked: an R package for fitting hierarchical models of wildlife occurrence and abundance. Journal of Statistical software 43, 10.

Flensted, K. K., et al. 2016. Red-listed species and forest continuity – A multi-taxon approach to conservation in temperate forests. Forest Ecology and Management 378: 144 – 159.

Fraser, L. H., et al. 2013. Coordinated distributed experiments: an emerging tool for testing global hypotheses in ecology and environmental science. Frontiers in Ecology and the Environment 11: 147 – 155.

Ganyushkin, D. A., K. V. Chistyakov, I. V. Volkov, D. V. Bantcev, E. P. Kunaeva, T. A. Andreeva, A. V. Terekhov, and D. Otgonbayar. 2018. Present glaciers of Tavan Bogd Massif in the Altai Mountains, Central Asia, and their changes since the Little Ice Age. Geosciences 8:1–35.

Gavin, M. C., J., McCarter, A., Mead, F., Berkes, J. R., Stepp, D., Peterson, and R., Tang. 2015. Defining biocultural approaches to conservation. Trends in ecology & evolution 30(3): 140 - 145.

Gaynor, K. M., C. E. Hojnowski, N. H. Carter, and J. S. Brashares. 2018. The influence of human disturbance on wildlife nocturnality. Science 360:1232–1235.

Gaynor, K. M., J., Brown, A., Moddleton, M., Power and J., Brashares. 2019. Landscapes of Fear: Spatial Patterns of Risk Perception and Response.

Geldmann, J., et al. 2013. Effectiveness of terrestrial protected areas in reducing habitat loss and population declines. Biological Conservation 161: 230 – 238.

Geldmann, J., A., Manica, N. D., Burgess, L., Coad and A., Balmford. 2019. A global-level assessment of the effectiveness of protected areas at resisting anthropogenic pressures. Proceedings of the National Academy of Sciences 116 (46): 23209–23215.

Giam, X. et al. 2012. Reservoirs of richness: least disturbed tropical forests are centres of undescribed species diversity. Proceedings of the Royal Society B: Biological Sciences 279: 67 – 76.

Gilbert, N. 2008. A quarter of mammals face extinction. Nature. https://doi.org/10.1038/455717a

Gippoliti, S. and C. Sousa 2004. The chimpanzee, Pan troglodytes, as an "umbrella" species for conservation in Guinea-Bissau, West Africa: opportunities and constraints. Folia Primatologica 75: 386.

Gompper, M. E., D. B. Lesmeister, J. C. Ray, J. R. Malcolm, and R. Kays. 2016. Differential habitat use or intraguild interactions: What structures a carnivore community? PLoS ONE 11(1):e0146055.

Grantham, H. S., A., Duncan, T. D. Evans, et al. 2020. Anthropogenic modification of forests means only 40% of remaining forests have high ecosystem integrity. Nature Communications 11: 5978.

Gray, C. L., S. L., Hill, T., Newbold, L. N., Hudson, L., Börger, S., Contu, et al. 2016. Local biodiversity is higher inside than outside terrestrial protected areas worldwide. Nature Communications 7(1): 1 - 7.

Greco, I., and F. Rovero. 2021. The African golden cat *Caracal aurata* in Tanzania: first record and vulnerability assessment. Oryx 55:212–115.

Greco, I., E. Fedele, M. Salvatori, M. Giampaoli Rustichelli, F. Mercuri, G. Santini, F. Rovero, L. Lazzaro, B. Foggi, et al. 2021. Guest or pest? Spatio-temporal occurrence and effects on soil and vegetation of the wild boar on Elba island.

Mammalian Biology 101:193–206.

Greenspan, E., and A. Giordano. 2021. A rangewide distribution model for the Pallas's cat (*Otocolobus manul*): identifying potential new survey regions for an understudied small cat. Mammalia 85:in press. doi.org/10.1515/mammalia-2020-0094.

Guillera-Arroita, G., J. J., Lahoz-Monfort, D. I., MacKenzie, B. A., Wintle, M. A., McCarthy. 2014. Ignoring imperfect detection in biological surveys is dangerous: A response to 'Fitting and interpreting occupancy models". PLoS ONE. 9: e99571.

Guisan, A. and N. E., Zimmermann. 2000. Predictive habitat distribution models in ecology. Ecological modelling, 135(2-3), pp.147-186.

Haddad, N. M., L. A., Brudvig, J., Clobert, K. F., Davies, A., Gonzalez, R. D., Holt, et al. 2015. Habitat fragmentation and its lasting impact on Earth's ecosystems. Science Advances 1: 1 – 9.

Hale R., and S. E. Swearer. 2016. Ecological traps: current evidence and future directions. Proceedings of the Royal Society B 283: 20152647.

Halfwerk, W., and H., Slabbekoorn. 2015. Pollution going multimodal: the complex impact of the human-altered sensory environment on animal perception and performance. Biology letters 11(4): 20141051.

Hansen, A. J., and R., Defries. 2007. Ecological Mechanisms Linking Protected Areas to Surrounding Lands. Ecological Applications 17: 974 – 988.

Hansen, A. 2011. Contribution of source–sink theory to protected area science. in Sources, Sinks and Sustainability (eds). In: Liu, J., V., Hull, A. T. Morzillo, and J. A. Wiens. Sources, sinks, and sustainability across landscapes. Pp: 339 – 360 Cambridge University Press.

Harcourt, A. H., S. A., Parks, and R., Woodroffe. 2001. Human density as an influence on species/area relationships: double jeopardy for small African reserves? Biodiversity and Conservation 10: 1011 – 1026.

Hatfield, R. S., J. Mwaura, S. Musila and L. O'Meara 2019. The first confirmed record of African golden cat *Caracal aurata* from Kenya since 1946. Journal of East African Natural History 108, 49–55.

Hegerl, C., N. Burgess, M. Nielsen, E. Martin, M. Ciolli and R. Rovero 2017. Using camera-trap data to assess the impact of bushmeat hunting on forest mammals in Tanzania. Oryx 51: 87–97.

Hoffmann, M., H. T. Craig, A., Angulo, et al. 2010. The Impact of Conservation on the Status of the World's Vertebrates. Science 330(6010): 1503–1509.

Hoffmann, S., C., Beierkuhnlein, R., Field, et al. 2018. Uniqueness of Protected Areas for Conservation Strategies in the European Union. Scientific Reports 8: 6445.

Holbrook, K. M. and B. A. Loiselle 2009. Dispersal in a neotropical tree, Virola flexusa (Myristicacae): does hunting of large vertebrates' limit seed removal? Ecology 90: 1449 – 1455.

Howard, C., C. H., Flather, and P. A., Stephens. 2020. A global assessment of the drivers of threatened terrestrial species richness. Nature Communications 11: 993.

IUCN, International Union for Conservation of Nature 2021. The IUCN Red List of Threatened Species. Available at: https://www.iucnredlist.org. Accessed on December 2022.

Jarvis, A., H. I. Reuter, A. Nelson, and E. Guevara. 2008. Hole-filled seamless SRTM data V4, International Centre for Tropical Agriculture (CIAT), Cali, Colombia. http://srtm.csi.cgiar.org.

Jayakody, S., A. M., Sibbald, I. J., Gordon, and X., Lambin. 2008. Red deer *Cervus elephus* vigilance behaviour differs with habitat and type of human disturbance. Wildlife biology 14(1): 81-91.

Jones, K. R., et al. 2018. One-third of global protected land is under intense human pressure. Science 360: 788 – 791.

Joppa, L. N. and A., Pfaff. 2009. High and far: biases in the location of protected areas. PLoS One 4: e8273.

Joseph, L. N., S. A. Field, C. Wilcox and H. P. Possingham2006. Presence-Absence versus Abundance Data for Monitoring Threatened Species. Conservation Biology 20(6): 1679 – 1687.

Kellner and Meredith. A Wrapper Around 'rjags' to Streamline 'JAGS' Analyses. 2021 Available at: https://cran.r-project.org/web/packages/jagsUI/jagsUI.pdf

Kery, M. 2002. Inferring the absence of a species: a case study of snakes. The Journal of wildlife management, pp.330-338.

Kéry, M. and J. A., Royle. 2008. Hierarchical Bayes estimation of species richness and occupancy in spatially replicated surveys. Journal of Applied Ecology, 45(2): pp.589-598.

Kéry, M., G. Guillera-Arroita and J.J. Lahoz-Monfort. 2013. Analysing and mapping species range dynamics using occupancy models. Journal of Biogeography 40(8): 1463 – 1474.

Kéry, M. and J. A. Royle 2016. Applied hierarchical modeling in ecology: analysis of distribution, abundance and species richness in R and BUGS. Vol. 1 Prelude and static models. Academic Press, London, UK, 783p. ISBN: 978-0-12-801378-6.

Kühl, H., F. Maisels, M. Ancrenaz and E. A. Williamson 2008. Best Practice Guidelines for Surveys and Monitoring of Great Ape Populations. IUCN SSC Primate Specialist Group, Gland, Switzerland.

Kunming-Montreal Global biodiversity framework 2022. Draft decision submitted by the President. Document n: CBD/COP/15/L.25 18 December 2022. Available: https://www.cbd.int/doc/c/e6d3/cd1d/daf663719a03902a9b116c34/cop-15-l-25-en.pdf

Lacher, T. E., A. D. Davidson, T. H. Fleming, E. P. Gómez-Ruiz, G. F. McCracken, N. Owen-Smith, C. A. Peres and S. B. Vander Wall. 2019. The functional roles of mammals in ecosystems. Journal of Mammalogy 100: 942 – 964.

Lama, S. T., J. G. Ross, D. Bista, A. P. Sherpa, G. R. Regmi, M. K. Suwal, P. Sherpa, J. Weerman, S. S. Lama, M. Thapa, and L. P. Poudyal. 2019. First photographic record of marbled cat *Pardofelis marmorata* Martin, 1837 (Mammalia, Carnivora, Felidae) in Nepal. Nature Conservation 32:19 – 34.

Lamberski, N. 2015. *Felidae*. Fowler's Zoo and Wild Animal Medicine 8:467–476.

Lambert, J. E. 2010. Primate seed dispersers as umbrella species: a case study from Kibale National Park, Uganda, with implications for Afrotropical forest conservation. American Journal of Primatology 73(1): 9 – 24.

Laurance, W., D., Carolina Useche, J., Rendeiro, et al. 2012. Averting biodiversity

collapse in tropical forest protected areas. Nature 489: 290–294.

Lawler, J. J., L. E. Aukema, J. B. Grant, B. S. Halpern, P. Kareiva, C. R. Nelson, K. Ohleth, J. D. Olden, M. A. Schlaepfer, B. R. Sillman, and P. Zaradic. 2006. Conservation science: a 20-year report card. Frontiers in Ecology and Environment 4: 473 – 480.

Leung, B., et al. 2020. Clustered versus catastrophic global vertebrate declines. Nature 588: 267 – 271.

Lewis, J. S., K. A. Logan, M. W. Alldredge, L. L. Bailey, S. VandeWoude and K. R. Crooks 2015. The effects of urbanization on population density, occupancy, and detection probability of wild felids. Ecological Application 25(7): 1880 –1895.

Li, J., G. B. Schaller, T. M. McCarthy, D. Wang, Z. Jiagong, P. Cai, L. Basang, and Z. Lu. 2013. A communal sign post of snow leopards (*Panthera uncia*) and other species on the Tibetan Plateau, China. International Journal of Biodiversity 2013: 370905.

Li, X., W. V. Bleisch, X. Liu, and X. Jiang. 2020. Camera-trap surveys reveal high diversity of mammals and pheasants in Medog, Tibet. Oryx 55: 177 – 180.

Linden, D. W., A. K. Fuller, J. A. Royle and M. P. Hare. 2017. Examining the occupancy–density relationship for a low-density carnivore. Journal of Applied Ecology 54: 2043 – 2052.

Lindenmayer, D.B., M.P., Piggott, and B.A., Wintle. 2013. Counting the books while the library burns: why conservation monitoring programs need a plan for action. Frontiers in Ecology and the Environment 11: 549 – 555.

Linkie, M., G., Guillera-Arroita, J., Smith, A., Ario, G., Bertagnolio, F., Cheong, et al. 2013. Cryptic mammals caught on camera: assessing the utility of range wide camera trap data for conserving the endangered Asian tapir. Biological Conservation 162: 107–115.

Lloyd, E. K. 2017. Behavioural flexibility in the Sanje mangaby (*Cercocebus sanjei*), Udzungwa Mountains, Tanzania. Ph.D. thesis in Anthropology. University of Texas, San Antonio, Texas, USA.

Lodberg-Holm, H. K., H. W., Gelink, A. G., Hertel, J. E., Swenson, M., Domevscik, and S.

M. J. G. Steyaert. 2019. A human-induced landscape of fear influences foraging behavior of brown bears. Basic and Applied Ecology 35: 18 - 27.

Loiseau, N., N. Mouquet, N. Casajus, N. et al. 2020. Global distribution and conservation status of ecologically rare mammal and bird species. Nature Communication 11: 5071.

Lomolino, M. V., B. R., Riddle, and R. J., Whittaker. 2016. Biogeography. OUP USA.

MacKenzie, D. I., J. D. Nichols, G. Lachman, S. Droege, J. A. Royle, and C. Langtimm. 2002. Estimating site occupancy rates when detection probabilities are less than one. Ecology 83:2248 –2255.

MacKenzie, D. I., J. D., Nichols, J. E., Hines, M. G. Knutson and A. B., Franklin. 2003. Estimating site occupancy, colonization, and local extinction when a species is detected imperfectly. Ecology, 84(8): 2200–2207.

MacKenzie, D. I., and J. D. Nichols 2004. Occupancy as a surrogate for abundance estimation. Animal Biodiversity Conservation 27(1): 461 – 467.

MacKenzie, D. I., and J. A. Royle. 2005. Designing occupancy studies: general advice and allocating survey effort. Journal of Applied Ecology 42: 1105 – 1114.

MacKenzie, D. I., J. D. Nichols, J. A. Royle, K. H. Pollock, J. E. Hines and L. L. Bailey. 2005. Occupancy Estimation and Modeling: Inferring Patterns and Dynamics of Species Occurrence. (eds) 1st. Edition. Elsevier, San Diego, CA, USA.

Magioli, M., K. M. P. M. de Barros Ferraz, A. G., Chiarello, M., Galetti, E., Z. F., Setz, A. P., Paglia, N., Abrego, M. C., Ribeiro and O., Ovaskainen. 2021. Land-use changes lead to functional loss of terrestrial mammals in a Neotropical rainforest. Perspectives in Ecology and Conservation, 19(2): 161-170.

Marion, S., A., Davies, U., Demšar, R. J., Irvine, P. A., Stephens, and J., Long. 2020. A systematic review of methods for studying the impacts of outdoor recreation on terrestrial wildlife. Global ecology and conservation 22: e00917.

Marsh, L. K. 2003. Primates in fragments: ecology and conservation. Springer US, pp: 539.

Marshall, A. R., H. I. O. Jørgensbye, F. Rovero, P. J. Platts, P. C. L. White and J. C. Lovett. 2010. The species–area relationship and confounding variables in a

threatened monkey community. America Journal of Primatology 72(4): 325 – 336.

Martin, E. H., N. Cavada, V. G. Ndibalema and F. Rovero. 2015. Modelling fine-scale habitat associations of medium-to-large forest mammals in the Udzungwa Mountains of Tanzania using camera trapping. Tropical Zoology 28(4): 137 – 151.

Martins, C. S. and C. B. Valladares-Padua. 2005. The black lion tamarin (*Leontopithecus chrysopygus*) as an umbrella species in the conservation of the biodiversity of patches of the Atlantic Rain Forest of Sao Paula's inland area. Bulletin of the American Society of Primatology 29: 11 – 13.

Martinez Marti C. 2011. The Leopard (*Panthera pardus*) and the Golden Cat (*Caracal aurata*) in Equatorial Guinea: A National Assessment of status, Distribution and Threat. Conservation International & Panthera, New York, USA.

Mathisen, M. K., W., Adam, and B., Zbigniew. 2018. Effects of forest roads on oak trees via cervid habitat use and browsing. Forest ecology and management 424: 378 - 386.

Mazerolle, M. J. 2019. Model selection and multimodel inference based on (Q)AIC(c). R package version 2.2-2. https://cran.r-project.org/package=AICcmodavg.

McBlain, M., K. A., Jones, and G., Shannon. 2020. Sleeping Eurasian oystercatchers adjust their vigilance in response to the behaviour of neighbours, human disturbance and environmental conditions. Journal of Zoology 312(2): 75 - 84.

McCabe, G., F. Rovero, D. Fernández, T. M. Butynski and T. T. Struhsaker. 2019. *Cercocebus sanjei*. The IUCN Red List of Threatened Species 2019: e.T4203A17955753. Downloaded on November 2020. Available on: https://dx.doi.org/10.2305/IUCN.UK.2019-3.RLTS.T4203A17955753.en.

McKenna, D., S., Naumann, K., A., McFarland Graf, and D., Evans. 2014. Literature Review, the ecological effectiveness of the Natura 2000 Network. ETC/BD report to the EEA, 30 pp.

McKinney, M. L. 2001. Role of human population size in raising bird and mammal threat among nations. Animal conservation 4(1): 45–57.

Meredith, M., and M. Ridout. 2014. Overlap: estimates of coefficient of overlapping for animal activity patterns. R package version 0.2.3. Available on: https://CRAN.R-project.org/package=overlap.

Millennium Ecosystem Assessment, 2005. Ecosystems and Human Well-being: Synthesis. Island Press, Washington, DC. Available at: https://www.millenniumassessment.org/documents/document.356.aspx.pdf

Miller, D. L., E. Rexstad, L. Thomas, L. Marshall and J. L. Laake. 2019. Distance Sampling in R. Journal of Statistical Software 89: 1 – 28.

Mittermeier, R. A., C. Valladares-Pádua, A. B. Rylands, A. A. Eudey, T. M. Butynski, J. U. Ganzhorn, R. Kormos, J. M. Aguiar and S. Walker 2006. Primates in Peril: The World's 25 Most Endangered Primates, 2004 –2006. Primate Conservation 20: 1 – 28.

Moll, R. J., K. Kilshaw, R. A. Montgomery, L. Abade, R. D. Campbell, L. A. Harrington, J. J. Millspaugh, J. D. S. Birks, and D. W. Macdonald. 2016. Clarifying habitat niche width using broad-scale, hierarchical occupancy models: a case study with a recovering mesocarnivore. Journal of Zoology 300: 177 – 185.

Moqanaki, E. M., N. Jahed, E. Malkhasyan, E. Askerov, M. S. Farhadinia, M. Kabir, M. Adibi Ali, J. Ud Din, L. Joolaee, N. R. Chahartaghi, and S. Otrowski. 2019. Distribution and status of the Pallas's cat in the south-west part of its range. Cat News Special Issue 13: 24 – 30.

Moqanaki, E. M., and S. Ross. 2020. Manul downlisted to Least Concern. Cat News 71: 15.

Muff, S., E. B.,Nilsen, R. B., C. R. O'Hara Nater. 2021. Rewriting results sections in the language of evidence. Trends in Ecology and Evolution 1 – 8.

Mugerwa, E. M., D. Sheil, P. Ssekiranda, M. Van Heist and P. Ezuma. 2012. Camera trap assessment of terrestrial vertebrates in Bwindi Impenetrable National Park, Uganda. African Journal of Ecology 51: 21 – 31.

Murdoch, J. D., T. Munkhzul, and C. Sillero-Zubiri. 2007. Do nature reserves adequately protect Pallas' cats in central Mongolia. Pages 17–20 *in* J. Hughes and R. Mercer, editors. Felid biology and conservation conference. WildCRU,

Oxford, United Kingdom.

Mwamende, K. A. 2009. Social organisation, ecology and reproduction in the Sanje mangabey (*Cercocebus sanjei*) in the Udzungwa Mountains National Park, Tanzania. M.Sc. Thesis, Victoria University of Wellington, New Zealand. Available at: http://researcharchive.vuw.ac.nz/xmlui/bitstream/handle/10063/1114/thesis.pdf?sequence=1&sa=U&ei=qblbU9DLE6Ki8QGrk4CACg&ved=0CB0QFjAA&usg=AFQjCNHPUJGQW_LC-eh4paOu558kAEe0ZQ

National Statistics Office of Mongolia. 2020. General Statistical Database. National Statistics Office of Mongolia, Ulan Bator, Mongolia.

Naldi, L., I., Greco, M., Ferretti, and M., Zaccaroni. Density Estimates and Habitat Preferences of the European Hare (*Lepus europaeus*) on Mountainous Areas in Italy. Mammal Study 45(2): 123 - 131.

Neilson, E. W., T. Avgar, C. Burton, K. Broadley, and S. Boutin. 2018. Animal movement affects interpretation of occupancy models from camera trap surveys of unmarked animals. Ecosphere 9: e02092.

Newmark, W. D. 1986. Species-area relationship and its determinants for mammals in western North American national parks. Biological Journal of the Linnean Society 28: 83 – 98.

Niedballa, J., R. Sollmann, A. Mohamed, J. Bender, and W. Andreas. 2015. Defining habitat covariates in camera-trap based occupancy studies. Scientific Reports 5:17041.

Nickel, B. A., J. P., Suraci, M. L., Allen, and C. C., Wilmers. 2020. Human presence and human footprint have non-equivalent effects on wildlife spatiotemporal habitat use. Biological Conservation 241: 108383.

Noon, B. R., L. L. Bailey, T. D. Sisk and K. S. McKelvey. 2012. Efficient species-level monitoring at the landscape scale. Conservation Biology 26: 432 – 441.

O'Brien, T.G., J. E. M., Baillie, L., Krueger and M., Cuke. 2010. The wildlife picture index: monitoring top trophic levels. Animal Conservation 13: 335–343.

Oberosler, V., C. Groff, A. Iemma, P. Pedrini, and F. Rovero. 2017. The influence of

human disturbance on occupancy and activity patterns of mammals in the Italian Alps from systematic camera trapping. Mammalian Biology 87: 50 – 61.

Oberosler, V., S. Tenan, E. F. Zipking and F. Rovero. 2020a. Poor management in protected areas is associated with lowered tropical mammal diversity. Animal Conservation 23: 171 – 181.

Oberosler, V., S, Tenan, E. F. Zipkin and F. Rovero. 2020b. When parks work: Effect of anthropogenic disturbance on occupancy of tropical forest mammals. Ecology and Evolution 10: 3881 – 3894.

Ordiz, A., R., Bischof, and J. E., Swenson. 2013. Saving large carnivores, but losing the apex predator? Biological Conservation 168: 128 - 133.

Osugi, S., S., Baek, T., Naganuma, K., Tochigi, M. L., Allen, & S. Koike. 2022. The effect of decreasing human activity from COVID-19 on the foraging of fallen fruit by omnivores. Ecology and Evolution, 12: e9657.

Otgonbayar, B., and B. Suuri. 2021. Diet of the Pallas's cat (*Otocolobus manul*) in Mongolian steppe habitat during a population peak of Brandt's voles. Journal of Arid Environment 193: 104583.

Ovaskainen, O., and J., Soininen. 2011. Making more out of sparse data: hierarchical modeling of species communities. Ecology 92: 289 – 295.

Pacifici, M., M., Di Marco, J. E. M., Watson. 2020a. Protected areas are now the last strongholds for many imperiled mammal species. Conservation Letters. 13: e12748.

Pacifici, M., C., Rondinini, J.R., Rhodes, et al. 2020b. Global correlates of range contractions and expansions in terrestrial mammals. Nature Communication 11: 2840.

Paddock, C. L., Bruford, M. W. and G. M. McCabe. 2020. Estimating the population size of the Sanje mangabey (*Cercocebus sanjei*) using acoustic distance sampling. America Journal of Primatology 82: e23083.

Parks, S. A., and A. H., Harcourt. 2002. Reserve Size, Local Human Density, and Mammalian Extinctions in U.S. Protected Areas. Conservation Biology 16: 800 – 808.

Parsons, A. W., T. Forrester, W. J. McShea, M. C. Baker-Whatton, J. J. Millspaugh and R. Kays. 2017. Do occupancy or detection rates from camera traps reflect deer density? Journal of Mammalogy 98(6): 1547 – 1557.

Pettorelli, N., et al. 2005. Using the satellite-derived NDVI to assess ecological responses to environmental change. Trends in Ecology & Evolution 20: 503 – 510.

Penone, C., B. G. Weinstein, C. H. Graham, T. M. Brooks, C. Rondinini, S. B. Hedges, A. D. Davidson and G. C. Costa. 2016. Global mammal beta diversity shows parallel assemblage structure in similar but isolated environments. Proceedings of the royal society B 283(1837): 20161028.

Pfaller, J. B., K. A., Bjorndal, M., Chaloupka, K. L., Williams, M. G., Frick, et al. 2013. Accounting for Imperfect Detection Is Critical for Inferring Marine Turtle Nesting Population Trends. PLOS ONE 8(4): e62326.

Pfeiffer, M., C. Dulamsuren, Y. Jäschke, and K. Wesche. 2018. Grasslands of China and Mongolia: spatial extent, land use and conservation. Chapter 8 *in* V. R. Squires, J. Dengler, H. Feng, and L. Hua, editors. Grasslands of the world: diversity, management and conservation. CRC Press, Boca Raton, Florida, USA.

Pimm, S. L., J. L. Gittleman, and T. M. Brooks. 1995. The future of biodiversity. Science 269: 347 – 350.

Pimm, S. L., C. N., Jenkns, R., Abell, T. M., Brook, J. L. Gittleman, L. N., Joppa, P. H., Raven, C. M., Roberts and J. O., Sexton. 2014. The biodiversity of species and their rates of extinction, distribution, and protection. Science 344(6187): 1246752.

Plummer, M. 2003. JAGS: A program for analysis of Bayesian graphical models using Gibbs sampling. Proceedings of the 3rd international workshop on distributed statistical computing; 2003: Vienna, Austria.

Poudel, B. S., P. G. Spooner, and A. Matthews. 2015. Temporal shift in activity patterns of Himalayan marmots in relation to pastoralism. Behavioral Ecology 26: 1345 – 1351.

Purvis, A., J. L. Gittleman, G. Cowlishaw, and G. M. Mace. 2000. Predicting extinction risk in declining species. Proceedings of the Royal Society of London B 267:

1947 – 1952.

QGIS Development Team. 2019. QGIS Geographic Information System. https://www.qgis.org/en/site/.

R Core Team. 2019. R: a language and environment for statistical computing. R Foundation for Statistical Computing, Vienna, Austria.

Reed, S. E., and A. M., Merenlender. 2008. Quiet, nonconsumptive recreation reduces protected area effectiveness. Conservation Letters 1(3): 146 - 154.

Richard, J.H. and S.D., Côté. 2016. Space use analyses suggest avoidance of a ski area by mountain goats. Journal of Wildlife Management 80: 387 - 395.

Ridout, M. S., and M. Linkie. 2009. Estimating overlap of daily activity patterns from camera trap data. Journal of Agricultural, Biological and Environmental Statistics 14: 322 – 337.

Ripple, W. J., J. E. Estes, R. L. Beschta, C. C. Wilmers, E. G. Ritchie, M. Hebblewhite, J. Berger, B. Elmhagen, M. Letnic, M. P. Nelson, et al. 2014. Status and ecological effects of the world's largest carnivores. Science 343: 1241484.

Ripple, W. J., T. M. Newsome, C. Wolf, R. Dirzo, K. T. Everatt, M. Galetti, M. W. Hayward, G. I. H. Kerley, T. Levi, P. A. Lindsey, et al. 2015. Collapse of the world's largest herbivores. Science Advances 1: e1400103.

Ripple, W. J., et al. 2017. Extinction risk is most acute for the world's largest and smallest vertebrates. Proceedings of the National Academy of Sciences 114: 10678 – 10683.

Roberts, R., R. Hamilton and D. R. Piperno. 2021. Tropical forests as key sites of the "Anthropocene": Past and present perspectives. PNAS 118(40): e2109243118.

Rodrìguez-Luna, E., A. Shedden and B. A. Solòrzano-Garcìa. 2013. A region-wide review of Mesoamerican primates: prioritizing for conservation. In: Marsh L. K. and C. A. Chapman (eds). Primates in fragments: complexity and resilience Developments in primatology: progress and prospects. Springer Science+Business Media New York, pp. 47 – 55.

Rogan, M. S., G. A. Balme, G. Distiller, R. T. Pitman, J. Broadfield, G. K. Mann, G. M. Whittington-Jones, L. H. Thomas and M. J. O'Riain. 2019. The influence of

movement on the occupancy–density relationship at small spatial scales. Ecosphere 10(8): e02807.

Rondinini, C., et al. 2011. Global habitat suitability models of terrestrial mammals. Philosophical Transactions of the Royal Society B: Biological Sciences 366: 2633 –2641.

Ross, S., A. Barashkova, T. Dhendup, B. Munkhtsog, I. Smelansky, D. Barclay, and E. Moqanaki. 2020. *Otocolobus manul*. The IUCN Red List of Threatened Species 2020: e.T15640A162537635.

Ross, S, A. Barashkova, V. Kirilyuk, and S. Naidenko. 2019*a*. The behaviour and ecology of the manul. Cat News Special Issue 13: 9 – 13.

Ross, S., E. M. Moqanaki, A. Barashkova, T. Dhendup, I. Smelansky, S. Naidenko, A. Antonevich, and G. Samelius. 2019*b*. Past, present and future threats and conservation needs of the Pallas's cat. Cat News Special Issue 13: 46 – 51.

Ross, S., B. Munkhtsog, and S. Harris. 2012. Determinants of mesocarnivore range use: relative effects of prey and habitat properties on Pallas's cat home-range size. Journal of Mammalogy 93: 1292 – 1300.

Ross, S., R. Kamnitzer, B. Munkhtsog, and S. Harris. 2010*a*. Den-site selection is critical for Pallas's cats (*Otocolobus manul*). Canadian Journal of Zoology 88: 905 – 913.

Ross, S., B. Munkhtsog, and S. Harris, 2010*b*. Dietary composition, plasticity, and prey selection of Pallas's cats. Journal of Mammalogy 91: 811 – 817.

Ross, S. 2009. Providing an ecological basis for the conservation of the Pallas's cat (*Otocolobus manul*). Dissertation, University of Bristol, Bristol, United Kingdom.

Rovero, F., T. T. Struhsaker, A. R. Marshall, T. A. Rinne, U. B. Pedersen, T. M. Butynski, C. L. Ehardt and A. S. Mtui. 2006. Abundance of diurnal primates in Mwanihana Forest, Udzungwa Mountains, Tanzania. International Journal of Primatology 27: 675 – 697.

Rovero, F., A, R. Marshall, T. Jones and A. Perking. 2009. The primates of the Udzungwa Mountains: Diversity, ecology and conservation. Journal of

Anthropological Sciences 87: 93 – 126.

Rovero, F., M., Tobler and J., Sanderson. 2010. Camera trapping for inventorying terrestrial vertebrates. Manual on field recording techniques and protocols for All Taxa Biodiversity Inventories and Monitoring.

Rovero, F., A. S. Mtui, A. S. Kitegile and M. R. Nielsen. 2012. Hunting or habitat degradation? Decline of primate populations in Udzungwa Mountains, Tanzania: an analysis of threats. Biological Conservation 146: 89 – 96.

Rovero, F., F., Zimmermann, D., Berzi and P., Meek. 2013. Which camera trap type and how many do I need?" A review of camera features and study designs for a range of wildlife research applications. Hystrix, It. J. Mamm. 24(2): 148–156.

Rovero, F., E. Martin, M. Rosa, J. A. Ahumada and D. Spitale. 2014a. Estimating Species Richness and Modelling Habitat Preferences of Tropical Forest Mammals from Camera Trap Data. PLoS ONE 9: e103300.

Rovero, F., M. Menegon, J. Fjeldsa, L. Collett, N. Doggart, C. Leonard, G. Norton, N. Owen, A. Perkin, D. Spitale and A. Ahrends. 2014b. Targeted vertebrate surveys enhance the faunal importance and improve explanatory models within the Eastern Arc Mountains of Kenya and Tanzania. Diversity and Distribution 20: 1438 – 1449.

Rovero, F., A. Mtui, A. Kitegile, P. Jacob, A. Araldi and S. Tenan. 2015. Primates Decline Rapidly in Unprotected Forests: Evidence from a Monitoring Program with Data Constraints. PLoS ONE 10(2): e0118330.

Rovero, F. and D. Spitale. 2016. Species-level occupancy analysis. In: Camera Trapping for Wildlife Research. Data in the Wild (eds F. Rovero & F. Zimmermann). pp. 68 – 64. Pelagic Publishing, Exeter, UK.

Rovero, F. and J. Ahumada. 2017. The Tropical Ecology, Assessment and Monitoring (TEAM) Network: an early warning system for tropical rain forests. Science of the Total Environment 574: 914 – 923.

Rovero, F., S., Shinyambala, A. Perkin and I. Greco. 2019. Minziro Nature Reserve Biodiversity Surveys 2018.

figshare.com/articles/Minziro_Nature_Reserve_Biodiversity_surveys_2018/10283822/1 [accessed 8 July 2020].

Rovero, F., C. Augugliaro, R. Worsøe Havmøller, C. Groff, F. Zimmermann, V. Oberosler, and S. Tenan. 2020. Co-occurrence of snow leopard *Panthera uncia*, Siberian ibex *Capra sibirica* and livestock: potential relationship and effects. Oryx 54: 118 – 124.

Rovero, F., J., Ahumada, P.A., Jansen, D., Sheil, P., Alvarez, K., Boekee, S., Espinosa, M. G. M., Lima, E. H., Martin, T. G., O'Brien, J., Salvador, F., Santos, M., Rosa, A., Zvoleff, C., Sutherland, and S., Tenan. 2020. A standardized assessment of forest mammal communities reveals consistent functional composition and vulnerability across the tropics. Ecography, 43: 75-84.

Rovero, F., and K., Roland Kays. 2021. Camera trapping for conservation. In: Wich, S. A. and A. K., Piel (eds) Conservation Technology. Oxford Academic, Oxford, GB.Rowcliffe, J. M., R. Kays, B. Kranstauber, C. Carbone, and P. A. Jansen. 2014. Quantifying levels of animal activity using camera trap data. Methods in Ecology and Evolution 5: 1170 – 1179.

Royle J. A. and M., Kery. 2007. A Bayesian state-space formulation of dynamic occupancy models. Ecology 88: 1813–1823.

Saura, S., Ö., Bodin, and M. J., Fortin. 2014. Stepping stones are crucial for species' long-distance dispersal and range expansion through habitat networks. Journal of Applied Ecology 51: 171 – 182.

Schieltz, J. M., and D. I. Rubenstein. 2016. Evidence based review: positive versus negative effects of livestock grazing on wildlife. What do we really know? Environmental Research Letters 11: 113003.

Schipper J., et al. 2008. The Status of the World's Land and Marine Mammals: Diversity, Threat, and Knowledge. Science 322(5899): 225 – 30.

Schirpke, U., C., Meisch, T. Marsoner and U. Tappeiner. 2018. Revealing spatial and temporal patterns of outdoor recreation in the European Alps and their surroundings. Ecosystem Services 13: 336 – 350.

Schlaepfer M. A., M. C. Runge and P. W. Sherman. 2002. Ecological and evolutionary

traps. Trends in Ecology and Evolution. 17: 474 – 480.

Schmitz, M. F., D. G. G., Matos, I., De Aranzabal, D., Ruiz-Labourdette, and F. D., Pineda, 2012. Effects of a protected area on land-use dynamics and socioeconomic development of local populations. Biological Conservation 149(1): 122 - 135.

Schulze, K., K., Knights, L., Coad, J., Geldmann, F., Leverington, A., Eassom, et al. 2018. An assessment of threats to terrestrial protected areas. Conservation Letters 11(3): e12435.

Scott, J. M., et al. 2001. Nature Reserves: Do They Capture the Full Range of America's Biological Diversity? Ecological Applications 11: 999 – 1007.

Semper-Pascual, A., et al. 2022. Occupancy winners in tropical protected forests: a pantropical analysis. Proceedings of the Royal Society B: Biological Sciences 289: 20220457.

Sévêque, S., L. K. Gentle, J. Lopez-Bao, W. Yarnell, and A. Uzal. 2020. Human disturbance has contrasting effects on niche partitioning within carnivore communities. Biological Reviews 95: 1689 – 1705.

Segar, J., H.M., Pereira, L. Baeten, et al. 2022. Divergent roles of herbivory in eutrophying forests. Nature Communication 13: 7837.

Smith, A.F., S., Ciuti, D., Shamovich, V., Fenchuk, B., Zimmermann, and M., Heurich. 2022. Quiet islands in a world of fear: Wolves seek core zones of protected areas to escape human disturbance. Biological Conservation 276: 109811.

Snow Leopard Network. 2014. Snow Leopard Survival Strategy. www.snowleopardnetwork.org.

Soofi, M., A. Ghoddousi, T. Zeppenfeld, S. Shokri, M. Soufi, A. Jafari, M. Ahmadpour, A. T. Qashqaei, L. Egli, T. Ghadirian, N. Raeesi Chahartaghi, B. Zehzad, B. H. Kiabi, I. Khorozyan, N. Balkenhol, and M. Waltert. 2018. Livestock grazing in protected areas and its effects on large mammals in the Hyrcanian forest, Iran. Biological Conservation 217: 377 – 382.

Spehar, S. N., B. Loken, Y. Rayadin and J. A. Royle. 2015. Comparing spatial capture–recapture modeling and nest count methods to estimate orangutan densities in the Wehea Forest, East Kalimantan, Indonesia. Biological Conservation 191:

185 – 193.

Supp, S. R., and S. K. M., Ernest. 2014. Species-level and community-level responses to disturbance: a cross-community analysis. Ecology 95: 1717 – 1723.

Suraci, J. P., M. Clinchy, L. Y. Zanette and C. C. Wilmers. 2019. Fear of humans as apex predators has landscape-scale impacts from mountain lions to mice. Ecology Letters 22: 1578 – 1586.

Suraci, J.P., Gaynor, K.M., Allen, M.L., Alexander, P., Brashares, J.S., et al. 2021. Disturbance type and species life history predict mammal responses to humans. Global Change Biology 27: 3718-3731.

Sutherland, C., M., Brambilla, P., Pedrini, and S., Tenan. 2016. A multiregion community model for inference about geographic variation in species richness. Methods in Ecology and Evolution 7: 783 – 791.

Steenweg, R. et al. 2017. Scaling-up camera traps: monitoring the planet's biodiversity with networks of remote sensors. Frontiers in Ecology and the Environment 15: 26 – 34.

Steffen, W., J., Grinevald, P., Crutzen and J., McNeill. 2011. The Anthropocene: conceptual and historical perspectives. Philosophical Transaction of the Royal Society A 369: 842–867.

Steffen, W., K., Richardson, J., Rockström, S. E., Cornell, I., Fetzer, E. M., Bennett, R., Biggs, S. R., Carpenter, W., de Vries, C. A. de Wit and C., Folke. 2015. Planetary boundaries: Guiding human development on a changing planet. Science 347: 6223.

Stewart, G. 2010. Meta-analysis in applied ecology. Biology Letters 6: 78 – 81.

Stuart, A. J. 2015. Late Quaternary megafaunal extinctions on the continents: a short review. Geological Journal 50: 338 – 363.

Tanwar, K.S., A. Sadhu, and Y.V., Jhala 2021. Camera trap placement for evaluating species richness, abundance, and activity. Scientific Reports 11: 23050.

Tempel, D. J. and R. J. Gutierréz. 2013. Relation between Occupancy and Abundance for a Territorial Species, the California Spotted Owl. Conservation Biology 27(5): 1087 – 1095.

Thieurmel, B., and A., Elmarhraoui. 2019. suncalc: Compute Sun Position, Sunlight Phases, Moon Position and Lunar Phase. R package version 0.5.0.

Tseveenmyadag, N. and B. Nyambayar. 2002. The impact of rodenticide used to control rodents on Demoiselle crane (*Anthropoides virgo*) and other animals in Mongolia. Mongolian Academy of Sciences and Peregrine Fund, Ulaanbaatar, Mongolia.

Tucker, M. A., K., Böhning-Gaese, W. F., Fagan, J. M., Fryxell, B., Van Moorter, S. C., Alberts, et al. 2018. Moving in the Anthropocene: Global reductions in terrestrial mammalian movements. Science 359(6374): 466 - 469.

Van Kuijk, M., M., De Jager, M., Van Oosterhout, L., De Laender, and M., Parahoe. 2022. Local abundances of terrestrial mammal and bird species around indigenous villages in Suriname. Conservation Science and Practice 4: e12699.

Venter, O. et al. 2016. Sixteen years of change in the global terrestrial human footprint and implications for biodiversity conservation. Nature Communications 7: 12558.

Visconti, P., S. H., Butchart, T. M., Brooks, P. F., Langhammer, D., Marnewick, S., Vergara, et al. 2019. Protected area targets post-2020. Science 364(6437): 239 - 241.

Watson, J. E. M., et al. 2018. The exceptional value of intact forest ecosystems. Nature Ecology and Evolution 2: 599 – 610.

Wearn, O. R. and P., Glover-Kapfer. 2017. Camera-trapping for conservation: A guide to best-practices. Woking, UK: WWF.

Wells, M. P., and T. O., McShane. 2004. Integrating Protected Area Management with Local Needs and Aspirations. Ambio 33: 513 – 519.

Wellington, K., C. Bottom, C. Merrill, and J. A. Litvaitis. 2014. Identifying performance differences among trail cameras used to monitor forest mammals. Wildlife Society Bulletin 38: 634 – 638.

Wilcove, D. S., and M., Wikelski. 2008. Going, Going, Gone: Is Animal Migration Disappearing. PLoS Biology 6(7): e188.

Williams, S. T., N. Maree, P. Taylor, S. R. Belmain, M. Keith, and L. H. Swanepoel. 2018.

Predation by small mammalian carnivores in rural agro-ecosystems: an undervalued ecosystem service? Ecosystem Services 30: 362 – 371.

Williams, D. R., C., Rondinini, and D., Tilman. 2022. Global protected areas seem insufficient to safeguard half of the world's mammals from human-induced extinction. Proceedings of the National Academy of Sciences 119: e2200118119.

Wilmers, C. C., A. C., Nisi, and N., Ranc. 2021. COVID-19 suppression of human mobility releases mountain lions from a landscape of fear. Current Biology 31(17): 3952 - 3955.

Wilson, T. L. and J. H. Schmidt. 2015. Scale dependence in occupancy models: implications for estimating bear den distribution and abundance. Ecosphere 6(9): 168.

Wilson, M. W., A. D., Ridlon, K. M., Gaynor, S. D., Gaines, A. C., Stier, and B. S., Halpern. 2020. Ecological impacts of human-induced animal behaviour change. Ecology letters 23(10): 1522 - 1536.

Wingard, J., M. Pascual, A. Rude, A. Houle, S. Gombobaatar, G. Bhattacharya, M. Munkhjargal, N. Conaboy, S. Myagmarsuren, T. Khaliun, T. Batsugar, and T. Bold. 2018. Silent steppe II: Mongolia's wildlife trade crisis, ten years later. Zoological Society of London, London, United Kingdom.

Wilson, E. O. 2016. Half-Earth: Our Planet's Fight for Life. Liveright Publishing Company, 2016.

Winters, A. M. 2006. Rodenticide use and secondary poisoning risks to non-target wildlife in central Mongolia. Thesis, Michigan State University, East Lansing, USA.

Wintle, B. A., et al. 2019. Global synthesis of conservation studies reveals the importance of small habitat patches for biodiversity. Proceedings of the National Academy of Sciences 116: 909 – 914.

Woodroffe, R., and J. R., Ginsberg. 1998. Edge Effects and the Extinction of Populations Inside Protected Areas. Science 280: 2126 – 2128.

Wooster, E.I.F., D., Ramp, E.J., Lundgren, A.J., O'Neill, E., Yanco, G.T., Bonsen, and A.D.,

Wallach. 2022. Predator protection dampens the landscape of fear. Oikos e09059.

World Bank. 2018. Population density (people per sq. km of land area)–Mongolia. World Development Indicators, The World Bank Group. https://data.worldbank.org. Accessed Jun 2020.

WWF. 2018. Living planet report—2018: aiming higher. Available at: http://scholar.google.com/scholar?hl=en&btnG=Search&q=intitle:LIVING+PLANET+REPORT+2004#0

WWF. 2020. Living planet report 2020 – bending the curve of biodiversity loss. Available at: https://icriforum.org/living-planet-report-2020-bending-the-curve-of-biodiversity-loss/

Zahler, P., B. Lhagvasuren, R. P. Reading, J. R. Wingard, S. Amgalanbaatar, S. Gombobaatar, N. Barton, and Y. Onon. 2004. Illegal and unsustainable wildlife hunting and trade in Mongolia. Mongolian Journal of Biological Sciences 2: 23 – 31.

Zhou, X. H., X. T. Wan, Y. H. Jin, and W. Zhang. 2016. Concept of scientific wildlife conservation and its dissemination. Zoological Research 37: 270 – 274.

Zimmermann, F., D. Foresti and F. Rovero. 2016. Behavioural studies. Chapter 8 in: Rovero, F. and D. Zimmermann. Camera trapping for wildlife research (eds). Pelagic Exeter, United Kingdom.

Zipkin, E. F., A., DeWan, and A. J., Royle. 2009. Impacts of forest fragmentation on species richness: a hierarchical approach to community modelling. Journal of Applied Ecology 46: 815 – 822.

Zipkin, E. F., A. J., Royle, D. K., Dawson, and S., Bates. 2010. Multi-species occurrence models to evaluate the effects of conservation and management actions. Biological Conservation 143: 479 – 484.

The African golden cat *Caracal aurata* in Tanzania: first record and vulnerability assessment

Ilaria Greco and Francesco Rovero

Abstract We report on the first population found in Tanzania of the Vulnerable African golden cat *Caracal aurata*, extending its documented range c. 200 km to the south and south-east. This is one of the least-known and truly forest-dependent felines in Africa, ranging across the Guinea–Congolian forest block. We recorded the new population in Minziro Nature Forest Reserve, north-west Tanzania, during a 3-month survey in 2018. We deployed 70 camera traps on a regular grid and obtained 33 detection events of the golden cat at 26% of sites, with a minimum of 10 individuals across 257 km². We estimated occupancy and detection probability and modelled these in relation to the distance of sampling sites to the forest edge, which coincides with both the Reserve boundary and proximity to human settlements surrounding the Reserve. Mean estimated occupancy was 0.41 ± SE 0.12 (mean detectability = 0.13 ± SE 0.05), with occupancy increasing significantly with distance from the forest edge. Detectability did not vary significantly with distance from the forest edge, but was higher for camera models that had a shorter trigger time. Our findings add to the scant data available for this species. It appears threatened by human activity, which we recorded both outside and within the Reserve, and the presence of the species indicates Minziro Forest is an important site for its conservation.

Keywords African golden cat, camera trapping, *Caracal aurata*, detection probability, edge effect, Minziro, occupancy modelling, Tanzania

Supplementary material for this article is available at doi.org/10.1017/S003060532000040X

The African golden cat *Caracal aurata* is an elusive, medium-sized felid categorized as Vulnerable on the IUCN Red List, regarded as the least-known wildcat in Africa and one of the least-studied felines (Bahaa-El-Din et al., 2015b). As the only truly forest-dwelling feline in Africa, it is threatened by deforestation, habitat destruction and snaring (Bahaa-El-Din et al., 2016). Although the population is believed to be decreasing (Bahaa-El-Din et al., 2015a), robust knowledge of the species is scant. The golden cat occurs in West and Central Africa, with an easternmost population recently confirmed in Kenya from a roadkill in the Aberdare Mountains (Hatfield et al., 2019). Western Tanzania has been regarded as potentially suitable for the species (Butynski et al., 2012), but no records have previously been reported. Here, we present the first record and results of habitat association modelling for a population of golden cat found in Tanzania in the course of a biodiversity survey in Minziro Nature Forest Reserve. We used a camera-trap survey, and occupancy analysis, to determine the distribution of the golden cat and its association with habitat edges and human disturbance.

Camera trapping was conducted in Minziro Nature Forest Reserve, north-west Tanzania, during 3 October–28 December 2018. Established in 2016 and formerly a reserve with lower protection status, it comprises 257 km² of flat, moist forest at a mean altitude of 1,150 m (Rovero et al., 2019). The northern boundary is the country border, merging with the Sango Bay Forest Reserve in Uganda. All other boundaries adjoin human-modified areas with settlements, plantations and patches of drier woodland and grassland (Fig. 1), with Kagera river and seasonal flooding to the east, and a paved road and several villages to the west. The Reserve is the easternmost extension in Tanzania of the Congo–Guinea forest, with fauna typical of West and Central Africa. The Reserve is heavily disturbed by illegal logging, burning, livestock grazing and fishing occurring in the area (Rovero et al., 2019). We found evidence of bushmeat hunting: we encountered hunters with dogs on one occasion and found a number of snares, presumably set for ungulates but potentially a threat to the golden cat and other species.

We surveyed 70 sites across the Reserve using a regular grid of 1–2 km² cell size, firstly surveying 40 camera sites and then 30 (Fig. 1), for a minimum of 30 days (mean 32 days) each. We used Browning (Morgan, USA), Cuddleback (Green Bay, USA) and UOVision (Shenzhen, China) cameras, with infrared flash and motion-activated sensor. The trigger speed was 0.15 s for Browning, and 1–2 s for Cuddleback and UOVision. Cameras were unbaited and attached to trees at c. 50 cm from the ground, facing a presumed animal trail.

The survey yielded 2,219 camera-days from 68 camera traps (two were stolen). We annotated images using *Wild.ID* and ran analyses using *R 3.6* (R Core Team, 2019). We calculated

Ilaria Greco (Corresponding author, orcid.org/0000-0002-6208-2465) Department of Biology, University of Florence, via Madonna del Piano 6, 50019 Sesto Fiorentino, Italy. E-mail ilaria.greco@unifi.it

Francesco Rovero* (orcid.org/0000-0001-6688-1494) Department of Biology, University of Florence, Sesto Fiorentino, Italy

*Also at: Tropical Biodiversity Section, MUSE–Museo delle Scienze, Trento, Italy

Received 12 December 2019. Revision requested 18 February 2020. Accepted 6 May 2020.

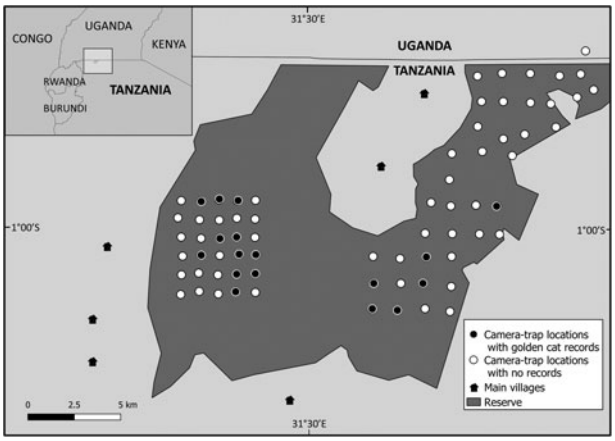

FIG. 1 Minziro Nature Forest Reserve, Tanzania, with camera-trap sites and records of the African golden cat *Caracal aurata*.

the number of golden cat detections per day, and used them to derive a relative abundance index. We plotted the species' daily activity pattern using hourly events. We then used single-season occupancy modelling (MacKenzie et al., 2002) to estimate golden cat occupancy (ψ) and detection probability (p) and their association with presumed covariates. We arranged golden cat detections/non-detections into a site-by-sampling occasion matrix; we chose 5 days as the resolution of the occasions as with poorly detected species this provides the best estimation of detectability, and hence occupancy (Rovero & Spitale, 2016). We built parsimonious models using the distance from each site to the closest Reserve border (i.e. forest edge) as a covariate. We derived these distances using *QGIS* (QGIS Development Team, 2019) and a 1:100,000 scale map. Based on our survey of human disturbance, we considered greater distance to the border as a proxy for increasing habitat quality and decreasing human disturbance. We assumed that both ψ and p increase with distance to border. For detection probability we also considered that camera-trap model could potentially influence detection. Using *unmarked* (Fiske & Chandler, 2011), we built all model combinations and ranked them according to the Akaike information criterion (AIC). We considered statistically supported models with $\Delta AIC < 2.00$ and used *AICcmodavg* (Mazerolle, 2019) to average parameter estimates.

After discarding 3,297 blank and set-up images, camera trapping yielded 4,244 photographs of 23 species of medium to large wild mammals (Supplementary Table 1), including 169 images of golden cats. These corresponded to 33 independent detection events of the species within 24-hour intervals at 17 sites (naïve occupancy = 0.26; Fig. 1). Based on individual pelage marks, we identified a minimum of 10 individuals. Pelage colouration varied from dark brown to sandy and golden (Plate 1). Animals were mainly active at night, with activity peaking at 19.00, 22.00 and 3.00, but were also detected in daylight (Supplementary Fig. 1). Based on occupancy model ranking (Table 1), we averaged the two most supported models, and the resultant mean estimated occupancy was 0.41 ± SE 0.12. Occupancy increased significantly with distance to the Reserve border (1.30 ± SE 0.54; Table 2, Fig. 2). Mean detection probability was 0.13 ± SE 0.05 and did not vary significantly with distance to the Reserve border but did vary between camera models, with Browning cameras having significantly higher values (Supplementary Table 2).

Our findings suggest that habitat intactness and human disturbance affect golden cat occurrence, with increased occupancy with increasing distance from the Reserve border

PLATE 1 African golden cat *Caracal aurata* photo-trapped in Minziro Nature Forest Reserve, Tanzania. The survey revealed golden/brown-reddish (a, c) and dark/light grey (b, d) morphotypes.

TABLE 1 Model ranking for occupancy (ψ) and detection probability (*p*) of the African golden cat *Caracal aurata* detected by camera trapping in Minziro Nature Forest Reserve (Fig. 1), Tanzania.

Models	No. of parameters	AIC[1]	Δ AIC	AIC weight	R^2
p (Camera model) ψ (Distance from closest edge)	5	198.88	0.00	0.59	0.27
p (Camera model + Distance from closest edge) ψ (Distance from closest edge)	6	200.50	1.62	0.26	0.27
p (.) ψ (Distance from closest edge)	3	203.44	4.56	0.06	0.16
p (Distance from closest edge) ψ (Distance from closest edge)	4	204.18	5.31	0.04	0.18
p (Camera model) ψ (.)	4	204.83	5.95	0.03	0.17
p (Camera model + Distance from closest edge) ψ (.)	5	205.68	6.80	0.02	0.18
p (.) ψ (.)	2	212.82	13.95	< 0.01	0.00
p (Distance from closest edge) ψ (.)	3	213.16	14.28	< 0.01	0.03

[1]Models were ranked according to the Akaike information criterion (AIC), with ΔAIC < 2 considered supported.

TABLE 2 Parameter estimates from the averaging of the two best supported models testing the effect of covariates on detection probability (*p*) and occupancy (ψ) of the African golden cat in Minziro Nature Forest Reserve (Fig. 1).

Model	Estimate ± SE	*Z*	P (>|*z*|)
ψ Distance from closest edge	1.30 ± 0.54	2.38	0.02
p Camera model—Browning	1.51 ± 0.64	2.36	0.02
p Camera model—UOVision	−0.57 ± 1.23	−0.47	0.64
p Distance from closest edge	−0.18 ± 0.30	0.61	0.54

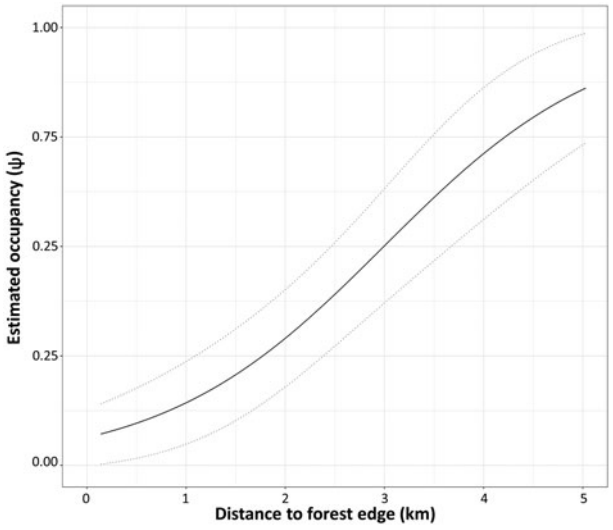

FIG. 2 Estimated occupancy (dotted lines show SE) of the golden cat in Minziro Nature Forest Reserve in relation to distance from the closest forest edge.

and human settlements. This matches the feline's known sensitivity to anthropogenic disturbance and its vulnerability in human-disturbed areas (Martinez Marti, 2011; Bahaa-El-Din et al., 2016). We documented a high incidence of human activities around and within the Reserve, potentially explaining the species' relatively higher occurrence in areas with dense, closed-canopy, continuous forests. A similar pattern has also been reported in Uganda (Mugerwa et al., 2012). Detection probability was greater with faster cameras, highlighting the importance of standardizing camera models in wildlife surveys: the best performing devices increase the probability of detecting elusive species. Although not exclusively nocturnal, the golden cat activity pattern showed peaks at night, mirroring the cathemeral behaviour reported by Bahaa-El-Din et al. (2015a). Peaks of golden cat activity may overlap with periods of low human presence and higher prey activity. The minimum number of 10 individual cats detected gives a naïve density of 4 per 100 km², suggesting that this population may not be as abundant as in other areas. Densities of 16 individuals per 100 km² have been reported in pristine habitats in Gabon, and densities similar to our estimates have been reported in highly disturbed and hunted areas (Bahaa-El-Din et al., 2016). It is possible that the presence of seasonally flooded forest and swamps, mainly on the eastern side of Minziro Nature Forest Reserve, make this habitat type suboptimal for the golden cat.

This is the first record of the little-known golden cat in Tanzania, c. 200 km east-south-east from the closest known populations in Uganda and Rwanda, potentially confirming anecdotal reports of the species in the contiguous Sango Bay Forest in Uganda in the mid 1990s (T. Davenport, pers. comm., 2019). Pelage pattern suggests the population in Tanzania may be the subspecies *Caracal aurata aurata*, with spots only on the abdomen and limbs (Bahaa-El-Din et al., 2015a). Given its isolation and the heavily modified habitat, we assume this population is genetically isolated, and thus Minziro Nature Forest Reserve may be an important site for the species' conservation. We also recorded the tree pangolin *Phataginus tricuspis* and giant pangolin *Smutsia gigantea*, both Endangered, and the first record in Tanzania of the fire-footed rope squirrel *Funisciurus pyrropus*. Considering the human encroachment we detected, and ineffective law enforcement, these findings indicate the need for appropriate protection of this forest.

  doi:10.1017/S003060532000040X

Acknowledgements We thank Tim Davenport and an anonymous reviewer for their constructive comments; Italy's Provincia Autonoma di Trento, MUSE–Science Museum, and the Italian NGO ACAV for funding; COSTECH and the Tanzanian Forest Service for research permission and assistance; Chief Conservator Bernard Mwigulu along with Hassan Omary, Twaha Mponzi and Alfred Mlenge for support; Michele Menegon for the loan of some cameras; and Andrew Perkin, Steven Shinyambala, Ruben Mwakisoma, Wilbrod Bayona and other assistants for field support.

Author contributions Study design, data collection: FR; data analysis: IG; writing: IG, FR.

Conflicts of interest None.

Ethical standards This research abided by the *Oryx* guidelines on ethical standards.

References

Bahaa-El-Din, L., Henschel, P., Butynski, T., Macdonald, D.W., Mills, D., Slotow, R. & Hunter, L. (2015a) The African golden cat *Caracal aurata*: Africa's least known feline. *Mammal Review*, 45, 63–77.

Bahaa-El-Din, L., Mills, D., Hunter, L. & Henschel, P. (2015b) *Caracal aurata.* In *The IUCN Red List of Threatened Species* 2015: e.T18306A50663128. dx.doi.org/10.2305/IUCN.UK.2015-2.RLTS.T18306A50663128.en [accessed 8 July 2020].

Bahaa-El-Din, L., Sollmann, R., Hunter, L., Slotow, R., Macdonald, D.W. & Henschel, P. (2016) Effects of human land-use on Africa's only forest-dependent feline: the African golden cat *Caracal aurata*. *Biological Conservation,* 199, 1–9.

Butynski, T.M., Douglas-Dufresne, H. & de Jong, Y.A. (2012) Identification, distribution and conservation status of the African golden cat *Caracal aurata* in Kenya. *Journal of East African Natural History,* 101, 3–16.

Fiske, I. & Chandler, R. (2011) *unmarked*: an *R* package for fitting hierarchical models of wildlife occurrence and abundance. *Journal of Statistical Software*, 43, 10.

Hatfield, R.S., Mwaura, J., Musila, S. & O'Meara, L. (2019) The first confirmed record of African golden cat *Caracal aurata* from Kenya since 1946. *Journal of East African Natural History,* 108, 49–55.

MacKenzie, D.I., Nichols, J.D., Lachman, G.B., Droege, S., Royle, J.A. & Langtimm, C.A. (2002) Estimating site occupancy rates when detection probabilities are less than one. *Ecology,* 83, 2248–2255.

Martinez Marti, C. (2011) *The Leopard (*Panthera pardus*) and the Golden Cat (*Caracal aurata*) in Equatorial Guinea: A National Assessment of Status, Distribution and Threat*. Conservation International & Panthera, New York, USA.

Mazerolle, M.J. (2019) *Model Selection and Multimodel Inference Based on (Q)AIC(c)*. R package version 2.2-1. cran.r-project.org/package=AICcmodavg [accessed 13 July 2020].

Mugerwa, B., Sheil, D., Ssekiranda, P., van Heist, M. & Ezuma, P. (2012) Camera trap assessment of terrestrial vertebrates in Bwindi Impenetrable National Park, Uganda. *African Journal of Ecology*, 51, 21–31.

QGIS Development Team (2019) *QGIS Geographic Information System. Open-Source Geospatial Foundation Project*. qgis.org [accessed July 2020].

R Core Team (2019) *R: A Language and Environment for Statistical Computing*. R Foundation for Statistical Computing, Vienna, Austria.

Rovero, F. & Spitale, D. (2016) Species-level occupancy analysis. In *Camera Trapping for Wildlife Research. Data in the Wild* (eds F. Rovero & F. Zimmermann), pp. 68–64. Pelagic Publishing, Exeter, UK.

Rovero, F., Shinyambala, S., Perkin, A. & Greco, I. (2019) *Minziro Nature Reserve Biodiversity Surveys 2018*. figshare.com/articles/Minziro_Nature_Reserve_Biodiversity_surveys_2018/10283822/1 [accessed 8 July 2020].

Received: 12 February 2021 | Revised: 15 July 2021 | Accepted: 27 August 2021

DOI: 10.1002/jwmg.22150

THE JOURNAL OF WILDLIFE MANAGEMENT | THE WILDLIFE SOCIETY

NOTE

Spatio-temporal occurrence and sensitivity to livestock husbandry of Pallas's cat in the Mongolian Altai

Ilaria Greco[1] | Valentina Oberosler[2] | Ibra Edoardo Monti[1] | Claudio Augugliaro[3] | Anna Barashkova[4] | Francesco Rovero[1,2]

[1]Department of Biology, University of Florence, via Madonna del Piano 6, 50019 Sesto Fiorentino, Italy

[2]MUSE—Museo delle Scienze, Corso del Lavoro e della Scienza 3, 38122 Trento, Italy

[3]Department of Ecology and Evolution, University of Lausanne, CH-1015, Lausanne, Switzerland and Wildlife Initiative, Bayangol District, 6th Khoroo, Micro District 10, Ulaanbaatar 210349, Mongolia

[4]Siberian Environmental Center, P. O. Box 547, 630090 Novosibirsk, Russia

Correspondence

Ilaria Greco, Department of Biology, University of Florence, via Madonna del Piano 6, 50019 Sesto Fiorentino, Italy.
Email: ilaria.greco@unifi.it

Funding information

Panthera Sabin Snow Leopard grants; Parco Natura Viva; Fondazione Arca; Wildlife Initiative; MUSE–Museo delle Scienze; Université de Lausanne; Altai Institute for Research and Conservation; Irbis Mongolia; Herbette Foundation; Gino Zobele fund

Abstract

Biased research and conservation efforts result in some faunal groups (e.g., small felids) being understudied, and hence these groups are often declining without adequate knowledge to manage for threat reduction. The Pallas's cat (*Otocolobus manul*) occurs across central and western Asia with declining populations and the largest population is likely in Mongolia. A potential threat to this felid is livestock encroachment across its range, including within protected areas, yet we lack a clear understanding of the impact of livestock husbandry on this cat. We used motion-sensitive camera data from 216 sites in 4 study areas in western Mongolia to study the occurrence probability of Pallas's cat in relation to habitat characteristics and occurrence of livestock, and conducted a local assessment within a strictly protected area where we obtained the highest number of detections. We estimated a relatively low occupancy (0.33 ± 0.10), which is associated with sites with natural vegetation, steeper slopes, and greater prey abundance. Occupancy also increased with increasing livestock occurrence, particularly large herds of sheep and goats. Such co-occurrence was partially adjusted by diel activity segregation, presumably to limit direct encounters. Our results suggest that the preferred habitat by Pallas's cat in the study region coincides with areas encroached by livestock. The Pallas's cat's

habitat is specialized and its dependence on areas that are increasingly used for grazing may eventually threaten the cat with habitat degradation, prey depletion, predation by dogs, and poisoning from pest control. Relevant conservation actions should regulate livestock encroachment within protected areas and improve grazing regimes. The Pallas's cat is an indicator species of mountainous and steppe ecosystems in central Asia; hence, further research towards the preservation of its populations would also benefit other key species across its range.

KEYWORDS

livestock husbandry, occupancy modelling, *Otocolobus manul*, Pallas's cat, regional assessment, small cat conservation, strictly protected area

Wildlife conservation has gained additional public attention because of the current extinction crisis (Pimm et al. 1995, Zhou et al. 2016). Research and conservation efforts are biased, with some faunal groups that are understudied and receive limited conservation funding (Lawler et al. 2006, Brodie 2009). Among mammals, the Felidae family is one of the most threatened taxa (Cardillo et al. 2004, Lamberski 2015), yet the majority of research and conservation effort has targeted the 7 species of large cats, while the 33 species of small cats have been largely overlooked (Brodie 2009). Less than 1% of conservation funding to all wild cats was devoted to small cats (Brodie 2009). Increased knowledge on the occurrence and vulnerability to changes of small cats is desirable. The use of motion-sensitive camera data from studies primarily focused on larger species or on the pool of medium to large mammals (Lama et al. 2019, Li et al. 2020, Greco and Rovero 2021) has potential to provide some of the missing data on small felids. We used data from a study on snow leopard (*Panthera uncia*) in western Mongolia to determine the spatio-temporal patterns of occurrence of the Pallas's cat (*Otocolobus manul*) and its sensitivity to environmental and anthropogenic factors, with a focus on the effects of grazing livestock.

The Pallas's cat, or manul, is a rare small felid with a vast but highly fragmented distribution in the steppes and mountainous areas of central and western Asia. Its dependence on cavities for shelter, vulnerability to aerial and terrestrial predators, and high dietary specialization underline its natural low density and patchy distribution (Ross et al. 2019*b*), making the species highly vulnerable (Ross et al. 2019*b*, Purvis et al. 2000). Although it was recently downlisted to least concern status by the International Union for Conservation of Nature (Moqanaki and Ross 2020), the species is declining (Chimed et al. 2021), with many populations that are small and isolated (Ross et al. 2020). While Mongolia is the stronghold of its distribution (Ross et al. 2020), only few inferential studies on their home range, spatial distribution, and density are available (Ross et al. 2019*b*, Anile et al. 2021, Chimed et al. 2021, Greenspan and Giordano 2021). Various factors threaten the Pallas's cat in Mongolia, including historical direct persecution for fur and medical uses (Barashkova and Smelansky 2011, Ross et al. 2020). Nonetheless, the greatest impact is thought to be caused by livestock overstocking, which causes habitat degradation due to heavy grazing (Ross et al. 2019*b*), an increase in predation by dogs (Farhadinia et al. 2016), and prey depletion due to eradication campaigns to reduce rodents (Delibes-Mateos et al. 2011, Ross et al. 2020). The number of domestic animals has exponentially increased in Mongolia in the last 20 years due to the worldwide demand for cashmere wool (National Statistical Office of Mongolia 2018). Livestock husbandry occurs throughout the country (Barashkova et al. 2007, Damdinsuren et al. 2008), and is permitted with few limitations even within protected areas according to the Mongolian Law on special protected areas (1994), with the exception of strictly protected areas (SPA). Despite the evidence that overstocking affects the Pallas's cat, quantitative knowledge on how livestock directly or indirectly affect Pallas's cat occurrence and activity pattern is scant.

We examined 4 areas across western Mongolia with different management regimes to estimate Pallas's cat occupancy (MacKenzie et al. 2002) in relation to habitat features, prey availability, and livestock grazing, and to investigate its diel activity pattern in relation to that of livestock. We hypothesized that 1) the cat's occupancy increases at sites that are steeper, have natural vegetation cover, and higher prey availability (Ross et al. 2012); 2) the cat's occupancy decreases at sites with higher livestock presence, or its diel activity pattern minimizes the overlap with that of domestic animals (Sévêque et al. 2020); and 3) large herds of goats and sheep have a greater effect on cat occupancy than the small herds of free-ranging, large-sized livestock (Augugliaro et al. 2020).

STUDY AREA

The Mongolian Altai Mountains extend from the northwestern part of Mongolia to the south, stretching over 900 km, and ranging 500–4,500 m above sea level. The area is characterized by a semi-arid and cold continental climate, with long cold winters reaching temperature of −25°C in January and short summers with little precipitation averaging 45 mm in July and 20°C. The landscape is characterized by rocky, steep, and dry mountains, with high plateaus dominated by dry steppe vegetation, and valley bottoms covered by coniferous trees and sparse shrubs.

We conducted the study in 4 areas within the Altai Mountains range of Mongolia in 2015–2019 (Figure 1). The Siilkhem National Park, Part B (Siilkhem B; 49°49′N, 89°44′E; 1,400 km^2) and the Tavan Bogd National Park (Tavan Bogd; 48°3′N, 88°37′E; 6,362 km^2) are located at the northwestern corner of the country, bordering Russia and China. Tavan Bogd is the largest protected area in Mongolia, with the highest elevation in the country (4,374 m) at Khuiten Uul Mountain. To the south, approximately 45 km from the Chinese border, lies the Khork Serkh (47°93′N, 90°99′E; 659 km^2), which is an SPA established in 1977, located between Bayan Olgii and Hovd provinces. The fourth area, Sutai massif (46°37′N, 93°35′E; 850 km^2), is an inland, remote and isolated area that had no legal protection when surveyed, but it was granted Nature Reserve status in 2020. All 4 study areas fell within the range of potentially suitable habitat for the Pallas's cat (Barashkova et al. 2019, Ross et al. 2020, Greenspan and Giordano 2021; Figure 1).

Beside the Pallas's cat, the community of medium to large mammalian species in western Mongolia includes a variety of large and meso carnivores including snow leopards, wolves (*Canis lupus*), wolverines (*Gulo gulo*), foxes

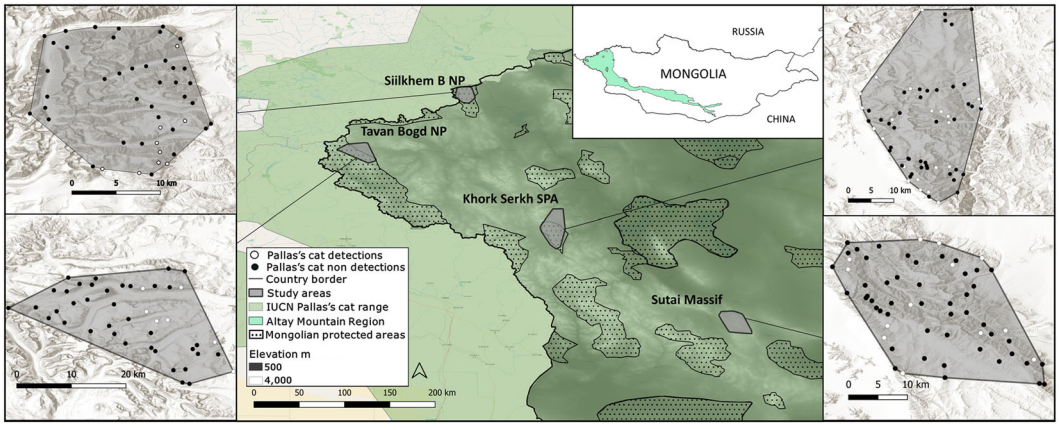

FIGURE 1 Western Mongolia with the 4 study areas: Siilkhem B National Park (sampled in 2015), Tavan Bogd National Park (2017), Khork Serkh Strictly Protected Area (2018), and Sutai Massif (2019). Pallas's cat distribution range is from the International Union for Conservation of Nature (IUCN) Red List website (Ross et al. 2020)

(*Vulpes vulpes*), lynxes (*Lynx lynx*), bears (*Ursus arctos*), and mustelids. Siberian ibexes (*Capra sibirica*), argali (*Ovis ammon*), and marmots (*Marmota marmota*) are the main wild herbivores. In the study area, human density is 1.5 person/km^2, with approximately 30% of the population being pastoral nomads or semi-nomads (Dagvadorj et al. 2009, World Bank 2018). Pastoralism is the primary form of livelihood in the country, with herder families moving seasonally to different grazing areas. In the province of Bayan Olgii alone, where the first 3 study areas are located, 2.2 million head of livestock were reported in 2018, 1.9 million of which were sheep and goats (National Statistics Office of Mongolia 2020). Except for the SPAs, traditional livestock husbandry is permitted in national parks only within limited use zones. Herd size can exceed 1,000 animals (Augugliaro et al. 2020), with large livestock (e.g., cows, yaks, horses) that are usually free-ranging in small clusters, while goats and sheep form large herds and are generally guarded by herders with dogs during the day and moved into corrals at night.

METHODS

Motion-sensitive cameras

For every study area, we collected motion-sensitive camera data in spring (Mar–Jun) from 2015 to 2019, sampling one study area per year with the exception of 2016 (Table S1, available in Supporting Information). We sampled 48–63 sites per study area (Table S1) with a criterion of ≥1.5 km between adjacent cameras. The regular design was constrained by topography and snow cover, and hence accessibility (Figure 1). Sampled sites covered 500–1,100 km^2 per study area at an elevation from 1,900 m to 3,500 m (Table S1). We placed motion-sensitive cameras on narrow valleys and ridges to maximize the chances to detect passing wildlife. Albeit aimed at primarily detecting snow leopards, such design and site selection proved efficient at detecting livestock and other wild mammals (Rovero et al. 2020) including the Pallas's cat. Pallas's cat and snow leopard occur at similar altitudinal ranges in the Altai Mountains (Snow Leopard Network 2014, Moqanaki et al. 2019), and display a comparable marking behavior (Allen et al. 2016). Such behavioral similarity, similar habitat preferences, and the relative homogeneity of the landscape, potentially allows the 2 species to use the same marking spots (Li et al. 2013). This further supports the effectiveness of site selection at detecting the Pallas's cat. We used heat-in-motion triggered cameras of different brands, and considered Reconyx (Holmen, WI, USA) as fast-triggered and other brands (Cuddeback, Green Bay, WI, USA; Browning, Birmingham, AL, USA; and UoVision, Shenzhen, China) as slow-triggered. We set cameras to work in continuous mode for 45–90 days (Table S1), with no delay between photographs; we used alkaline batteries, which outperform other types at cold temperatures. We placed motion-sensitive cameras on rock piles at approximately 50 cm from the ground. Upon retrieving cameras, we annotated images using the open-source software Wild.ID (Fegraus and MacCharty 2016).

Covariates

We used 8 environmental and anthropogenic covariates potentially associated to Pallas's cat occupancy (ψ) and detection probability (p). We selected covariates from a broader set of candidate variables (Table S2, available in Supporting Information) to avoid collinearity, based on Pearson's correlation coefficient ($r = 0.5$ as threshold). Hence, we used the motion-sensitive camera trigger speed (fast and slow) and sampling effort (camera days) as potentially affecting detectability. We derived the relative abundance index (RAI) of the pooled domestic species (i.e., livestock), with a 15-minute interval and normalized by the sampling effort, as an indicator of the intensity of livestock passage. We used site slope, site aspect, study area, and land cover (bare ground, managed ground, natural vegetation) as predictors of occupancy, and the occurrence probability of livestock modeled across sampling sites. We preferred this metric over the RAI of livestock as a predictor of Pallas's cat occupancy because we assumed it

more accurately measured the diffused presence of livestock across the landscape given it accounts for imperfect detection (MacKenzie et al. 2002, MacKenzie and Royle 2005).

We conducted a second analysis using only data from Khork Serkh SPA, where we obtained the highest number of detections of both Pallas's cat and livestock, which enabled us to conduct more detailed analysis of the target species. In addition, for Khork Serkh SPA we distinguished small-sized and large-sized livestock, and modeled their occupancy separately to determine the relative impact on Pallas's cat given their different herding and rearing management regimes (Augugliaro et al. 2020). The use of a greater number of motion-sensitive cameras in this area relative to other areas allowed us to also record small-sized species. Therefore, we recorded detections of voles (*Alticola* spp.) and pikas (*Ochotona* spp.) as preferred Pallas's cat prey (Ross et al. 2010*b*), and used independent photographs to compute their RAI, which we then used as a covariate of Pallas's cat occupancy.

To estimate livestock occupancy, we merged the number of domestic animals and human detections into a single category (i.e., livestock) and 2 categories (i.e., small and large livestock) for all study areas and the area sampled in 2018, respectively, and used single-season occupancy models. We modeled occupancy in relation to distance to the herders' tents or houses (i.e., ger) and elevation; we also fitted the distance to herders' houses to detectability, on the assumption that livestock herds would be more compact and hence more easily detected where closer to houses. Based on Akaike's Information Criterion (AIC) and model-averaging procedures described below, we derived occupancy estimates at motion-sensitive camera sites, and used them as a covariate of Pallas's cat occupancy models. We extracted all environmental variables using the geo-processing tools available in Quantum GIS (QGIS Development Team 2019), with the land cover extracted using the GLC2000 dataset (European Commission 2003) and altitudes extracted using a 30-m digital elevation model (Jarvis et al. 2008).

Occupancy modeling

We used single-season occupancy models (MacKenzie et al. 2002) to study the spatial patterns of the Pallas's cat in relation to covariates. Occupancy (ψ) is defined as the proportion of sites a species is expected to occur while accounting for imperfect detection, expressed in probability scale. Given the limitations of estimating true occupancy from point detectors within a continuous habitat, we interpreted occupancy as the proportion of area occupied (Neilson et al. 2018). For the multiple-area analysis, we summarized detection and non-detection data in a 2-dimensional array $Y_{i,j}$ of 216 sites × 131 sampling occasions, using a resolution of 1 day. Its elements $y_{i,j}$, denoted if the cat was detected ($y = 1$) or undetected ($y = 0$) at site i during sampling occasion j. We used NA to denote that a site was not sampled during a specific occasion. We ran models using the package unmarked (Fiske and Chandler 2011) in the R environment (R Core Team 2019). We standardized continuous covariates to have mean of zero and unit variance, built models with various combinations of covariates, and included the null model (i.e., no covariates). We ranked models according to the principle of parsimony, using the AIC and considered as equally best-supported those with $\Delta AIC < 2$ (Burnham and Anderson 2002). In the case of multiple best models, we used a model-averaging method through the package AICmodavg (Mazerolle 2019) to estimate the relative importance of the parameters and predicted occupancy and detection probabilities from the averaged models. We used the same procedure for the analysis on Khork Serkh SPA data but without using study area, and including the RAI of prey and the occupancy of both large- and small-sized livestock as covariates. For this study area we also mapped the occupancy values estimated at the scale of motion-sensitive camera sites and derived from the averaged models.

Analysis of diel activity pattern

To investigate activity patterns of livestock and Pallas's cat, we used a kernel density estimation function implemented in the R package overlap (Meredith and Ridout 2014), which allowed us to compute activity distribution

curves for the 2 groups and carry out a pairwise comparison. Hence, we considered all the domestic species as a single category (i.e., livestock) and used the time converted in radians of each independent event (>30 min) of cats and livestock to create temporal density curves (Zimmermann et al. 2016). Specifically, to determine whether the cat shifted diel activity depending on the intensity of site use by livestock, we built 2 density curves for the Pallas's cat: 1 for its detections at sites where livestock were also detected (i.e., RAI of livestock > 0) and 1 for detections at sites where livestock were not detected (RAI = 0). This resulted in 111 sites with and 105 sites without livestock occurrences, corresponding to 63 and 44 detections of Pallas's cat in the 2 subsets, respectively. Thus, to simultaneously compare Pallas's cat and livestock activities and test if the cat's diel activity shifts across the 2 scenarios, we plotted each of the cat's density curves with the one of livestock activity across the whole area. We then tested for significant differences between the 2 pairs of curves with a Wald test (Zimmermann et al. 2016). By using the R package activity (Rowcliffe et al. 2014), we computed overlap coefficient (Δ) between the 2 sets of curves, and specifically used Δ_4 for the scenario with livestock and Δ_1 for the one without livestock, in relation to the number of cat's detections (Meredith and Ridout 2014). We then computed 1,000 bootstraps iterations on the overlap values to estimate 95% confidence intervals (Ridout and Linkie 2009). The coefficient assesses the degree of overlap from 1 (complete overlap) to 0 (no overlap). Finally, we used the Welch 2-sample *t*-test to assess if the 2 generated distributions of Δ values were significantly different.

RESULTS

We obtained 1,298 images of Pallas's cats, corresponding to 107 detection events at 52 sites of the 216 sampled, between 2,223 m and 3,300 m in elevation, through 13,890 camera days across all study areas, with an average of 62 camera days per sampling unit (Table 1, S1). We detected 7 domestic species (Table S3, available in Supporting Information) at 111 sites, with an overall mean estimated occurrence probability of 0.51 (Siilkhem B ψ = 0.55, Tavan Bogd ψ = 0.41, Khork Serkh SPA ψ = 0.57, Sutai Massif ψ = 0.52). The highest numbers of raw detections (538) and occupancy (0.57) of livestock were recorded at Khork Serkh SPA. Livestock occupancy (as a whole category and considering small- and large-sized livestock separately) increased at lower elevations and in proximity to the herders' camps across the 4 study areas and in the focal area (Table 2; Table S4, available in Supporting Information).

For both the overall and the focal area assessment, multiple Pallas's cat occupancy models were best-supported (Table 3). Pallas's cat average estimated occupancy was 0.33 ± 0.10 (SE), and was lower in Tavan Bogd compared to other study areas (Figure 2A). Estimated detection probability was low (p = 0.02 ± 0.003) and increased where cameras had faster (p = 0.03 ± 0.003) than slower trigger speeds (p = 0.01 ± 0.004). Occupancy was higher in areas with sparse and natural vegetation (ψ = 0.73 ± 0.11) than with bare and managed ground (Table 4; Figure 2B) and it increased significantly with livestock occupancy (Table 4; Figure 2C). In Khork Serkh, the occurrence probability of

TABLE 1 Number of independent events per day and naïve occupancy of domestic species (i.e., livestock, dogs, and humans) and Pallas's cat, and the number of sites where the cat was detected. Data were collected using cameras in the 4 study areas in western Mongolia, 2015–2019

		Livestock		Pallas's cat		
Study area	Protection level	Events	Naïve ψ	Events	Naïve ψ	Number of successful sites
Siilkhem B	National park	316	0.44	11	0.19	9
Tavan Bogd	National park	138	0.29	10	0.16	7
Khork Serkh	Strictly protected	538	0.60	62	0.37	23
Sutai Massif	Unprotected	244	0.62	24	0.21	13

TABLE 2 Parameter estimates from model-averaging of the best-supported models for the occupancy (ψ) and detection (p) probability of livestock in western Mongolia, 2015–2019. For the assessment across the 4 study areas, we considered all livestock, humans, and dogs as a single category, while for the focal area assessment, we considered small- and large-sized livestock separately. Parameters include elevation and distance to herders' tents or houses (i.e., ger)

Parameter	Estimates	SE	*Z*	*P*
Four areas, western Mongolia—livestock				
ψ distance to closest ger	−1.11	0.50	2.21	0.03
ψ elevation	−0.38	0.31	1.23	0.21
p distance to closest ger	−0.62	0.18	3.41	<0.01
Focal area, Khork Serkh—small-sized livestock				
ψ distance to closest ger	−1.92	0.64	−2.99	<0.01
ψ elevation	−0.84	0.35	−2.36	0.02
p distance to closest ger	−0.63	0.24	−2.66	<0.01
Focal area, Khork Serkh—large-sized livestock				
ψ distance to closest ger	−0.57	0.49	1.16	0.25
ψ elevation	−0.38	0.31	1.25	0.22
p distance to closest ger	−0.45	0.23	1.96	0.04

the Pallas's cat increased significantly with increasing occupancy of sheep and goats ($\beta = 1.25 \pm 0.47$, $P < 0.01$; Figure 3; Table 4) and the occupancy of large livestock was not retained in the best models, showing a positive but non-significant effect. Similar to the model for all areas, the cat's occupancy increased in habitat with natural vegetation ($\psi = 0.70 \pm 0.12$, $P = 0.01$). Moreover, occupancy tended to increase with increasing steepness of the terrain ($\beta = 0.79 \pm 0.42$, $P = 0.05$), and higher relative abundance of rodents ($\beta = 0.67 \pm 0.41$, $P = 0.09$; Table 4; Figure 3).

Overall, Pallas's cat displayed a cathemeral behavior with multiple peaks of activity through the 24 hours (Figure 4), with detections during 1400–1700 that were less frequent. Across the 4 areas, the overlap between Pallas's cat and livestock curves was lower at sites where livestock was also detected ($\Delta = 0.28$, 95% CI = 0.25–0.31) than at sites where livestock was not detected ($\Delta = 0.45$, 95% CI = 0.41–0.49; Figure 4). The difference in activity pattern was significant in the former case ($W = 20.44$, $P < 0.001$) and non-significant in the latter ($W = 2.26$, $P = 0.13$). The t-test for differences in activity overlaps between the 2 scenarios had a significant outcome ($P < 0.001$).

DISCUSSION

Motion-sensitive camera detections of Pallas's cat from snow leopard surveys in the Mongolian Altai Mountains enabled us to evaluate the spatio-temporal patterns and responses of this little-known felid to a suite of covariates, with a particular focus on the sensitivity to grazing livestock. Previous information on Pallas's cat occupancy was limited to local ecological knowledge (Chimed et al. 2021). We are aware of the limitations of our sampling that primarily targeted the snow leopard (Rovero et al. 2020), and we acknowledge that occupancy may simply reflect the proportion of area used by the Pallas's cat (Efford and Dawson 2012, Neilson et al. 2018). Yet, being a metric that accounts for imperfect detection, its usefulness to assess habitat associations has been revealed by many studies (Niedballa et al. 2015, Gompper et al. 2016, Moll et al. 2016, Greco et al. 2021).

TABLE 3 Summary of the single-species single-season occupancy (ψ) and detection (p) models of the Pallas's cat across the 4 study areas and for the focal area (i.e., Khork Serkh Strictly Protected Area), in western Mongolia, 2015–2019. We ranked models using Akaike's Information Criterion (AIC), and considered models with ΔAIC < 2.00 equally best-supported. Only the 10 top models and the null models are shown. We also provide number of parameters (K) and Akaike weights (w_i). Focal area models included a relative abundance index (RAI) of domestic livestock, dogs, and humans (domestics), and of prey species

Models	K	AIC	ΔAIC	w_i
Across the 4 areas—western Mongolia				
p (trigger speed) ~ ψ (habitat cover + study area)	8	1,145.84	0.00	0.59
p (trigger speed) ~ ψ (occupancy domestics + habitat cover)	6	1,147.33	1.50	0.28
p (trigger speed) ~ ψ (habitat cover)	5	1,149.45	3.61	0.10
p (trigger speed) ~ ψ (aspect + study area + habitat cover)	9	1,159.93	6.09	0.03
p (trigger speed) ~ ψ (aspect + habitat cover)	8	1,167.31	21.48	0.00
p (trigger speed) ~ ψ (aspect + study area + habitat cover)	11	1,167.83	21.99	0.00
p (trigger speed) ~ ψ (slope + study area)	7	1,170.19	24.36	0.00
p (trigger speed) ~ ψ (slope + habitat cover)	6	1,170.27	24.43	0.00
p (trigger speed) ~ ψ (aspect + occupancy domestics + slope + habitat cover)	10	1,171.01	25.17	0.00
p (trigger speed) ~ ψ (slope + occupancy domestics + study area)	8	1,171.54	25.70	0.00
p (1) ~ ψ (1)	2	1,180.76	34.63	0.00
Focal area—Khork Serkh Strictly Protected Area				
p (trigger speed + RAI domestics) ~ ψ (occupancy small livestock + RAI prey + slope + habitat cover)	9	581.12	0.00	0.43
p (trigger speed + RAI domestics) ~ ψ (occupancy small livestock + slope + habitat cover)	8	582.74	1.62	0.19
p (trigger speed + RAI domestics) ~ ψ (slope × occupancy small livestock + habitat cover)	9	583.98	2.86	0.10
p (trigger speed + RAI domestics) ~ ψ (occupancy small livestock + habitat cover)	7	584.70	3.58	0.07
p (trigger speed + RAI domestics) ~ ψ (occupancy large livestock + habitat cover + slope)	8	586.05	4.93	0.04
p (trigger speed + RAI domestics) ~ ψ (occupancy small livestock + slope)	6	586.20	5.08	0.03
p (trigger speed + RAI domestics) ~ ψ (slope × occupancy small livestock)	7	586.97	5.85	0.02
p (trigger speed + RAI domestics) ~ ψ (occupancy small livestock + RAI prey + slope)	7	587.05	5.93	0.02
p (trigger speed + RAI domestics) ~ ψ (occupancy large livestock + habitat)	7	588.60	7.48	0.01
p (trigger speed + RAI domestics) ~ ψ (RAI prey + habitat cover + slope)	8	588.68	7.56	0.00
p (1) ~ ψ (1)	2	647.60	66.48	0.00

Moreover, our inference is related to the gradient of protected areas encroached by livestock (2 national parks, 1 SPA, 1 area that was not protected at the time of sampling), and not to the wider steppe ecosystem in western Mongolia. The moderate occupancy and very low detectability we estimated are broadly consistent with the presumed low density of this species (Ross et al. 2012, Anile et al. 2021), while the proportion of sites used on sites sampled is comparable with that of Chimed et al. (2021). The significantly lower occupancy in Tavan Bogd may

THE JOURNAL OF WILDLIFE MANAGEMENT

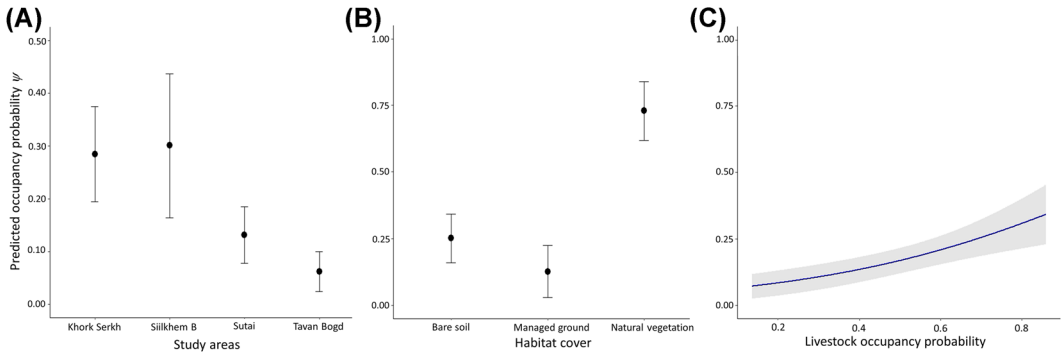

FIGURE 2 Estimated occupancy probability (ψ) of the Pallas's cat in western Mongolia, spring 2015–2019, in relation to A) the study areas, B) the 3 main habitat land cover types, and C) the occupancy of domestic animals (SE in grey). Values are in probability scale and are derived from averaging the best-supported models

TABLE 4 Parameter estimates from model-averaging of the best-supported models of Pallas's cat occupancy (ψ) and detection (p) probability across 4 study areas and a focal area in western Mongolia, 2015–2019

Parameter	Estimates	SE	Z	P
Across the 4 areas—western Mongolia				
ψ habitat cover–natural vegetation	2.11	0.49	4.30	<0.01
ψ habitat cover–managed ground	−0.88	0.83	1.06	0.29
ψ occupancy of domestic animals	0.44	0.22	1.96	0.04
ψ study area–Tavan Bogd NP	−1.78	0.68	2.63	<0.01
ψ study area–Siilkhem B NP	0.07	0.72	0.11	0.92
ψ study area–Sutai Massif	−0.96	0.55	1.75	0.08
p trigger speed – slow	−0.77	0.36	2.17	0.03
Focal area—Khork Serkh Strictly Protected Area				
ψ abundance of small-sized livestock	1.25	0.47	2.62	<0.01
ψ habitat cover–natural vegetation	2.52	1.00	2.52	0.01
ψ habitat cover–managed ground	1.42	1.41	1.01	0.31
ψ slope	0.79	0.42	1.88	0.05
ψ relative abundance of prey species	0.67	0.41	1.66	0.09
p trigger speed–slow	−1.68	0.57	2.96	<0.01
p RAI domestics[a]	−0.15	0.13	1.14	0.26

[a]Relative abundance index of domestic livestock, dogs, and humans.

indicate that this area is suboptimal for this felid, likely because it is generally higher in elevation and has more extensive glacial and snow cover relative to the other areas (Ganyushkin et al. 2018). The Pallas's cat appears to prefer areas that are steep, with natural vegetation and higher occurrence of prey, matching the high habitat and dietary specialization known for this species (Ross et al. 2019*a*, Chimed et al. 2021, Greenspan and Giordano 2021). The importance of areas with vegetation emerged clearly from both analyses (i.e., the entire region and the focal area of Khork Serkh SPA), while a weak preference for steep areas only emerged from the focal area. For this area

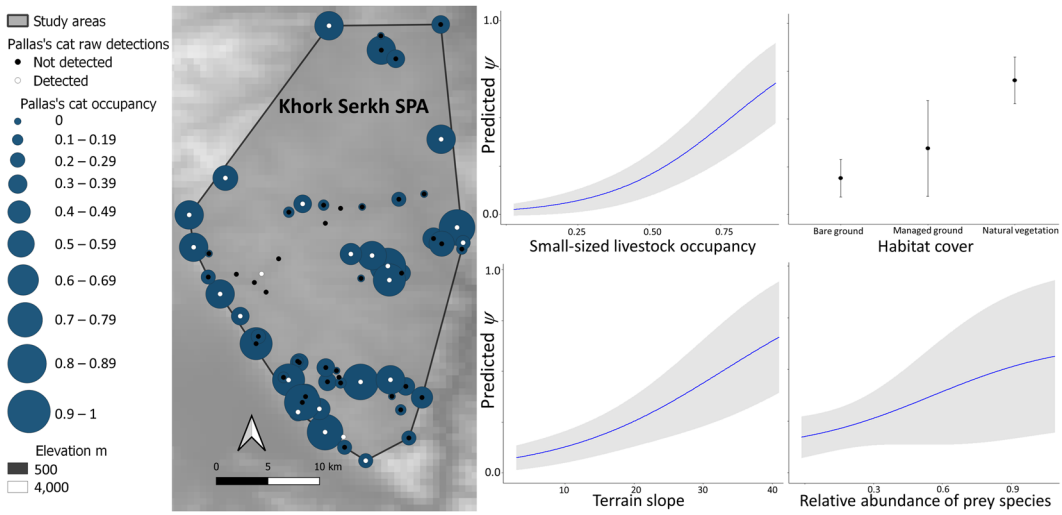

FIGURE 3 Occupancy probability distribution of the Pallas's cat in Khork Serkh Strictly Protected Area (2018), western Mongolia. Circles indicate occupancy probability, with larger ones representing higher values. We modeled occupancy as a function of the occupancy of small-sized domestic animals (i.e., sheep and goats), habitat land cover type, slope, and relative abundance of prey species

we could also consider prey availability in the model, and this variable too resulted to be weakly associated to Pallas's cat's occupancy. The weak association may have been affected by natural fluctuations in the abundance of prey (Andreassen et al. 2021, Otgonbayar and Suuri 2021) or our placement of motion-sensitive cameras to target snow leopard may have biased low the detection of small animals. Similar to the effect of land cover, the positive association with the occupancy of livestock was revealed in both assessments, and it was relatively more attributable to small-sized livestock in the focal area. Pallas's cat was significantly more detectable in all study areas when using fast-trigger motion-sensitive cameras, as reported for other elusive felids and small mammals (Wellington et al. 2014, Greco and Rovero 2021).

The positive association of the Pallas's cat with vegetated and prey-rich habitat where also grazing livestock occur is partially in contrast to our hypothesis. Such spatial association may be due to the higher abundance of prey species near camps due to fertilization promoting vegetation growth (Bülow-Olsen 1980, Ross 2009) or areas with natural vegetation that are associated with a greater presence of pikas and other small rodents (Ross 2009). The presence of livestock could also trigger a form of mesopredator release, with herding dogs and livestock that might disperse larger carnivores (Ross 2009, Anile et al. 2021). The convergence in habitat preferences between domestic species and Pallas's cat suggests that the preferred habitat by the cat in the study region coincides with areas encroached by livestock. The spatial association is especially pronounced with sheep and goats that are managed as large herds and represent the majority of livestock, being therefore of potential greater impact on the vegetated areas (Augugliaro et al. 2020). Thus, the Pallas's cat is able to populate the preferred habitat despite its use by livestock; however, in line with our hypothesis, a coping mechanism is the shift in the diel activity pattern of the felid at grazing sites in the direction of minimizing temporal activity overlap with livestock, which are usually reared in corrals at night in the study region, particularly for small-sized livestock (Augugliaro et al. 2020). In view of these results, we suggest that the convergence between Pallas's cat preferred habitat and grazing areas of livestock may represent a serious, impending threat to the felid, as suggested by its shift in diel activity pattern to limit direct encounters. Temporal niche partitioning in response to anthropogenic disturbance is known from a range of other study systems where wild species co-occur with humans and livestock, with animals minimizing risk by shifting the temporal, rather than the spatial niche (Poudel et al. 2015, Oberosler et al. 2017, Gaynor et al. 2018).

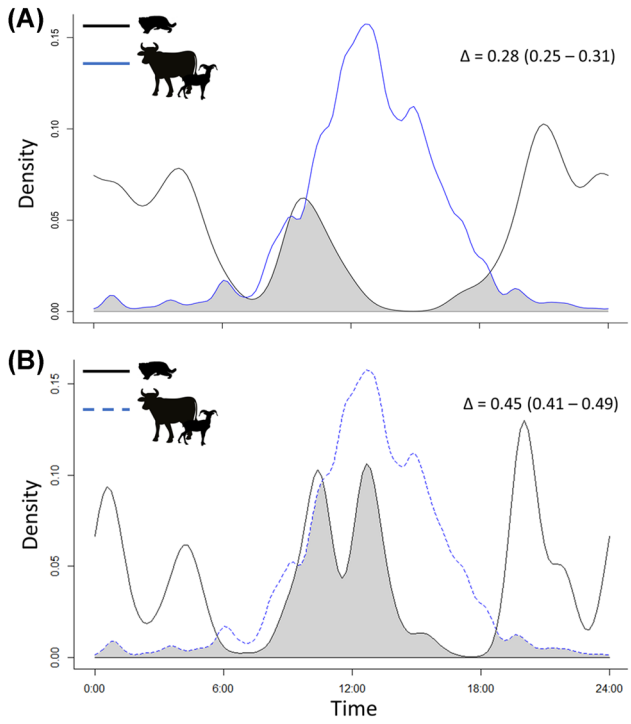

FIGURE 4 Temporal overlap in activity between the Pallas's cat and livestock in western Mongolia, 2015–2019. The figure displays the diel activity pattern of the felid A) at sites where livestock were detected (111 sites, 63 cat's detections) and B) at sites where livestock were not detected (105 sites, 44 cat's detections). Both Pallas's cat activity curves were plotted against the diel activity pattern of livestock across the whole area, to point out the felid's variation in activity pattern. The coefficient (Δ) assessed the degree of overlap between the diel activity curves of the 2 taxa (1 = complete overlap, 0 = no overlap)

When considering that livestock numbers have markedly increased across Mongolia over the last decades (Berger et al. 2013, Pfeiffer et al. 2018), and that we also recorded diffused livestock presence into protected areas (this study, Augugliaro et al. 2020, Salvatori et al. 2021), our findings are of conservation concern for a number of reasons. First, the Pallas's cat is specialized in its habitat choice, and only uses a small fraction of area available within the steppe ecosystem (10–30%; Ross et al. 2019*a*); it is dependent on areas that are protected but also increasingly used for grazing, which may eventually threaten the cat from habitat degradation affecting the abundance of small rodents, hence progressively reducing prey availability (Cao et al. 2016, Schieltz and Rubenstein 2016). Second, the proximity of preferred areas to herders' houses and camps implies higher chances of Pallas's cat predation by dogs, considered one of the most important causes of human-related deaths of these cats (Ross 2009; Barashkova 2012, 2017), and poisoning, directly as a predator control method or as consequence of poisoning of Pallas's cat's primary prey for pest or disease control (Tseveenmyadag and Nyambayar 2002). This latter threat is particularly critical for Mongolia (Winters 2006). The detrimental effects of such practices and overharvesting are also currently threatening marmot (*Marmota* spp.) species (Zahler et al. 2004, Clayton 2016), on whose cavities Pallas's cats are dependent on for denning and resting sites (Ross et al. 2010*a*). These concerns are augmented when considering that hunting of Pallas's cats is still permitted in Mongolia (Murdoch et al. 2007, Barclay et al. 2019) where Pallas's cats were traded until recently on local markets (Wingard et al. 2018), poaching of this species within protected areas has been documented as frequently occurring (Murdoch et al. 2007), and Pallas's cats are occasionally shot when mistaken for marmots (Ross et al. 2019*b*). Field observations from our sampling reported

Pallas's cat skins found in several nomads' tents across 3 out of 4 areas (F. Rovero, University of Florence, and C. Augugliaro, University of Lausanne, personal observation).

Habitat degradation resulting from livestock grazing has detrimental effects on large mammals (Ripple et al. 2014, 2015; Soofi et al. 2018), while a general trend of total abundance declining with grazing is also documented for small mammals (Schieltz and Rubenstein 2016). But studies on the specific effects on small carnivores are few and with contrasting outcomes (Blaum et al. 2007*a*, 2007*b*, 2009; Bösing et al. 2014; Williams et al. 2018). For example, a study in South Africa reported that stocking rate of livestock was inversely related to local abundance of small- and medium-sized predators, including felids (Blaum et al. 2009). While our data on the Pallas's cat do not provide for inference on population trends, the consistency in the results across study areas with different protection regimes and between the regional and the focal area indicates that the causalities we suggest to explain the spatio-temporal responses of Pallas's cat to livestock are founded.

MANAGEMENT IMPLICATION

We suggest that the most relevant conservation actions for Pallas's cat should include regulations of livestock encroachment within protected areas by improving enforcement efficacy. Additionally, in consideration of the cat's association with natural vegetation and prey abundance, we suggest improving protection for this habitat and banning the eradication campaigns of rodents through poisoning. We further believe that a review of its legal status in Mongolia based on updated and quantitative evidence should be carried out. Because our knowledge of Pallas's cat ecology, behavior, distribution, and population status is scarce, further research on their populations is required for the conservation of the species and to benefit other key species across its range.

ACKNOWLEDGMENTS

We are grateful to P. R. Krausman, J. K. Sheppard, and 2 anonymous reviewers for valuable comments to an earlier version of the manuscript. We thank the Ministry of Environment and Tourism of Mongolia for providing the research permit, the Altai Mountain Protected Area Authority, and C. Janchvlamdan for the technical support and help with logistics. Fototrappolaggio, University of Lausanne, Altai Institute for Research and Conservation, and Snow Leopard Conservancy provided a share of the motion-sensitive cameras. We are thankful to all participants in the expeditions, particularly M. Krofel, C. Groff, R. Havmøller, R. Rizzoli, B. Rosembaum, D. Ciaramella, F. Zimmermann, P. Christe, and P. Zorer for the valuable contribution to the fieldwork. We also thank A. Marchetto and S. Palmarini for classifying camera images. The study was funded by Panthera (Sabin Snow Leopard Grants to FR); MUSE—Museo delle Scienze, Italy; Green Initiative; Natural History Museum of Denmark; University of Lausanne; Irbis Mongolia; Altai Institute for Research and Conservation; Parco Natura Viva, Italy; and Herbette Foundation, Switzerland. VO was supported by the Gino Zobele Fund.

ETHICS STATEMENT

For our research, no animals were handled and permission to conduct the study was granted by the Ministry of Environment and Tourism of Mongolia (protocol number 10/1674).

ORCID

Ilaria Greco http://orcid.org/0000-0002-6208-2465
Valentina Oberosler http://orcid.org/0000-0002-7019-9858
Ibra Edoardo Monti http://orcid.org/0000-0001-5268-8386
Claudio Augugliaro http://orcid.org/0000-0002-1815-1777
Francesco Rovero http://orcid.org/0000-0001-6688-1494

REFERENCES

Allen, M., H. Wittmer, E. Setiawan, S. Jaffe, and A. J. Marshall. 2016. Scent marking in Sunda clouded leopards (*Neofelis diardi*): novel observations close a key gap in understanding felid communication behaviours. Scientific Report 6: 35433.

Andreassen, H. P., J. Sundell, F. Ecke, S. Halle, M. Haapakoski, H. Henttonen, O. Huitu, J. Jacob, K. Johnsen, E. Koskela, et al. 2021. Population cycles and outbreaks of small rodents: ten essential questions we still need to solve. Oecologia 195: 601–622.

Anile, S., C. Augugliaro, B. Munkhtsog, F. Dartora, A. Vendraminn, G. Bombieri, and C. Nielsen. 2021. Density and activity patterns of Pallas's cats *Otocolobus manul* in central Mongolia. Wildlife Research 48:264–272.

Augugliaro, C., P. Christe, C. Janchivlamdan, H. Baymanday, and F. Zimmermann. 2020. Patterns of human interaction with snow leopard and co-predators in the Mongolian western Altai: current issues and perspectives. Global Ecology and Conservation 24:e01378.

Barashkova, A. 2012. New data on Pallas's cat in Tyva. Steppe Bulletin 35:44–48. [In Russian].

Barashkova, A. N. 2017. Manul. Pages 313–317 *in* Red Data Book of the Altai Republic. Government of Altai Republic, Gorno-Altaisk, Russia. [In Russian].

Barashkova, A., and I. Smelansky. 2011. Pallas's cat in the Altai Republic, Russia. Cat News 54:4–7.

Barashkova, A., I. Smelansky, S. Goryunova, and S. Naidenko. 2007. Pallas's cat: investigation for saving (clarifying conservation status in Russia). Siberian Environmental Center, Novosibirsk, Russia.

Barashkova, A., I. Smelansky, V. Kirilyuk, S. Naidenko, A. Antonevich, M. Gritsina, K. Zhumabai Uulu, M. Koshkin, N. Battogtokh, B. Otgonbayar, A. Grachev, and A. Lissovsky. 2019. Distribution and status of the manul in Central Asia and adjacent areas. Cat News Special Issue 13:14–23.

Barclay, D., I. Smelansky, E. Nygren, and A. Antonevich. 2019. Legal status, utilisation, management and conservation of manul. Cat News Special Issue 13:37–40.

Berger, J., B. Buuveibaatar, and C. Mishra. 2013. Globalization of the cashmere market and the decline of large mammals in Central Asia. Conservation Biology 27:679–689.

Blaum, N., E. Rossmanith, A. Popp, and F. Jeltsch. 2007*a*. Shrub encroachment affects mammalian carnivore abundance and species richness in semiarid rangelands. Acta Oecologica–International Journal of Ecology 31:86–92.

Blaum, N., E. Rossmanith, M. Schwager, and F. Jeltsch. 2007*b*. Responses of mammalian carnivores to land use in arid savanna rangelands. Basic and Applied Ecology 8:552–564.

Blaum, N., B. Tietjen, and E. Rossmanith. 2009. Impact of livestock husbandry on small- and medium-sized carnivores in Kalahari savannah rangelands. Journal of Wildlife Management 73:60–67.

Bösing, B. M., D. H. Haarmeyer, J. Dengler, J. U. Ganzhorn, and U. Schmiedel. 2014. Effects of livestock grazing and habitat characteristics on small mammal communities in the Knersvlakte, South Africa. Journal of Arid Environments 104: 124–131.

Brodie, J. F. 2009. Is research effort allocated efficiently for conservation? *Felidae* as a global case study. Biodiversity and Conservation 18:2927–2939.

Bülow-Olsen, A. 1980. Changes in the species composition in an area dominated by *Deschampsia flexuosa* (L) trin. as a result of cattle grazing. Biological Conservation 18:257–270.

Burnham, K. P., and D. R. Anderson. 2002. Model selection and multimodel inference. Springer, New York, New York, USA.

Cao, C., L. Shuai, X. Xin, Z. Liu, Y. Song, and Z. Zeng. 2016. Effects of cattle grazing on small mammal communities in the Hulunber meadow steppe. PeerJ 4:e2349.

Cardillo, M., A. Purvis, W. Sechrest, J. L. Gittleman, J. Bielby, and G. M. Mace. 2004. Human population density and extinction risk in the world's carnivores. PLoS Biology 2:e197.

Chimed, O., J. S. Alexander, G. Samelius, P. Lkhagvajav, L. Davaa, N. Bayasgalan, and K. Sharma. 2021. Examining the past and current distribution of Pallas's cat in Southern Mongolia. Mammalian Biology 101:811–816.

Clayton, E. 2016. *Marmota sibirica*. The IUCN Red List of Threatened Species 2016:e.T12832A22258643.

Dagvadorj, D., L. Natsagdorj, J. Dorjpurev, and B. Namkhainyam. 2009. Mongolian assessment report on Climate Change 2009. Ministry of Environment, Nature and Tourism, Ulan Bator, Mongolia.

Damdinsuren, B., J. E. Herrick, D. A. Pyke, B. T. Bestelmeyer, and K. M. Havstad. 2008. Is rangeland health relevant to Mongolia? Rangelands 30:25–29.

Delibes-Mateos, M., T. A. Smith, C. N. Slobodchikoff, and J. E. Swenson. 2011. The paradox of keystone species persecuted as pests: a call for the conservation of abundant small mammals in their native range. Biological Conservation 144: 1335–1346.

Efford, M. G., and D. K. Dawson. 2012. Occupancy in continuous habitat. Ecosphere 3(4):1–15.

European Commission. 2003. Global Land Cover 2000 database. European Commission, Joint Research Center. https://forobs.jrc.ec.europa.eu/products/glc2000/glc2000.php

Farhadinia, M. S., E. M. Moqanaki, and M. A. Adibi. 2016. Baseline information and status assessment of manul (Pallas's cat; *Otocolobus manul* Pallas, 1776) in Iran. Cat News Special Issue 2016:38–42.

Fegraus, E., and J. MacCharty. 2016. Camera trap data management and interoperability. Chapter 4 *in* F. Rovero and F. Zimmermann, editors. Camera trapping for wildlife research. Pelagic Publishing, Exeter, United Kingdom

Fiske, I., and R. Chandler. 2011. Unmarked: an R package for fitting hierarchical models of occurrence and abundance. Journal of Statistical Software 43:1–23.

Ganyushkin, D. A., K. V. Chistyakov, I. V. Volkov, D. V. Bantcev, E. P. Kunaeva, T. A. Andreeva, A. V. Terekhov, and D. Otgonbayar. 2018. Present glaciers of Tavan Bogd Massif in the Altai Mountains, Central Asia, and their changes since the Little Ice Age. Geosciences 8:1–35.

Gaynor, K. M., C. E. Hojnowski, N. H. Carter, and J. S. Brashares. 2018. The influence of human disturbance on wildlife nocturnality. Science 360:1232–1235.

Gompper, M. E., D. B. Lesmeister, J. C. Ray, J. R. Malcolm, and R. Kays. 2016. Differential habitat use or intraguild interactions: What structures a carnivore community? PLoS ONE 11(1):e0146055.

Greco, I., E. Fedele, M. Salvatori, M. Giampaoli Rustichelli, F. Mercuri, G. Santini, F. Rovero, L. Lazzaro, B. Foggi, et al. 2021. Guest or pest? Spatio-temporal occurrence and effects on soil and vegetation of the wild boar on Elba Island. Mammalian Biology 101:193–206.

Greco, I., and F. Rovero. 2021. The African golden cat *Caracal aurata* in Tanzania: first record and vulnerability assessment. Oryx 55:212–115.

Greenspan, E., and A. Giordano. 2021. A rangewide distribution model for the Pallas's cat (*Otocolobus manul*): identifying potential new survey regions for an understudied small cat. Mammalia 85:574–587.

Jarvis, A., H. I. Reuter, A. Nelson, and E. Guevara. 2008. Hole-filled seamless SRTM data V4, International Centre for Tropical Agriculture (CIAT), Cali, Colombia. http://srtm.csi.cgiar.org

Lama, S. T., J. G. Ross, D. Bista, A. P. Sherpa, G. R. Regmi, M. K. Suwal, P. Sherpa, J. Weerman, S. S. Lama, M. Thapa, and L. P. Poudyal. 2019. First photographic record of marbled cat *Pardofelis marmorata* Martin, 1837 (Mammalia, Carnivora, Felidae) in Nepal. Nature Conservation 32:19–34.

Lamberski, N. 2015. *Felidae*. Fowler's Zoo and Wild Animal Medicine 8:467–476.

Lawler, J. J., L. E. Aukema, J. B. Grant, B. S. Halpern, P. Kareiva, C. R. Nelson, K. Ohleth, J. D. Olden, M. A. Schlaepfer, B. R. Sillman, and P. Zaradic. 2006. Conservation science: a 20-year report card. Frontiers in Ecology and Environment 4:473–480.

Li, J., G. B. Schaller, T. M. McCarthy, D. Wang, Z. Jiagong, P. Cai, L. Basang, and Z. Lu. 2013. A communal sign post of snow leopards (*Panthera uncia*) and other species on the Tibetan Plateau, China. International Journal of Biodiversity 2013: 370905.

Li, X., W. V. Bleisch, X. Liu, and X. Jiang. 2020. Camera-trap surveys reveal high diversity of mammals and pheasants in Medog, Tibet. Oryx 55:177–180.

MacKenzie, D. I., J. D. Nichols, G. Lachman, S. Droege, J. A. Royle, and C. Langtimm. 2002. Estimating site occupancy rates when detection probabilities are less than one. Ecology 83:2248–2255.

MacKenzie, D. I., and J. A. Royle. 2005. Designing occupancy studies: general advice and allocating survey effort. Journal of Applied Ecology 42:1105–1114.

Mazerolle, M. J. 2019. Model selection and multimodel inference based on (Q)AIC(c). R package version 2.2-2. https://cran.r-project.org/package=AICcmodavg

Meredith, M., and M. Ridout. 2014. Overlap: estimates of coefficient of overlapping for animal activity patterns. R package version 0.2.3. https://CRAN.R-project.org/package=overlap

Moll, R. J., K. Kilshaw, R. A. Montgomery, L. Abade, R. D. Campbell, L. A. Harrington, J. J. Millspaugh, J. D. S. Birks, and D. W. Macdonald. 2016. Clarifying habitat niche width using broad-scale, hierarchical occupancy models: a case study with a recovering mesocarnivore. Journal of Zoology 300:177–185.

Moqanaki, E. M., N. Jahed, E. Malkhasyan, E. Askerov, M. S. Farhadinia, M. Kabir, M. Adibi Ali, J. Ud Din, L. Joolaee, N. R. Chahartaghi, and S. Otrowski. 2019. Distribution and status of the Pallas's cat in the south-west part of its range. Cat News Special Issue 13:24–30.

Moqanaki, E. M., and S. Ross. 2020. Manul downlisted to Least Concern. Cat News 71:15.

Murdoch, J. D., T. Munkhzul, and C. Sillero-Zubiri. 2007. Do nature reserves adequately protect Pallas' cats in central Mongolia. Pages 17–20 *in* J. Hughes and R. Mercer, editors. Felid biology and conservation conference. WildCRU, Oxford, United Kingdom.

National Statistics Office of Mongolia. 2020. General Statistical Database. National Statistics Office of Mongolia, Ulan Bator, Mongolia.

Neilson, E. W., T. Avgar, C. Burton, K. Broadley, and S. Boutin. 2018. Animal movement affects interpretation of occupancy models from camera trap surveys of unmarked animals. Ecosphere 9:e02092.

Niedballa, J., R. Sollmann, A. Mohamed, J. Bender, and W. Andreas. 2015. Defining habitat covariates in camera-trap based occupancy studies. Scientific Reports 5:17041.

Oberosler, V., C. Groff, A. Iemma, P. Pedrini, and F. Rovero. 2017. The influence of human disturbance on occupancy and activity patterns of mammals in the Italian Alps from systematic camera trapping. Mammalian Biology 87:50–61.

Otgonbayar, B., and B. Suuri. 2021. Diet of the Pallas's cat (*Otocolobus manul*) in Mongolian steppe habitat during a population peak of Brandt's voles. Journal of Arid Environment 193:104583.

Pfeiffer, M., C. Dulamsuren, Y. Jäschke, and K. Wesche. 2018. Grasslands of China and Mongolia: spatial extent, land use and conservation. Chapter 8 *in* V. R. Squires, J. Dengler, H. Feng, and L. Hua, editors. Grasslands of the world: diversity, management and conservation. CRC Press, Boca Raton, Florida, USA.

Pimm, S. L., J. L. Gittleman, and T. M. Brooks. 1995. The future of biodiversity. Science 269:347–350.

Poudel, B. S., P. G. Spooner, and A. Matthews. 2015. Temporal shift in activity patterns of Himalayan marmots in relation to pastoralism. Behavioral Ecology 26:1345–1351.

Purvis, A., J. L. Gittleman, G. Cowlishaw, and G. M. Mace. 2000. Predicting extinction risk in declining species. Proceedings of the Royal Society of London B 267:1947–1952.

QGIS Development Team. 2019. QGIS Geographic Information System. https://www.qgis.org/en/site/

R Core Team. 2019. R: a language and environment for statistical computing. R Foundation for Statistical Computing, Vienna, Austria.

Ridout, M. S., and M. Linkie. 2009. Estimating overlap of daily activity patterns from camera trap data. Journal of Agricultural, Biological and Environmental Statistics 14:322–337.

Ripple, W. J., J. E. Estes, R. L. Beschta, C. C. Wilmers, E. G. Ritchie, M. Hebblewhite, J. Berger, B. Elmhagen, M. Letnic, M. P. Nelson, et al. 2014. Status and ecological effects of the world's largest carnivores. Science 343:1241484.

Ripple, W. J., T. M. Newsome, C. Wolf, R. Dirzo, K. T. Everatt, M. Galetti, M. W. Hayward, G. I. H. Kerley, T. Levi, P. A. Lindsey, et al. 2015. Collapse of the world's largest herbivores. Science Advances 1:e1400103.

Ross, S. 2009. Providing an ecological basis for the conservation of the Pallas's cat (*Otocolobus manul*). Dissertation, University of Bristol, Bristol, United Kingdom.

Ross, S., A. Barashkova, T. Dhendup, B. Munkhtsog, I. Smelansky, D. Barclay, and E. Moqanaki. 2020. *Otocolobus manul*. The IUCN Red List of Threatened Species 2020:e.T15640A162537635.

Ross, S., A. Barashkova, V. Kirilyuk, and S. Naidenko. 2019*a*. The behaviour and ecology of the manul. Cat News Special Issue 13:9–13.

Ross, S., R. Kamnitzer, B. Munkhtsog, and S. Harris. 2010*a*. Den-site selection is critical for Pallas's cats (*Otocolobus manul*). Canadian Journal of Zoology 88:905–913.

Ross, S., E. M. Moqanaki, A. Barashkova, T. Dhendup, I. Smelansky, S. Naidenko, A. Antonevich, and G. Samelius. 2019*b*. Past, present and future threats and conservation needs of the Pallas's cat. Cat News Special Issue 13:46–51.

Ross, S., B. Munkhtsog, and S. Harris, 2010*b*. Dietary composition, plasticity, and prey selection of Pallas's cats. Journal of Mammalogy 91:811–817.

Ross, S., B. Munkhtsog, and S. Harris. 2012. Determinants of mesocarnivore range use: relative effects of prey and habitat properties on Pallas's cat home-range size. Journal of Mammalogy 93:1292–1300.

Rowcliffe, J. M., R. Kays, B. Kranstauber, C. Carbone, and P. A. Jansen. 2014. Quantifying levels of animal activity using camera trap data. Methods in Ecology and Evolution 5:1170–1179.

Salvatori, M., S. Tenan, O. Oberosler, C. Augugliaro, P. Christe, C. Groff, M. Krofel, F. Zimmermann, and F. Rovero. 2021. Co-occurrence of snow leopard, wolf and Siberian ibex under livestock encroachment into protected areas across the Mongolian Altai. Biological Conservation 261:109294.

Schieltz, J. M., and D. I. Rubenstein. 2016. Evidence based review: positive versus negative effects of livestock grazing on wildlife. What do we really know? Environmental Research Letters 11:113003.

Sévêque, S., L. K. Gentle, J. Lopez-Bao, W. Yarnell, and A. Uzal. 2020. Human disturbance has contrasting effects on niche partitioning within carnivore communities. Biological Reviews 95:1689–1705.

Snow Leopard Network. 2014. Snow Leopard Survival Strategy. www.snowleopardnetwork.org

Soofi, M., A. Ghoddousi, T. Zeppenfeld, S. Shokri, M. Soufi, A. Jafari, M. Ahmadpour, A. T. Qashqaei, L. Egli, T. Ghadirian, N. Raeesi Chahartaghi, B. Zehzad, B. H. Kiabi, I. Khorozyan, N. Balkenhol, and M. Waltert. 2018. Livestock grazing in protected areas and its effects on large mammals in the Hyrcanian forest, Iran. Biological Conservation 217:377–382.

Tseveenmyadag, N., and B. Nyambayar. 2002. The impact of rodenticide used to control rodents on Demoiselle crane (*Anthropoides virgo*) and other animals in Mongolia. Mongolian Academy of Sciences and Peregrine Fund, Ulaanbaatar, Mongolia.

Wellington, K., C. Bottom, C. Merrill, and J. A. Litvaitis. 2014. Identifying performance differences among trail cameras used to monitor forest mammals. Wildlife Society Bulletin 38:634–638.

Williams, S. T., N. Maree, P. Taylor, S. R. Belmain, M. Keith, and L. H. Swanepoel. 2018. Predation by small mammalian carnivores in rural agro-ecosystems: an undervalued ecosystem service? Ecosystem Services 30:362–371.

Wingard, J., M. Pascual, A. Rude, A. Houle, S. Gombobaatar, G. Bhattacharya, M. Munkhjargal, N. Conaboy, S. Myagmarsuren, T. Khaliun, T. Batsugar, and T. Bold. 2018. Silent steppe II: Mongolia's wildlife trade crisis, ten years later. Zoological Society of London, London, United Kingdom.

Winters, A. M. 2006. Rodenticide use and secondary poisoning risks to non-target wildlife in central Mongolia. Thesis, Michigan State University, East Lansing, USA.

World Bank. 2018. Population density (people per sq. km of land area)–Mongolia. World Development Indicators, The World Bank Group. https://data.worldbank.org. Accessed Jun 2020.

Zahler, P., B. Lhagvasuren, R. P. Reading, J. R. Wingard, S. Amgalanbaatar, S. Gombobaatar, N. Barton, and Y. Onon. 2004. Illegal and unsustainable wildlife hunting and trade in Mongolia. Mongolian Journal of Biological Sciences 2:23–31.

Zhou, X. H., X. T. Wan, Y. H. Jin, and W. Zhang. 2016. Concept of scientific wildlife conservation and its dissemination. Zoological Research 37:270–274.

Zimmermann, F., D. Foresti, and F. Rovero. 2016. Behavioural studies. Chapter 8 *in* F. Rovero and F. Zimmermann, editors. Camera trapping for wildlife research. Pelagic, Exeter, United Kingdom.

Associate Editor: James Sheppard.

SUPPORTING INFORMATION

Additional supporting information may be found in the online version of the article at the publisher's website.

How to cite this article: Greco, I., V. Oberosler, I. E. Monti, C. Augugliaro, A. Barashkova, and F. Rovero. 2021. Spatio-temporal occurrence and sensitivity to livestock husbandry of Pallas's cat in the Mongolian Altai. Journal of Wildlife Management 1–16. https://doi.org/10.1002/jwmg.22150

Received: 12 May 2022 | Revised: 8 November 2022 | Accepted: 29 November 2022

DOI: 10.1002/ecs2.4427

ECOSPHERE
AN ESA OPEN ACCESS JOURNAL

ARTICLE

Methods, Tools, and Technologies

Calibrating occupancy to density estimations to assess abundance and vulnerability of a threatened primate in Tanzania

Ilaria Greco[1] | **Christina Lynette Paddock**[2,3] | **Gráinne Michelle McCabe**[3] | **Claudia Barelli**[1] | **Steven Shinyambala**[4] | **Arafat S. Mtui**[4] | **Francesco Rovero**[1,5]

[1]Department of Biology, University of Florence, Sesto Fiorentino, Italy

[2]School of Biosciences, Cardiff University, Cardiff, UK

[3]Bristol Zoological Society, Bristol, UK

[4]Udzungwa Ecological Monitoring Centre, c/o Udzungwa Mountains National Park, Mang'ula, Tanzania

[5]MUSE—Museo delle Scienze, Trento, Italy

Correspondence
Ilaria Greco
Email: ilaria.greco@unifi.it

Funding information
Bristol Zoological Society; Fondazione Foresta Futura; MUSE—Museo delle Scienze; NERC Natural Environmental Research Council, Grant/Award Number: NE/N007980/1; Primate Conservation, Grant/Award Number: #1443; Tropical Ecology Assessment and Monitoring (TEAM) Network; Wild Planet Trust

Handling Editor: Alessio Mortelliti

Abstract

The current decline of mammals worldwide makes quantitative population assessments crucial, especially for range-restricted and threatened species. However, robust abundance estimations are challenging for elusive or otherwise difficult to detect species. Alternative metrics requiring only presence/absence data, that is, occupancy, are possible but calibration with independent density estimates should be foreseen, although rarely performed. Here, we calibrated density estimates from acoustic surveys to occupancy estimates from camera-trapping detections to derive the abundance of the endangered Sanje mangabey (*Cercocebus sanjei*) across its entire range in the Udzungwa Mountains of Tanzania. We found marked occupancy–density relationships for the two forest blocks where this primate occurs and used them to derive spatially explicit density estimates. Occupancy increased in montane forest zones at mid-elevation but decreased slightly with proximity to forest borders. We predicted an average density (±SE) of 0.26 ± 0.05 groups/km^2 in the national park and 0.24 ± 0.06 in the nature reserve. Accordingly, and given the much larger area of the reserve, the average predicted individual abundance was 1555 ± 325 and 2471 ± 571 in the national park and nature reserve, respectively. We found higher density and abundance in the nature reserve compared with previous studies. Given the past disturbance and poorer protection in the nature reserve relative to the national park, our results instill optimism for the status of the species, although occupancy analysis highlighted the potential vulnerability of this primate to human disturbance. Our approach appears valuable for spatially explicit density estimations of elusive species, and provides robust assessments of vulnerability and identification of priority areas for conservation of threatened populations.

KEYWORDS
acoustic distance sampling, camera-trapping, *Cercocebus sanjei*, density estimation, endangered species, occupancy, Udzungwa Mountain National Park

INTRODUCTION

In the Anthropocene, wildlife species are experiencing an unprecedented decline, with 26% of mammals currently threatened with extinction (International Union for Conservation of Nature [IUCN], 2021). While the highest concentration of threatened and range-restricted species are found in tropical forests, these represent one of the most affected biomes, with habitat loss and harvesting that disproportionally impact mammals (Roberts et al., 2021; Schipper et al., 2008). Nonhuman primates are among the most threatened order of mammals, with ~65% of the 504 existing species being threatened with extinction and ~75% of the populations facing decline (Estrada et al., 2017; Fernández et al., 2022). By functioning as seed dispersers, these species serve a critical ecological role in forest regeneration, affecting plant species diversity and demography (e.g., Andresen et al., 2018; Holbrook & Loiselle, 2009; Lambert, 2010). For these reasons, nonhuman primates are considered excellent ecological indicators and are highly sensitive to anthropogenic disturbance (Marsh, 2003; Rodrìguez-Luna et al., 2013). Therefore, research and conservation efforts focused on primates may have the added benefits of preserving important ecological functions as well as other species (Gippoliti & Sousa, 2004; Lambert, 2010; Martins & Valladares-Padua, 2005). However, the quantitative knowledge on abundance, conservation status, and vulnerability of threatened primates needed to promote sound conservation remains limited (Estrada et al., 2017), and rarely does this cover the entire range of species (e.g., Davenport et al., 2022).

A key limiting issue of such assessments is the pervasive difficulty of estimating population abundance and its spatial variation, especially for rare and elusive free-ranging animals. Hence, accounting for imperfect detection is important, especially for species that are difficult to detect, and methods that include it are highly recommended (e.g., Cavada et al., 2019; Spehar et al., 2015). In place of direct counts of individuals or groups, a practical approach is the use of detection/nondetection data (Joseph et al., 2006; Kühl et al., 2008). The latter are suitable for estimating occupancy, which is broadly considered a surrogate for abundance, and can be modeled with spatial covariates to assess species response to drivers of change (Kéry & Royle, 2016; Linden et al., 2017; MacKenzie et al., 2002, 2006). However, the assumption of a positive relationship between the two metrics is often untested and ideally requires the calibration of occupancy with independently derived density estimates (Linden et al., 2017).

Here, we present the results of an approach that calibrates occupancy from camera-trapping detections to density from acoustic surveys to estimate population abundance and spatial variation of an endangered primate in relation to both environmental and anthropogenic factors. We selected the Sanje mangabey (*Cercocebus sanjei*, Mittermeier et al., 2006) for this study, an IUCN-endangered, predominantly ground-dwelling, and frugivorous primate first described in 1979 and occurring only in two separated forests in the Udzungwa Mountains of south-central Tanzania (Ehardt et al., 2005; McCabe et al., 2019; Rovero et al., 2006). The area is of outstanding importance for biodiversity conservation (Burgess et al., 2007; Rovero, Menegon, et al., 2014) and a high-priority area for primate conservation in Tanzania (Davenport et al., 2013).

Despite several ecological studies, robust knowledge on population abundance and habitat association remains preliminary, with studies rarely targeting the whole species range with consistent methodology. Earlier estimations of population abundance were based on crude extrapolations of home-range data from a few groups (e.g., Ehardt, 2001; Ehardt et al., 2005; Rovero et al., 2009). More recently, Paddock et al. (2020) used acoustic detections to estimate density using a distance sampling approach, hence taking into account imperfect detection. This method enabled group detection using the distinctive mangabey whoop-gobble long-call, which is given by males in each group in the mornings, allowing for remote sensing without the need for visual observations of this elusive species. However, effort was limited to a single survey across a spatially and numerically limited set of listening posts, and the analysis did not consider spatial covariates. Similarly, habitat associations have been studied with camera traps, but only for parts of the species range (Martin et al., 2015; Oberosler et al., 2020a; Rovero, Martin, et al., 2014) and considered only a few environmental and anthropogenic variables. Studies showed that camera traps are very efficient at detecting this ground-dwelling species (Hegerl et al., 2017; Martin et al., 2015; Oberosler et al., 2020a), which is instead very rarely sighted by human observations (Barelli et al., 2013; Rovero et al., 2012).

Here, we aimed to provide more accurate quantification of abundance and density of this elusive and iconic

species by integrating camera-trapping and acoustic data to overcome previous limitations, particularly the difficulties associated with collecting systematic and spatially comprehensive density data from acoustic detections. Thus, we used camera-trap data collected consistently in both forests, and hence across most of the species' range, to calibrate spatially explicit occupancy estimates to density from acoustic surveys, and used the regression to derive density estimates across the species' range. Moreover, by integrating visual counts of group size, we also predicted individual densities and total population abundance. Lastly, we also aimed to determine spatial patterns of occurrence in relation to both habitat and potential anthropogenic disturbance to better assess habitat associations and vulnerability of this endangered and iconic primate.

MATERIALS AND METHODS

Study area

The Udzungwa Mountains in south-central Tanzania (7°40′–8°40′ S and 35°10′–36°50′ E; Figure 1) represent the largest block within the Eastern Arc Mountains and the richest in biodiversity (Rovero, Menegon, et al., 2014). Part of the area is protected as Udzungwa Mountain National Park (1990 km^2), established in 1992, whereas the remaining part is preserved either as nature reserve or forest reserve (Rovero et al., 2009). The two forests where the Sanje mangabeys occur are Mwanihana (MW, 167 km^2) within the Udzungwa Mountain National Park, and Uzungwa Scarp Nature Reserve (USNR, 372 km^2), which is approx. 150 km to the southwest (Figure 1). These areas are both east-facing escarpment slopes ranging in elevation between 290 and 2100 m above sea level (asl), with a gradient of vegetation cover from lowland deciduous to montane evergreen and upper montane bamboo forests. Lowland zones in both areas are dominated by regenerating and secondary forest due to past logging and degradation, whereas the higher elevations are mainly characterized by undisturbed, closed-canopy forest. The two forests share similar ecological characteristics (Appendix S1: Table S1), but different management regimes: MW has effective law enforcement being in a well-protected national park, while USNR is less efficiently protected (Rovero et al., 2012) and more degraded (Oberosler et al., 2020a; Rovero, Menegon, et al., 2014). In fact, the nature reserve is a forest island surrounded by small villages and suffers from logging, habitat destruction, and illegal hunting, whereas MW has minor anthropogenic disturbance from the villages located east of the park boundary.

Data collection: Acoustic and camera-trapping surveys

Acoustic detection data were collected by Paddock et al. (2020) during the dry season (June–November 2017), at 28 survey locations (MW: $N = 13$; USNR: $N = 15$; Figure 1).

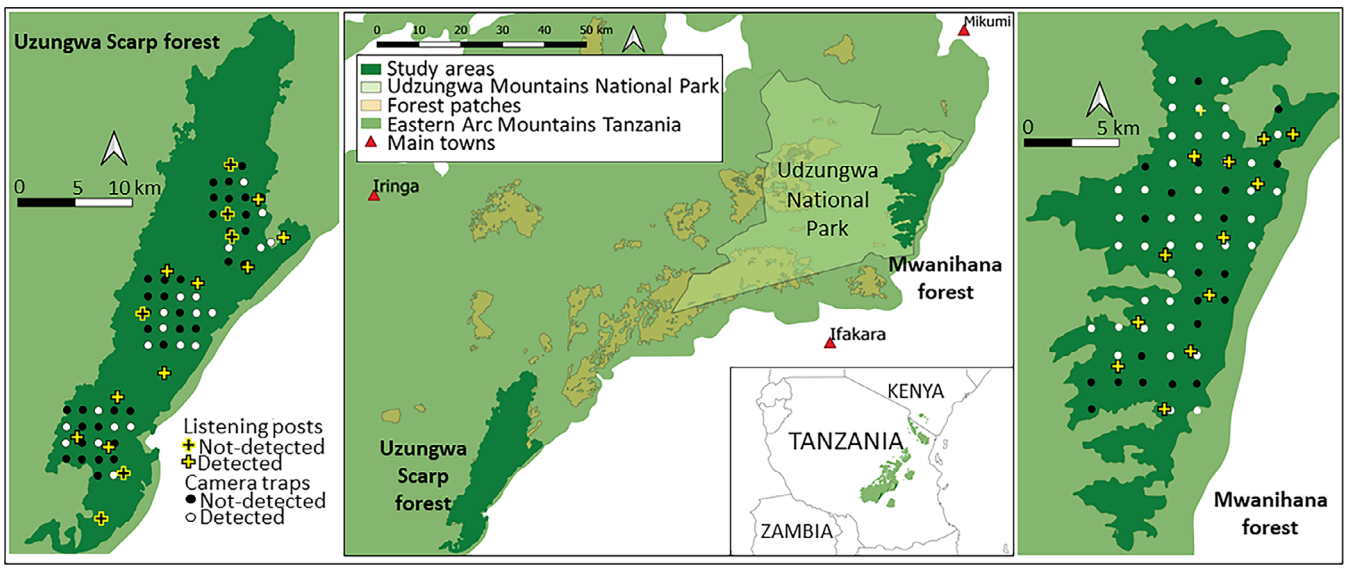

FIGURE 1 Map of the study area in Tanzania (central panel and inset), with the two forest blocks (Mwanihana forest and Uzungwa Scarp Nature Reserve) where the Sanje mangabey (*Cercocebus sanjei*) occurs (left and right panels). In these two forests, black and white dots represent camera-trap locations (white are those where mangabeys were detected), whereas crosses represent the listening posts where acoustic surveys were made (yellow are those where mangabeys were detected).

The listening posts were located randomly inside cells of a systematic grid, with a minimum distance between locations of 2 km (Figure 1), which is in line with the known home-range size of the target species (Ehardt et al., 2005). The distance to each mangabey vocalization heard was estimated by three independent observers and the distance and direction mapped to estimate the position of the group. Estimates included in the analyses were truncated at 1 km as it was unlikely calls were accurately detectable over this distance. Data collection was carried out in the morning, between 07:00 and 09:00, when the Sanje mangabey is known to call at the highest frequencies (Ehardt et al., 2005), and every survey was conducted once (further details in Paddock et al., 2020).

Camera-trapping surveys were conducted in both forests in the same period as the acoustic survey (i.e., July–November 2017). Data in MW were collected through the Tropical Ecology Assessment and Monitoring (TEAM) Network project (Rovero & Ahumada, 2017), which follows a standardized and systematic protocol for monitoring medium-to-large terrestrial mammals, and the same protocol was extended in USNR. Thus, for each forest, we placed three consecutive arrays of 20 camera traps (Reconyx HC500, Reconyx Inc., Holmen, WI, USA) for a total of 60 camera stations per forest (Figure 1). Cameras were located based on a systematic grid of 2-km^2 cell size and deployed in the field for a minimum of 30 consecutive days. Inside each cell, camera traps were placed on the closest wildlife trail to the centroid of the cell and attached to trees at approximately 50 cm from to the ground, facing the presumed trail at approximately 2–3 m distance. The total sampling effort yielded 1839 camera days for MW and 1792 for USNR (Appendix S1: Table S1) from 117 camera-trap sites overall, as three were damaged, with a mean effort per camera of 31 days for both study areas.

Data collection: Covariates

We derived six covariates that could affect the species spatial distribution both in terms of density and occupancy and used them as proxies of environmental and anthropogenic factors. Thus, we considered: (1) habitat cover, extracted from the GLC2000 dataset (European Commission, 2004) and based on Food and Agriculture Organization of the United Nations habitat classification (i.e., broadleaf evergreen forest and deciduous forest), (2) elevation, extracted from a 90-m digital elevation model raster, (3) ground slope, (4) distance from the camera location to the closest river, and (5) distance to the closest forest border. Values were extracted using the built-in tools in the open-source software QGIS (QGIS Development Team, 2019). Based on Pearson's correlation coefficient (threshold = 0.5), these variables were not collinear.

Data analyses

Group density estimates

We reanalyzed data from Paddock et al. (2020) with the aim of building density estimation models with account of anthropogenic and environmental covariates. We used the package "Distance" (Miller et al., 2019) in R (R Core Team, 2018) to model the probability of detection and estimate Sanje mangabey groups' density from distance data. We built and compared several model combinations using different detection functions and covariates, to find the best fitting detection function. The best model was selected using Akaike information criteria (AIC) where the best model was considered at $\Delta AIC = 0$. We did not use adjustment terms as covariates were involved (Miller et al., 2019). Given the limited sample size ($N = 28$ listening posts), we only used elevation, ground slope, and distance to the closest reserve border as density covariates (see next section on assumptions of covariate relationship with density and occupancy). We averaged covariate value across a 1-km buffer around each listening post since Sanje mangabeys are generally heard within such area. Group densities were calculated for each study forest and then extrapolated considering the total available forest area (MW = 150.59 km^2 and USNR = 314.48 km^2; Marshall et al., 2010).

Occupancy modeling

Sanje mangabey occupancy (ψ) accounting for imperfect detection (p) was estimated using single-species single-season occupancy modeling (MacKenzie et al., 2002). Occupancy is the proportion of sites where the target species is expected to occur when the likelihood to record it is smaller than 1, namely when the nondetection of the species does not imply its absence from the site (MacKenzie et al., 2002). We built a single model for both forests. The input data consisted of a matrix of sampled sites i by the sampling occasions j, filled with species detections (1) and nondetections (0). This consisted in a matrix of 117 sites and 137 sampling occasions. We scored as NA a site that was not sampled during a specific occasion. We first built a null model with constant detection and occupancy, and then selected the best supported model for the detection probability by fitting distance to the closest forest border and habitat type. In fact, previous studies assessed that the former could influence the detection probability of a range

of species in either direction (Greco & Rovero, 2021; Rovero, Martin, et al., 2014), likely triggering increasing shyness or boldness. Moreover, detectability could also be affected by the density of forest floor vegetation in different habitat types, leading to changes in the efficiency of camera at detecting animals (Greco et al., 2021). We did not use camera-trap effort as potential covariate for the detection probability because our effort was homogeneous across cameras. We then used the best supported detection model (Appendix S1: Table S2) to model occupancy. Occupancy probability was modeled as a function of (1) habitat type, (2) elevation, (3) ground slope, (4) distance to the closest reserve border, and (5) distance to the closest river. We expected occupancy to increase away from the forests' borders, where anthropogenic disturbance may be higher, and that would increase in association with an optimal environment for the Sanje mangabeys, such as closer to watercourses, in association with broadleaves evergreen forests, and at mid-elevation. We also expected averaged site-specific occupancy to be higher in the national park compared with the nature reserve (Oberosler et al., 2020a; Paddock et al., 2020). Finally, we ranked all the occupancy models with different combinations of variables against the null model. Models were run using the package "unmarked" (Fiske & Chandler, 2011) in R. Model selection and ranking was based on the AIC score, with $\Delta AIC < 2$ representing best supported models. If multiple models resulted top ranked, we followed Dormann et al.'s (2018) procedure to averaging predictions: we computed predictions on link scale for each best supported model, back-transformed them to response scale, and averaged predictions. Using the best models, we predicted occupancy across the forest areas by using a grid of 100 × 100 m pixels populated with site covariate values (Rovero & Spitale, 2016). This was done by using the "predict" function and plotted the result on a map using the "levelplot" function in the R package "lattice" (Sarkar, 2008).

Density to occupancy calibration

Given that listening post locations might not perfectly overlap with just one pixel of predicted occupancy, we averaged predicted occupancy values from the nine pixels centered on each listening post. We then regressed density values from survey sites on these predicted occupancy values to determine the relationships. We used generalized linear models with a gamma distribution and log-link function for each population within the two forests to test the relationship between the two metrics, with occupancy values as the independent variable and density values as the dependent variable ($N = 13$ sites for MW and $N = 9$ sites for USNR). Contrary to MW, USNR had sites with no acoustic records, and we assumed that these reflected nondetections rather than absence. Hence, we did not include them in the analyses. We chose a gamma distribution as the data are continuous and positive (Bolker, 2008) and because we hypothesized that the relationship might not be linear. This is because as occupancy increases along the 0–1 gradient, density may increase at a higher rate given it is not bounded. Based on the calibration results, we derived density (±SE) estimates from the occupancy values at the 100 × 100 m resolution, using the function "predict" in the package "stats" (Chambers & Hastie, 1992). We averaged density values to predict group density in each forest and multiplied them by the forest area to predict group abundance. Lastly, we derived individual density and abundance by using an average count of 39.2 individuals per group in MW ($N = 5$) and 31.7 in USNR ($N = 3$; Paddock et al., 2020).

RESULTS

Three occupancy models were best supported (Table 1), resulting in an average (±SE) site-specific estimated occupancy probability (ψ) of 0.64 ± 0.10 and 0.48 ± 0.09 in MW and USNR, respectively (Figure 2), with lower occupancy in USNR than MW (Welch two-sample t test: $t = 3.57$; df = 110.32; p value <0.001). In addition, occupancy decreased with elevation ($\beta = -1.36 \pm 0.41$; $p < 0.01$), it was higher in broadleaf evergreen forest ($\beta = 2.38 \pm 0.71$; $p < 0.01$) and increased with distance to protected area border ($\beta = 0.58 \pm 0.31$; $p = 0.06$; Figure 2; Table 2). Conversely, the detection probability (p) decreased away from the border ($\beta = -0.24 \pm 0.09$; $p < 0.01$; Table 2). Spatially explicit occupancy maps are shown in Appendix S1: Figure S1.

Acoustic density estimations were best fitted by a half-normal detection function and with the distance to the closest reserve border as the variable retained (goodness of fit = 0.69; Appendix S1: Table S2). Occupancy values at the listening posts successfully predicted density estimates from acoustic surveys for both MW ($\beta = 1.90 \pm 0.92$ SE; $p = 0.03$; $R^2 = 0.32$) and USNR ($\beta = 2.49 \pm 0.93$ SE; $p = 0.03$; $R^2 = 0.36$; Figure 3). The spatially explicit densities derived from such relationships (Figure 4) were significantly higher in MW than in USNR (Welch two-sample t test: $t = 16.65$; df = 51,988; p value <0.001), and resulted in an estimated mean ± SE density of 0.26 ± 0.05 groups/km^2 and 0.24 ± 0.06, respectively. These estimates translated into 39.66 ± 8.28 mangabey groups across MW and 77.94 ± 18.01 across USNR. Predicted population size using available mean group counts resulted in 1555 ± 324.58 and

TABLE 1 Results of the occupancy models (top five and null model) for the Sanje mangabey (*Cercocebus sanjei*) in two forests, Mwanihana and Uzungwa Scarp Nature Reserve in Tanzania, detected by camera traps in 2017.

Occupancy models	No. parameters	AIC	ΔAIC	R^2
p (Distance to closest reserve border) ~ ψ (Distance to closest reserve border + Habitat + Elevation)	**6**	**1228.26**	**0.00**	**0.57**
p (Distance to closest reserve border) ~ ψ (Distance to closest reserve border + Habitat + Elevation + Distance to closest river + Slope)	**8**	**1229.92**	**1.66**	**0.58**
p (Distance to closest reserve border) ~ ψ (Distance to closest reserve border + Habitat + Elevation + Slope)	**7**	**1230.09**	**1.84**	**0.57**
p (Distance to closest reserve border) ~ ψ (Distance to closest reserve border + Elevation)	5	1241.59	13.33	0.51
p (Distance to closest reserve border) ~ ψ (Distance to closest reserve border + Habitat + Distance to closest river)	4	1241.73	13.47	0.51
p (1) ~ ψ (1)	2	1320.06	91.81	0.00

Note: Model ranking is based on the Akaike information criterion (AIC), with models having ΔAIC < 2.00 considered best supported (appearing in boldface).

2471 ± 570.88 individual monkeys in MW and USNR, respectively, corresponding to an estimated individual density of 10.32 ± 2.16 individuals/km^2 in MW and 7.86 ± 1.82 in USNR (Table 3).

DISCUSSION

By integrating density estimation from acoustic surveys with spatially explicit occupancy predictions, we derived density with account for spatial heterogeneity across the entire range of the endangered Sanje mangabey, hence refining the population estimates by Paddock et al. (2020), which were based on acoustic surveys at a limited sample of sites. Occupancy modeling also allowed us to determine habitat associations across the species' range and assess potential vulnerability of this nonhuman primate species to anthropogenic disturbance.

The use of occupancy as a cost-effective population assessment tool when abundance estimation is complex has long been recognized (e.g., MacKenzie et al., 2006; Noon et al., 2012; Wilson & Schmidt, 2015) and rests on an assumed positive relationship between occupancy and density (MacKenzie & Nichols, 2004). Such relationship is inherently complex because occupancy asymptotes at 1. In our study, the design of 2-km^2 grid cell size used for camera-trapping broadly matched the documented home range of Sanje mangabey (Ehardt et al., 2005; Mwamende, 2009). Hence, given that the grid cell size was close to the target species' home range, occupancy and abundance should broadly correspond (Linden et al., 2017), which likely underlines the occupancy–density relationship we found. Indeed, several studies highlighted how the spacing of detectors in relation to the home-range and movement pattern of the target species influenced the relationship (Rogan et al., 2019; Tempel & Gutierréz, 2013), with appropriate designs being those where such spacing matches the target species' home-range size, so to assume independence of detections (Clare et al., 2015; Tempel & Gutierréz, 2013; Wilson & Schmidt, 2015). In addition, the use of camera-trapping to estimate occupancy in continuous habitats is problematic due to the inherent violation of the closure assumption, given that camera traps are point detectors and animals regularly move in and out of sampled "sites" (Neilson et al., 2018). However, this issue makes estimated occupancy from camera detections a biased approximation of true occupancy, especially when low-density species move fast across large areas, hence saturating occupancy when density may be low (Lewis et al., 2015; Neilson et al., 2018; Parsons et al., 2017).

Findings from studies that investigated both forests found that the northern forest appears well protected compared with the southern one (Oberosler et al., 2020b), with the population in the nature reserve forest that has suffered decades of poor protection and, as a result, it is highly threatened and with lower density (Paddock et al., 2020). Our predictions of average group density per forest are broadly in line with those presented by Paddock et al. (2020) in that density was significantly higher in MW than in USNR; however, we estimated relatively higher density in USNR than from the acoustic distance sampling data alone (i.e., 0.22 vs. 0.15 groups/km^2 and

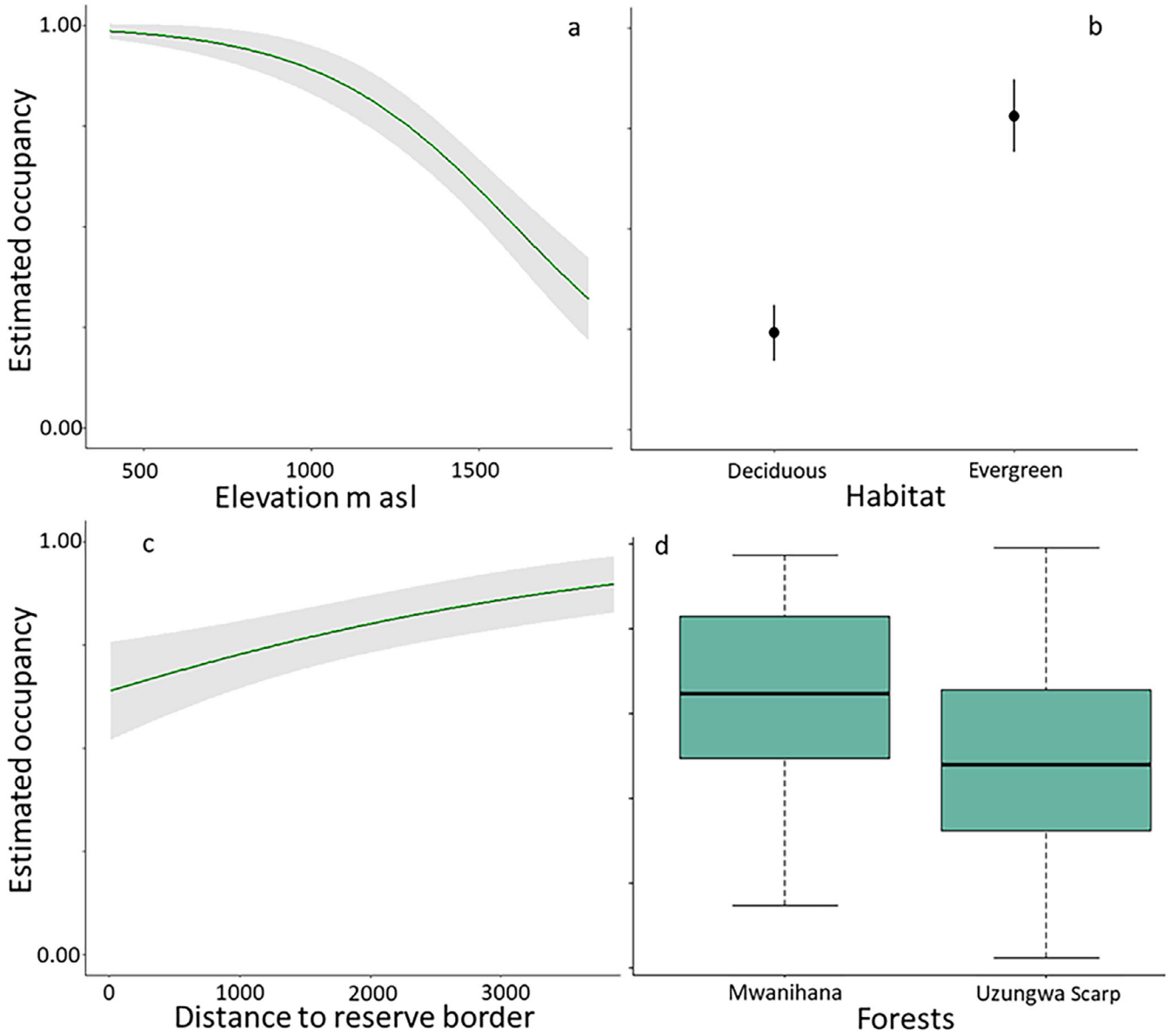

FIGURE 2 Bivariate predictions of estimated occupancy probability with SE from the averaging of the predictions of the three best supported models for the Sanje mangabey (*Cercocebus sanjei*) in relation to: (a) elevation, (b) forest type, and (c) distance to the closest forest border. Additionally, (d) shows the box plot for site-specific occupancy values divided by forest, where central bold lines depict medians, boxes show interquartile range with lower and upper quartile values, and whiskers indicate minimum and maximum values.

TABLE 2 Parameter estimates from the averaging of the best supported models of Sanje mangabey (*Cercocebus sanjei*): occupancy (ψ) and detection (*p*) probability estimates across the two study areas (Mwanihana forest and Uzungwa Scarp Nature Reserve) in Tanzania.

Parameters	Estimate	SE	*z*	*p*
ψ Distance to closest edge	0.58	0.32	1.85	0.06
ψ Habitat—evergreen	2.38	0.70	3.38	<0.01
ψ Elevation	−1.36	0.41	3.29	<0.01
ψ Slope	0.12	0.26	0.47	0.64
ψ Distance to closest river	0.36	0.25	1.44	0.15
p Distance to closest edge	−0.24	0.09	2.71	<0.01

69.6 vs. 45.9 groups for ours and the earlier study, respectively). This divergence may be caused by the spatially limited sample of listening posts used by Paddock et al. (2020) in comparison to the diffuse grid of camera traps we deployed, as well as the single acoustic survey event conducted for that study that may have caused a lower overall detection of the target species. The higher group density we estimated in USNR compared with previous studies translated into a higher overall abundance of approximately 4.026 ± 875.61 individuals in both forests (vs. 3167 ± 436.62 estimated by Paddock et al., 2020), 61% of which are estimated to occur in USNR given its much larger area than MW. We caution that the conversion

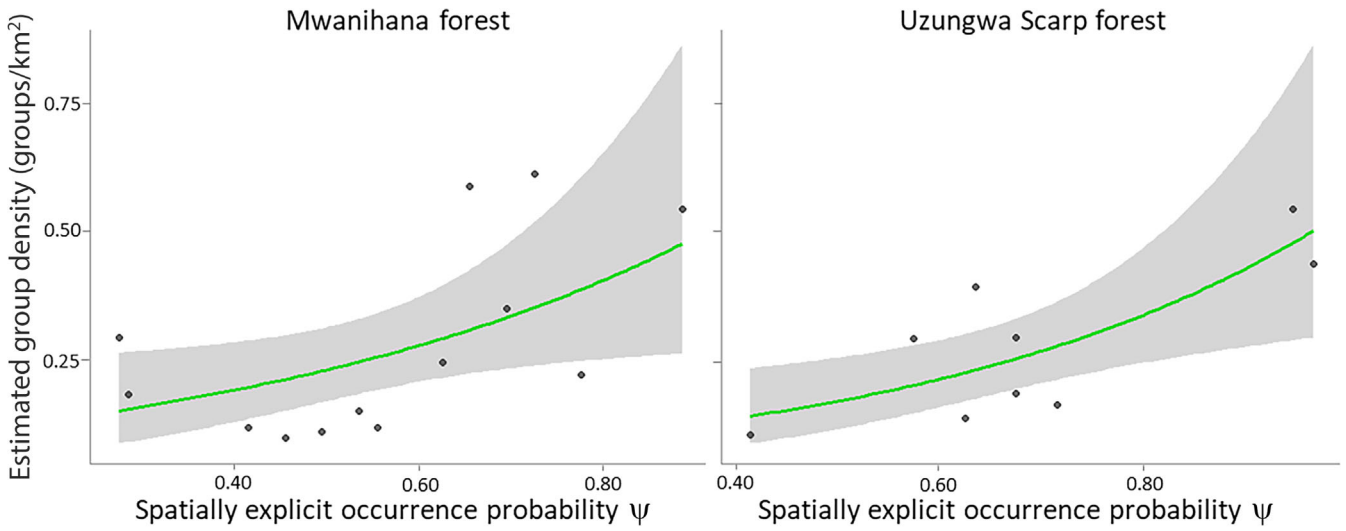

FIGURE 3 Relationship between occupancy and acoustic density estimates derived in Mwanihana (left, $N = 13$ listening posts) and Uzungwa Scarp forests (right, $N = 9$), Tanzania, where the Sanje mangabey (*Cercocebus sanjei*) was studied. The graph represents the result of a generalized linear model with gamma distribution and log-link function. Shaded area represents SE.

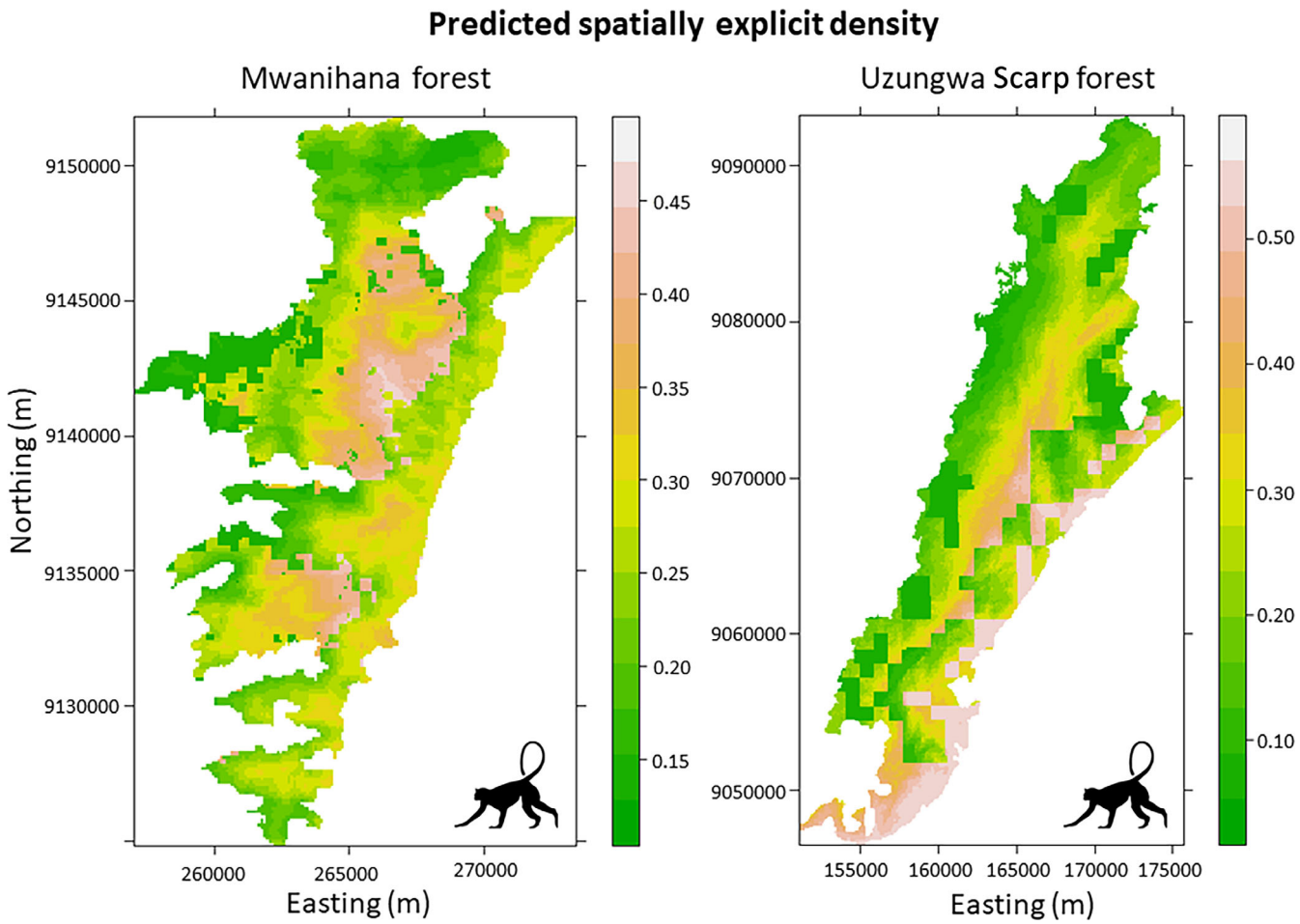

FIGURE 4 Maps of the predicted group density of the Sanje mangabey (*Cercocebus sanjei*) in Mwanihana forest (left) and Uzungwa Scarp forest (right), Tanzania.

TABLE 3 Estimated group density, number of groups, population size, and individual density of the Sanje mangabey (*Cercocebus sanjei*) in Mwanihana forest (MW) and Uzungwa Scarp Nature Reserve (USNR), Tanzania.

Metric	Forest	Parameter estimate	SE	Range
Group density (groups/km^2)	MW	0.26	0.05	0.12–0.47
	USNR	0.24	0.06	0.05–0.56
No. groups	MW	39.66	8.28	19.22–70.93
	USNR	77.94	18.01	16.24–177.18
Population size	MW	1554.63	324.58	753.48–2780.34
	USNR	2470.63	570.88	514.86–5616.59
Individual density (individuals/km^2)	MW	10.32	2.16	5.00–18.46
	USNR	7.86	1.82	1.64–17.86

from groups to individuals' abundance may be biased by the relatively small sample of group counts available ($N = 8$; Paddock et al., 2020) and needs therefore to be considered with this limitation in mind for future improvements. However, population estimates with methods that account for imperfect detection (Paddock et al., 2020) and with data from across the species' range (this study) were lacking (see review in Paddock et al., 2020); hence, our study provides for an important and comprehensive contribution to refine the species' conservation status and as a baseline for future studies.

The lower group density in USNR compared with MW mirrors results from earlier occupancy analyses from camera-trapping data (Hegerl et al., 2017; Oberosler et al., 2020a, 2020b) and is likely explained by the elevated anthropogenic encroachment that has affected USNR for decades, mainly in the form of illegal hunting, tree cutting, and charcoal making (Oberosler et al., 2020a; Rovero et al., 2012). Such disturbance is seemingly more impactful on the strictly arboreal and folivorous colobine monkeys that underwent severe declines in USNR, being the target of selective hunting techniques (Rovero et al., 2012, 2015), while the predominantly ground-dwelling and frugivorous mangabeys appear not to be specifically targeted by hunters and better adapted to exploit more heterogeneous and lightly disturbed habitats (Ehardt et al., 2005; Lloyd, 2017; Rovero, Martin, et al., 2014). Yet, their lower density in USNR than MW (with a seemingly lower group size in the former forest; Paddock et al., 2020) and the results of occupancy analyses suggest that the mangabey is vulnerable to human disturbance. In fact, the decreasing occupancy in proximity to protected area borders coincides in the insulated USNR with proximity to densely human-populated areas, which surround the entire forest block. Indeed, the grid of camera traps distributed across most of the species' range allowed us to study spatial variation in occurrence, and hence abundance. Elevation and gross habitat type emerged as important predictors consistently for both populations. Sanje mangabeys displayed a general preference for sub-montane forest at mid-elevation, with higher occurrence roughly between 500 and 1000 m asl. These areas of presumed optimal habitat for the species generally consist of evergreen forest with greater mean basal area than elsewhere (Cavada et al., 2016), indicating predominance of closed-canopy and old-growth forest. Nonetheless, our results indicated that deciduous forest zones were also used, likely reflecting the great niche flexibility of the Sanje mangabey, which is known to exploit mosaic forests, thanks to its diet predominantly based on seeds and invertebrates (Ehardt et al., 2005; Lloyd, 2017; McCabe et al., 2019; Rovero et al., 2012).

In conclusion, the approach we tested, based on calibrating occupancy to independent density estimations, appears valuable for spatially explicit density estimations of poorly detected species such as the Sanje mangabey, provided that the sampling design is appropriate to relate the two inherently different metrics. Our analysis provided for the first comprehensive assessments of the abundance and vulnerability of this primate, identifying priority areas for conservation, especially the forest areas at lower elevation and close to human settlements. While the relatively higher abundance of Sanje mangabeys in the less protected USNR than earlier reported gives cause for optimism, this forest continues to suffer from illegal human encroachment, calling for the need of increased protection and mitigation of anthropogenic threats.

AUTHOR CONTRIBUTIONS

Francesco Rovero conceived the study. Ilaria Greco and Christina Lynette Paddock analyzed the data, with the contribution of Francesco Rovero. Christina Lynette Paddock, Gráinne Michelle McCabe, Claudia Barelli, Steven Shinyambala, and Arafat S. Mtui conducted fieldwork. Ilaria Greco and Francesco Rovero wrote the manuscript and all authors contributed critically to the drafts.

ACKNOWLEDGMENTS

We thank the subject-matter editor and two reviewers for their insightful comments and suggestions that helped us improve the original manuscript. We are grateful to the Tanzania Wildlife Research Institute, Tanzania Commission for Science and Technology, Tanzania National Parks, Tanzania Forest Service Agency, and Tanzania Commission for Science and Technology for research permissions. Wardens and staff of TANAPA's Udzungwa Mountains National Park and TFS's Uzungwa Scarp Nature Reserve are particularly thanked for the invaluable assistance and support given. For camera-trapping, we thank Ruben Mwakisoma, Emilian Omari, Aggrey Uisso, and several other field assistants. For the Sanje Mangabey Project, we thank all field assistants for their critical help, particularly Yahaya Sama, Bakari Ponda, Loy Loishoki, and Saidi Malendula. We also thank Dr. Andrew Bowkett for participating in the baseline camera-trapping survey in Uzungwa Scarp, and Dr. David Fernandez as co-director of the Sanje Mangabey Project. Funding and equipment for camera-trapping were provided by Fondazione Foresta Futura (Italy), Wild Planet Trust (UK), MUSE—Museo delle Scienze, and the Tropical Ecology Assessment and Monitoring (TEAM) Network. Funding for the acoustic surveys was provided by the UK Natural Environment Research Council (NERC; CASE Studentship NE/N007980/1), Bristol Zoological Society as the NERC CASE industry partner, and Primate Conservation Inc. (#1443).

CONFLICT OF INTEREST STATEMENT

The authors have not disclosed any competing interests.

DATA AVAILABILITY STATEMENT

Data (Greco et al., 2023) are available from Figshare: https://doi.org/10.6084/m9.figshare.21915237.

ETHICS STATEMENT

Ethics approval was not required for this study since no animals were handled or disturbed for this research.

ORCID

Ilaria Greco https://orcid.org/0000-0002-6208-2465
Francesco Rovero https://orcid.org/0000-0001-6688-1494

REFERENCES

Andresen, E., V. Arroyo-Rodriguez, and M. Ramos-Robles. 2018. "Primate Seed Dispersal: Old and New Challenges." *International Journal of Primatology* 39(3): 443–65.

Barelli, C., J. F. Gallardo Palacios, and F. Rovero. 2013. "Variation in Primate Abundance along an Elevational Gradient in the Udzungwa Mountains of Tanzania." In *High Altitude Primates. Developments in Primatology: Progress and Prospects*, edited by N. Grow, S. Gursky-Doyen, and A. Krzton, 211–26. New York: Springer.

Bolker, B. M. 2008. "Probability and Stochastic Distributions for Ecological Modeling." In *Ecological Models and Data in R*, 103–46. Princeton, NJ: Princeton University Press. https://doi.org/10.2307/j.ctvcm4g37.7.

Burgess, N. D., T. M. Butynski, N. J. Cordeiro, N. H. Doggart, J. Fjeldså, K. M. Howell, F. B. Kilahama, et al. 2007. "The Biological Importance of the Eastern Arc Mountains of Tanzania and Kenya." *Biological Conservation* 134: 209–31.

Cavada, N., C. Barelli, M. Ciolli, and F. Rovero. 2016. "Primates in Human-Modified and Fragmented Landscapes: The Conservation Relevance of Modelling Habitat and Disturbance Factors in Density Estimation." *PLoS One* 11: e0148289.

Cavada, N., S. Tenan, C. Barelli, and F. Rovero. 2019. "Effects of Anthropogenic Disturbance on Primate Density at the Landscape Scale." *Conservation Biology* 33: 873–82.

Chambers, J. M., and T. J. Hastie. 1992. *Statistical Models in S*. Pacific Grove, CA: Wadsworth and Brooks/Cole.

Clare, J. D., E. M. Anderson, and D. M. MacFarland. 2015. "Predicting Bobcat Abundance at a Landscape Scale and Evaluating Occupancy as a Density Index in Central Wisconsin." *Journal of Wildlife Management* 79(3): 469–80.

Davenport, T. R. B., S. J. Machaga, N. E. Mpunga, S. P. Kimiti, W. Mwalwengele, O. Mwaipungu, and P. M. Makumbule. 2022. "A Reassessment of the Population Size, Demography, and Status of Tanzania's Endemic Kipunji *Rungwecebus kipunji* 13 Years on: Demonstrating Conservation Success." *International Journal of Primatology* 43: 317–38.

Davenport, T. R. B., K. Nowak, and A. Perkin. 2013. "Priority Primate Areas in Tanzania." *Oryx* 48(1): 39–51.

Dormann, C. F., J. M. Calabrese, G. Guillera-Arroita, E. Matechou, V. Bahn, K. Bartoń, C. M. Beale, et al. 2018. "Model Averaging in Ecology: A Review of Bayesian, Information-Theoretic, and Tactical Approaches for Predictive Inference." *Ecological Monographs* 88: 485–504.

Ehardt, C. L. 2001. "The Endemic Primates of the Udzwunga Mountains, Tanzania." *African Primates* 4: 15–26.

Ehardt, C. L., T. P. Jones, and T. M. Butynski. 2005. "Protective Status, Ecology and Strategies for Improving Conservation of *Cercocebus sanjei* in the Udzungwa Mountains, Tanzania." *International Journal of Primatology* 263: 557–83.

Estrada, A., P. A. Garber, A. B. Rylands, C. Roos, E. Fernandez-Duque, A. Di Fiore, K. A. I. Nekaris, et al. 2017. "Impending Extinction Crisis of the World's Primates: Why Primates Matter." *Science Advances* 3: e1600946.

European Commission. 2004. *Global Land Cover for the Year 2000*, edited by E. Bartholomé, A. Belward, R. Beuchle, H. Eva, S. Fritz, A. Hartley, P. Mayaux, and H. J. Stibig. Luxembourg: Luxembourg Office for Official Publications of the European Communities, Catalogue Number LB-55-03-099-ENC.

Fernández, D., D. Kerhoas, A. Dempsey, J. Billany, G. McCabe, and E. Argirova. 2022. "The Current Status of the World's Primates: Mapping Threats to Understand Priorities for Primate Conservation." *International Journal of Primatology* 43: 15–39.

Fiske, I., and R. Chandler. 2011. "Unmarked: An R Package for Fitting Hierarchical Models of Occurrence and Abundance." *Journal of Statistical Software* 43: 1–23.

Gippoliti, S., and C. Sousa. 2004. "The Chimpanzee, *Pan troglodytes*, as an "Umbrella" Species for Conservation in Guinea-Bissau, West Africa: Opportunities and Constraints." *Folia Primatologica* 75: 386.

Greco, I., E. Fedele, M. Salvatori, M. Giampaoli Rustichelli, F. Mercuri, G. Santini, F. Rovero, et al. 2021. "Guest or Pest? Spatio-Temporal Occurrence and Effects on Soil and Vegetation of the Wild Boar on Elba Island." *Mammalian Biology* 101: 193–206.

Greco, I., and F. Rovero. 2021. "The African Golden Cat *Caracal aurata* in Tanzania: First Record and Vulnerability Assessment." *Oryx* 55(2): 212–5.

Greco, I., F. Rovero, C. L. Paddock, G. M. McCabe, C. Barelli, S. Shinyambala, and A. Mtui. 2023. "Greco_et_al_Ecosphere." Figshare. Dataset. https://doi.org/10.6084/m9.figshare.21915237.v1.

Hegerl, C., N. Burgess, M. Nielsen, E. Martin, M. Ciolli, and F. Rovero. 2017. "Using Camera-Trap Data to Assess the Impact of Bushmeat Hunting on Forest Mammals in Tanzania." *Oryx* 51: 87–97.

Holbrook, K. M., and B. A. Loiselle. 2009. "Dispersal in a Neotropical Tree, *Virola flexusa* (Myristicacae): Does Hunting of Large Vertebrates Limit Seed Removal?" *Ecology* 90: 1449–55.

International Union for Conservation of Nature (IUCN). 2021. "The IUCN Red List of Threatened Species." https://www.iucnredlist.org.

Joseph, L. N., S. A. Field, C. Wilcox, and H. P. Possingham. 2006. "Presence-Absence versus Abundance Data for Monitoring Threatened Species." *Conservation Biology* 20(6): 1679–87.

Kéry, M., and J. A. Royle. 2016. *Applied Hierarchical Modeling in Ecology: Analysis of Distribution, Abundance and Species Richness in R and BUGS. Vol. 1: Prelude and Static Models*. London: Academic Press, 783 pp.

Kühl, H., F. Maisels, M. Ancrenaz, and E. A. Williamson. 2008. *Best Practice Guidelines for Surveys and Monitoring of Great Ape Populations*. Gland: IUCN SSC Primate Specialist Group.

Lambert, J. E. 2010. "Primate Seed Dispersers as Umbrella Species: A Case Study from Kibale National Park, Uganda, with Implications for Afrotropical Forest Conservation." *American Journal of Primatology* 73(1): 9–24.

Lewis, J. S., K. A. Logan, M. W. Alldredge, L. L. Bailey, S. VandeWoude, and K. R. Crooks. 2015. "The Effects of Urbanization on Population Density, Occupancy, and Detection Probability of Wild Felids." *Ecological Applications* 25(7): 1880–95.

Linden, D. W., A. K. Fuller, J. A. Royle, and M. P. Hare. 2017. "Examining the Occupancy–Density Relationship for a Low-Density Carnivore." *Journal of Applied Ecology* 54: 2043–52.

Lloyd, E. K. 2017. "Behavioural Flexibility in the Sanje Mangaby (*Cercocebus sanjei*), Udzungwa Mountains, Tanzania." PhD thesis in Anthropology, University of Texas.

MacKenzie, D. I., and J. D. Nichols. 2004. "Occupancy as a Surrogate for Abundance Estimation." *Animal Biodiversity and Conservation* 27(1): 461–7.

Mackenzie, D. I., J. D. Nichols, G. Lachman, S. Droege, A. J. Royle, and C. Langtimm. 2002. "Estimating Site Occupancy Rates when Detection Probabilities Are Less than One." *Ecology* 83: 2248–55.

MacKenzie, D. I., J. D. Nichols, J. A. Royle, K. H. Pollock, J. E. Hines, and L. L. Bailey. 2006. *Occupancy Estimation and Modeling: Inferring Patterns and Dynamics of Species Occurrence*, 1st ed. Amsterdam: Elsevier.

Marsh, L. K. 2003. *Primates in Fragments: Ecology and Conservation*. Boston, MA: Springer US, 539 pp.

Marshall, A. R., H. I. O. Jørgensbye, F. Rovero, P. J. Platts, P. C. L. White, and J. C. Lovett. 2010. "The Species–Area Relationship and Confounding Variables in a Threatened Monkey Community." *American Journal of Primatology* 72(4): 325–36.

Martin, E. H., N. Cavada, V. G. Ndibalema, and F. Rovero. 2015. "Modelling Fine-Scale Habitat Associations of Medium-to-Large Forest Mammals in the Udzungwa Mountains of Tanzania Using Camera Trapping." *Tropical Zoology* 28(4): 137–51.

Martins, C. S., and C. B. Valladares-Padua. 2005. "The Black Lion Tamarin (*Leontopithecus chrysopygus*) as an Umbrella Species in the Conservation of the Biodiversity of Patches of the Atlantic Rain Forest of Sao Paula's Inland Area." *Bulletin of the American Society of Primatology* 29: 11–3.

McCabe, G., F. Rovero, D. Fernández, T. M. Butynski, and T. T. Struhsaker. 2019. "*Cercocebus sanjei*. The IUCN Red List of Threatened Species." 2019: e.T4203A17955753. https://doi.org/10.2305/IUCN.UK.2019-3.RLTS.T4203A17955753.en.

Miller, D. L., E. Rexstad, L. Thomas, L. Marshall, and J. L. Laake. 2019. "Distance Sampling in R." *Journal of Statistical Software* 89: 1–28.

Mittermeier, R. A., C. Valladares-Pádua, A. B. Rylands, A. A. Eudey, T. M. Butynski, J. U. Ganzhorn, R. Kormos, J. M. Aguiar, and S. Walker. 2006. "Primates in Peril: The World's 25 Most Endangered Primates, 2004–2006." *Primate Conservation* 20: 1–28.

Mwamende, K. A. 2009. "Social Organisation, Ecology and Reproduction in the Sanje Mangabey (*Cercocebus sanjei*) in the Udzungwa Mountains National Park, Tanzania." MSc thesis, Victoria University of Wellington. http://researcharchive.vuw.ac.nz/xmlui/bitstream/handle/10063/1114/thesis.pdf?sequence=1&sa=U&ei=qblbU9DLE6Ki8QGrk4CACg&ved=0CB0QFjAA&usg=AFQjCNHPUJGQW_LC-eh4paOu558kAEe0ZQ.

Neilson, E. W., T. Avgar, A. C. Burton, K. Broadley, and S. Boutin. 2018. "Animal Movement Affects Interpretation of Occupancy Models from Camera-Trap Surveys of Unmarked Animals." *Ecosphere* 9(1): e02092.

Noon, B. R., L. L. Bailey, T. D. Sisk, and K. S. McKelvey. 2012. "Efficient Species-Level Monitoring at the Landscape Scale." *Conservation Biology* 26: 432–41.

Oberosler, V., S. Tenan, E. F. Zipkin, and F. Rovero. 2020a. "Poor Management in Protected Areas Is Associated with Lowered Tropical Mammal Diversity." *Animal Conservation* 23: 171–81.

Oberosler, V., S. Tenan, E. F. Zipkin, and F. Rovero. 2020b. "When Parks Work: Effect of Anthropogenic Disturbance on Occupancy of Tropical Forest Mammals." *Ecology and Evolution* 10: 3881–94.

Paddock, C. L., M. W. Bruford, and G. M. McCabe. 2020. "Estimating the Population Size of the Sanje Mangabey (*Cercocebus sanjei*) Using Acoustic Distance Sampling." *American Journal of Primatology* 82: e23083.

Parsons, A. W., T. Forrester, W. J. McShea, M. C. Baker-Whatton, J. J. Millspaugh, and R. Kays. 2017. "Do Occupancy or Detection Rates from Camera Traps Reflect Deer Density?" *Journal of Mammalogy* 98(6): 1547–57.

QGIS Development Team. 2019. "QGIS Geographic Information System." Open-source Geospatial 475 Foundation Project. http://qgis.osgeo.org.

R Core Team. 2018. *R: A Language and Environment for Statistical Computing*. Vienna: R Foundation for Statistical Computing.

Roberts, R., R. Hamilton, and D. R. Piperno. 2021. "Tropical Forests as Key Sites of the 'Anthropocene': Past and Present Perspectives." *Proceedings of the National Academy of Sciences* 118(40): e2109243118.

Rodrìguez-Luna, E., A. Shedden, and B. A. Solòrzano-Garcìa. 2013. "A Region-Wide Review of Mesoamerican Primates: Prioritizing for Conservation." In *Primates in Fragments: Complexity and Resilience Developments in Primatology: Progress and Prospects*, edited by L. K. Marsh and C. A. Chapman, 47–55. New York: Springer Science + Business Media.

Rogan, M. S., G. A. Balme, G. Distiller, R. T. Pitman, J. Broadfield, G. K. Mann, G. M. Whittington-Jones, L. H. Thomas, and M. J. O'Riain. 2019. "The Influence of Movement on the Occupancy–Density Relationship at Small Spatial Scales." *Ecosphere* 10(8): e02807.

Rovero, F., and J. Ahumada. 2017. "The Tropical Ecology, Assessment and Monitoring (TEAM) Network: An Early Warning System for Tropical Rain Forests." *Science of the Total Environment* 574: 914–23.

Rovero, F., A. R. Marshall, T. Jones, and A. Perking. 2009. "The Primates of the Udzungwa Mountains: Diversity, Ecology and Conservation." *Journal of Anthropological Sciences* 87: 93–126.

Rovero, F., E. Martin, M. Rosa, J. A. Ahumada, and D. Spitale. 2014. "Estimating Species Richness and Modelling Habitat Preferences of Tropical Forest Mammals from Camera Trap Data." *PLoS One* 9: e103300.

Rovero, F., M. Menegon, J. Fjeldsa, L. Collett, N. Doggart, C. Leonard, G. Norton, et al. 2014. "Targeted Vertebrate Surveys Enhance the Faunal Importance and Improve Explanatory Models within the Eastern Arc Mountains of Kenya and Tanzania." *Diversity and Distribution* 20: 1438–49.

Rovero, F., A. S. Mtui, A. Kitegile, P. Jacob, A. Araldi, and S. Tenan. 2015. "Primates Decline Rapidly in Unprotected Forests: Evidence from a Monitoring Program with Data Constraints." *PLoS One* 10(2): e0118330.

Rovero, F., A. S. Mtui, A. S. Kitegile, and M. R. Nielsen. 2012. "Hunting or Habitat Degradation? Decline of Primate Populations in Udzungwa Mountains, Tanzania: An Analysis of Threats." *Biological Conservation* 146: 89–96.

Rovero, F., and F. Spitale. 2016. "Species-Level Occupancy Analyses." In *Camera Trapping for Wildlife Research. Data in the Wild*, edited by F. Rovero and F. Zimmermann, 68–94. Exeter: Pelagic Publishing.

Rovero, F., T. T. Struhsaker, A. R. Marshall, T. A. Rinne, U. B. Pedersen, T. M. Butynski, C. L. Ehardt, and A. S. Mtui. 2006. "Abundance of Diurnal Primates in Mwanihana Forest, Udzungwa Mountains, Tanzania." *International Journal of Primatology* 27: 675–97.

Sarkar, D. 2008. *Lattice: Multivariate Data Visualization with R*. New York: Springer. http://lmdvr.r-forge.r-project.org.

Schipper, J., J. S. Chanson, F. Chiozza, N. A. Cox, M. Hoffmann, V. Katariya, J. Lamoreux, et al. 2008. "The Status of the World's Land and Marine Mammals: Diversity, Threat, and Knowledge." *Science* 322(5899): 225–30.

Spehar, S. N., B. Loken, Y. Rayadin, and J. A. Royle. 2015. "Comparing Spatial Capture–Recapture Modeling and Nest Count Methods to Estimate Orangutan Densities in the Wehea Forest, East Kalimantan, Indonesia." *Biological Conservation* 191: 185–93.

Tempel, D. J., and R. J. Gutierréz. 2013. "Relation between Occupancy and Abundance for a Territorial Species, the California Spotted Owl." *Conservation Biology* 27(5): 1087–95.

Wilson, T. L., and J. H. Schmidt. 2015. "Scale Dependence in Occupancy Models: Implications for Estimating Bear Den Distribution and Abundance." *Ecosphere* 6(9): 168.

SUPPORTING INFORMATION

Additional supporting information can be found online in the Supporting Information section at the end of this article.

How to cite this article: Greco, Ilaria, Christina Lynette Paddock, Gráinne Michelle McCabe, Claudia Barelli, Steven Shinyambala, Arafat S. Mtui, and Francesco Rovero. 2023. "Calibrating Occupancy to Density Estimations to Assess Abundance and Vulnerability of a Threatened Primate in Tanzania." *Ecosphere* 14(3): e4427. https://doi.org/10.1002/ecs2.4427